THE UNIVERSITY OF MICHIGAN

INDUSTRY PROGRAM OF THE COLLEGE OF ENGINEERING

DIFFUSION OF GLYCEROL AND SODIUM CHLORIDE IN RESINS AND ANALYSIS OF ION EXCLUSION AND OTHER SOLID-LIQUID MASS TRANSFER PROCESSES

Muhammad T. Tayyabkhan

A dissertation submitted in partial fulfillment
of the requirements for the degree of
Doctor of Philosophy in The
University of Michigan
1959

November, 1959

IP-404

Doctoral Committee:

Professor Robert R. White, Chairman
Professor Julius T. Banchero
Professor Stuart W. Churchill
Professor Wilfred Kaplan
Professor Robert W. Parry

ACKNOWLEDGMENTS

I wish to thank the following:

Professor R. R. White, for his encouragement, stimulation, patience and understanding.

Professors W. Kaplan, R. C. Bartels and B. A. Galler for generous contribution of time and valuable help in various mathematical problems.

Professors J. T. Banchero, S. W. Churchill and R. W. Parry for advice and criticism.

Miss Helen Sherman and Mrs. B. Nachman without whose moral support this research might not have been completed.

Dr. Murray Douglas for stimulating technical discussions.

Many friends including Miss V. Chang, Mrs. V. Douglas, Mr. S. P. Mathur, Mr. M. Melbin, Mr. D. Mongia, Mr. M. Mascarenhas, Mr. M. Sanghvi, Mr. K. S. Sanvordenker, and Mr. H. E. Zellink.

Staff of Industry Program.

Chemical and Metallurgical Engineering Office and Shop Staff.

Dow Chemical Company for providing the resin.

J. N. Tata endowment and the Chemical and Metallurgical Engineering Department and Graduate School of The University of Michigan for financial support during this research.

TABLE OF CONTENTS

PREFACE

This thesis is written in two parts. The first part involves an experimental study and the second part is concerned with utilizing the experimentally determined results as parameters in mathematical models. Because of the difference in the subject matter and its treatment, the author considers it advantageous to have each of the two parts of the thesis complete and self-contained. Each part has its own table of contents, introduction, summary, conclusions, and bibliography. The equation and figure numbers and the references to the literature in each part apply only to that part and there are no cross references between the two parts.

The experimental study, Part I of this thesis, is written in such a style that the first 15 to 20 pages of this part give a complete report of the study including the problem, the method of its solution and conclusions. All details of the explanations and the methods, including experimental procedure, mathematical equations and solutions, correlation of data and literature survey are deferred from consideration until after a somewhat comprehensive but brief and rapid report of the study is given in the first few pages. In the present thesis these details are grouped together in the last section of Part I.

In the opinion of the author, a report such as this thesis has two functions: (1) Communicating to the reader "useful" "information content" of the research and (2) Recording all the details of the research as reference for other workers in the field. The first is the function of a journal article; the second is the function of a specialized handbook. The organization of the report that has been used in Part I of the thesis (i.e., separation of all methodological details from the central report which is

given in the first few pages) performs the function of "communicating" more efficiently than the conventional style of writing dissertations without sacrificing the function of "recording".

Part II of this thesis grew from the attempts to reproduce laboratory and pilot plant data from the physical characteristics that were determined experimentally (and reported in Part I of this thesis). The author was forced to organize and integrate, for his own use, material reported by several workers in fields of chromatography and ion exchange. The objective of the author is to communicate this organization to the reader; and consequently a "text-book style" is employed in an attempt to help the reader develop an "understanding" of the entire area of the field under consideration. Numerous illustrations are used and various concepts are introduced in order of increasing complexity.

OVERALL PLAN OF THE THESIS

This thesis is in two parts:

The first part involves an experimental study of the diffusion of sodium chloride and glycerol in solid resin particles. The sodium form of a cation-exchange resin, Dowex 50, is used. Diffusivities or diffusion coefficients are determined and some equilibrium data are obtained.

The second part involves a mathematical analysis of the performance and design of a fixed bed ion-exclusion column. Mathematical models are postulated and discussed. Some experimental data available in literature are compared with the models.

PART I

DIFFUSION OF GLYCEROL AND SODIUM CHLORIDE IN DOWEX 50

TABLE OF CONTENTS FOR PART I

TABLE OF CONTENTS FOR PART I (CONT'D)

LIST OF TABLES

LIST OF FIGURES

LIST OF FIGURES (CONT'D)

NOMENCLATURE

c	the concentration of the solute at a distance r from the center of the resin sphere and at time t. (gm or gm mols/cm^3)
C	the molar concentration of (diffusing solute diffusing ion) within a resin particle. (gm-moles/cu^3)
D	the diffusivity or the diffusion coefficient of glycerol or sodium chloride in the resin. (cm^2/sec)
F	the Faraday constant (23.060 cal/abs. volt g-equiv.)
n	variable of summation for a series of terms.
N	the number of data points.
q	the total amount of sodium chloride or glycerol left in the resin at time t. (gm or gm-mols)
q_o	the total equilibrium amount of sodium chloride or glycerol present in the resin before the elution, i.e. at time t equal to zero. (gm or gm-mols)
q^*	the value of q on the plot of data that coincides with the origin of the master plot, superpositioned for fitting the data. (gm or gm-mols)
r	distance from the center of the resin sphere. (cm)
R	the radius of the resin spheres. (cm)
$\check{R}$	the sum of the squares of the errors for "least squares fit" of the data.
t	the time. (seconds)
T	the absolute temperature. (°K)
t^*	the value of t on the plot of data that coincides with the origin of the master plot, superpositioned for fitting the data. (seconds)
x	the degree of cross linking of the resin Dowex 50, expressed as percent divinyl-benzene.
Z	the electrochemical valence of the ions.
ϕ	the flux of diffusing solute or diffusing ions (gm-moles/(sq.cm)(sec))
φ	the dimensionless time ($\pi^2 Dt/R^2$).
$\bar{\varphi}$	the electric potential.

SUMMARY
(For Part I)

An experimental study indicated that diffusion according to Fick's Law is an adequate model for describing mass transfer of NaCl and glycerol in the solid phase Dowex 50. Several baskets, each containing one gram of uniform resin particles, were first saturated with a solution and then subjected for different amounts of time to a stream of distilled water that carried away the solutes diffusing out of the resin. The solutes remaining in the resin were extracted and their amounts were determined. Equilibrium absorption and diffusivities were determined by making a two constant fit of the data to a "diffusion model".

The variables studied were: (1) Resin Cross Linkage - 2% to 12% DVB; (2) Temperature - 25 to 80°C; (3) Concentrations in the Equilibrating solution; (4) Resin Particle Size; (5) Flow Rate of the Eluting Distilled water. Diffusivities increase with decrease in cross-linkage and with increase in temperature. The ratio of the diffusivities of NaCl or glycerol in the resin to that in water is between 0.2 and 0.35 for 2% DVB and between 0.025 and 0.1 for 12% DVB. Diffusivities were found to be independent of the variables 3, 4 and 5 above. The equilibrium absorption also increased with decrease in cross-linkage and increase in temperature.

The analytic solution of the "diffusion model" is in the form of an infinite series that does not converge rapidly. A method of curve fitting by super-positioning a master plot has been developed for making a two constant fit of the data to the analytic solution. Besides being very rapid, the method of super-positioning has the advantage of having

less bias than many alternative methods. The variation in superpositioning, among different persons fitting the same data, was found to be less than the scatter of the experimental data.

Possible utilization of the experimental technique and the mathematical solutions for studying diffusion of ions for ion-exchange systems have been discussed briefly.

I. INTRODUCTION

There are processes of commercial and laboratory interest such as ion exclusion and chromatography in which a liquid mixture is passed over a bed of solids and components of the mixture are transferred between the liquid and the solid. The rates of transfer in these processes depend on the resistance in the liquid phase and that in the solid phase. The transfer of mass in a liquid phase passing over beds of solids has been studied by many researchers in the past and generalized correlations for predicting the transfer resistances (C2, S1) are available in the literature. For predicting the resistances in the solid phase, on the other hand, there are no general methods and very little data have been published.

For the present study, a typical ion-exclusion system, Dowex 50-sodium chloride-glycerol-water has been selected.* A small bed containing one gram of the resin, Dowex 50, is taken and the mass transfer resistance in the liquid is eliminated by passing the liquid over the bed at high velocities.

The solid phase itself consists of an aggregate of small particles and direct measurements of the concentrations of materials in the solid phase, i.e., within each particle, are not possible. The total amounts of materials present in the solid phase, however, can be determined

---

* The system has some commercial importance since an aqueous solution containing both NaCl and glycerol is obtained as a by-product in soap manufacture. See References (P2) and (A1) for separation of these materials by ion exclusion.

A brief description of ion exclusion is given in Section 11 of Detailed Discussions.

by extracting them quantitatively from the resin particles. Data on the total amount of the materials present in the solid phase during an unsteady state elution (or desorption) of the solid are correlated to give the resistance to mass transfer within the solid phase.

In more complex processes such as ion-exchange and the chemical reactions catalyzed by ion-exchange resins, mass transfer between a solid and a liquid is one of several phenomena occurring simultaneously. An understanding of the mass transfer studied in the present research can be extended to these processes.

II. GENERAL PLAN

It is postulated that the process of mass transfer within the resin particles obeys Fick's Law of Diffusion wherein "diffusivity" is a proportionality constant relating rate to a driving force which is concentration gradient.

Uniform, spherical resin particles are saturated with solutions of glycerol and sodium chloride in water to establish constant initial concentrations through the spheres. These spheres are subsequently subjected to a constant boundary condition of zero concentration at the surface of the spheres. This is accomplished by passing distilled water at high velocities past the resin particles which carries away the materials diffusing out of the resin spheres. The amount of glycerol and sodium chloride remaining in the resin particles at different times of elution is determined experimentally.

The following partial differential equation represents a material balance for an element of volume within a resin particle. Radial symmetry is assumed.

$$D\left(\frac{\partial^2 c}{\partial r^2} + \frac{2}{r}\frac{\partial c}{\partial r}\right) = \frac{\partial c}{\partial t}$$

D is the diffusivity of the solute

c is the concentration of the solute at a distance r from the center of the resin sphere and at time t.

The initial concentration in the resin particle is the equilibrium concentration. The boundary condition is a zero concentration at the surface of the spheres.

The analytic solution of this equation has been obtained. It gives c as a function of r and t. This can be integrated over the resin spheres to give the total amount of materials present in the resin spheres at different times. The data may now be fitted to this integrated solution to give the values of the equilibrium concentrations and the diffusivities.

The applicability of this diffusion model and other assumptions involved are stated and justified, as far as possible, in the section on the discussion of results.

III. THE EXPERIMENTAL PROCEDURE

Baskets made from stainless steel wire screen were filled with a weighed amount (one gram) of ion-exchange resin. The resin particles were spherical and uniform in size.* Figure 1 shows a typical basket.

These baskets were immersed for about 12 hours in a solution containing sodium chloride and glycerol in order to bring the resin to equilibrium with the surrounding solution.

Each basket was placed in a rubber conduit and distilled water was pumped at high velocities through the assembly as indicated in Figure 2. During this time, sodium chloride and glycerol transferred out of the resin particles and were carried away by the stream of the distilled water.

The process was interrupted suddenly by pulling the basket out of the conduit without discontinuing the flow. A synchronized electric timer recorded the time for which each basket was subjected to the stream of eluting distilled water.

The amounts of materials remaining in the resin particles after the elution with distilled water were determined by extracting them from the resin in 100 ccs. of distilled water and analyzing the solution thus obtained.

Data from a typical experimental run described above are shown in Table I.

---

* Details on screening and preparation of the resin are given in Section 2 of the Detailed Discussions.

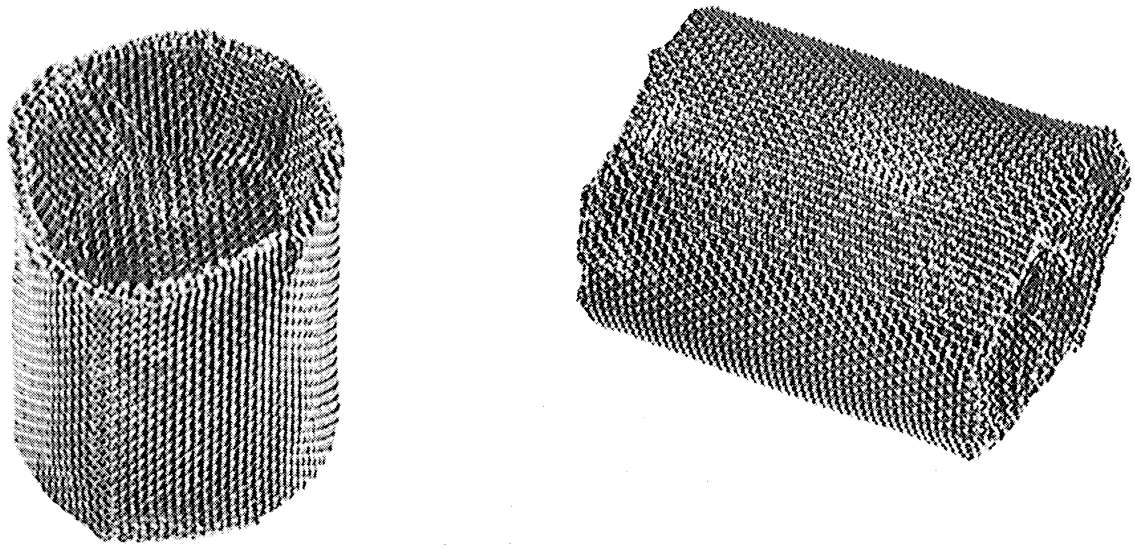

Figure 1. A Typical Basket Containing One Gram of Dowex 50. (Size: 1 inch x 3/4 inches diameter).

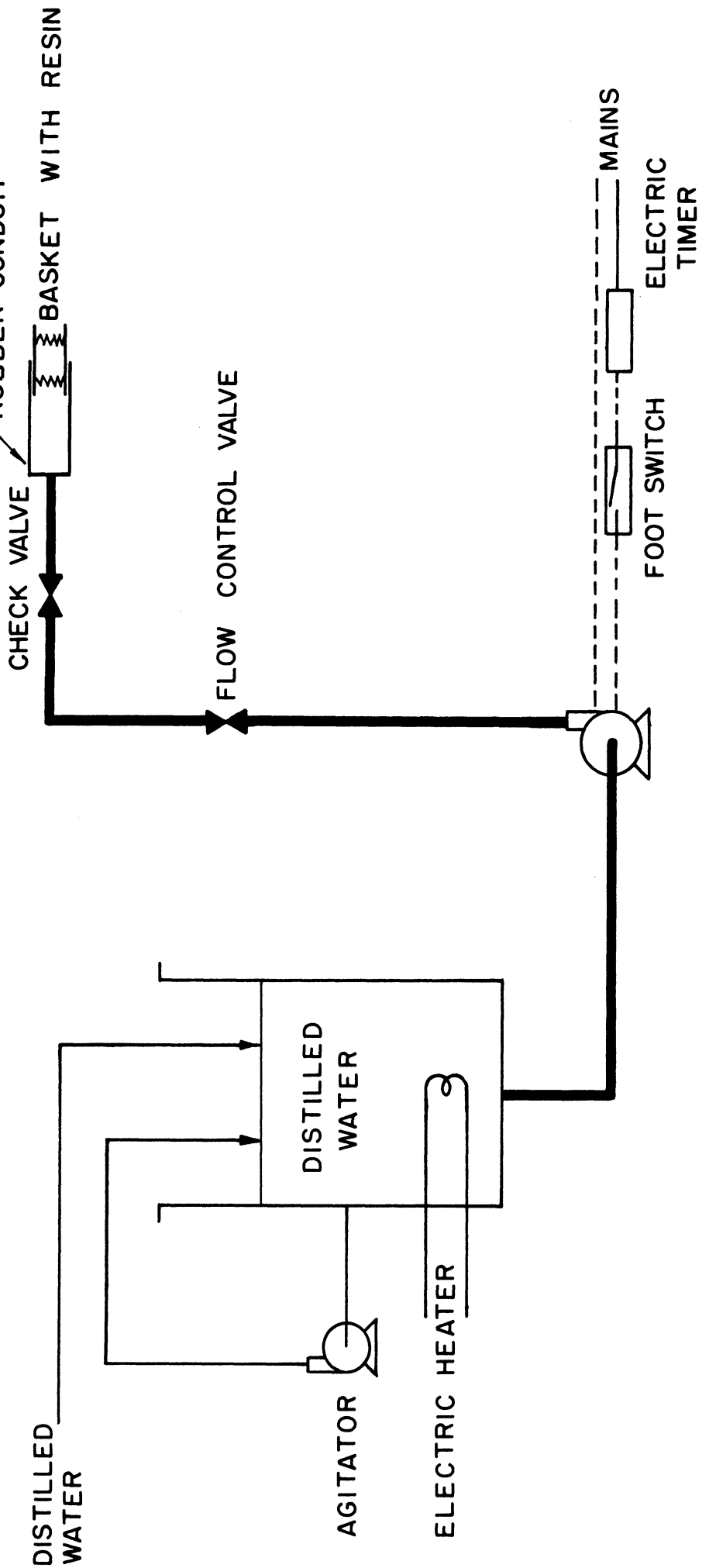

Figure 2. Sketch of Equipment Used for Diffusion Study.

TABLE I

DATA FROM A TYPICAL RUN

Run Number: 7-10
Temperature: (26.0 ± .2) °C
Cross Linkage of the resin: 8% divinyl benzene
Weight of resin each basket: One gram (air dry) at 50% relative humidity and 25 °C
Resin saturation time: 16 hours
Saturating solution: 9.80 wt.% Sodium Chloride and
9.49 wt.% Glycerol

Time for Elution in Minutes	Total Amount of Solutes Remaining in the Resin	
	mgm. Glycerol	mgm. Sodium Chloride
0.037	39.8	
0.078	36.4	8.8
0.133	35.6	7.94
0.190	33.2	6.24
0.320	30.0	5.91
0.475	27.15	5.19
0.573	25.07	4.08
0.847	23.15	3.56
1.003	20.4	2.98
1.010	20.4	2.63
1.545	15.92	1.90
1.645	14.68	1.48
2.060	13.6	1.062
2.598	8.95	0.48
3.465	7.34	0.30
4.497	4.955	0.125
0	45.2*	11.7*

* The amounts of gycerol and sodium chloride at the zero elution time are included here only for comparison. They are not part of the data, but are obtained from the correlation of the data according to the method described in the next section.

IV. EVALUATING DIFFUSIVITIES FROM THE DATA

The amount of sodium chloride and glycerol remaining in the ion exchange resin at the time, t, depends on the amount that was present in equilibrium with the saturating solution at time zero and the resistance to the transfer of the materials from the resin to the eluting stream of water. The data giving q, the amount of sodium chloride or glycerol left in the resin at time, t, are correlated to give the amount at equilibrium and the diffusivity of the solute in the resin phase.

Assuming the diffusion model and Fick's Law, a material balance for an element of volume within a resin particle gives the following partial differential equation.

$$D\left(\frac{\partial^2 c}{\partial r^2} + \frac{2}{r}\frac{\partial c}{\partial r}\right) = \frac{\partial c}{\partial t}$$

where D is the diffusivity of the solute in $cm^2/sec.$

c is the concentration of the solute at a distance r from the center of the resin sphere and at time, t.

Radial symmetry is assumed within the resin particle.

The initial concentration is the equilibrium concentration. The boundary condition is the zero concentration at the surface of the resin particles.

This defines a boundary value problem and its solutions are discussed in Section 6 of Miscellaneous Details. The analytic solution of the problem gives the concentrations of the materials as a function of r and t. This solution is integrated over the resin spheres to give

the following equation which expresses q, the total amount of sodium chloride, or glycerol, remaining in the resin phase as a function of time, t.

$$\frac{q}{q_o} = \frac{6}{\pi^2} \sum_{n=1}^{\infty} \frac{1}{n^2} e^{-\frac{n^2 \pi^2 Dt}{R^2}}$$

where q_o is the total equilibrium amount of sodium chloride or glycerol present in the resin before the elution (in gram mols.),

D is the diffusivity in $cm^2/sec.$,

and R is the radius of the resin spheres in centimeters.

Generally 15 to 20 data points of q versus t are obtained for each run. These are fitted to the above equation to obtain the values q_o and D.

A new method of fitting the data to this equation has been worked out in this study. It involves superpositioning of a master plot of q/q_o versus Dt/R^2. Details of this method of superpositioning as well as other methods of handling the above equation are discussed in Section 7 of the Detailed Discussions.

V. RESULTS

Table II shows the diffusivities of sodium chloride and glycerol in Dowex 50 with 8% divinyl benzene at 25°C. As can be seen from the table, the same values of diffusivities are obtained for different concentrations of equilibrating solutions, different resin sizes and different flow rates of the eluting distilled water. This justifies the use of the diffusion model.

Figures 3 and 4 show the diffusivities of sodium chloride and glycerol in wet Dowex 50 as a function of temperature and the cross linkage of the resins (measured as percent divinyl benzene content). For comparison diffusivities of glycerol (W4) and sodium chloride (T3) in water are also shown on the figures.

Resins containing 2, 4, 8, and 12% divinyl benzene were used in the study. As the cross linking (percent divinyl benzene) increases, the diffusivities are reduced.

Diffusivities increase with increased temperatures. For resin with 8% divinyl benzene, a plot of the logarithms of diffusivities versus the reciprocals of the absolute temperatures gave straight lines for the experiments at 25°C., 55°C., and 78°C. For other cross-linkages only two temperatures were investigated; 25°C. and 65°C; and the straight lines were drawn on the log D versus 1/T plot as mentioned above. (See Figures 3 and 4.)

Figures 5 and 6 are the cross plots from the Figures 3 and 4 showing diffusivities as a function of percentage divinyl benzene in the resin.

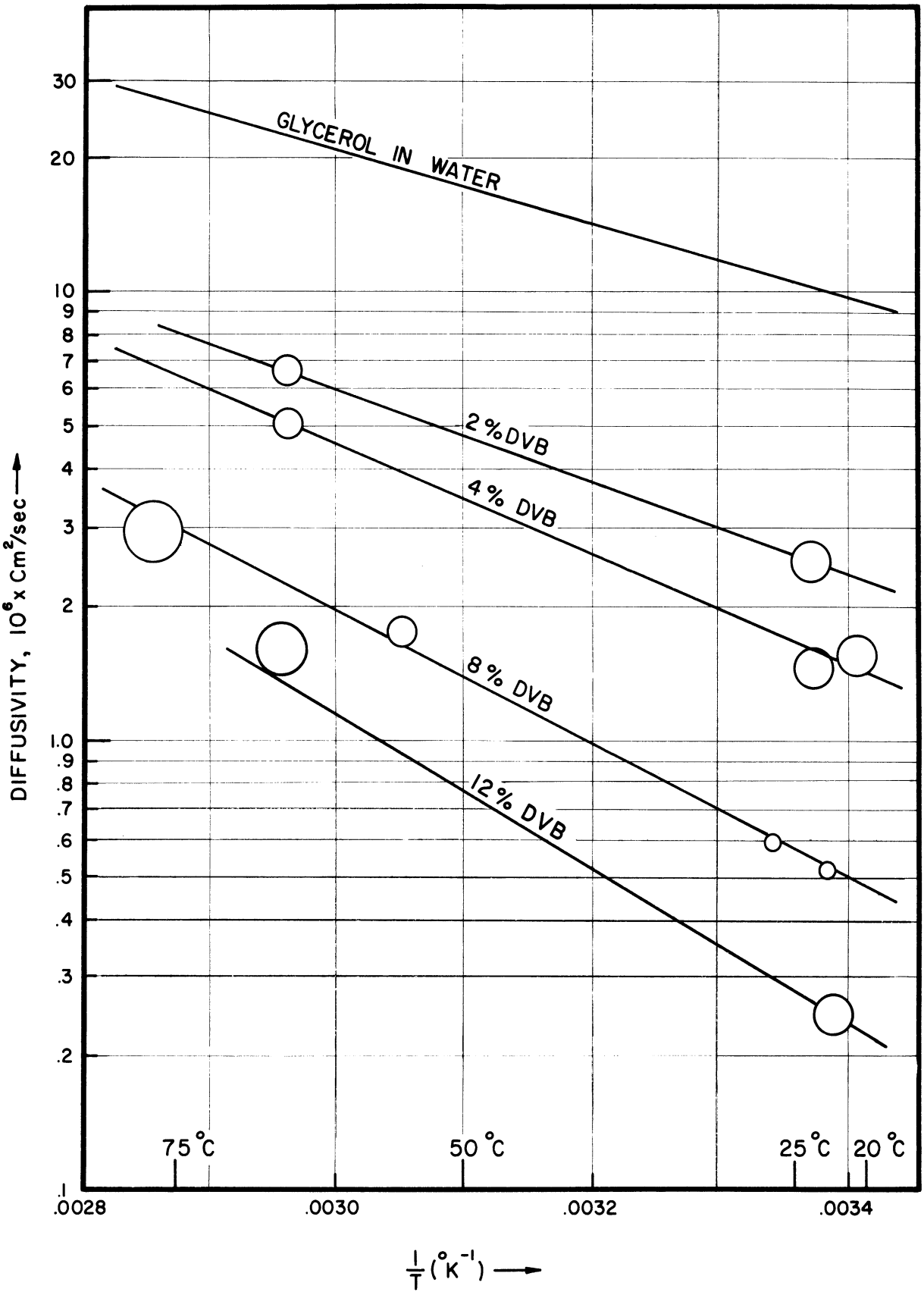

Figure 3. Diffusivity of Glycerol in Dowex 50 (Equilibrating Soln. 30% Glycerol, 5% NaCl by wt)

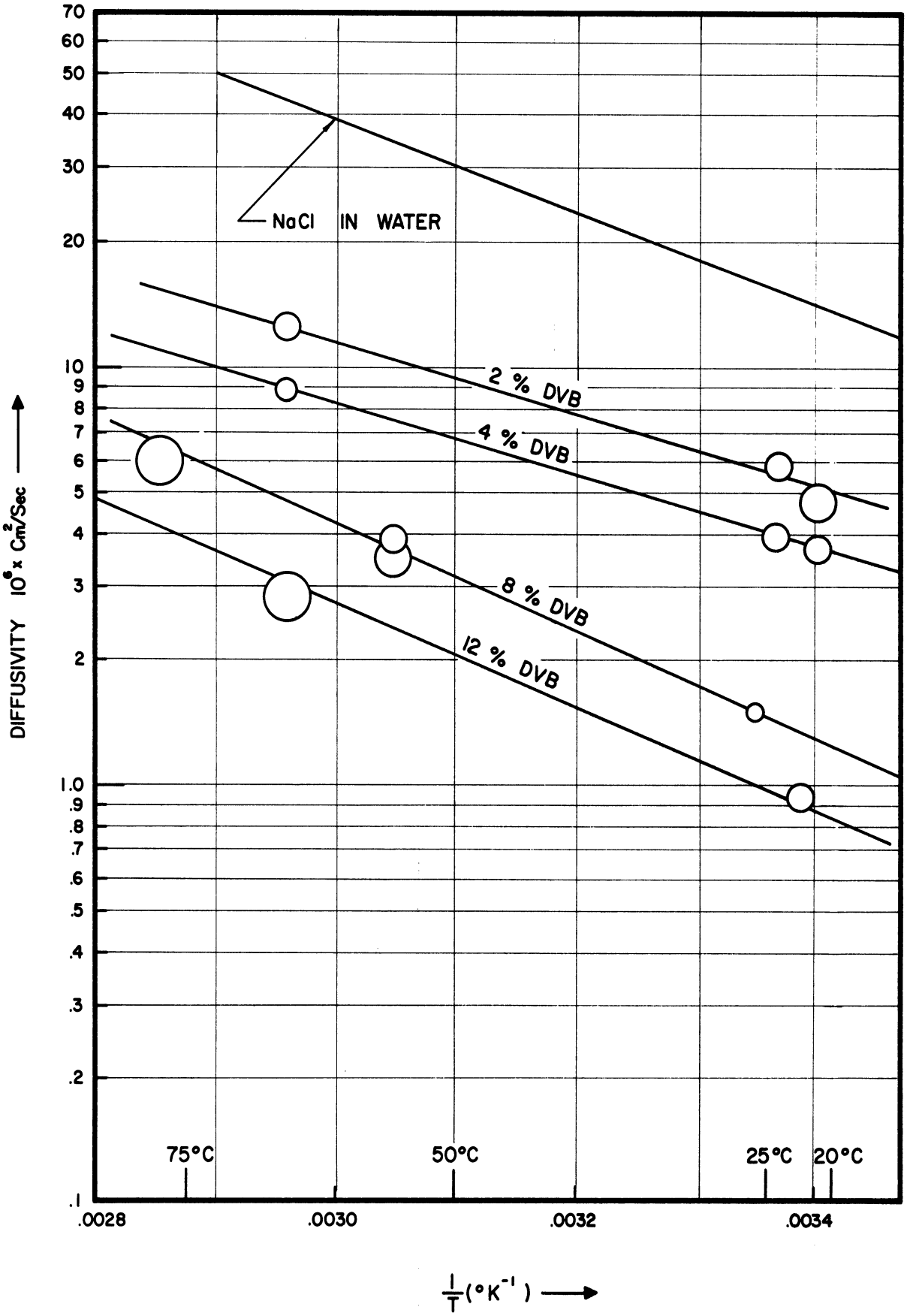

Figure 4. Diffusivity of Sodium Chloride in Dowex 50. (Equilibrating Soln. 30% Glycerol, 5% Nacl by wt)

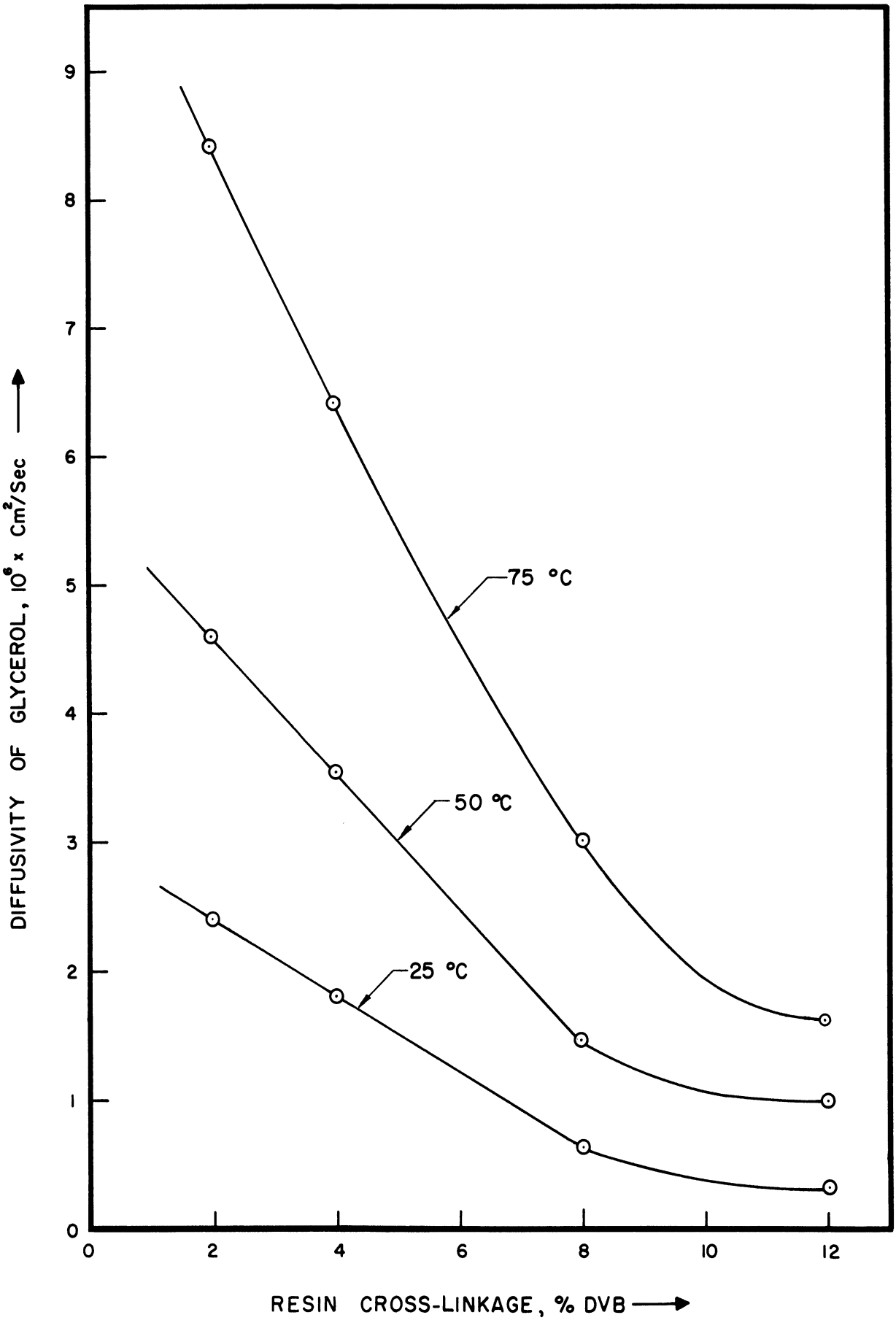

Figure 5. Diffusivity of Glycerol in Dowex 50 (Na-form) as a Function of the Cross-linkage of the Resin.

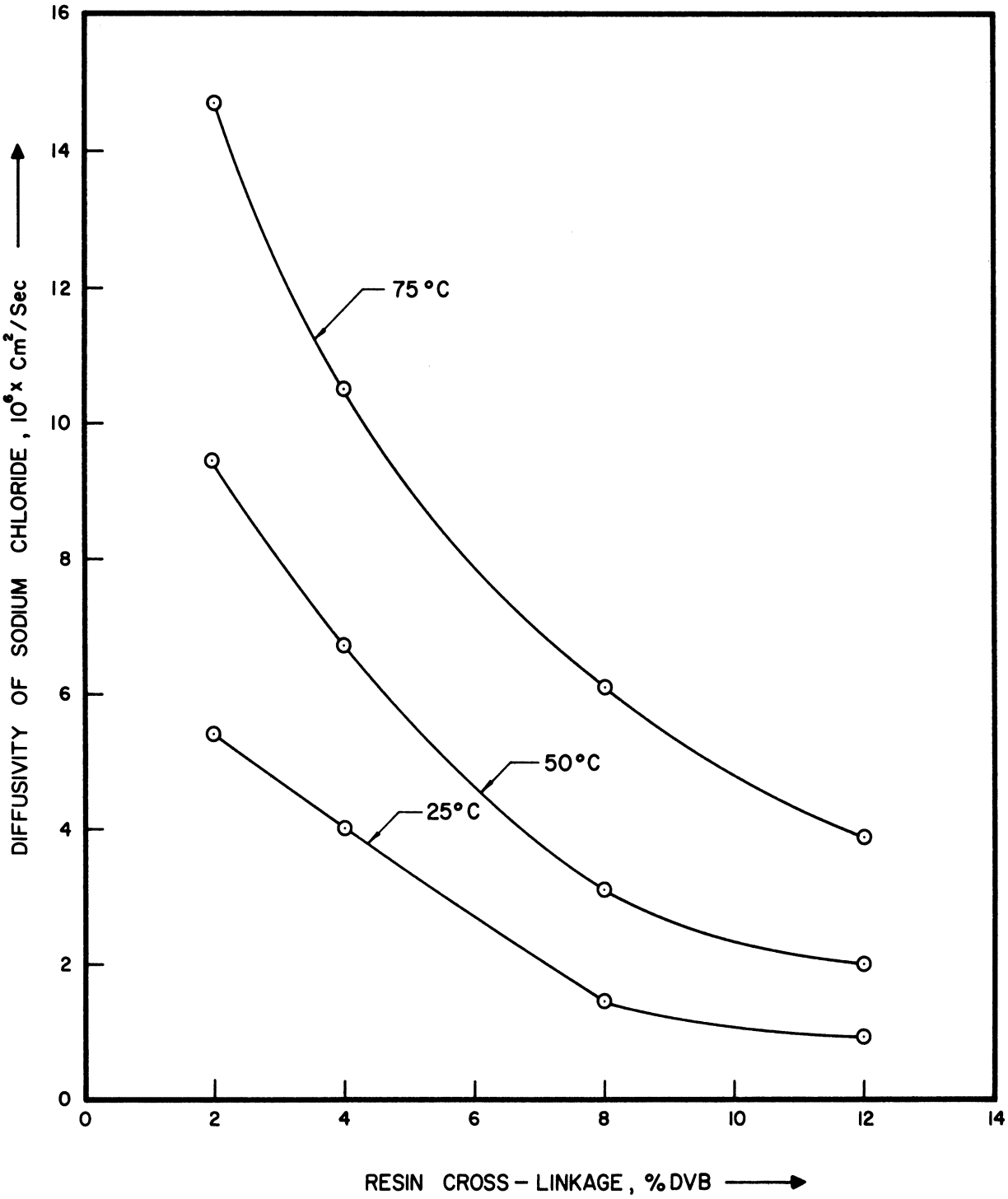

Figure 6. Diffusivity of NaCl in Dowex 50 (Na-form) as a Function of the Cross-linkage of the Resin.

TABLE II

DIFFUSIVITIES OF SODIUM CHLORIDE AND GLYCEROL IN DOWEX 50W X 8% DVB AT 25°C

	Diameter of Resin Particles mms.	Wt. of the Resin in Each Basket gms.	Suprfcl Velocity Eluting Water cms/sec	Conc. of Equlbm. Solution wt.% NaCl	Glycrl	Diffusivity in the Resin $\frac{cm.}{sec.} \times 10^6$ NaCl	Glycerol
Diffusivity of Sodium Chloride as a function of concentrations	0.6083	1.000	150	2	0	1.25±0.2	
	0.6083	1.000	150	5	0	1.5 ±0.2	
	0.6083	1.000	150	10	0	1.4 ±0.2	
	0.6083	1.000	150	10	10	1.45±0.2	
	0.6083	1.000	150	15	5	1.3 ±0.2	
Diffusivity of glycerol as a Function of Concentrations	0.6083	1.000	150	2	2		0.57±0.05
	0.6083	1.000	150	0	10		0.50±0.05
	0.6083	1.000	150	2	25		0.54±0.05
	0.6083	1.000	150	10	10		0.57±0.05
	0.6083	1.000	150	15	5		0.50±0.05
Diffusivities as a Function of Particle Size	0.6083	1.000	150	10	10	1.45±0.2	0.57±0.05
	0.450	1.000	150	10	10	1.45±0.2	
	0.450	1.000	150	10	10	1.4 ±0.2	0.55±0.07
Diffusivities as a Function of Flow Rates	0.6083	1.000	150	10	10	1.45±0.2	0.57±0.05
	0.6083	1.000	30	10	10	1.4 ±0.2	0.55±0.05
Diffusivities as a Function of the Weight of the Resin Sample	0.6083	1.000	150	10	10	1.45±0.2	0.57±0.05
	0.6083	0.500	150	10	10	1.4 ±0.2	0.55±0.05
	0.6083	2.000	150	10	10	1.4 ±0.2	0.53±0.05

Diffusivities of sodium chloride and glycerol in Dowex 50 are between 2 and 30% of the corresponding values of the diffusivities in water at the same temperature. For the temperature range 20 to 80°C for both sodium chloride and glycerol, the ratio of their diffusivities in Dowex 50 to those in water lies within the band shown in Figure 7.

Figures 8 and 9 shows the equilibrium data obtained in this study. The limited range of concentrations covered was chosen from the range of concentrations encountered in industrial separations of glycerol and sodium chloride. The ordinates in Figures 8 and 9 are milligrams of glycerol and sodium chloride in one gram of bone dry resin, since these values are obtained directly from the data for each run and they are independent of the swelling and shrinking of the resin and the volume changes accompanying the same.

The amounts of sodium chloride and glycerol absorbed by the resin at equilibrium increases with decreased divinyl benzene cross-linkage. Temperature produces, comparatively, a small effect on the equilibrium values. For higher percentages of divinyl benzene in the resin, the effect of temperature on the equilibrium absorption is smaller than that for lower percentages of divinyl benzene.

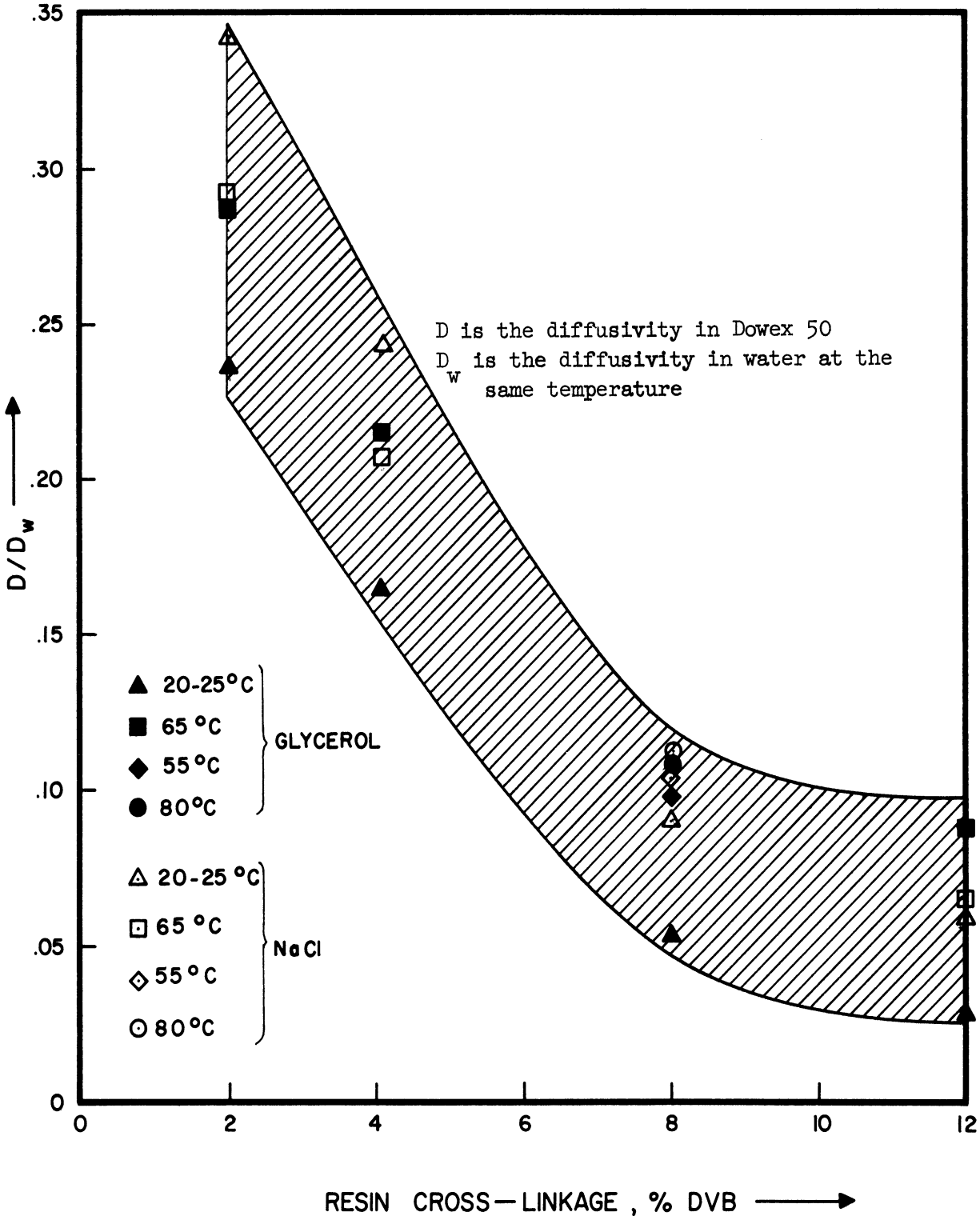

Figure 7. Ratio of the Diffusivities of Glycerol and NaCl in Dowex 50 to Their Diffusivities in Water as a Function of the Resin Cross-linkage.

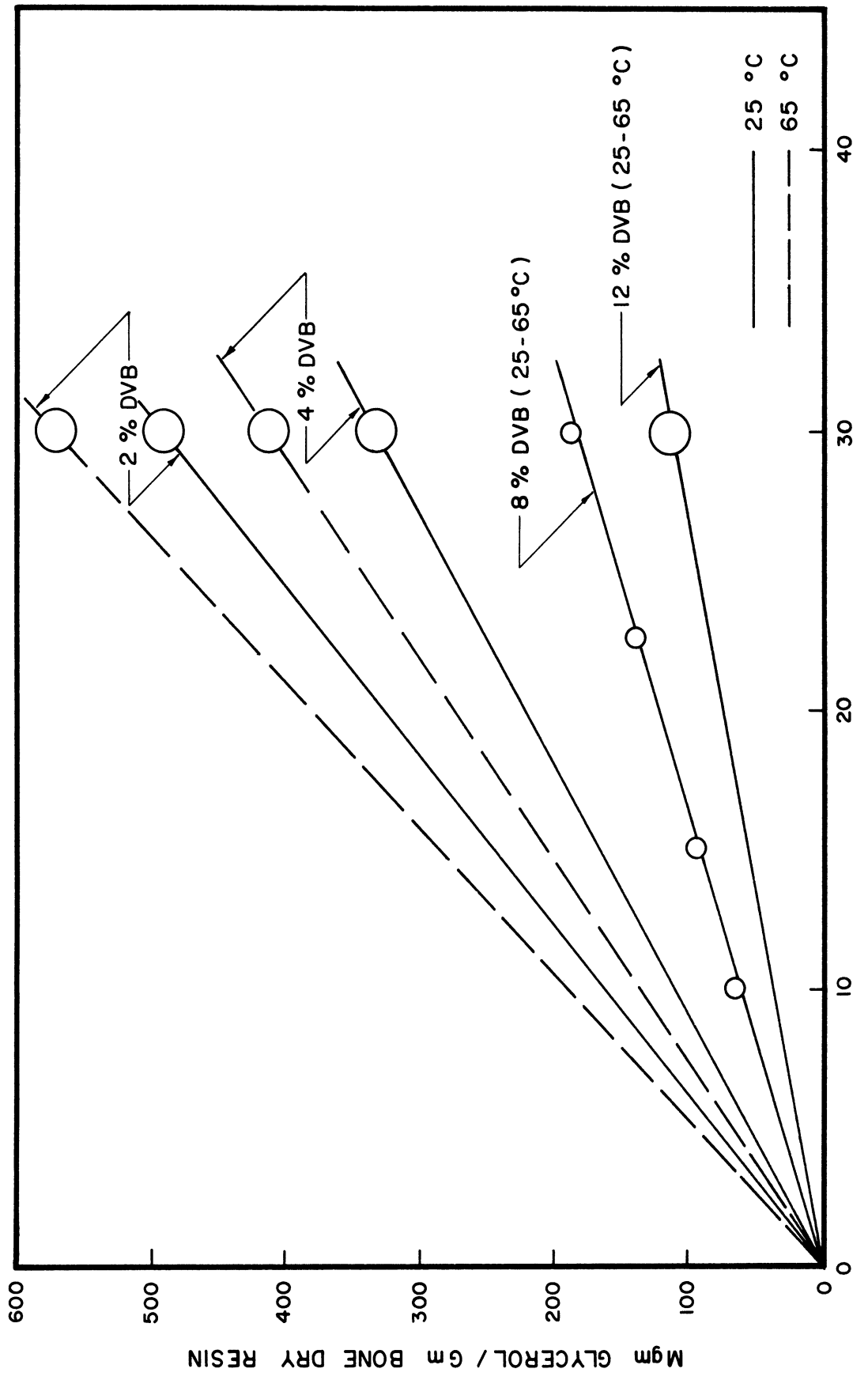

Figure 8. Equilibrium Data for Glycerol in Dowex 50 (Na-form).

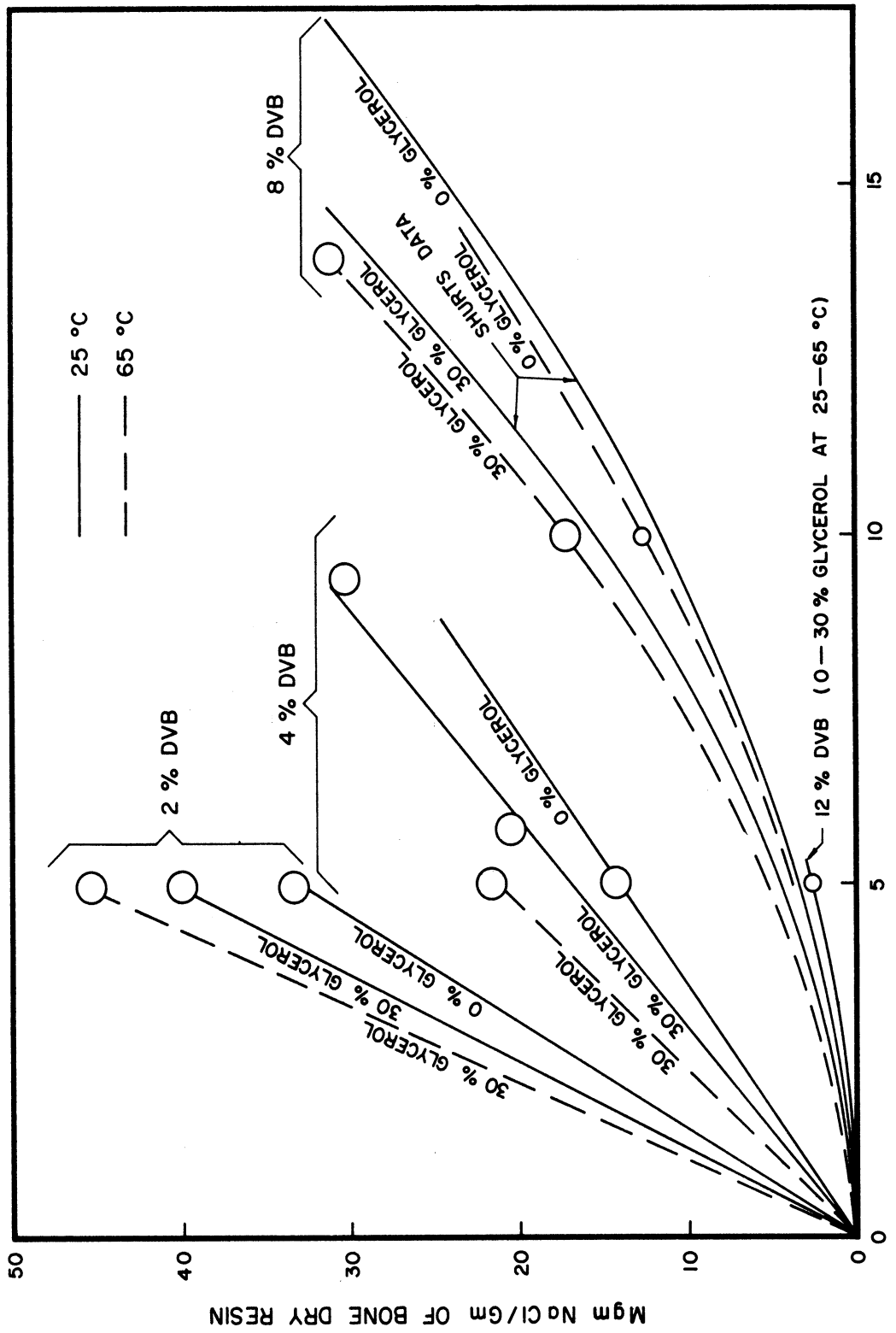

Figure 9. Equilibrium Data for NaCl in Dowex 50 (Na-form).

VI. DISCUSSION OF RESULTS

Application of the diffusion model for correlation of the data taken in this research involves several assumptions. They are stated below and their justifications are discussed.

Assumption: 1.

The amount of material transferred from the resin to the eluting water is so small compared to the flow rates of the eluting water that the concentrations of the components in the bulk of the eluting water is always negligibly small.

Justification: The total amount of sodium chloride eluted is of the order of 10 mgms. The total amount of glycerol eluted is of the order of 100 mgms. The time for elution is generally between 5 seconds and 2 minutes. The flow rate of eluting distilled water is about 16 litres per minute. This means that the concentrations of the solutes in the bulk of the distilled water would be of the order of 5 p pm for sodium chloride and 50 p pm for glycerol.

More than 99% of the equilibrating solution in the interstices between the particles is displaced in less than a second. This was established by performing the experiments with baskets containing glass beads instead of resin particles.

Assumption: 2.

The resin particles are perfectly spherical and completely uniform in size. All the particles are subject to identical external conditions at the surface. There is complete radial symmetry within the resin particles.

Justifications: The resin was wet screened and only the particles caught between the screen wires of a particular mesh screen were used. Broken and non-spherical particles were rejected by rolling. The resin treatment is fully described in Section 2 of Detailed Discussions.

Identical external conditions at the surface of the particles are insured by high flow rates of the eluting water. Runs using baskets containing 0.5 grams, 1 gram and 2 grams of the resin gave the same results as can be seen from Table II. Radically different shapes** of the baskets also gave the same results.

Assumption: 3.

Before elution with distilled water the resin particles have no concentration gradients within them and they are at equilibrium with a known saturating solution.

Justification: The diffusivities obtained from the data suggest that 2 to 10 minutes are enough for 99% of the equilibration process. Actually the resin was in contact with the equilibrating solution for 12 hours before each run.

Assumption: 4.

The resistance to mass transfer in the liquid phase, i.e., from the surface of the resin spheres to the bulk of the eluting distilled water is negligibly small and the concentrations of sodium chloride and glycerol in the liquid right at the surface of the

---

** See Figures 1, 13.

resin particles is zero, the same as that in the bulk of the eluting water.

Justification: Mass transfer coefficients in the liquid phase calculated from the correlations in the literature for flow through a packed bed of spheres give very high values for the flow rates involved. Also, in this research, it was found that reducing the flow rate of the eluting water to one fifth of its value gave the same results. (See Table II.)

Assumption: 5.

At the interface of the resin and the liquid a thermodynamic equilibrium always exists, and consequently the concentrations of the solutes in the resin phase at the surface of the resin are zero.

Justification: No justification other than the fit of the data to the mathematical model based on all the assumptions listed here.

Assumption: 6.

For the transfer of sodium chloride and glycerol in the wet resin phase, Fick's law of diffusion is applicable, using concentration gradients as the driving force; and the diffusivities (or the diffusion coefficients) of the components is independent of the concentrations of the components.

Justification: The experimental results in Table II show that for the resin with 8% divinyl benzene the diffusivity is not a function of the concentrations in the range of 0 to 15% sodium

chloride and 0 to 25% glycerol. Unfortunately, this is not the most severe set of conditions and for the resins with a smaller degree of cross linkage, which swell and shrink more with changes in concentrations, the diffusivities may be functions of the concentrations.

Table II shows that the same diffusivities are obtained from the data on the different sizes of the resin particles. This shows that the diffusion model is applicable.

Assumption: 7.

The diameter of the resin particles remains constant.

Justification: For the resin with 8% divinyl benzene, the change in diameter with the changes in concentrations in the range of 0 to 15% sodium chloride and 0 to 25% glycerol is less than 4%(S2). For the resins with a smaller degree of cross linkage, there would be greater changes in diameters with changes in concentrations.

When a resin shrinks, the diffusivity is likely to be reduced. Also the path for diffusion gets smaller. In a sense these two effects are compensating.

In all calculations in this thesis, the value of the diameter of the resin particles in distilled water was used.

For one cross linkage of the resin, 8% divinyl benzene, and one temperature, 25°C, it is possible to compare the equilibrium amounts of sodium chloride and glycerol obtained in this study with the values reported by Shurts and White (S2,S3) and Whitcombe, Banchero and White (W2).

Table III shows that there is a fairly good agreement. This is interesting since the data of the other researchers were taken under static conditions of equilibrium, whereas the values in this thesis have been obtained from fitting unsteady state rate data.

The mechanism for mass transfer in the resin phase, postulated in this thesis, is diffusion. The diffusion model explains a very wide range of data adequately. For most runs, the 15 points of data covered a complete range in which 10% to 95% of the total amount of the solutes present in the resin was eluted by distilled water at different times.

The diffusion model explains the mass transfer of both an electrolyte, sodium chloride, and a non-electrolyte, glycerol. Its applicability is further validated by the agreement of the values of the equilibrium amounts with those in the literature and by the fact that the same values of diffusivities are obtained from the runs with different sizes of the resin particles (see Table II).

The diffusivities of the solutes in the resin are small--of the order of 10^{-6} cm^2/sec. They are a fraction of the corresponding diffusivities in water. This suggests that even for very low flow rates, the major resistance to mass transfer between the aqueous and the resin phase would be in the solid phase, and the mass transfer operation in most laboratory and commercial ion-exclusion columns would be controlled by the diffusion in the resin phase.

Because of low values of diffusivities, many ion-exchange reactions may also be expected to be controlled by the diffusion of the ions in and out of the resin particles. Determination of diffusivities in such cases would be very useful in evaluating ion-exchange processes.

TABLE III

EQUILIBRIUM ABSORPTION OF SODIUM CHLORIDE AND GLYCEROL
IN DOWEX 50 WITH 8% DVB AT 25 °C

Concentrations of the Solutes in Aqueous Phase		Milligram of Solute Per Gram of Air Dry Resin				
		Glycerol		Sodium Chloride		
wt.% Glycerol	wt.% NaCl	From Curve Fitting of Data in This Study	Calculated from Shurts Correlation (S1,S2)	From Curve Fitting of Data in This Study	Calculated From Shurts Correlation (S1,S2)	Reported by Whitcombe (W2)
26.6	1.859	130	120			
4.85	15.0	25	24.7	22.5	24.4	28.1
1.91	2.3	7.5	7.5	1.0	0.86	9.9
9.66	9.94	45	45.7	11.	10.0	11.5
9.54	0	38	37.4			
0	2.02			.8	.716	.82
0	4.95			3.7	2.9	3.32
0	10.01			11	9.25	11.6

The experimental technique used in this study can be used directly for determining diffusivities of the ions if it is assumed that the ion exchange reactions are very rapid and the rates are controlled by the diffusion of the materials in and out of the resin particles. A possible experimental method for such a study and the applicable equations, etc., are discussed in Section 12 of Detailed Discussions.

VII. CONCLUSIONS
(For Part I)

1. The mass transfer of NaCl and glycerol within the solid phase Dowex 50 (immersed in water) can be described by a mechanism assuming Fick's Law of Diffusion where the rate of transfer of materials is proportional to the concentration gradients and the proportionality constant is the diffusivity.

2. For the resin with 8% of the cross-linking divinyl benzene and at room temperature, the diffusivities of NaCl and glycerol are independent of the concentrations of these materials.

3. In the temperature range of 25 to 80°C, the diffusivities of NaCl and glycerol are reduced as the cross-linkage of the resin (measured as percent divinyl benzene) is increased.

4. For the resins with 2 to 12% cross-linking divinyl benzene, the diffusivities of NaCl and glycerol are increased with increase in temperature. For a given cross-linkage, a plot of logarithm of diffusivity versus the reciprocal of absolute temperature gives a straight line.

5. The diffusivities of NaCl and glycerol in the resin phase are a fraction of their diffusivities in water at the same temperature. The value of this fraction decreases with the increase in the cross-linkage of the resin. For the temperature range of 25 to 80°C and for both solutes, the value of this fraction is between 0.2 and 0.35 for 2% divinyl benzene and it is between 0.025 and 0.1 for 12% divinyl benzene.

6. In view of conclusion 5, it is highly probable that in most ion exclusion and ion exchange column operations, the total resistance to mass transfer is controlled by the resistance in the solid phase.

7. The amounts of NaCl and glycerol absorbed by the resin at equilibrium decrease with increase in cross-linkage of the resin.

8. The amounts of NaCl and glycerol absorbed by the resin at equilibrium increase with increase in temperature, the effect being greater for the resin with a small degree of cross linkage and almost negligible for the resin with 12% divinyl benzene.

9. The method of superpositioning a master-plot on the data provides an adequate method of making a two constant fit to data to obtain the values of diffusivity and the amount absorbed at equilibrium.

VIII. DETAILED DISCUSSIONS

1. Structure and Properties of the Resin

The resin used in this study was Dowex 50W which is the trade name of a synthetic cation exchange resin made by Dow Chemical Company. Chemically, it is a sulfonated polystyrene resin, cross linked with divinyl benzene. A schematic representation of the chemical structure of the Na-form of Dowex 50W would be[52]:

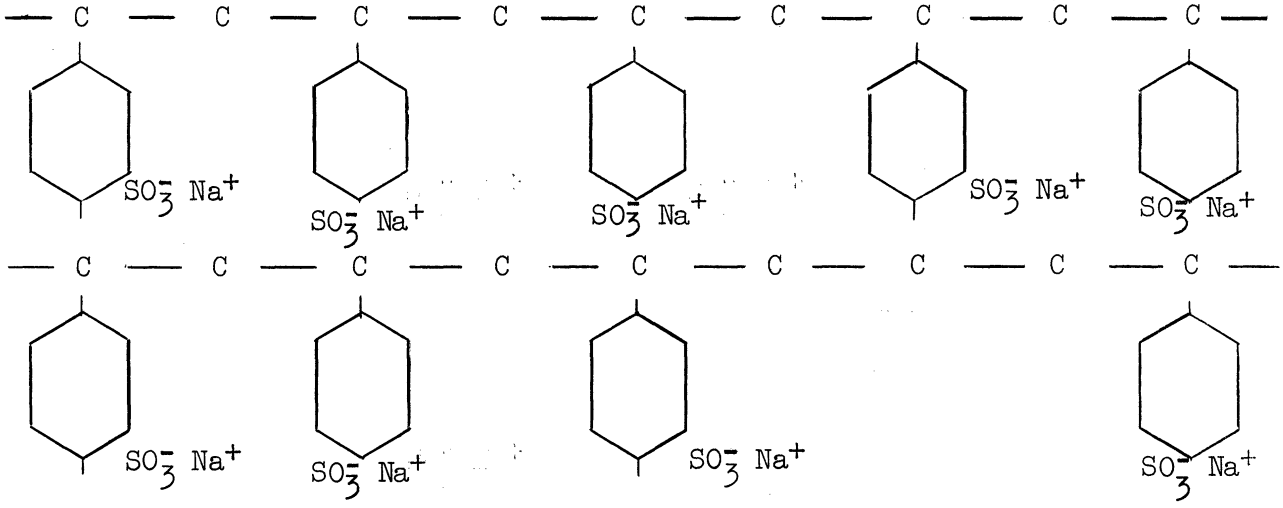

The degree of crosslinking of the polystyrene chains is controlled by the amount of divinyl benzene used in the manufacture of the resin, and the resins with different cross-linkage were supplied by the manufacturer. In this study, resin with two, four, eight and twelve percent divinyl benzene was used. The degree of cross linking is often indicated by the manufacturer by the symbol "X"; thus Dowex 50W X 8 or Dowex 50 X 8% DVB indicates 8% divinyl benzene.

The sulfonate groups SO_3H or SO_3Na groups are the active ion exchange groups and when the resin is used as a cation exchange resin it exchanges the Na or H ion from these active groups for other cations. Other cation or anion exchange resins have other active groups such as

NH_2, COOH, etc. Since in this study only sulfonated resin Dowex 50W was used, the following discussion shall be limited to this resin. For more details on different kinds of resins references (B1,K2) are suggested.

Industrially available Dowex 50 is hard, tough and usually spherical. When immersed in water, or any other polar solvent, it swells, supposedly due to solvation of the ionic groups. The extent of the swelling is controlled by the amount of crosslinking in the resin network. Table IV gives the moisture contents and swelling of the resins used in this study. The swollen resin is a homogeneous phase distinct from external solution. It may be considered as a solution in which complete dissociation of the SO_3Na group has occurred and Na^+ ions are free to diffuse throughout the resin phase so long as electroneutrality is maintained.

It should be emphasized that the resin particle is not a two phase porous solid with rigid channels. Instead it is a concentrated solution of a high molecular weight polymer in water. When the resin is immersed in an aqueous solution of some neutral material (non polar, non ionizable), such as glycerol, a thermodynamic phase equilibrium is established between the resin phase and the aqueous phase, and the neutral material is distributed between the two phases. In the case of an ionizable material, a similar phase equilibrium is established between the resin phase and the external solution, in addition to which a chemical equilibrium between the exchangeable cations is established within the resin phase. If the cation of an ionic solution is the same as the form of a cation exchange resin, e.g., NaCl and Na form of Dowex 50, the chemical equilibrium is of no consideration.

TABLE IV

MOISTURE CONTENTS AND SWELLING CHARACTERISTICS OF DOWEX 50 (Na FORM) IN WATER

Cross Linkage % Divinyl Benzene	Moisture Content in Air at 25°C and 50% Relative Humidity	Ratio of the Diameter of Resin Particles Immersed in Water to That in Air at 25°C and 50% R.H.	Ratio of the Volume of the Resin Particle Immersed in Water to That in Air at 25°C and 50% R.H.	Moisture Content of Swollen Resin in Water
2	18%	1.58	4.0	81%
4	18%	1.35	2.5	67%
8	18%	1.18	1.65	53%
12	17%	1.11	1.4	45%

2. Screening and Treatment of the Resin Used

For this study it was desired that the resin be:

1. In the sodium form,
2. spherical in shape,
3. without internal fractures,
4. closely sized.

Batches of resin supplied by the Dow Chemical Company were soaked in water and examined with a microscope for internal fractures. Most batches of Dowex 50 show internal fractures. Few of the Dowex 50W have internal fractures.* Internal fractures are possibly related to the manufacturing process for the resin and it was found that for a given batch either almost all of the particles had internal fractures or almost none did. Batches of finer sized resin were generally freer of internal fractures than batches of larger size resins. The batches with internal fractures were rejected.

The resin was already supplied in sodium form. However, it was treated repeatedly with saturated solution of sodium chloride and then washed with distilled water until free of chloride ions. The washing was done to remove the sodium chloride absorbed by the resin.

Batches of 20-50 mesh and 50-100 mesh resins treated as above were screened wet. For any one size desired, the resin particles that

---

* Resin carrying the extra designation, Dowex 50W is a special grade resin which is sulfonated under conditions giving a particularly uniform product. This resin is also lighter in color then Dowex 50 due to less charring of the organic polymer base.

were caught between the wires of the screen were collected, rejecting both the particles that went through the screen as well as the particles that were retained on the top of the screen.

The carefully sized resin particles were dried in a constant temperature, constant humidity room at 25°C and 50% relative humidity. The dry particles were rolled on a smooth stainless steel plate that was slightly inclined. The spherical particles rolled smoothly and the broken particles stayed on the plate and were rejected.

After rolling these particles were again treated with saturated NaCl solution, washed free of chloride and dried in a constant temperature, constant humidity room. This treatment was to take care of some ion exchange that usually took place between the material of the screen wire and the Na-form of the resin during wet screening.

The diameter of the treated particles was measured under a microscope with the help of a calibrated eye piece. For a batch of any one crosslinkage and particle size desired, about 50-100 particles were measured and a mean diameter was calculated. Table V gives the sizes of the resin particles used in this study.

3. Methods of Analyzing NaCl and Glycerol

The solutions used for equilibrating the resin contained from 1.0 to 30 percent by weight of the NaCl and glycerol in water. The solution obtained after extracting the solutes from the resin phase contained a few parts per million of NaCl and glycerol.

Because of the low concentrations involved in most of the solutions analyzed, methods that depend on physical properties such as

TABLE V

SCREENING AND SIZE OF RESIN PARTICLES USED

Cross Linkage of Dowes 50 Na-Form Resin	Tyler Screen Used		Diameter of the Particles in Distilled Water			Percent of Particles Broken or Non-Spherical
	Mesh Size	Screen Opening	Average	Range for 95% of Particles	Sample Size	
8% DVB	28	0.589 mms	0.6083 mms	± 0.0315 mms	129 particles	2 - 3%
8% DVB	35	0.417 mms	0.45 mms	± 0.03 mms	47 particles	0%
2% DVB	16	0.991 mms	0.965 mms	± 0.04 mms	50 particles	2%
4% DVB	24	0.701 mms	0.691 mms	± 0.03 mms	50 particles	0%
12% DVB	24	0.701 mms	0.706 mms	± 0.03 mms	50 particles	2%

density and refractive index were eliminated. The methods selected for NaCl analysis are independent of the glycerol content of the solution and that used for glycerol analysis is independent of the sodium chloride content.

A. Sodium Chloride Analysis

Sodium chloride content of the solutions used for equilibrating the resin were determined by titrating for chloride ions according to Fajan's method (W5). Tenth normal silver nitrate is used as the standard with dichloroflourescein as the indicator which gives a very sharp end point under artificial light. Shurts (S2) has shown that the presence of glycerol does not interfere at all with Fajan's titration. The expected error is about one part in a thousand.

Sodium chloride content of the very dilute solutions, obtained upon extracting the solutes from the resin phase, was determined by a Flame Photometer. A Beckman instrument, "model B", was used. Since the sodium content in the solution to be analysed was only a few parts per million, much care was required to avoid sodium contamination.* Fortunately, there is no source of potassium ions which is the most interfering contamination in this method of analysis.

Twenty standard solutions of NaCl covering a range of one to 500 parts per million were prepared by diluting a tenth normal solution. Their emmission at the wavelength of 5890 Å.u. was measured and this calibration curve is shown in Figure 10. The curve was reproducible over a

* The distilled water used for dilution and extraction of solutes from the resin was passed through an ion exchange deionizer to remove traces of Na and other ions. Standard solutions were stored in polyethylene bottles.

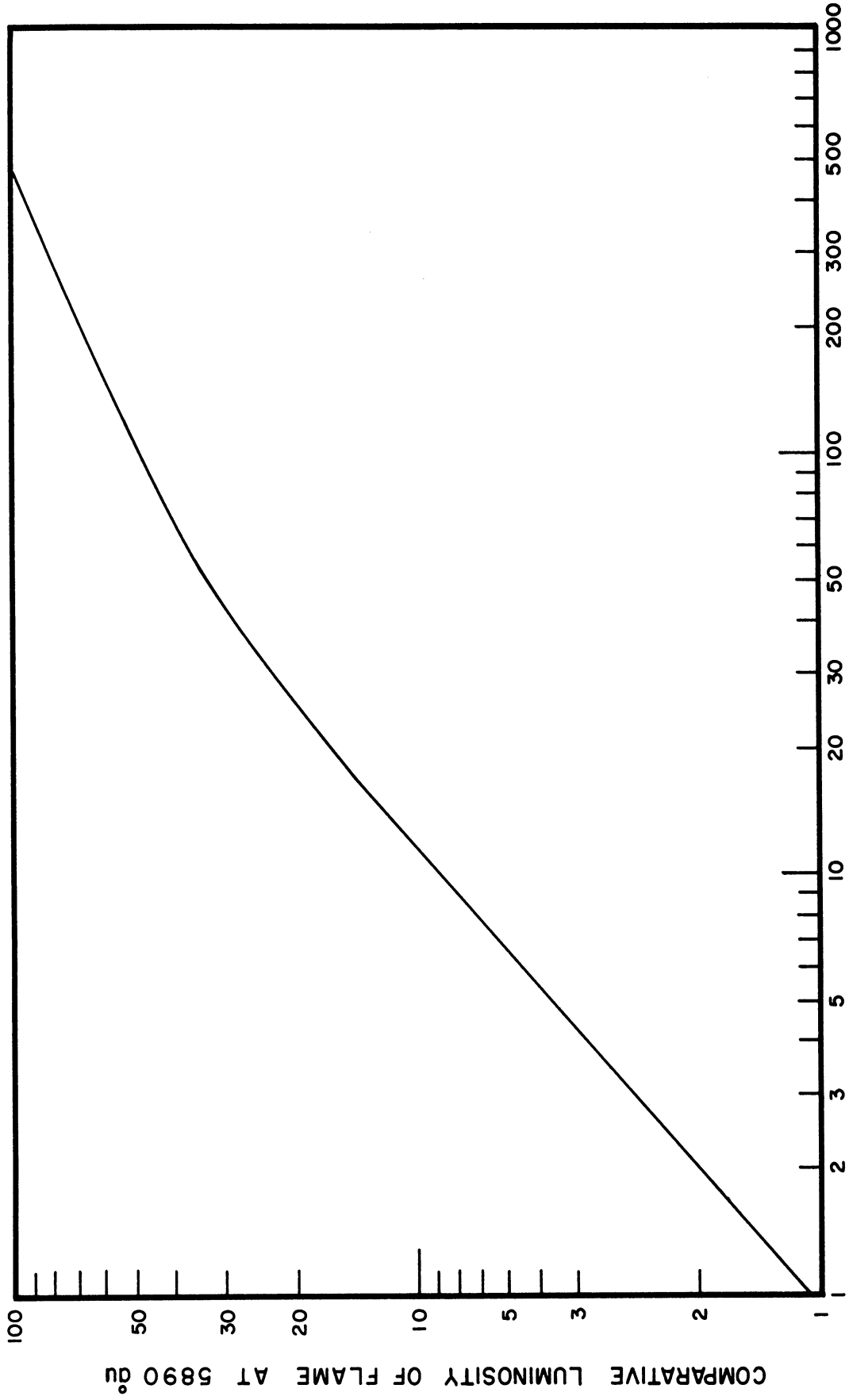

Figure 10. Calibration Curve for Analyzing NaCl Solutions with Flame Spectrophotometer.

period of several months. A calibration curve was made for every time that an analysis was performed. The expected error of analysis is about one part in 50. For the data from two runs, the concentrations of Na^+ determined by flame photometer were checked against the concentration of Cl^- determined by nephlometric method. The agreement was very good.

B. Glycerol Analysis

Glycerol was analysed by oxidizing it with periodic acid and then determining the excess periodate (S5,J1). The following reaction takes place quantitatively and smoothly in dilute aqueous solution at room temperature.

$$CH_2OH \cdot CHOH \cdot CH_2OH + 2HIO_4 \rightarrow 2CH_2O + HCOOH + 2HIO_3 + H_2O$$

Glycerol Periodic Acid

The excess periodate can be determined in the presence of iodate by the reaction:

$$IO_4^- + 2I^- + 2H^+ \rightarrow IO_3^- + H_2O + I_2$$

This reaction must be carried out in a solution with pH $\geq$ 5, otherwise iodate will oxidize iodide. This is accomplished by buffering the solution with an excess of sodium by carbonate. The iodine released is determined by adding a measured amount of arsenite and then titrating the excess arsenite with standard iodine solution using starch as an indicator.

The following detailed procedure (N3) was used:

Two mls. of normal sulfuric acid was pipetted into a 125 ml. Erlenmeyer flask and exactly one ml. of 0.1 molar periodic acid was added. The sample containing up to 3.5 mgm. of glycerol was then added and

enough water to make a volume of approximately 10 ml. The contents of the flask were then mixed and allowed to stand for one hour at room temperature (it may stand longer if more convenient). Approximately 5 ml. of 7% sodium bicarbonate solution was then added and, after thorough mixing, exactly two ml. of 0.11 normal sodium arsenite solution was added. (Sodium arsenite solution is prepared by dissolving sodium hydroxide pellets and arsenous oxide, As_2O_3, in water.) Two drops of 50% Potassium Iodide were mixed in and the flask was allowed to stand 10 minutes or more at room temperature. Four drops of the starch indicator were added and the solution was titrated with 0.025 Normal Iodine solution to a definite blue color using a microburette. A blank was run in parallel.

Titre of the sample minus titre of the blank is equal to the titre equivalent to periodic acid reduced. One milli-equivalent of periodic acid is reduced by 23 mgms. of glycerol.

As mentioned above, a sample containing up to 3.5 mgm of glycerol may be used. The solutions obtained on extracting the solutes from the resin contained one to 100 mgms. of glycerol in 100 ccs. Generally, aliquots containing two to three mgms. of glycerol were used for the analysis. Samples of the solutions used for equilibrating the resin were diluted and glycerol content determined again by the above method. The error in the analysis was about one part in 50.

4. Details of the Experimental Equipment Used

A. Equilibrating Tank

Figure 11 shows the tank in which the resin was saturated with equilibrating solution. The tank was a 12 inch diameter by 12 inch bell

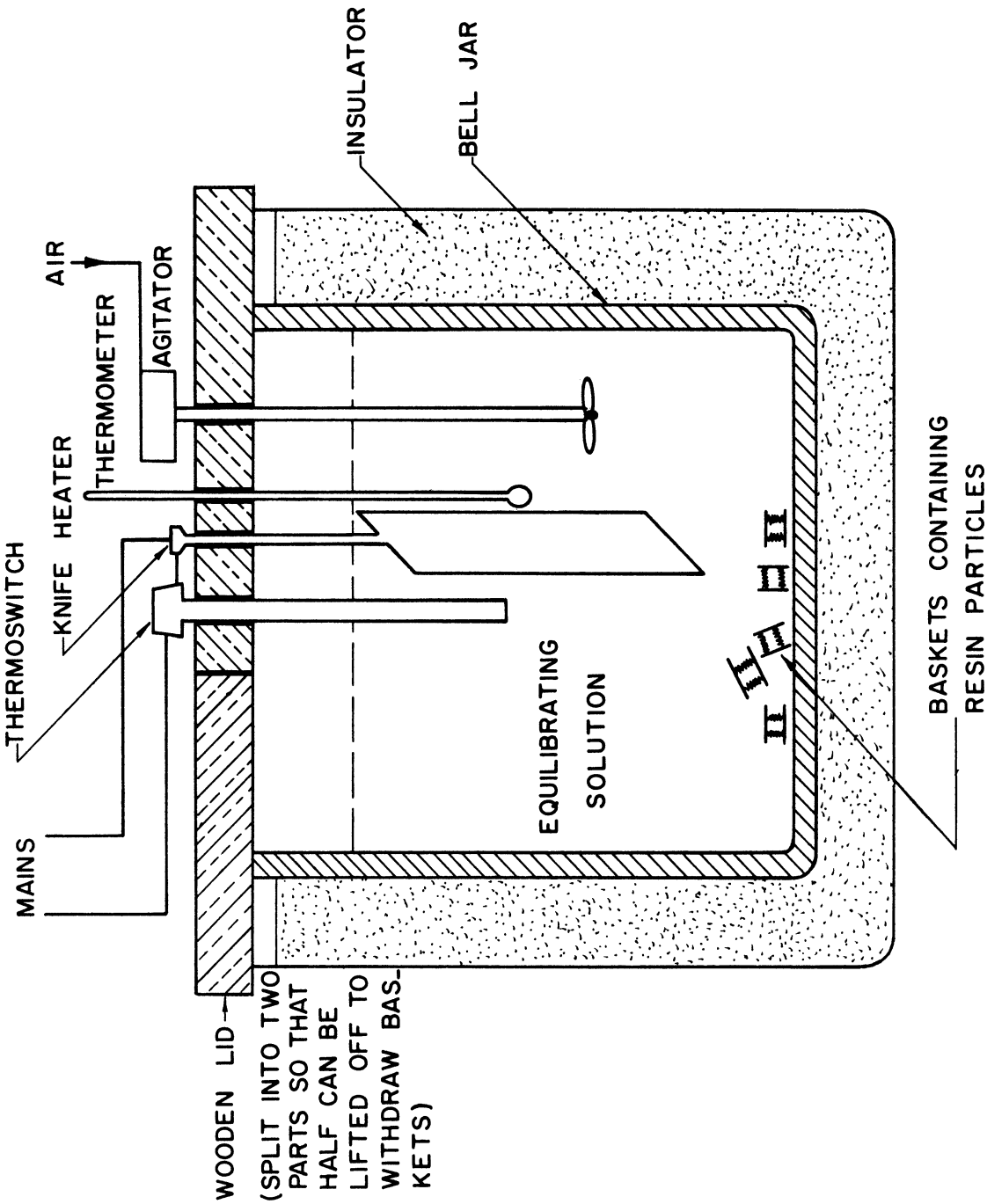

Figure 11. Sketch of the Tank Used for Equilibrating the Resin.

jar. It was usually two-thirds filled with the solution. It was insulated against heat loss. A Fenwell thermoswitch controlled the temperature to within 0.2°C. A 500 watt knife heater was used. A small air driven glass stirrer was used for agitation.

B. Resin Baskets

Figure 1 shows the shape of the resin baskets that were made. They were about 0.5 inches in diameter. The overall length of the basket was about one inch and the length of the resin chamber was 1/4 inch to 1/2 inch. When wet, the swollen resin occupied all this space. For each resin crosslinkage and particle size studied, there were 15 identical baskets, containing 1.000 gram of resin weighed at 25°C and 50% relative humidity. For resin with 8% divinyl benzene, additional sets of baskets containing one half and two grams of resin were also prepared.

Baskets were made by folding pieces of stainless steel screens as shown in Figure 12. After making a cylinder of the screen, one end was closed up, the weighed amount of resin was placed inside and then the other end closed up. The screen sizes were chosen such that the opening in the screen was smaller than the diameter of the dry resin.

Figure 13 shows the alternative shape of the resin baskets that was tried to ensure that the data did not depend on the shape of the baskets.

C. Equipment for the Elution of the Solutes from the Resin

Figure 2 shows a sketch of the equipment. Distilled water was held in a 50 gallon stainless steel tank. It had a small 1/8 horsepower

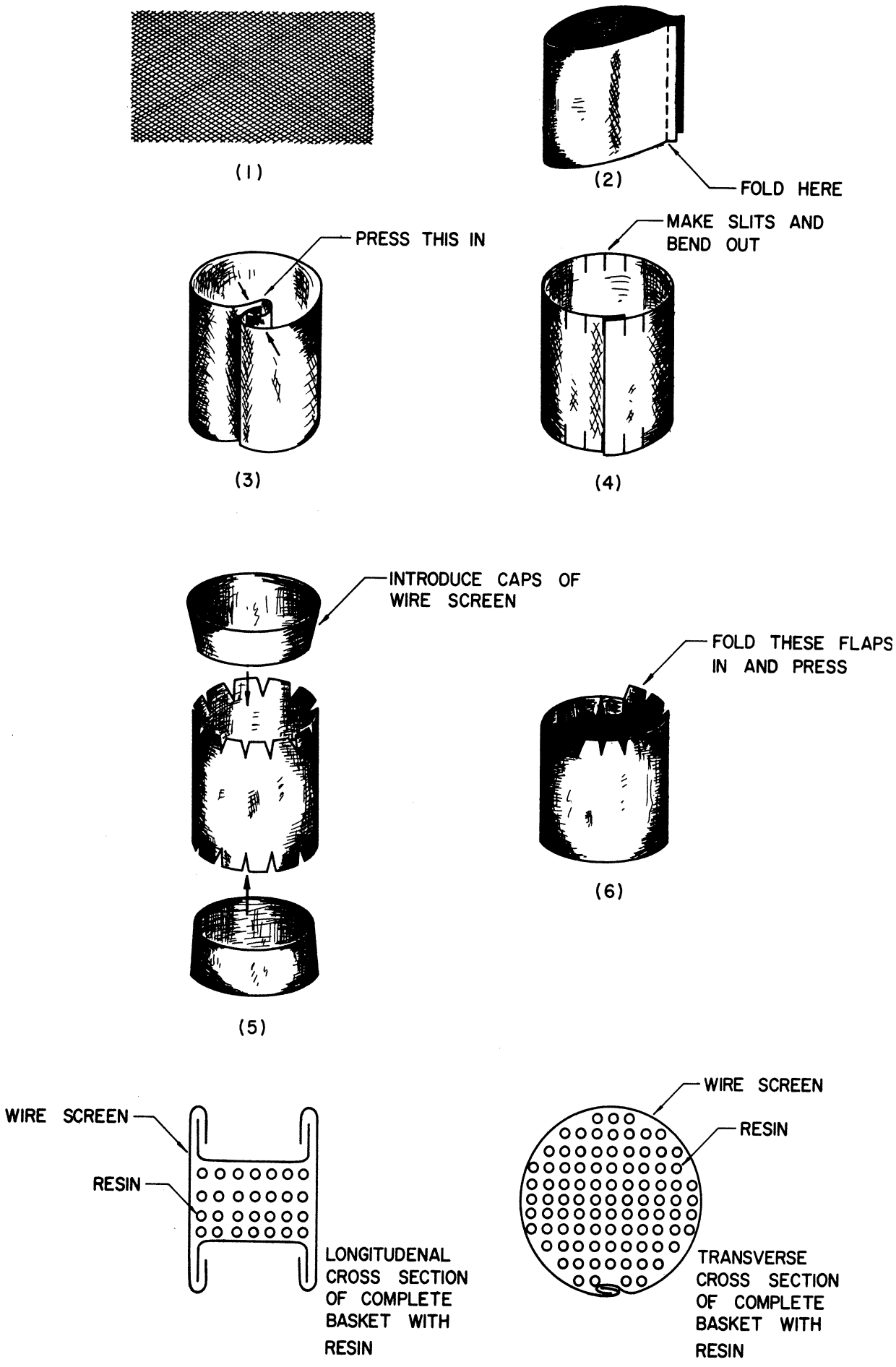

Figure 12. Method of Folding Screen to Make Baskets for Resin. Numbers (1) through (6) show the various steps in a sequence.

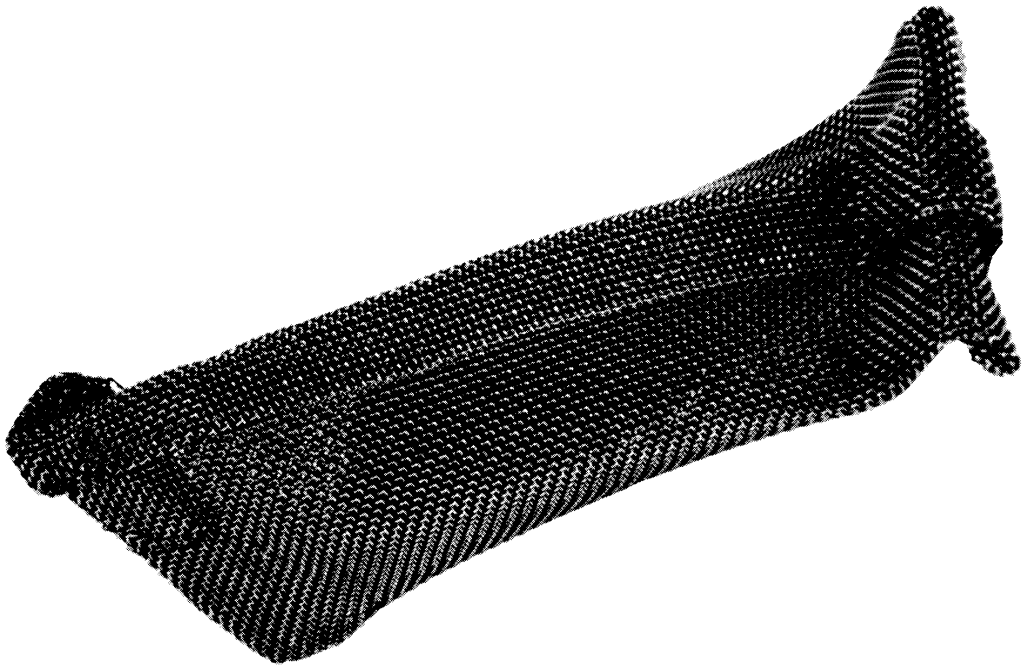

Figure 13. Alternate Shape of the Baskets Used.
(Size: 2 inches x 3/4 inches)

recirculation pump used for agitation. There were 6000 watt electric heaters. The temperature was controlled by a Fenwell thermoswitch mounted on a floating platform in the tank. The tank and the pipe line through the main pump were insulated. The temperature drop between the water in the tank and that flowing past the resin basket was less than one degree centrigrade for 80°C runs.

The pipe line between the distilled water tank and the resin basket was a 3/4 inch copper piping. The pump used for pumping water past the resin basket had a capacity of six gallons per minute. The time lag between turning on the foot switch and establishing of full flow of the pump was less than 0.1 second. The check valve prevented back flow and the trapping of air in the lines when the baskets were changed.

5. Experimental Procedure

The difficult experimental problem is that of getting information about the concentrations in the solid resin phase. Since the resin phase is dispersed into small particles, direct measurement within the resin phase are not generally possible*, and this information has to be obtained by making measurements in the liquid phase and using some kind of a material balance to deduce the values of the concentrations in the resin phase.

---

* The use of radioactive isotopes make some measurements of average values of the concentrations of these isotopes within the resin particles possible. See Section 10 of Detailed Discussion.

The amount of the materials present in the resin may be extracted by another solvent such as water and analysed. In such a procedure, a source of possibly large errors, is the difficulty of separating the resin particles from the adhering liquid. For example, the amounts of materials absorbed by the resin at equilibrium can not easily be obtained by immersing the resin in an equilibrating solution, draining off the equilibrating solution and extracting the materials absorbed by the resin. The adhering film of the equilibrium solution would be very difficult to separate and would cause large errors.

In the present study the technique of elution was chosen primarily to handle the problem mentioned above. The experimental conditions were such that, presumably, the film of the liquid adjacent to the resin particles has zero concentrations and, hence, is of no consequence in determining the amount of materials remaining in the resin particles by extracting the latter. On the other hand, for the case of absorption of materials by the resin, a similar experimental procedure of passing a saturating solution past a small amount of resin would not be practical since the adhering film of liquid would contain substantial amounts of materials.

The actual extracting of the materials remaining in the resin phase after a certain amount of elution time, was carried out in three stages. The resin basket was extracted with 30 ccs. of distilled water for 10 minutes for each stage of the extraction. The three extracts were collected together and the total volume was made up to 100 ccs. by adding distilled water. It was then analyzed for sodium chloride and glycerol. Further extraction of materials from the resin showed that more

than 99.7% of the total amount of the materials in the resin were generally extracted in the three stages.

Some experimental precautions were necessary to prevent air from being trapped in the interstices between the resin particles. During the elution run, if trapped air were present, it sometimes took several seconds for all of the air to be removed from the interstices, and very unreproducible data were obtained. The following procedure avoided trapping air. During equilibration, the baskets were immersed in the equilibrating solution gradually, allowing the air from the interstices to be displaced by the solution. Just before the elution run, each basket was inserted into a piece of rubber conduit under the equilibrating solution and the conduit containing the basket was attached to the system for pumping distilled water. The liquid seal was maintained and air pockets were prevented from developing upstream of the basket. A check valve very close to the down stream end of the pumping system prevented a back flow of water through the pump and the formation of air pockets in the lines when the pump was stopped.

6. Diffusion in a Sphere with Constant Boundary Conditions

A. The Differential Equation and Analytic Solutions

Applying Fick's Law of diffusion to the transient problem in spherical coordinates, a material balance (or the equation of continuity), gives the following partial differential equation (C1)

$$D\left(\frac{\partial^2 c}{\partial r^2} + \frac{2}{r}\frac{\partial c}{\partial r}\right) = \frac{\partial c}{\partial t}$$

where D is the diffusivity or the diffusion coefficient in cm^2/sec,

c is the concentration of the component in gm-mols/cc. Note that c is a function of r and t.

r is the distance from the centre of the sphere in cms.

t is the time in seconds.

The above equation assumes radial symmetry within the spheres and isotropic diffusion properties.

Additional boundary conditions are required to define a problem involving partial differential equations completely. For the problem under consideration in this thesis, initially the concentration in the sphere is uniform and has a value c_o gm-mols/cc. Then, during the diffusion run, at all times, the concentration is zero at the surface of the sphere. At the center of the sphere $\frac{\partial c}{\partial r} = 0$, because of radial symmetry.

These boundary conditions can be listed as:

$$c = c_o \quad \text{for all} \quad r \quad \text{at} \quad t = 0$$

$$c = 0 \quad \text{at} \quad r = R \quad \text{for all} \quad t$$

$$\frac{\partial c}{\partial r} = 0 \quad \text{at} \quad r = 0 \quad \text{for all} \quad t$$

Figure 14 shows the boundary conditions and the region of (r,t) plane in which the diffusion equation is to be solved.

Let the diffusivity, D, be a constant. This is an assumption and its validity has been considered in the discussion section.

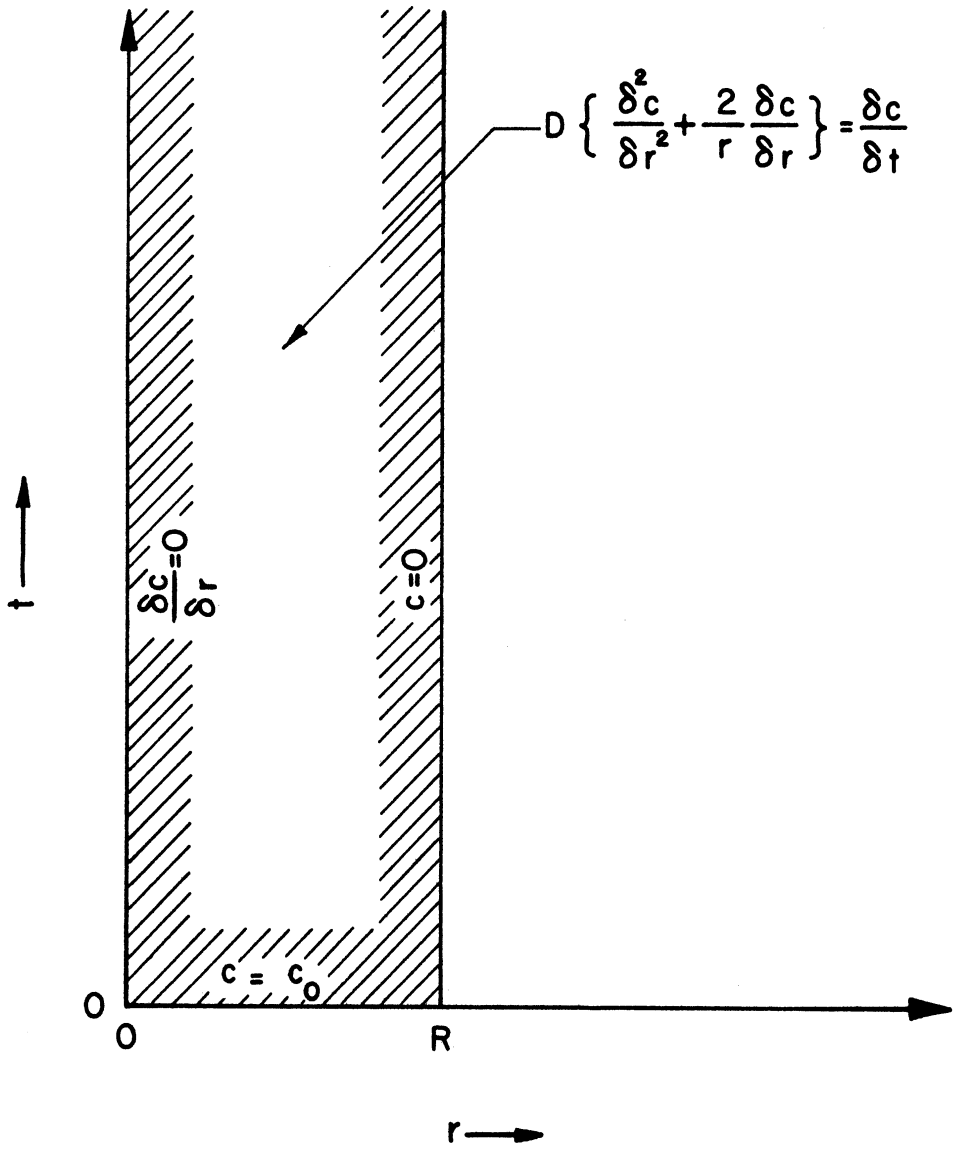

Figure 14. The Boundary Value Problem for Diffusion in a Sphere.

Analytic solutions to this problem have been obtained by two methods (C1): separation of variables method using Fourier Series (C3) and operational methods using Laplace Transforms (C4). The solutions obtained from these two methods are equivalent, though of different forms. The Laplace transform method gives the solution in the form of a series which is rapidly convergent for small values of time. The Fourier Series method gives a series that converges rapidly for large values of time.

The solution obtained by Laplace transforms is (C4):

$$c = c_o - \frac{Rc_o}{r} \sum_{n=0}^{\infty} \left\{ \operatorname{erfc}\left[\frac{2Rn + (R-r)}{2\sqrt{Dt}}\right] - \operatorname{erfc}\left[\frac{2Rn + (R+r)}{2\sqrt{Dt}}\right] \right\}$$

$$\text{where} \quad \operatorname{erfc}(\beta) = \frac{2}{\sqrt{\pi}} \int_{\beta}^{\infty} e^{-x^2} dx$$

The solution obtained by the Fourier series method is (C3):

$$c = -\frac{2Rc_o}{\pi r} \sum_{n=1}^{\infty} \frac{(-1)^n}{n} \sin\left(\frac{n\pi r}{R}\right) e^{-\frac{D\pi^2 n^2 t}{R^2}} \qquad (I)$$

If q is the total amount (gm-mols) of a component present in the sphere at any time t, then

$$q = \int_o^R (4\pi r^2) c \, dr$$

Using the Fourier series solution, Equation (I) for c, and interchanging the order of summation and integration we get,

$$q = -8Rc_o \sum_{n=1}^{\infty} \frac{(-1)^n}{n} e^{-\frac{D\pi^2 n^2 t}{R^2}} \int_o^R r \sin\left(\frac{n\pi r}{R}\right) dr \qquad (II)$$

Consider,

$$\int_o^R r \sin\left(\frac{n\pi r}{R}\right) dr$$

Here r is a variable of integration only. Let $x = \frac{n\pi r}{R}$.

Then,

$$\int_0^R r \sin\left(\frac{n\pi r}{R}\right) dr$$

$$= \int_0^{n\pi} \frac{R}{n\pi} x \,(\sin x)\, \frac{R\,dx}{n\pi}$$

$$= \frac{R^2}{n^2\pi^2} \int_0^{n\pi} x \cdot \sin x \cdot dx$$

$$= \frac{R^2}{n^2\pi^2} \left[- x \cos x + \sin x\right]_0^{n\pi} \qquad \text{(Integrating by parts)}$$

$$= \frac{R^2}{n^2\pi^2} \left[- n\pi\,(-1)^n\right]$$

$$= - \frac{R^2(-1)^n}{n\pi} \qquad \text{(III)}$$

Substituting Equation (III) in Equation (II), we get,

$$q = 8Rc_o \sum_{n=1}^{\infty} \frac{(-1)^n R^2 (-1)^n}{n^2\pi} e^{- \frac{D\pi^2 n^2 t}{R^2}}$$

$$= \frac{8R^3 c_o}{\pi} \sum_{n=1}^{\infty} \frac{1}{n^2} e^{-n^2\left(\frac{\pi^2 Dt}{R^2}\right)}$$

If q_o is the total amount of the component present in the sphere initially, then

$$q_o = (4/3)\pi R^3 c_o$$

and

$$\frac{q}{q_o} = \frac{6}{\pi^2} \sum_{n=1}^{\infty} \frac{1}{n^2} e^{-n^2\varphi} \qquad \text{(IV)}$$

where

$$\varphi = \frac{\pi^2 Dt}{R^2}$$

References (C5) and (I1) report this final solution, Equation (IV).

Equation (IV) shows that the fraction of the initial total amount present in the sphere is a function of only one variable φ. φ, in a sense, is the dimensionless time. As φ goes from zero to infinity, q/q_o varies from one to zero.

Equation (IV) is also applicable if q and q_o represent, not just the amounts in one sphere, but the total amounts present in any definite batch of uniform spherical particles.

B. Numerical Values of the Fraction Retained as a Function of Dimensionless Time

The series in Equation (IV) converges very slowly for small values of φ. Values of φ corresponding to the q/q_o of 0.5-0.9, are 3.0 to 0.1. In this range we need more than 20 terms to get an accuracy of 0.001 in q/q_o.

Fortunately, the function given in Equation (IV) has been computed on a digital computer by Reichenberg (R1). Table VI gives the numerical values of q/q_o as a function of φ, taken from Reichenberg. For any φ in the table, the error in the values of q/q_o is less than 0.001.

Other less accurate numerical evaluations of the function given in Equation (IV) are also available in the literature. Tölke (T2) has tabulated many functions that arise from solutions of diffusion equations. His tabulations are good for two significant figures.

There is the following connection between the Theta-Functions and the function in Equation (IV).

TABLE VI

NUMERICAL VALUES OF THE SOLUTION
OF THE DIFFUSION EQUATION IN A SPHERE
WITH CONSTANT BOUNDARY CONDITIONS (R1)

$$\frac{q}{q_o} = \frac{6}{\pi^2} \sum_{n=1}^{\infty} \frac{1}{n^2} e^{-\frac{n^2\pi^2 Dt}{R^2}}$$

$\frac{\pi^2 Dt}{R^2}$	$\frac{q}{q_o}$	$\frac{\pi^2 Dt}{R^2}$	$\frac{q}{q_o}$	$\frac{\pi^2 Dt}{R^2}$	$\frac{q}{q_o}$	$\frac{\pi^2 Dt}{R^2}$	$\frac{q}{q_o}$
0	1.00						
0.00036	0.98	0.1070	0.68	0.522	0.38	1.91	0.09
0.00141	0.96	0.1226	0.66	0.569	0.36	2.03	0.08
0.0032	0.94	0.1391	0.64	0.620	0.34	2.16	0.07
0.0057	0.92	0.1577	0.62	0.675	0.32	2.32	0.06
0.0091	0.90	0.177	0.60	0.734	0.30	2.50	0.05
0.0132	0.88	0.199	0.58	0.798	0.28	2.72	0.04
0.0183	0.86	0.222	0.56	0.868	0.26	3.01	0.03
0.0241	0.84	0.246	0.54	0.944	0.24	3.41	0.02
0.0309	0.82	0.273	0.52	1.028	0.22	4.11	0.01
0.0386	0.80	0.301	0.50	1.120	0.20	∞	0.00
0.0473	0.78	0.332	0.48	1.224	0.18		
0.0570	0.76	0.365	0.46	1.340	0.16		
0.0678	0.74	0.400	0.44	1.468	0.14		
0.0797	0.72	0.438	0.42	1.623	0.12		
0.0928	0.70	0.479	0.40	1.80	0.10		

From Equation (IV),

$$\frac{d}{d\varphi}\left(\frac{q}{q_o}\right) = -\frac{6}{\pi^2}\sum_{n=1}^{\infty} e^{-n^2\varphi}$$

and

$$-\frac{\pi^2}{6}\frac{d}{d\varphi}\left(\frac{q}{q_o}\right) = \sum_{n=1}^{\infty} e^{-n^2\varphi} = \sum_{n=1}^{\infty} \left(e^{-\varphi}\right)^{n^2} \qquad (V)$$

The function θ_3 is defined (W2) as,

$$\theta_3(z,x) = 1 + 2\sum_{n=1}^{\infty} x^{n^2} \cos 2nz$$

Putting $e^{-\varphi}$ for x, and 0 for z,

$$\theta_3(0,e^{-\varphi}) = 1 + 2\sum_{n=1}^{\infty} \left(e^{-\varphi}\right)^{n^2}$$

Hence, from Equation (V),

$$-\frac{\pi^2}{6}\frac{d}{d\varphi}\left(\frac{q}{q_o}\right) = \frac{1}{2}\left\{\theta_3(0,e^{-\varphi}) - 1\right\}$$

and

$$\frac{q}{q_o} = \frac{3}{\pi^2}\int_o^{\varphi}\left\{1 - \theta_3(0,e^{-\varphi})\right\} d\varphi$$

Jahnke and Emde (J2) have tabulated θ_3 function. This can be integrated either numerically or graphically to give q/q_o as a function of φ.

7. Two Constant-Curve Fitting of the Diffusion Data

If a batch of uniform spherical particles containing a total amount, q_o, gram molecules of a component, homogeneously distributed within the spheres, is suddenly subjected to zero concentrations at the

surface of the spheres, then the amount q gm.mols. of the component retained within the spheres at the time t seconds is given by:*

$$\frac{q}{q_o} = \frac{6}{\pi^2} \sum_{n=1}^{\infty} \frac{1}{n^2} e^{-n^2\left(\frac{\pi^2 Dt}{R^2}\right)} \qquad \text{(VI)}$$

where D is the diffusivity in the spheres, $cm^2/sec.$

and R is the radius of the spheres, cm.

Experimentally, in this study, the data obtained give values of q for different values of t. The values of R, the size of the particles, is known. Values of q_o, the initial amount, (which is the same as the equilibrium amount since the particles were intially equilibrated to obtain uniform concentration within the particles) and D, the diffusivity, are to be obtained by making a two constant fit to the data.

A. Direct Extrapolation

It is not possible to extrapolate the data of q versus t directly to zero time to obtain the value of q_o. From Equation (VI),

$$dq/dt = \frac{6Dq_o}{R^2} \sum_{n=1}^{\infty} e^{-\frac{n^2\pi^2 Dt}{R^2}}$$

and the slope of a plot of q versus t has an infinite slope at t = 0. Such a plot would start at q_o and be tangential to the q axis at the value of t = 0. Figure 15 shows such a plot. This makes direct extrapolation almost impossible.

B. Approximation for Small Values of Time

For very small values of time, Boyd et al. (B2) have approximated Equation (VI) by

$$q/q_o = 1 - 1.08\,\pi\sqrt{Dt}/R^2 \qquad \text{(VII)}$$

* For the derivation and discussion see the preceding section.

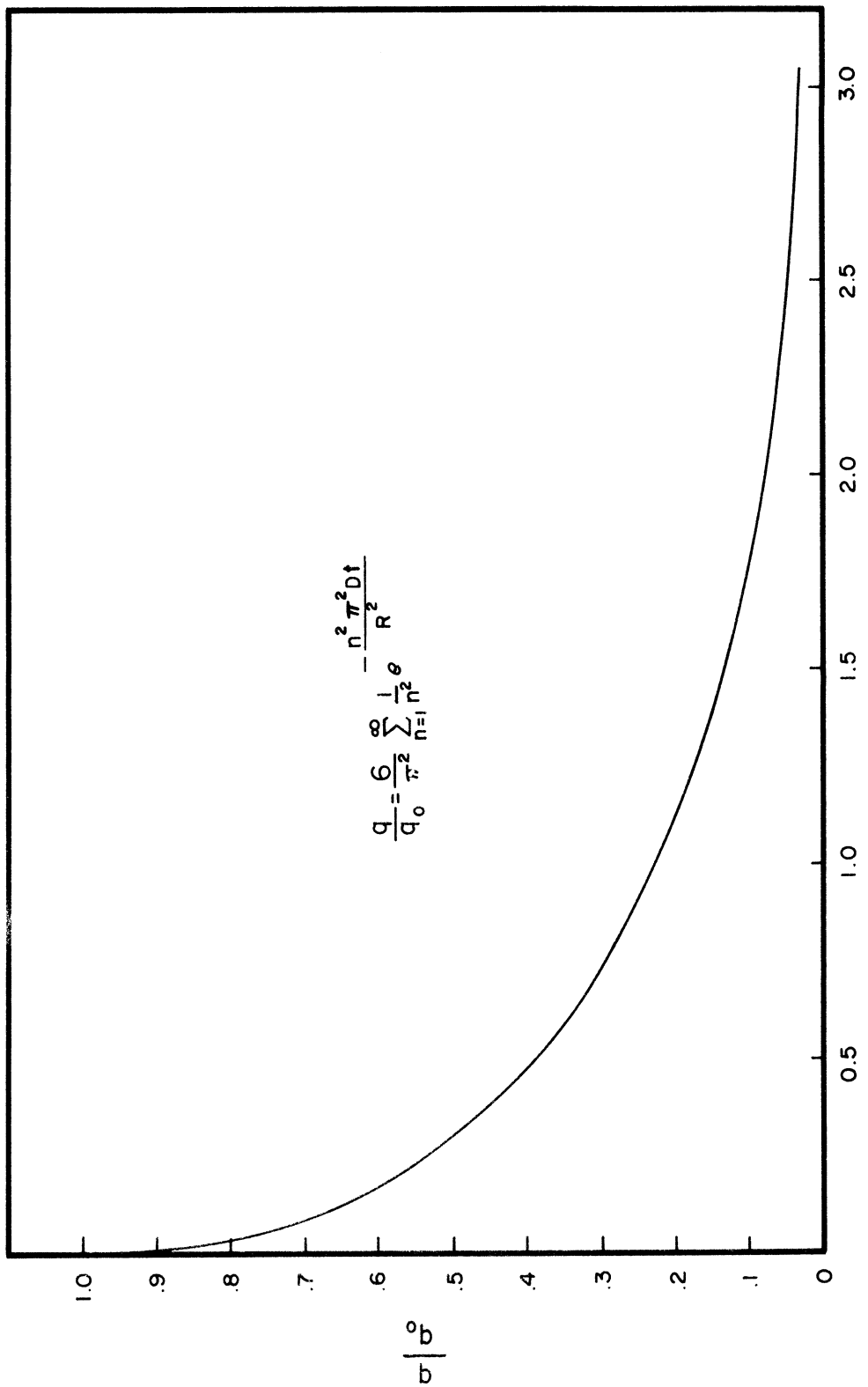

Figure 15. Plot on Linear Scale, of Fraction of Material Remaining in a Sphere versus Dimensionless Time.

In the range of the applicability of Equation (VII) a plot of q versus $\sqrt{t}$ gives a straight line and it is possible to extrapolate this to zero time to get q_o. The slope of such a line gives the diffusivity. This procedure has been used by Pope (G1) and others for similar studies.

This procedure is biased in favor of the data points for short values of time. The smaller the value of time for a data point, the greater the weight it exerts in determining the values of q_o and D, though, experimentally, the smaller the time, the lesser the accuracy of its measurement.

This happens because the "square root of time" scale is distorted such as to spread out the points for small values of time and to cramp in together the points for large values of time.

There is an additional difficulty in using Equation (VII). The equation, essentially, amounts to considering the sphere as a semi-infinite solid and is valid, at best, only for the first 30 to 40% of the diffusion process. This means that only the data for comparatively short values of time may be used. As can be seen from the tabulated values for Equation (VI), in Table VI, the first 30% of the diffusion takes place very rapidly*, and much more well spaced data for q and r may be obtained where q/q_o is between 0.3 and 0.7, rather than between 0.7 and 1.0 as required for the use of Equation (VII).

C. Two Constant Least Squares Fit

It is possible to make a least squares fit to the data of q versus t for determining the best values of q_o and D in Equation (VII).

---

* For most runs in this study 30% of the material was removed from the spherical particles in 5 to 15 seconds.

If q_i and t_i are the data for i = 1, 2, ..., N for the N-data points, then the sum of the squares of the errors, $\overset{v}{R}$, is given by:

$$\overset{v}{R} = \sum_{i=1}^{N} [q_i - \frac{6q_o}{\pi^2} \sum_{n=1}^{\infty} \frac{1}{n^2} e^{- \frac{n^2\pi^2 Dt}{R^2}}]^2 \qquad \text{(VIII)}$$

The best values of q_o and D are to be obtained to minimize this expression. When the value of R has been minimized, $\partial\overset{v}{R}/\partial D$ and $\partial\overset{v}{R}/\partial q_o$ are each equal to zero.

Differentiating the above expression for $\overset{v}{R}$, we get:

$$\frac{\partial \overset{v}{R}}{\partial D} = \sum_{i=1}^{N} 2[q_i - \frac{6q_o}{\pi^2} \sum_{n=1}^{\infty} \frac{1}{n^2} e^{- \frac{n^2\pi^2 Dt_i}{R^2}}][+ \frac{6q_o}{\pi^2} \sum_{n=1}^{\infty} \frac{\pi^2 t_i}{R^2} e^{- \frac{n^2\pi^2 Dt_i}{R^2}}]$$

$$= \frac{12q_o}{R^2} \sum_{i=1}^{N} [q_i - \frac{6q_o}{\pi^2} \sum_{n=1}^{\infty} \frac{1}{n^2} e^{- \frac{n^2\pi^2 Dt_i}{R^2}}][\sum_{n=1}^{\infty} e^{- \frac{n^2\pi^2 Dt_i}{R^2}}] t_i$$

$$\frac{\partial \overset{v}{R}}{\partial q_o} = \sum_{i=1}^{N} 2[q_i - \frac{6q_o}{\pi^2} \sum_{n=1}^{\infty} \frac{1}{n^2} e^{- \frac{n^2\pi^2 D_i t}{R^2}}][- \frac{6}{\pi^2} \sum_{n=1}^{\infty} \frac{1}{n^2} e^{- \frac{n^2\pi^2 Dt_i}{R^2}}]$$

$$= - \frac{12}{\pi^2} \sum_{i=1}^{N} [q_i - \frac{6q_o}{\pi^2} \sum_{n=1}^{\infty} \frac{1}{n^2} e^{- \frac{n^2\pi^2 D_i t}{R^2}}][\sum_{n=1}^{\infty} \frac{1}{n^2} e^{- \frac{n^2\pi^2 Dt_i}{R^2}}]$$

Hence the values of q_o and D which give the least square fit to the data are implicitly defined by the following two equations:

$$\sum_{i=1}^{N} [q_i - \frac{6q_o}{\pi^2} \sum_{n=1}^{\infty} \frac{1}{n^2} e^{- \frac{n^2 D\pi^2 t_i}{R^2}}][\sum_{n=1}^{\infty} e^{- \frac{n^2\pi^2 Dt_i}{R^2}}] t_i = 0 \qquad \text{(IX)}$$

$$\sum_{i=1}^{N} [q_i - \frac{6q_o}{\pi^2} \sum_{n=1}^{\infty} \frac{1}{n^2} e^{- \frac{n^2\pi^2 Dt_i}{R^2}}][\sum_{n=1}^{\infty} \frac{1}{n^2} e^{- \frac{n^2\pi^2 Dt_i}{R^2}}] = 0 \qquad \text{(X)}$$

These are non-linear simultaneous equations and the values of q_o and D that satisfy these equations can be obtained by trial and error, as shown below.

Let us first note, that the functions,

$$\sum_{n=1}^{\infty} \frac{1}{n^2} e^{-n^2\varphi} \quad \text{and} \quad \sum_{n=1}^{\infty} e^{-n^2\varphi}$$

have been tabulated in the literature.

The function $\sum_{n=1}^{\infty} \frac{1}{n^2} e^{-n^2\varphi}$ arises from the solution of the diffusion equation* and its value can be obtained from Table VI. The function $\sum_{n=1}^{\infty} e^{-n^2\varphi}$ is the θ_3 function* and its value is tabulated by Janke and Ende (J2).

Equations (IX) and (X) can be rearranged to give:

$$q_o = \frac{\sum_{i=1}^{N} \left(q_i t_i \sum_{n=1}^{\infty} e^{-\frac{n^2\pi^2 D t_i}{R^2}} \right)}{\frac{6}{\pi^2} \sum_{i=1}^{N} \left(\sum_{n=1}^{\infty} \frac{1}{n^2} e^{-\frac{n^2\pi^2 D t_i}{R^2}} \right) \left(\sum_{n=1}^{\infty} e^{-\frac{n^2\pi^2 D t_i}{R^2}} \right) t_i} \qquad \text{(XI)}$$

and

$$q_o = \frac{\sum_{i=1}^{N} \left(q_i \sum_{n=1}^{\infty} e^{-\frac{n^2\pi^2 D t_i}{R^2}} \right)}{\frac{6}{\pi^2} \sum_{i=1}^{N} \left(\sum_{n=1}^{\infty} \frac{1}{n^2} e^{-\frac{n^2\pi^2 D t_i}{R^2}} \right)} \qquad \text{(XII)}$$

Different trial values of D are taken; the values of q_o are calculated according to Equations (XI) and (XII) using the tables for $\sum_{n=1}^{\infty} \frac{1}{n^2} e^{-n^2\varphi}$ and $\sum_{n=1}^{\infty} e^{-n^2\varphi}$. The correct value of D is the one which gives the same value of q_o by the two equations. The values of D and q_o thus obtained give the "least squares" fit to the data.

The procedure described above is lengthy and time consuming. The data of this investigation are not, in fact, accurate enough to

---

* See Section 5 of Detailed Discussions

necessitate too elaborate a curve fitting procedure. A much simpler method of superpositioning of curves, described later, was developed in this study. However, for two runs, data were fitted by the least squares method described above and the values of q_o and D obtained agreed with those obtained by the superpositioning method within the error of experimental measurements.

There is a fundamental objection to the procedure for the least squares fit described above. It fits the q versus t data considering, as the error, the difference between the experimental and the "curve-fitted" values of q at the different measured values of t. On a "q" versus "t" plot, it considers the deviation of the data points in the q direction as the error. This would be meaningful if the experimental measurements of time "t" were absolutely correct. In the present study, however, the error in the measured values of t are of the same order of magnitude as that in q. In view of this fact, the above procedure for least squares fit introduces an arbitrary bias.

It is possible to work out a curve fitting procedure that would minimize the sum of the squares of the deviations of the data taken in any arbitrary direction. The choice of the direction, should depend on other information about the data, such as the accuracy of the variables measured. Lacking other definite criteria for choice, it seems reasonable, intuitively, that the deviations of the data should be measured in the direction normal to the curve "fitted" to the data.

D. Method of Superpositioning

In Equation (VI) q/q_o is a unique function of Dt/R^2. Figure 15 shows a plot of q/q_o versus Dt/R^2. From this figure a plot of q versus

t may be obtained for any particular values of q_o and D/R^2 simply by multiplying the ordinates by q_o and multiplying the abscissa by R^2/D. If Figure 15 were drawn on a sheet of elastic rubber, then the entire two parameter family of the plots of q versus t for the different values of q_o and D/R^2 can be obtained simply by stretching (and compressing) the rubber sheet in proper proportions along the q and the t axes.

If q/q_o and π^2Dt/R^2 are plotted on a logarithmic scale, Figure 16 is obtained. Once again log (q/q_o) is a unique function of log (Dt/R^2); but for different values of q_o and π^2D/R^2, a plot of (log q) versus (log t) will be exactly the same in shape as Figure 16, and will be displaced laterally along the (log q) and (log t) axes by the amounts (log $1/q_o$) and (log π^2D/R^2) respectively.

Hence, in order to make a two constant fit of the data of q versus t, the data is plotted on a logarithmic paper. A master plot of q/q_o versus π^2Dt/R^2 is made on a transparent logarithmic paper on the same scale as the data. Now the master plot is moved horizontally and vertically, without any rotation at all, over the plot of the data until a good fit is obtained. When such a fit is obtained, the point on the master plot with the coordinates $q/q_o = 1$ and $\pi^2Dt/R^2 = 1$ coincides with some point, say (q^*,t^*) on the paper on which the data is plotted. The coordinates of this point q^* and t^* are read. Then the constants of the fit are obtained simply from the relations

$$q_o = q^*$$

$$R^2/D\pi^2 = t^* .$$

The errors in the measurement of the data may be indicated on the plot of the data by marking, instead of a point (q,t), a small

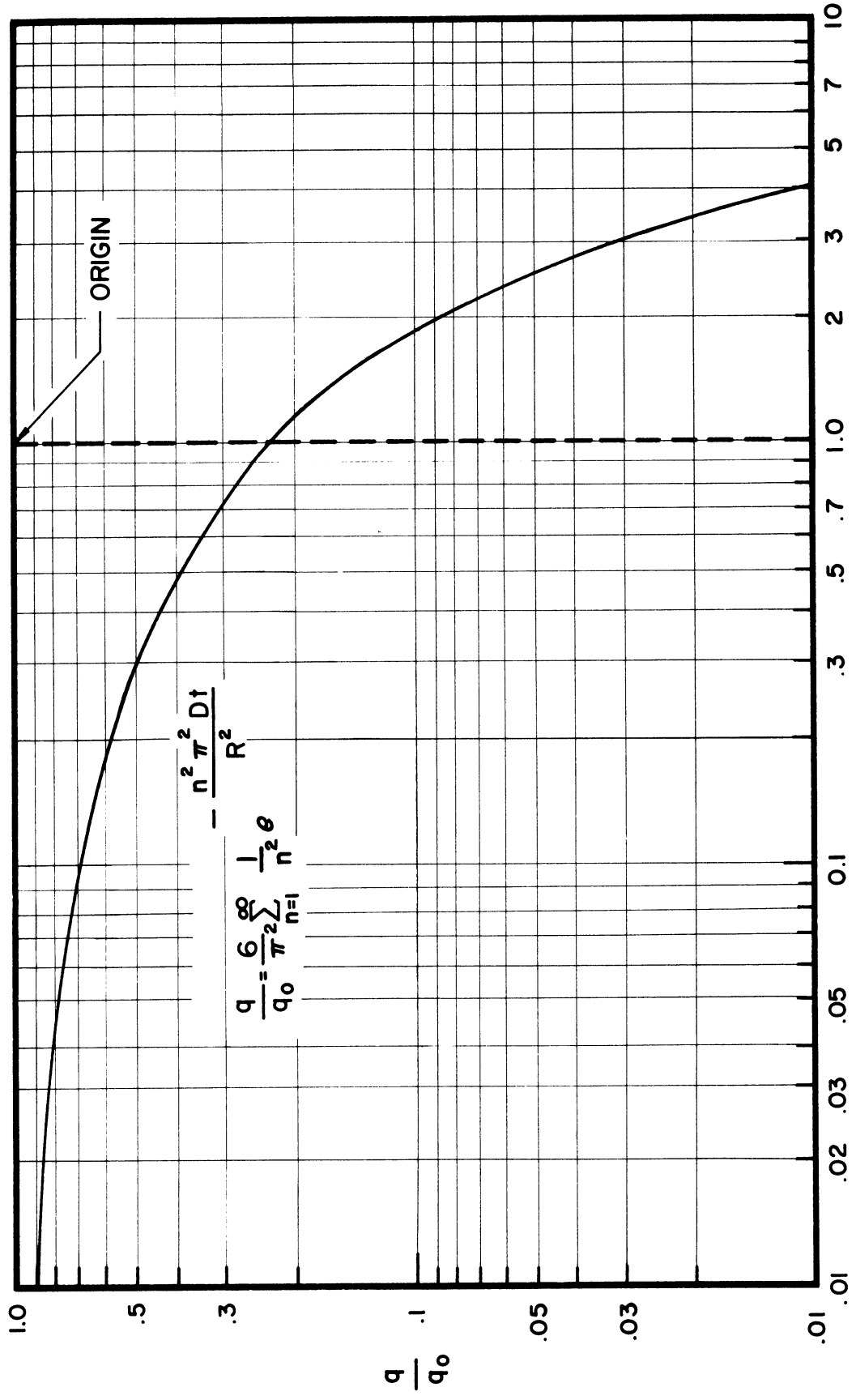

Figure 16. Fraction of Materials Remaining in a Sphere versus Dimensionless Time Plotted on a Logarithmic Scale. (Master plot for use in curve fitting.)

rectangle of the sides (Δt and Δq) equal to the estimated errors. During superpositioning of the master plot for curve fitting, it may be remembered that the data point lies anywhere within this rectangle. Thus the more unreliable data give the greater leeway in fitting.

Figure 17 shows data from a typical run, plotted on the logarithmic scale and fitted by the method described here. As can be seen the range of q/q_o covered by the data is from 0.9 to 0.05, i.e., the diffusion equation is fitted to a very wide range of the elution process.

The superpositioning is fairly sensitive if the data covers a reasonable range of q/q_o. It is interesting to note that in this method of curve fitting, the information content of the data in the range of $\pi^2 Dt/R^2 = 1$ is utilized equally in determining both q_o and D whereas the information in the data for short time is utilized more for determining q_o and the information in the data for large values of time is utilized more for determining D.

E. Reliability of the Method of Superpositioning

To get some information about the reliability of the method of superpositioning, a run of 35 data points was taken and the data were plotted on three logarithmic papers--the first had the 18 odd numbered data points of the run, the second had 17 even numbered data points and the third had all the 35 data points. All the three sets of data were fitted by superpositioning a master plot and the values of q^* and t^* were obtained. The values obtained in the three fits agreed with each other.

Repeatedly, at intervals of several weeks, the same three sets of data were fitted again by superpositioning. The consistancy of the fit over a period of time was thus checked.

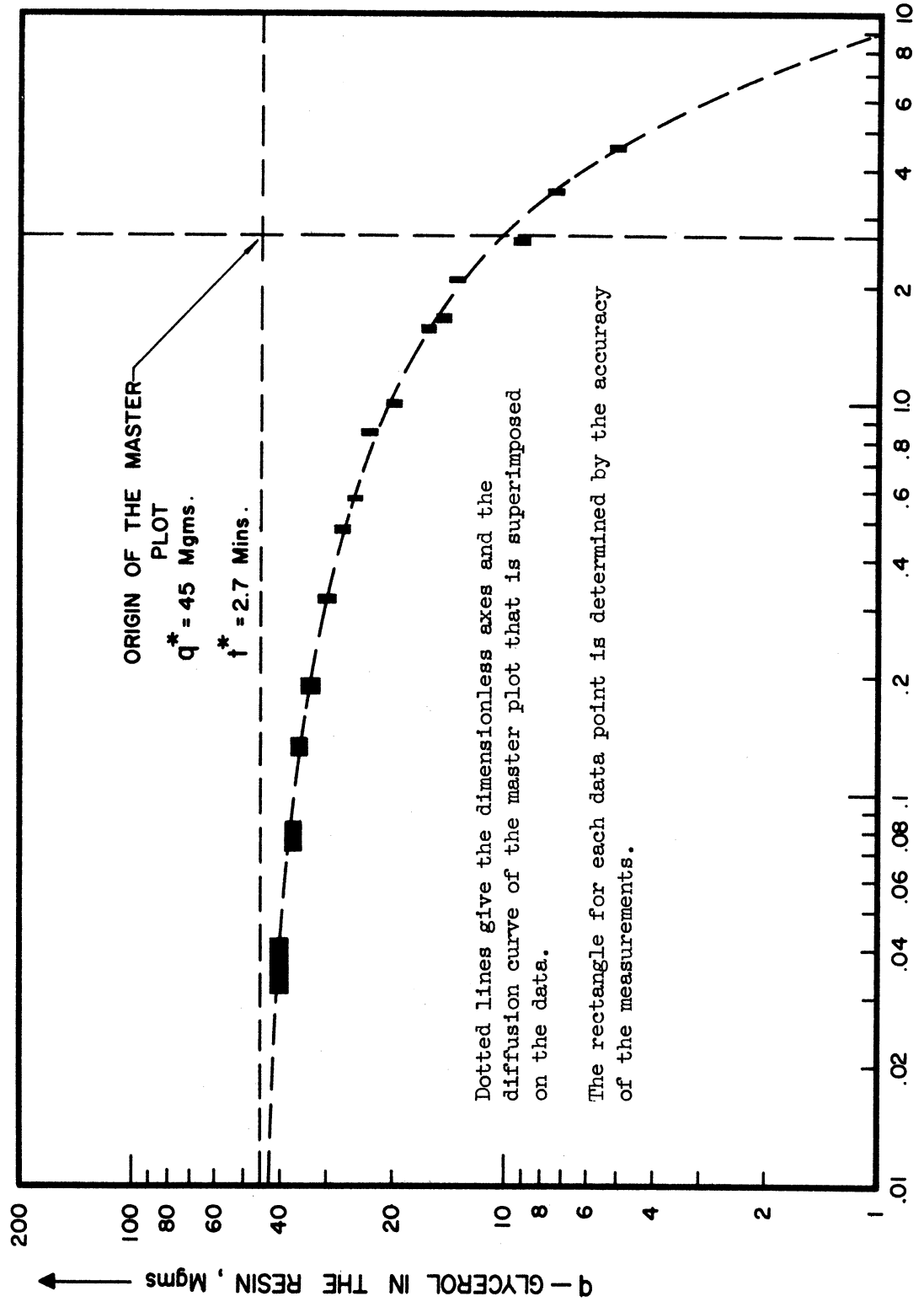

Figure 17. Data and Curve Fitting for a Typical Run. (Run Number 7-11)

The same three sets of data were fitted by nine other people--members of faculty and graduate students at the University. Values of q* and t* estimated by them are shown in Table VII. They agreed well with the values estimated by the author, and were within the experimental error.

8. Accuracy and Reproducibility of the Data

All measurements of the values of time for elution have an expected absolute error of $\pm$ 0.005 minutes. An electric timer indicated time in hundredths of minutes and it could be interpolated to indicate .002 minutes.

Accuracy of the glycerol and sodium chloride analysis was about one part in 50. For very low concentrations (5 to 50 ppm), the accuracy was about one part in 25. For high concentration ranges (200 to 1000 ppm), the accuracy was about one part in 100.

Figure 18 shows the data obtained for two identical runs. They indicate good reproducibility. The diffusivity obtained from the data was used to calculate the values for the solid curve in the figure, representing the fit of the data. Figure 19 shows the same data plotted on a logarithmic scale. The actual "fitting" of the data in order to determine diffusivities, was done on a logarithmic plot, as explained in the preceding section.

The equilibrium data shown in Figures 8 and 9 in the "Results" sections are based on very few actual measurements as indicated on the figures. They also cover only a limited range of concentrations.

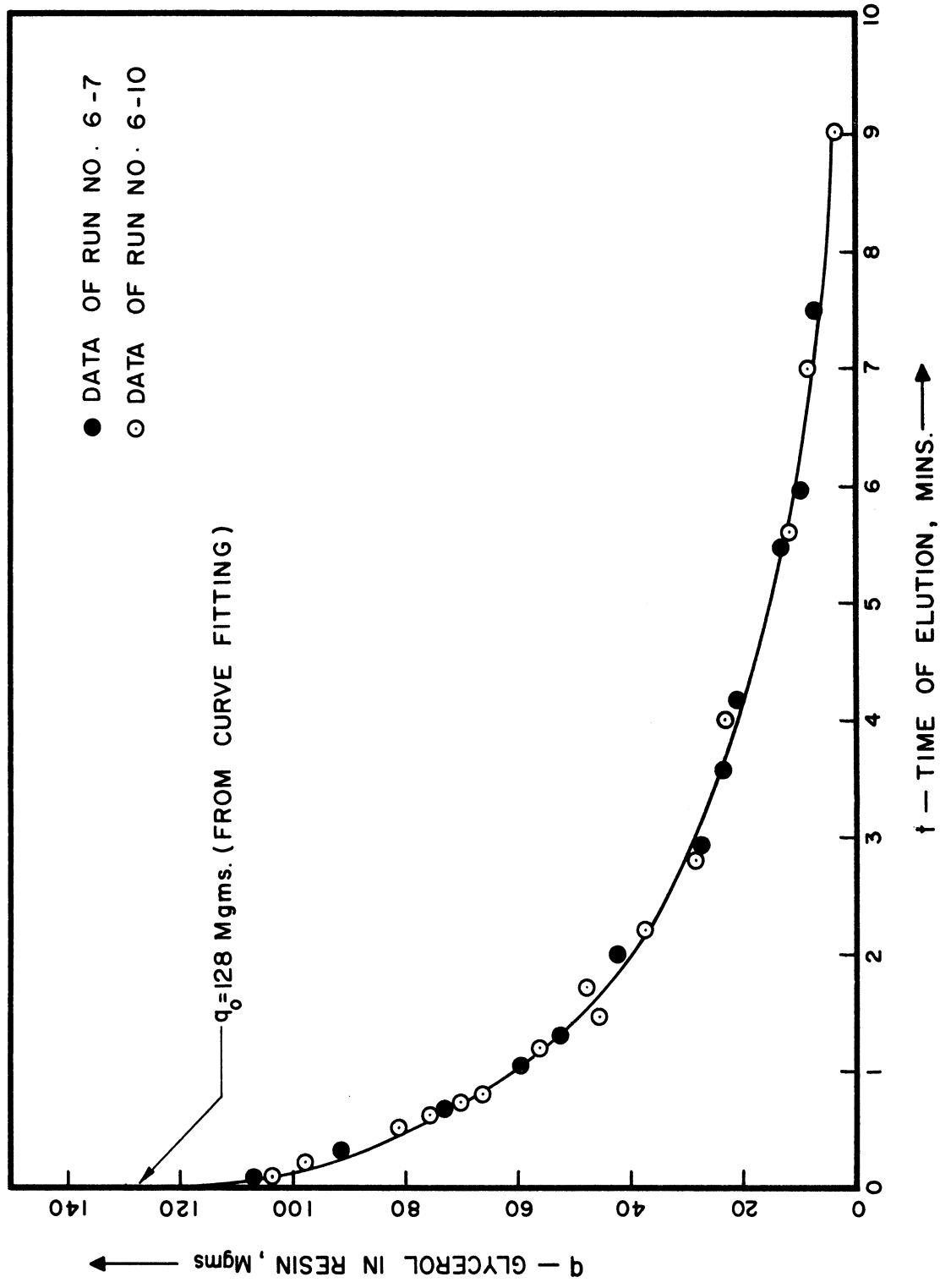

Figure 18. Reproducibility of Data and Fit of the Data to Diffusion Mechanism.

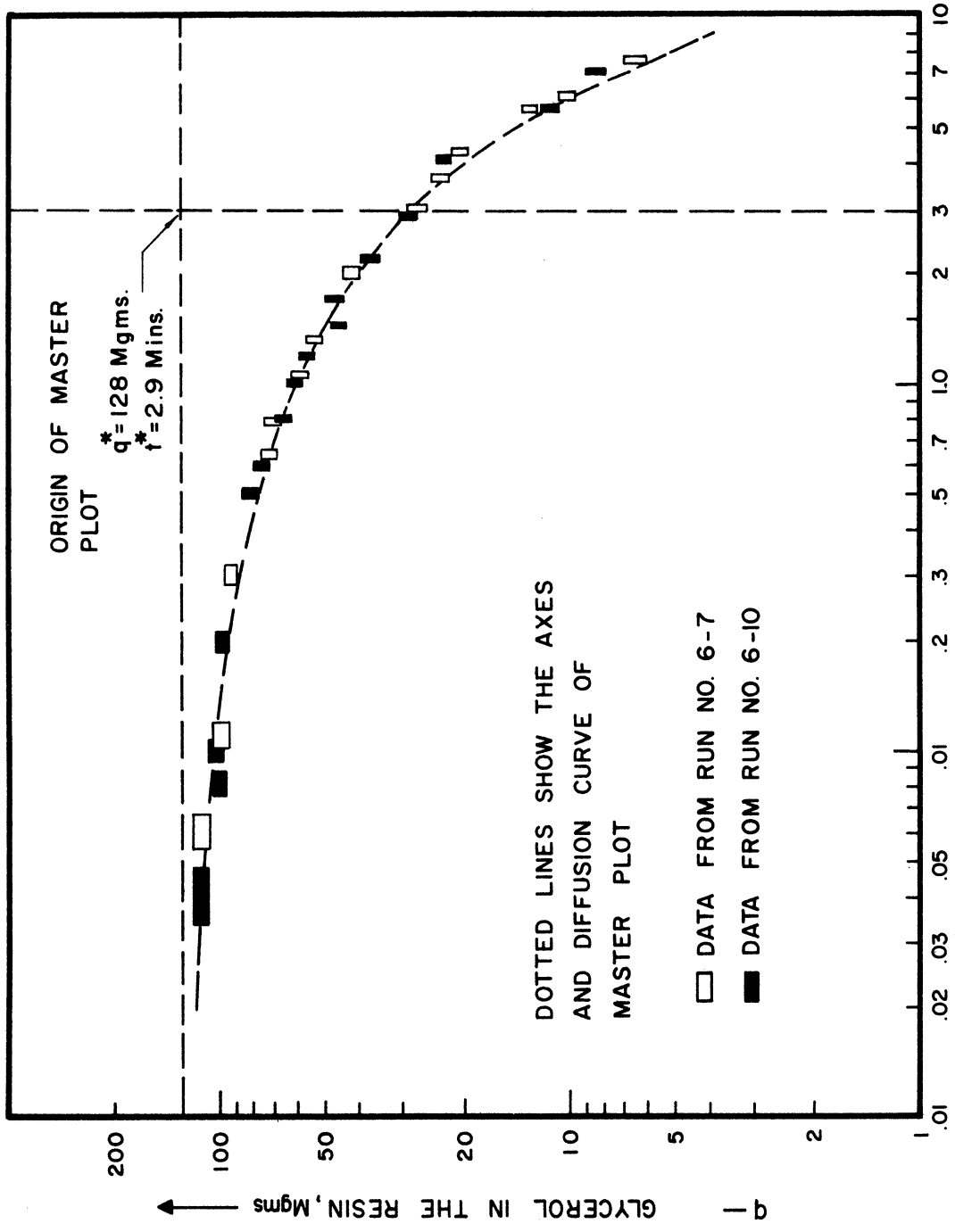

Figure 19. Reproducibility of Data, and Fit of the Data to Diffusion Mechanism.

TABLE VII

RELIABILITY OF CURVE FITTING BY SUPERPOSITIONING OF A MASTER PLOT OVER DATA

	Odd Numbered Data Points		Even Numbered Data Points		Total Data Points	
Number of Data Points	18		17		35	
Person Fitting the Data	Values Obtained by Curve Fitting by Superpositioning Master Plot					
	q*	t*	q*	t*	q*	t*
Author on May 12					10.0	1.45
Author on May 20					9.8	1.51
Author on June 10					10.1	1.43
Author on July 1					10.05	1.445
Author on July 16					9.9	1.47
Subject 1	10.15	1.45	10.35	1.41	10.15	1.445
Subject 2	10.3	1.39	10.3	1.37	9.97	1.445
Subject 3	10.25	1.41	10.0	1.43	10.15	1.40
Subject 4	10.15	1.43	10.15	1.405	9.95	1.48
Subject 5	10.4	1.42	10.05	1.50	10.15	1.42
Subject 6	10.5	1.40	10.3	1.39	9.9	1.50
Subject 7	10.35	1.41	10.2	1.44	10.05	1.43
Subject 8	10.2	1.43	10.15	1.45	10.15	1.43
Subject 9	10.45	1.41	10.2	1.45	10.0	1.46

9. Table of All Runs Made

TABLE VIII

RUNS MADE FOR DIFFUSION STUDY

Run Number	Resin Cross Linkage % DVB	Temp. °C	Conc. of Equilibrating Soln.		Results from the Run			
			Glycerol wt.%	NaCl wt.%	Glycerol		Sodium Chloride	
					mgms per gm of Air Dry Resin at Equilibrium	Diffusivity $\frac{cm^2}{sec} \times 10^6$	mgm per gm of Air Dry Resin at Equilibrium	Diffusivity $\frac{cm^2}{sec} \times 10^6$
5-2	8	Room	10	0	38±2	.50±.03		
5-6	8	Room	10	10	46±2	.53±.03	11±2	1.4±.15
5-17	8	Room	2	2	7.5±.3	.57±.05		
5-24	8	23	5	15	25±1	.50±.03	22.5±1	1.3±.2
6-10	8	23	25	2	128±3	.54±.03		
7-3	8	27	0	2			.8±.05	1.25±.2
7-6	8	26	0	5			3.7±.3	1.5±.15
7-7	8	25	0	10			11.5±.5	1.4±.1
7-8*	8	25	10	10			11.5±.5	1.45±.2
7-9*	8	26	10	10	42±1	.55±.07	11.0±.5	1.4±.2
7-11	8	26	10	10	44±1	.57±.03	11.5±.5	1.45±.13
8-5**	8	26	10	10	45±2	.55±.05	11±1	1.40±.1
8-6	8	26	10	10	44±1	.53±.05	10±1	1.40±.15
8-9	8	77-79	30	10	165±15	2.9±.2	17±1	5.9±.5
8-23	8	55	30	10	150±15	1.8±.2	14±1	3.5±.3
8-26	8	55	15	15	77±3	1.8±.2	26±1	3.8±.2
9-16	4	24	30	10	129±10	1.45±.05	12±1	3.7±.3
10-1	12	22	30	5	47±3	.25±.02	1.2±.2	0.93±.05
10-2	4	21	30	5	137±15	1.6±.2	8.2±.5	3.35±.3
10-3	2	22	30	5	200±2.0	1.8±.2	17±1.5	4.7±.5
10-14	4	24	0	5			5.6±.5	3.9±.3
10-15	2	24	0	5			14±1	5.8±.5
10-16	4	24	35	0	170±15	1.7±.2		
10-17	2	24	35	0	285±20	2.6±.2		
10-20	12	65	30	5	47±3	1.85±.07	.98±.05	2.8±.4
10-21	4	65	30	5	165±10	5.0±.2	8.7±.5	8.9±.6
10-22	2	65	30	5	235±15	6.7±.3	18.5±.3	12.5±1.5

* These runs were made with different size of resin particles.

** This run was made at a third the normal flow rate of eluting water.

NOTE: Data for each of the runs indicated on the above table are given in the Appendix II.

10. Related Literature

For overall survey of ion exchange a book by Kunin (K2) and two books edited by Nachod (N1) and (N2) are recommended.

The phenomenon and process of ion exclusion are described by Simpson and Wheaton (S4), and Wheaton and Bauman (W1).

Separation of sodium chloride and glycerol by ion exclusion are discussed by Asher and Simpson (A1) and Prielipp and Keller (P2). Some consideration to the economics of this separation is given by Keller et al. (K1). Phase equilibrium data for the system, glycerol-sodium chloride-water-Dowex 50 have been obtained and correlated by Shurts and White (S2),(S3). Their data are for a resin with 8% divinyl benzene and room temperature. They cover a wide range of concentrations.

Gregor, Collins, and Pope (G1) have studied diffusion of neutral molecules in a cation exchange resin by a technique similar to the one used in this dissertation. They have studied diffusion of isobutyl acetate, isobutyl alcohol, ethyl acetate, methyl acetate, ethanol and urea in cation exchange resin in different ionic forms.

Self diffusion of ions in a resin has received some attention in literature. Radioactive isotopes have been used in these studies. Generally the resin is saturated with a solution and then it is subjected to another solution with the same concentrations but containing radioactive isotopes of the ions under consideration. Tetenbaum and Gregor (T1) have studied self diffusion of cations and anions in Dowex 50 (12 and 15% DVB) at equilibrium. Richman and Thomas (R2) have reported self diffusion of sodium ions in Amberlite resins. Boyd and Soldano (B3, B4, B5, B6) have studied self diffusion of cations, anions, and water molecules.

The technique of using a small amount of resin (approximately a differential bed) was used by Boyd, Adamson, and Myers (B2) for studying ion exchange kinetics. The liquid flow rates in glass apparatus were low. Tetenbaum and Gregor (T1) mentioned above have used the same experimental set up and have discussed the problem of the flow rates. Bieber, Steidler, and Selke (B1) and Selke et al. (S1) have used this so called "shallow bed technique" for studying mass transfer in the liquid phase for ion-exchange processes.

11. Description of Ion Exclusion

If an ion exchange resin is immersed for a sufficient time in an aqueous solution of sodium chloride and glycerol phase equilibrium is established between the resin phase and the aqueous phase. If it is a cation exchange resin in the sodium form--as has been used in this thesis--no ion exchange reactions take place and the equilibrium is purely a physical equilibrium. In such cases one finds that the resin absorbs glycerol very much more than it does sodium chloride. In other words, the equilibrium constant for glycerol, expressed as the ratio of concentration in the resin phase to that in the external solution, is much larger than that for sodium chloride.

This is a specific example of ion exclusion. Generally speaking, however, an ion exchange resin, immersed in a polar solvent, preferentially absorbs non-electrolytes and non-ionizable materials rather than electrolytes and ionizable materials. Hence, the term "ion exclusion" is used to describe this phenomenon.

The same term "ion exclusion" is also applied to a process in which ionic and non-ionic materials are separated by utilizing the phenomenon of ion exclusion. Such a separation may be accomplished, for instance, by taking a column of resin in sodium form, feeding a small amount of a solution containing both sodium chloride and glycerol to be separated, and then eluting the absorbed materials from the resin by passing fresh distilled water through the column. Since the resin preferentially absorbs most of the glycerol fed to the column, most of the sodium chloride leaves the column in the first part of the effluent. Glycerol is subsequently eluted, or extracted, out of the solid resin by distilled water and leaves the column in the latter part of the effluent. In a sense, the column operates like the well known chromatographic columns and the separation is similar to chromatographic separations.

For more information on ion exclusion, References (W1), (N2), and (S4) from the Bibliography are recommended.

12. Diffusion-Controlled Ion-Exchange (Area of Future Research)

The diffusivities of NaCl and glycerol in Dowex 50 are only a fraction of their diffusivities in water. This suggests that in case of ion exchange, the reaction rates may be controlled by the diffusion of the ions in the solid phase. If so, the experimental technique used in the present study can be adopted as explained below, to obtain diffusivities of ions in the resin.

Consider a monovalent ion exchange reaction,

$$R^{-}H^{+} + Na^{+} \rightarrow R^{-}Na^{+} + H^{+}$$

where R is the immobile anion of the resin matrix.

If the rate of such a reaction is diffusion controlled, it would be determined by the diffusivities of the Na^+ and the H^+ ions in the resin. During the reaction, the diffusion of Na^+ ions into the resin particle and the diffusion of H^+ ions out of the resin particle take place simultaneously.

Due to the difference in the diffusivities of Na^+ and H^+ ions in the resin, electrical potentials will be generated in the resin particles, and, consequently, the driving force for the mass transfer of the ions will be a combination of two potentials - the chemical potential or the concentration gradient and the electrical potential.

For the case under consideration, following Nernst - Planck equations are applicable (H1).

$$\phi_1 = - D_1 [\text{grad } C_1 + Z_1 C_1 (F/RT) \text{ grad } \bar{\varphi}] \qquad \text{(i)}$$

$$\phi_2 = - D_2 [\text{grad } C_2 + Z_2 C_2 (F/RT) \text{ grad } \bar{\varphi}] \qquad \text{(ii)}$$

where ϕ is the flux

D is the diffusivity of individual ions

C is the molar concentration

Z is the electrochemical valence of the ions

F is the Faraday constant

R is the gas constant

T is the absolute temperature

$\bar{\varphi}$ is the electric potential

and the subscripts 1 and 2 refer to the two ion species under consideration.

Electroneutrality requires that the total equivalent concentration of the two reacting ions be constant throughout the resin particle, since the concentration of the fixed ionic groups on the resin matrix is constant.

Hence

$$Z_1C_1 + Z_2C_2 = \text{constant} \qquad \text{(iii)}$$

The absence of electric current gives

$$Z_1\phi_1 + Z_2\phi_2 = 0 \qquad \text{(iv)}$$

Equations (i) through (iv) have to be solved simultaneously.

With the use of Equation (iii) and (iv), Equations (i) and (ii) can be combined to give the following:

$$\phi_1 = - \left[\frac{D_1D_2\ (Z_1^2C_1 + Z_2^2C_2)}{D_1Z_1^2C_1 + D_2Z_2^2C_2}\right] \text{grad } C_1 \qquad \text{(v)}$$

The quantity in the brackets may be considered a diffusion coefficient which is dependent on the concentrations.

Using Equation (v) in place of Fick's law, the problem of diffusion in a resin particle has been set up by Helfferich and Plesset (H1). The problem is non-linear since the "effective diffusivity" is not a constant. The problem has been solved numerically by the above authors on a digital computer for two cases: (i) exchange of monovalent ions in the resin and (ii) exchange between monovalent and divalent ions. The tables of numerical values of the solutions have been reported (H1, P1).

Figure 20 shows graphically their solution for the exchange of monovalent ions. The curve for fractional attainment of equilibrium as a function of time, depends on the values of the diffusivities of both the ions.

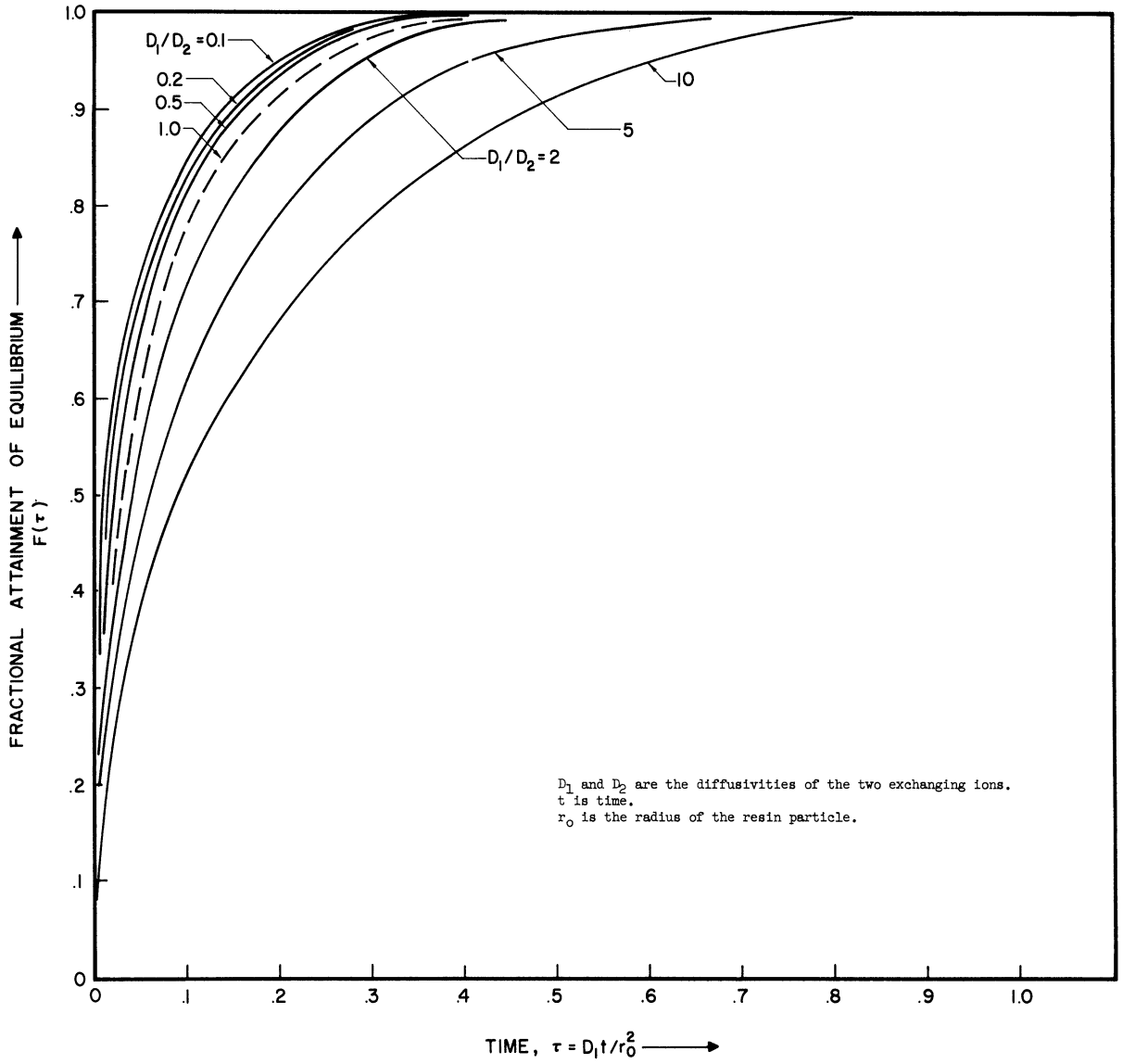

Figure 20. Fractional Attainment of Equilibrium versus Dimensionless Time for Diffusion Controlled Monovalent Ion Exchange Reaction.

In Figure 20, the curve for the parameter $D_1/D_2 = 1$, coincides with the curve obtained for the diffusion of a single molecular species without any chemical reaction, such as the one shown in Figures 15 and 16 of this thesis.

An experimental technique very similar to the one used in the present study may be utilized to obtain diffusivities of ions in the resin. For example, baskets containing a cation exchange resin can be equilibrated with sodium chloride solution. Each basket may be placed in a conduit and hydrochloric solution of desired strength may be pumped at high velocities. The baskets may be removed from the stream of the HCl solution at different times and the amount of Na^+ ions remaining in the resin may be extracted with HCl solutions of the same strength as that used for the run. The data may then be fitted to the diffusion mechanism by using Helfferich and Plesset's numerical solution to give the equilibrium value, the diffusivity of Na^+ ions and the ratio of the diffusivity of H^+ ion to that of Na^+ ion. This means that a "three constant fit" has to be made to the data.

In the cases where equilibrium values may already be known, only a two constant fit has to be made.

BIBLIOGRAPHY FOR PART I

A1 Asher, D. R. and Simpson, D. W. J. Phy. Chem., 60, (1956), 518.

B1 Bieber, H., Steidler, F.E., and Selke, W.A. Chem. Engr. Prog. Symp. No. 14, 50, (1954), 17.

B2 Boyd, G.E., Adamson, A.W., and Myers, L.S. J Amer. Chem. Soc. 69, (1947), 2830.

B3 Boyd, G.E., and Soldano, B.A. J. Amer. Chem. Soc. 75, (1953), 6091.

B4 Boyd, G.E., and Soldano, B.A. J. Amer. Chem. Soc. 75, (1953), 6099.

B5 Boyd, G.E., and Soldano, B.A. J. Amer. Chem. Soc. 75, (1953), 6105.

B6 Boyd, G.E. and Soldano, B.A. J. Amer. Chem. Soc. 75, (1953), 6107.

C1 Carslaw, H.S., and Jaeger, J.C. Conduction of Heat in Solids. (Oxford Univ. Press, Sec. Ed. (1959), 9, 17, 233.

C2 Chilton, T.H., and Colburn, A.P. Ind Eng. Chem. 26, (1935), 1183.

C3 Churchill, R.V. Fourier Series and Boundry Value Problems. McGraw Hill, (1941), 112-113.

C4 Churchill, R.V. Modern Operational Mathematics in Engineering. McGraw Hill, (1944), 122.

C5 Crank, J. The Mathematics of Diffusion. Oxford: (1956), 84-98.

D1 Dowex: Ion Exchange, Dow Chemicals., Midland, Mich.

G1 Gregor, H.P., Collins, F.C., and Pope, Martin, J. Colloid Sc. 6, (1951), 304.

H1 Helfferich, F., and Plesset, M.S. J. Chem. Physics. 28, (No 3), March (1958), 418.

I1 Ingersoll, L.R. and Zobel, O.J. Mathematical Theory of Heat Conduction. Berlin: Ginn and Co., 1913.

J1 Jackson, E.L. Organic Reactions. 2, Wiley, (1944), 341-375.

J2 Jahnke, E. and Emde, F. "Tables of Function." Fourth Ed., (Dover Publishers), 41-45.

K1 Keller, H.W., Michalson, A.W., and Payne, A.D. J. Amer. Oil Chem. Soc., 33, (Oct. '56), 435.

K2 Kunin, R. Ion Exchange Resins. John Wiley and Sons, 2nd Ed., 1958.

N1 Nachod, F.C. Ion Exchange: Theory and Applications. Academic Press, 1949.

N2 Nachod, F.C. Ion Exchange Technology. Ed. Nachod, F.C. and Schubert, J., Academic Press, 1956.

N3 Neish, A.C. Analytical Methods for Bacterial Fermentations. National Research Council of Canada, Saskatoon, Nov. 25, 1952, NRC. No. 2952. Prairie Regional Laboratory; Report No. 46-83 (2nd Ed).

P1 Plesset, M.S., Helfferich, F., and Franklin, J.N. J. Chem. Physics., 28, (No. 11), (Nov. 1958), 1064.

P2 Prielipp, G.E. and Keller, H.W. J. Amer. Oil Chem. Soc., 33, (March 1956), 103.

R1 Reichenberg, D. J. Amer. Chem. Soc., 75, (1953), 596.

R2 Richman, D. and Thomas, H.C. J. Phy. Chem., 60, (1956), 237.

S1 Selke, W.E., Bard, Y., Pasternak, A.D., and Aditua, S.K. Jour. A.I.Ch.E., 2, (No. 4), (1956), 468.

S2 Shurts, E. Univ. of Michigan Thesis, 1954.

S3 Shurts, E. and White, R.R. Journ. A.I.Ch.E., 3, (No. 2), (1957), 183.

S4 Simpson, D.W. and Wheaton, R.M. Chem. Eng. Progress., 50, (No. 1), (1954), 45.

S5 Smith, G. Frederick. Analytical Application of Periodic Acid and Iodic Acid. 5th Ed., G.F. Smith Chem. Co., Columbus, Ohio, 1950.

T1 Tetenbaum, M. and Gregor, H.P. J. Phy. Chem., 58, (1954), 1156.

T2 Tölke, Friedrich. Praktische Funktion enlehre. Springer, Berlin: 1943. Lithoprinted by Edwards Bros. Inc., Ann Arbor, Michigan.

T3 Treybel, R.E. Mass-Transfer Operations. McGraw-Hill, (1955), 25.

W1 Wheaton, R.M. and Bauman, W.C. Annals of the N.Y. Acad. of Sciences. 57, Art 3, (Nov. 11, 1953), 159.

W2 Whitcombe, J.A., Banchero, J.T., and White, R.R. C.E.P. Symposium Series, 50, (No. 14), (1954), 73.

W3 Whittaker and Watson. Modern Analysis. 4th Edition, Cambridge (Eng) Univ. Press, (1943), 464.

W4 Wilke, C.R. Chem Eng. Prog. 45, (1949), 218.

W5 Willard, H.H., and Furman, N.H. Elementary Quantitative Analysis. D. Van Nostrand Co. NY, 3rd Ed., (1940), 182.

PART II

ANALYSIS OF UNSTEADY STATE FIXED BED OPERATION FOR ION EXCLUSION AND OTHER SOLID-LIQUID MASS TRANSFER PROCESSES

TABLE OF CONTENTS FOR PART II

TABLE OF CONTENTS FOR PART II (CONT'D)

LIST OF FIGURES (CONT'D)

LIST OF FIGURES (CONT'D)

LIST OF FIGURES (CONT'D)

LIST OF FIGURES (CONT'D)

NOMENCLATURE

A_x — the area of the cross-section of the column. (cm^2)

c — Concentration of the solute in the liquid phase (gms or gm mols/cm^3)

C — Concentration of the solute in the liquid phase (gms or gm mols/cm^3)

$\bar{c}$ — the average concentration of the solute in the solid. (gms or gm mols/cm^3)

c_F — the concentration of the solutes in the feed. (gm or gms mols/cm^3)

c^* — the concentration in the liquid that would in equilibrium with the concentration in the solid. (gms or gm mols/cm^3)

c^*_s — the concentration in the solid that would be in equilibrium with the concentration in the liquid. (gms or gm mols/cm^3)

D — the diffusivity of the solutes in the solid phase. (cm^2/sec)

D_L — the longitudinal diffusivity in the liquid. (cm^2/sec)

G — the ratio of the concentrations of glycerol (or NaCl) in the liquid to that in the feed solution.

k — the coefficient for mass transfer across the liquid film. It is the amount of a material transferred per unit area of interface in unit time for a unit concentration difference across the liquid film.

K — the equilibrium constant i.e. the ratio of concentration of the solute in the solid to that in the liquid phase at equilibrium.

k_s — the coefficient for mass transfer in the solid phase. It is the amount of material transferred per unit area of interface in unit time for a unit concentration difference between the interface and the bulk of the solid.

L — the length of the bed. (cm)

q — the concentration of the solute in the solid phase. (gms or gms mols/cm^3)

Q — the average concentration of the solute in the solid phase. (gms or gm mols/cm^3)

R	the radius of the spherical particles. (cm)
$\bar{S}$	the interface area between the solid and the liquid per unit volume of the bed. (cm^2/cm^3 of the bed)
S	the ration of the concentrations of glycerol (or NaCl) in the liquid to that in the feed solution.
t	time from the start of the feed to the column. (sec)
t_o	the time for which a slug of the solution is fed to the column. (sec)
u	the superficial velocity of the liquid flowing through the bed. (cm/sec)
V	the volume of the bed between the inlet end of the bed and the point at a distance x from the inlet end. (cm^3)
V_e	the volume of the effluent that has flown out of the bed. (cm^3)
V_F	volume of the feed
V_T	total volume of the bed. (cm^3)
x	the distance from the inlet end of the bed. (cm)
z	a dimensionless measure of the distance from the inlet end of the bed. $z = \frac{D(1-\epsilon)x}{uR^2}$
$\bar{z}$	$\frac{Dk(1-\epsilon)x}{uR^2}$ generalized dimensionless distance from the entrance of the bed.
θ	$\frac{\epsilon}{(1-\epsilon)k}\left(\frac{ut}{x\epsilon} - 1\right)$ ratio of dimensionless time to dimensionless distance.
θ	is dimensionless time. $\theta = \frac{D}{R^2}\left(t - \frac{x\epsilon}{u}\right)$
ϵ	the porosity of the bed i.e. the fraction of the bed that is not filled with the solid. (cm^3 void/cm^3 of the bed)

NOMENCLATURE (CONT'D)

∇^2	the Laplacian in the space coordinates within the solid phase.
α	the porosity of the bed when the concentration of the solute is zero.
β	the coefficient in Equation (38) that expresses porosity as a function of concentration. (cm^3/gm or gms mol)
τ	variable of integration for integrating over the volume of the solid.
ρ	the distance of a point inside the solid particle as a fraction of the radius.
$[\frac{\partial q}{\partial r}]_{r=R}$	the concentration gradient from the surface of a solid partical into its interior.

Subscripts:

1,2,i,j	represent the different solutes.
G	represents Glycerol.
S	represents NaCl.

Superscripts:

0	represents absence of the other solute.
1	represents presence of the other solute.

SUMMARY
(For Part II)

Solid-liquid mass transfer processes that are carried out by passing the liquid over a fixed bed of solid particles are studied with the help of mathematical models.

Besides a brief explanation of the general principles and classification of the models, eleven models are discussed in increasing order of complexity. Effect of swelling and shrinkage of the solid with change in concentration and the effect of interdependent equilibria for solutes producing concentration and dilution effects are considered. Two other models are discussed in considerable detail:

(1) Equilibrium column operation with non-linear equilibrium characteristics;

(2) Linear equilibrium and "diffusion" in the solid as the controlling mass transfer resistance.

They produce two typical "kinds" of waves that are produced by many other mechanisms and phenomena.

For each model x-t contour diagrams which indicate level curves of concentration surfaces are discussed as a visual aid to understanding the model. The relation between operating and system variables (i.e. values of parameters in the model) and the prominent characteristics of effluent curves (such as symmetry and skewness, sharp and trailing edges, peak position, etc.) predicted by the model is discussed. Solution of a complex model may be estimated graphically from the solution of simpler models with the help of x-t contour diagrams.

Data available in literature on an ion exclusion column operation with the system ethylene-glycol-water-Dowex 50 are reproduced within the estimated experimental error by a model with the following assumptions: (1) linear equilibrium; (2) mass transfer rates controlled by "diffusion" in the solid phase; (3) piston flow and no longitudinal diffusion in the liquid. Diffusivities of ethylene glycol in Dowex 50 obtained from "fitting" the data to the model are 2.1, 1.9, 1.3 and 0.35 x 10^{-6} cm^2/sec for the resin with 2, 4, 8 and 24% DVB respectively.

For the system glycerol-NaCl-water-Dowex 50, typical data curves from literature are analyzed by considering several models in order of increasing complexity, where each successive complicating mechanism is introduced from the consideration of the preceding model. The dilution of the leading edge of NaCl curve is only partially reproduced by the models considered. For data involving concentrated feed solutions, the long trailing edge in the glycerol effluent curves could not be reproduced and models that consider flow patterns and velocity profiles in the liquid are suggested by the analysis.

I. INTRODUCTION

In a typical ion-exclusion process, a solution containing a mixture of two dissolved solutes is passed over a bed of ion-exchange resin particles. The solutes are absorbed by the resin, the amounts absorbed being determined by equilibrium characteristics and mass transfer resistances. Usually a limited amount of the solution is fed to the column and then fresh solvent is passed to extract the absorbed solutes back from the resin.

For typical ion-exclusion operation, the degree of absorption of the two solutes is different; consequently two separate concentration waves for the two solutes appear in the effluent from the column. The solute that is preferentially absorbed by the resin is retained longer in the bed than the other solute which is less absorbed by the resin, and the preferentially absorbed solute consequently appears later in the effluent. Figure 1 gives typical effluent waves obtained from an ion-exclusion column.

These waves must be evaluated for the design of an ion-exclusion process. Purities and recoveries can then be estimated from these waves. A process may be satisfactory if the area of overlap of the waves is small. Separation between the peaks may also be an important criterion. The peak heights give the maximum concentrations in the effluent. For sharp peaks, large amounts of the materials would be concentrated in a small volume and this may have economic advantages. For "spread-out" waves, the materials are diluted to very large volumes.

In practice, many "kinds" of effluent waves are obtained depending on the physical characteristics of the system and the values of the

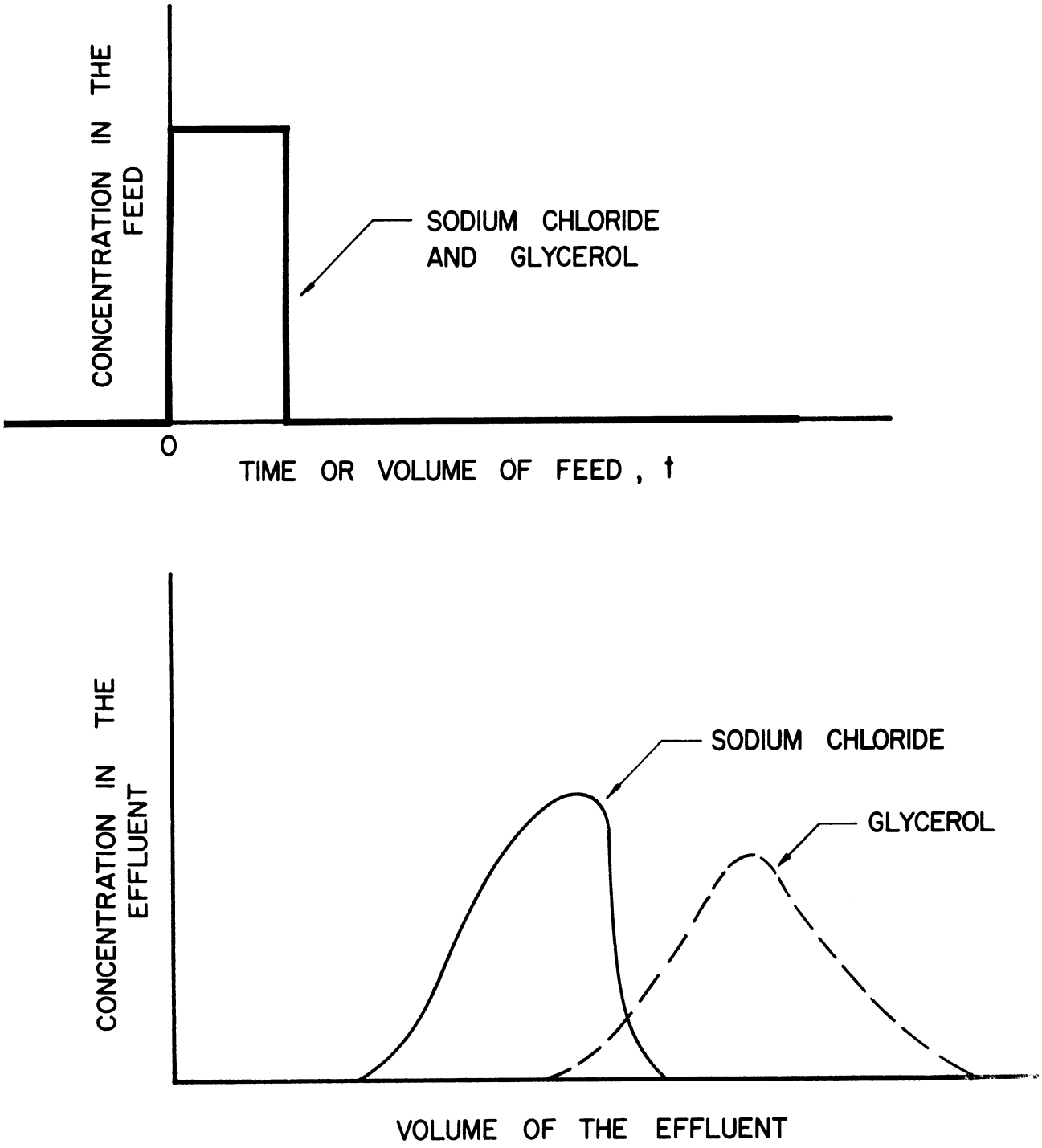

Figure 1. Typical Effluent Waves from an Ion-Exclusion Column.

design variables. The important physical characteristics are the equilibria between the solid and the liquid and the mass transfer resistances. Some of the important design variables are:

1) the volume of the bed;

2) the flow rate of the liquid;

3) the volume of the feed solution;

4) concentrations of solutes in the feed;

5) the diameter of the particles.

Figure 2 gives a few of the various "kinds" of the effluent waves that may be obtained.

The focus of this part of the dissertation is the relation between the effluent waves and the variables mentioned above. It is studied here with the aid of mathematical models.

A mathematical model is a set of mathematical equations that express the physical characteristics of the system of materials and the elementary mechanisms supposedly operating in the process under consideration. In the present study a differential equation is written expressing the material balance in a differential section of an ion-exclusion column. Other physical characteristics such as the mass transfer resistances and the solid-liquid equilibria are described by additional equations.

For the many possible physical characteristics of the systems and the many mechanisms that may be postulated, different mathematical models may be formulated. For example, the solid-liquid equilibrium may be linear or non-linear; the mass transfer resistances may or may not be negligible.

Several such different models are discussed in the next chapter. For the simpler models, analytic solutions of the differential equations

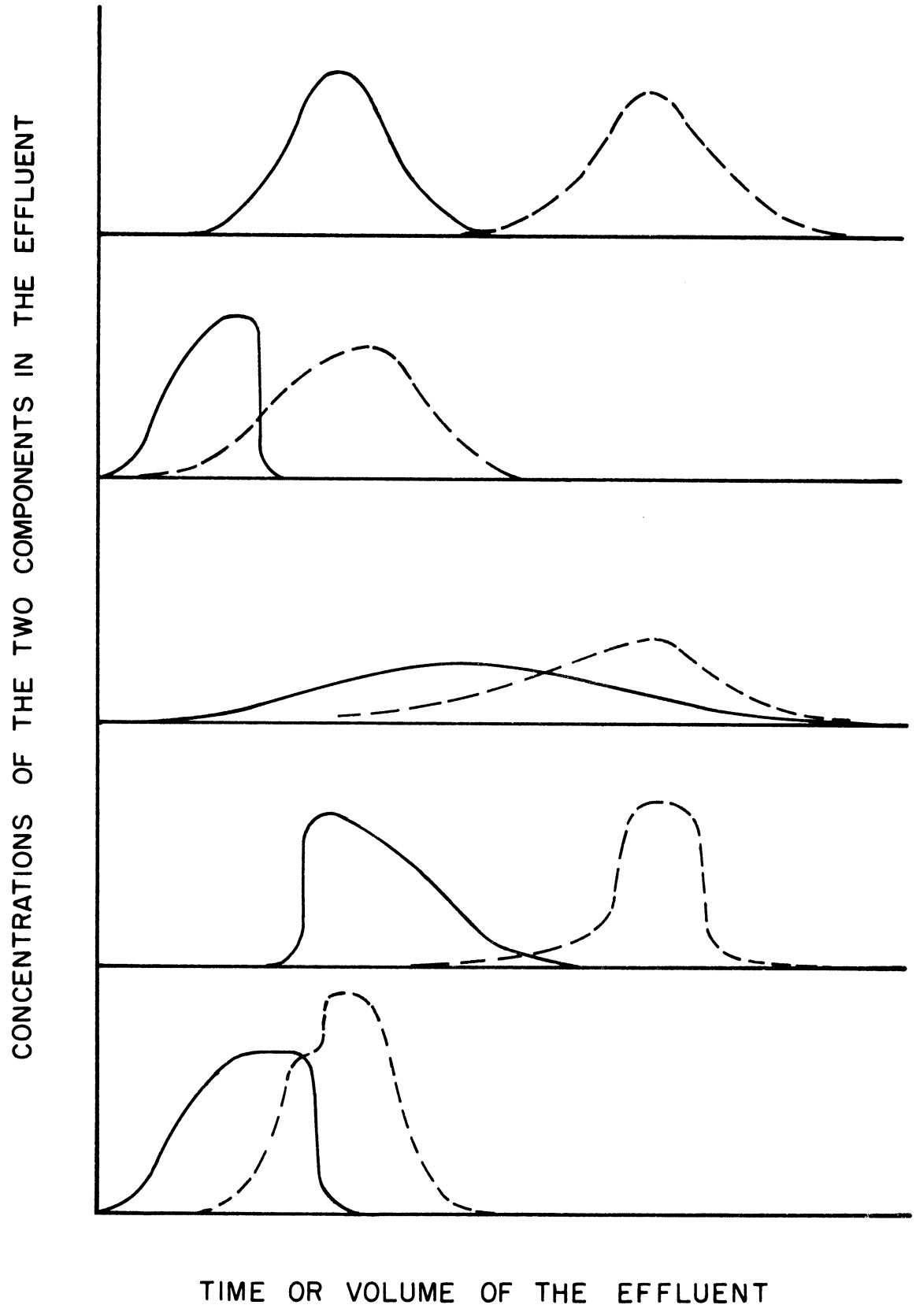

Figure 2. Different "kinds" of Effluent Waves From Ion-Exclusion Columns.

are possible. For more complex models, such as those involving non-linear equilibria, numerical solutions are suggested and the expected properties of the solutions are discussed qualitatively.

The emphasis in the next chapter is on the understanding of the "simpler" models. The use of an x-t contour diagram is advocated as an aid to understanding the characteristics of the effluent waves (such as the peak position, peak height, sharp and diffused trailing edges, etc.) predicted by the different simple models. The simpler models throw into relief the significant variables responsible for some of the basic characteristics of the effluent waves.

The following two models are treated in considerable detail.

(1) The operation of a column is such that the mass transfer resistances are negligible. The equilibrium between the solid and the liquid is arbitrary and non-linear. Model A (i) (b) .

(2) The mass transfer rate is controlled by the diffusion of the solute in the solid phase. The equilibrium is linear. Model B (i) (a) .

These models produce two typical "kinds" of effluent waves. Other mechanisms and phenomena frequently produce effluent waves "similar" to those produced by one of the above two models. For instance, swelling or shrinking of the solid tends to produce skewed waves which are also produced by non-linear equilibrium. Mass transfer resistances generally tend to disperse a wave symmetrically as it progress down a column.

The general problem involving both the non-linear equilibria and mass transfer resistances has not been solved. However, some

estimate of the solution can be made by approximating the equations to fit the above two models. In other words, frequently the effect of non-linear equilibrium and mass transfer resistances operating jointly, may be roughly estimated by considering their effects separately.

This is illustrated in Section III where attempts are made to predict and/or explain some ion exclusion data available in literature. The system glycerol-sodium chloride-water-Dowex 50 has been selected because equilibrium data of this system have been obtained by Shurts and White (S4, S5) and the diffusivities of the solutes in the resin are available from the research reported in Part I of this thesis.

The discussion of the mathematical models for ion-exclusion process is equally applicable to other mass transfer processes such as liquid-solid chromatography and to the processes involving complete saturation or elution of a fixed bed of solids.

II. MATHEMATICAL MODELS

1. Material Balance and General Discussion of the Basic Equations

An equation representing the material balance on a differential section of a resin bed has been written for each of the mathematical models considered here. Such an equation mathematically states that the net flow of a given material into a differential section of a bed is equal to the accumulation of the net contents of that material in the section. The accumulation includes the amount of the material in the liquid phase (i.e., in the voids of the bed), as well as the material absorbed in the solid phase.

The following equation describes the material balance for an arbitrary component, i, for several of the models considered here.

$$-\frac{\partial}{\partial x}(uC_i) = \frac{\partial}{\partial t}(\epsilon C_i + (1 - \epsilon) Q_i) \qquad (i)$$

Where i equals 1, 2, ... for the different solutes present, and

C_i = the concentration of the component i in the liquid phase,

Q_i = the average concentration of the component in the solid phase,

ϵ = the porosity of the bed, i.e., the fraction of the bed that is filled with the liquid,

u = the superficial velocity of the liquid flowing through the bed,

x = the distance along the bed in the direction of the flow of the liquid,

t = the time.

C_i and Q_i are functions of x and t.

The left side of the equation represents the net influx per unit volume of the differential bed of the component i due to the flow of the liquid solution through the bed. The right hand side of the equation is the consequent accumulation. The first term in the brackets is the amount of the component i in the liquid phase and the second term denotes the amount in the solid phase.

The equation is applicable under the assumptions of slug flow of the solution through the bed, absence of transverse concentration gradients in the bed, and no longitudinal mixing in the liquid. For more general cases that do not make these assumptions, additional terms would be present in the equation. These will be discussed later.

For each solute in the system, a separate material balance equation, such as Equation (1) may be written. The system of equations representing these material balances is solved simultaneously with another set of equations relating C_i and Q_i, that depend primarily on the physical characteristics of the system. Such a set of equations may be represented functionally by Equation (2) below:

$$f_i(C_1, C_2, \ldots, C_N, \quad Q_1, Q_2, \ldots, Q_N) = 0$$
$$i = 1, 2, \ldots, N \qquad (2)$$

For instance, under certain conditions column operation, the resistances to mass transfer may be negligible and at every point in the column the solid would then be in equilibrium with the solution. In that case,

the set of Equations (2) used in such a model would describe the equilibrium relations between the concentrations of the solutes in the solid and the liquid phases.

This second set of equations relating Q_i and C_i and representing the physical characteristics of system (such as equilibria and the mass transfer mechanisms), is used as the basis for classifying the various models considered here. These will be discussed further in the next section.

The material balance, Equation (1) described above, is a hyperbolic partial differential equation and it indicates certain characteristics of the propagation of disturbances. If the concentration of a component is changed suddenly at the entrance of the bed (at x=0), then the disturbance is propagated into the bed (to other values of x) in due course of time. In the x-t plane this propagation takes place along a line known as the characteristic of the differential equation. As a consequence of this propagation, break through curves and concentration waves are obtained in the effluent. The actual shapes of the waves and the break through curves are determined by the characteristics of the equilibria and the mass transfer resistances, which are represented by the second set of equations mentioned above.

The term $\frac{\partial}{\partial t}\{(1-\epsilon)Q_i\}$ in Equation (1) (the material balance equation) represents the instantaneous rate of transfer of the component i from the liquid phase into the solid phase. At times it may be more convenient to replace this by other mathematical expressions representing the rate of transfer of the component per unit volume of the bed. For example, if it is assumed that the diffusion of the component in the solid

phase controls the rate of mass transfer, then the above term may be replaced by the expression

$$- D\, S\left[\frac{\partial q}{\partial r}\right]_{r=R}$$

Where D is the diffusivity in the solid, S is the surface area of the solid per unit volume of the bed and $\left[\frac{\partial q}{\partial r}\right]_{r=R}$ is the concentration gradient from the surface of the particle into its interior.

If the superficial velocity, u, and porosity, ϵ, are assumed to be constant, the material balance equation becomes

$$u \frac{\partial C_i}{\partial x} + \epsilon \frac{\partial C_i}{\partial t} + (1-\epsilon) \frac{\partial Q_i}{\partial t} = 0$$

The distance along the bed, x, and the time, t, are the independent coordinates. The following transformation of coordinates,

$$z = \frac{1-\epsilon}{u} x$$

$$\theta = t - \frac{\epsilon}{u} x$$

simplifies the equation and reduces it to

$$\frac{\partial C_i}{\partial z} + \frac{\partial Q_i}{\partial \theta} = 0$$

Analytical as well as numerical solutions are often obtained more readily from the simplified equation.

The transformation mentioned above redefines the independent coordinates - distance along the bed, and time. Figure 3 shows the relation between the original and the transformed coordinates graphically. The "new" distance, z, is a multiple of the original distance, x. The

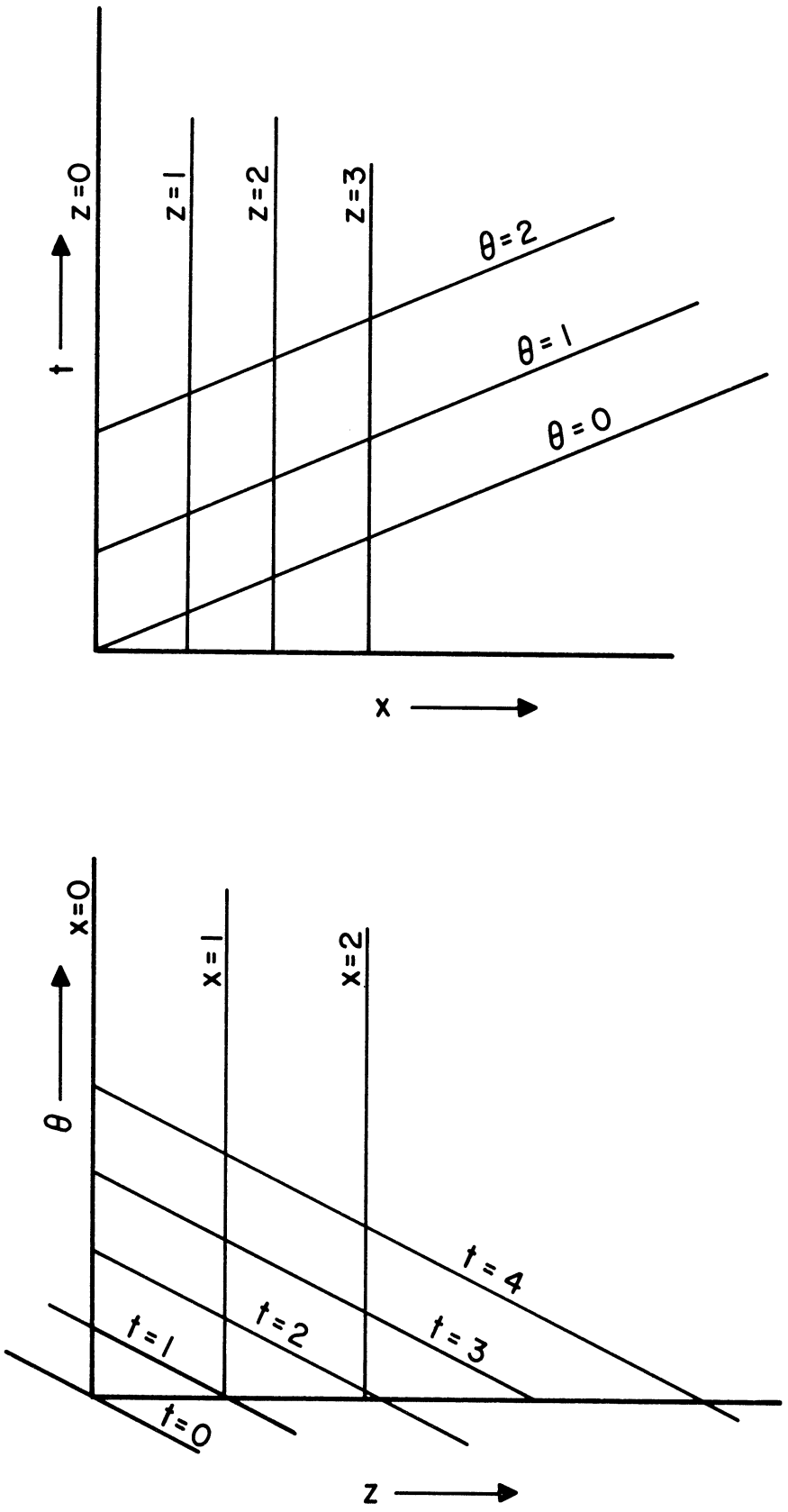

Figure 3. Transformation of Coordinates for Material Balance.

$$z = \frac{1-\epsilon}{u} x$$

$$\theta = t - \frac{\epsilon}{u} x$$

The "new" time coordinate, however, is a moving coordinate. At any point in the bed, the value of θ is zero when the first slug of liquid that entered the bed at the start of the process, reaches that point. It is as if the "new" time, θ, were measured at each point in the bed by a different clock, and each of these clocks were started when the first slug of liquid that entered the bed passed that point in the bed.

2. General Classification of the Models Considered

In a subsequent section of this chapter, various mathematical models for unsteady state, fixed bed, solid-liquid mass transfer operations are discussed in detail. The various models are introduced in increasing order of complexity. This sequence also follows a somewhat logical order of classification.

The main bases of the logical classification are the different physical characteristics of the system involved, such as equilibria and resistances to mass transfer.

If the resistance to mass transfer is almost negligible, a column may operate in such a fashion that the solid is always in equilibrium with the liquid surrounding it. Such an operation is called the equilibrium column operation. Non-equilibrium column operation is negatively defined as one which is not an equilibrium column operation.

If the equilibrium between the solid and liquid phases is linear, (i.e., the ratio of the concentration of a component in the solid to that in the liquid is independent of its concentration in the liquid) the solution of the mathematical models is simplified. This is the reason for classifying the models into those that assume linear equilibrium

and those that do not assume linear equilibrium. It is possible to have all the four combinations of the equilibrium and non-equilibrium column operations, and the linear and non-linear equilibria.

If more than one solute is present, the equilibrium characteristics of one solute may or may not depend on the concentrations of the other solutes. This gives the classification of "independent" and "interdependent" equilibria.

For the case of non-equilibrium column operations, different models are formulated for the different assumptions about the rates of mass transfer. For example, the mass transfer may be controlled by the rates of diffusion in the solid phase, or by the rates of transfer through the liquid film surrounding a solid.

Each of the different models mentioned above give a mathematical relation between the average concentration of the component i in the liquid phase, C_i, and that in the solid phase, Q_i. A set containing as many relations as there are solutes, is obtained. This set may be a set of algebraic equations, differential equations, or integro-differential equations. For example, in equilibrium column operation with n solutes there will be n equations describing the equilibrium functions, as follows:

$$Q_i = f(C_1, C_2, \ldots, C_n)$$

$$i = 1, 2, 3, \ldots, n .$$

Consider, as a second example, the case of non-equilibrium column operation where the diffusion in the solid is assumed to be the controlling resistance. For any component, i, the following differential

equation describes diffusion.

$$\nabla^2 q_i = \frac{1}{D} \frac{\partial q}{\partial t} \tag{3}$$

Where q_i is the concentration of the component i within the solid phase.

D is the diffusivity in the solid phase,

and

∇^2 is the Laplacian in the space coordinates within the solid phase.

The boundary condition is that, at all times, the value of q at the surface of the solid is given by the equation,

$$[q_i]_{\text{surface}} = f(C_1, C_2, \ldots, C_i, \ldots, C_n) \tag{4}$$

The average concentration in the solid, Q_i, is given by integrating q_i over the volume of the solid, τ, and then dividing it by the volume of the solid.

$$Q_i = \frac{1}{\tau} \int_{\tau} q_i \, d\tau \tag{5}$$

A set of equations (3), (4), and (5) for all the n solutes together defines the mathematical relation between the average concentration in the liquid phase, C_i, and that in the solid phase, Q_i.

As mentioned in the section on material balances this set of relations between C_i and Q_i has to be solved simultaneously with the material balance equations.

The effect of longitudinal diffusion in the liquid and that of the possible shrinkage and swelling of the solid particles are considered in some of the models. They modify the material balance equations mentioned above.

3. x-t Contour Diagrams

Consider a bed of solids over which a solution is passed. Let the initial concentration of the solution in the solid be zero. The solid absorbs the solute from the solution and eventually it gets saturated. Figure 4A represents the solution entering the column. Figures 4 B, C, and D give typical concentration curves in the effluent for different lengths of the column.

All these concentration curves for the different lengths of the column can be represented graphically by one x-t contour diagram as shown in Figure 5. x, the abscissa of the diagram, is the distance from the end of the column where the liquid is introduced. t, the ordinate of the diagram is time. The concentration of the liquid, c, is a function of x and t. In a three dimensional space, (x, t, c), this represents a surface. On an x-t plane, the level curves of this surface, or the contours of this surface, may be plotted. This gives the x-t contour diagram.

In Figure 5, the various curves represent the loci of the points in x-t plane at which the value of c is a constant. The t-axis (i.e., x=0), represents the entrance of the bed. The values of c along this axis represent the concentration history of the solution fed to the column. The x-axis, where t=0, represents the conditions in the column at the start of the operation.

A cross-section of the concentration surface taken at any particular value of x, along a vertical line, gives the effluent concentration history for the length of the column equal to x. Curves B, C, and D in Figure 4 are such cross sections of the contour diagram in Figure 5.

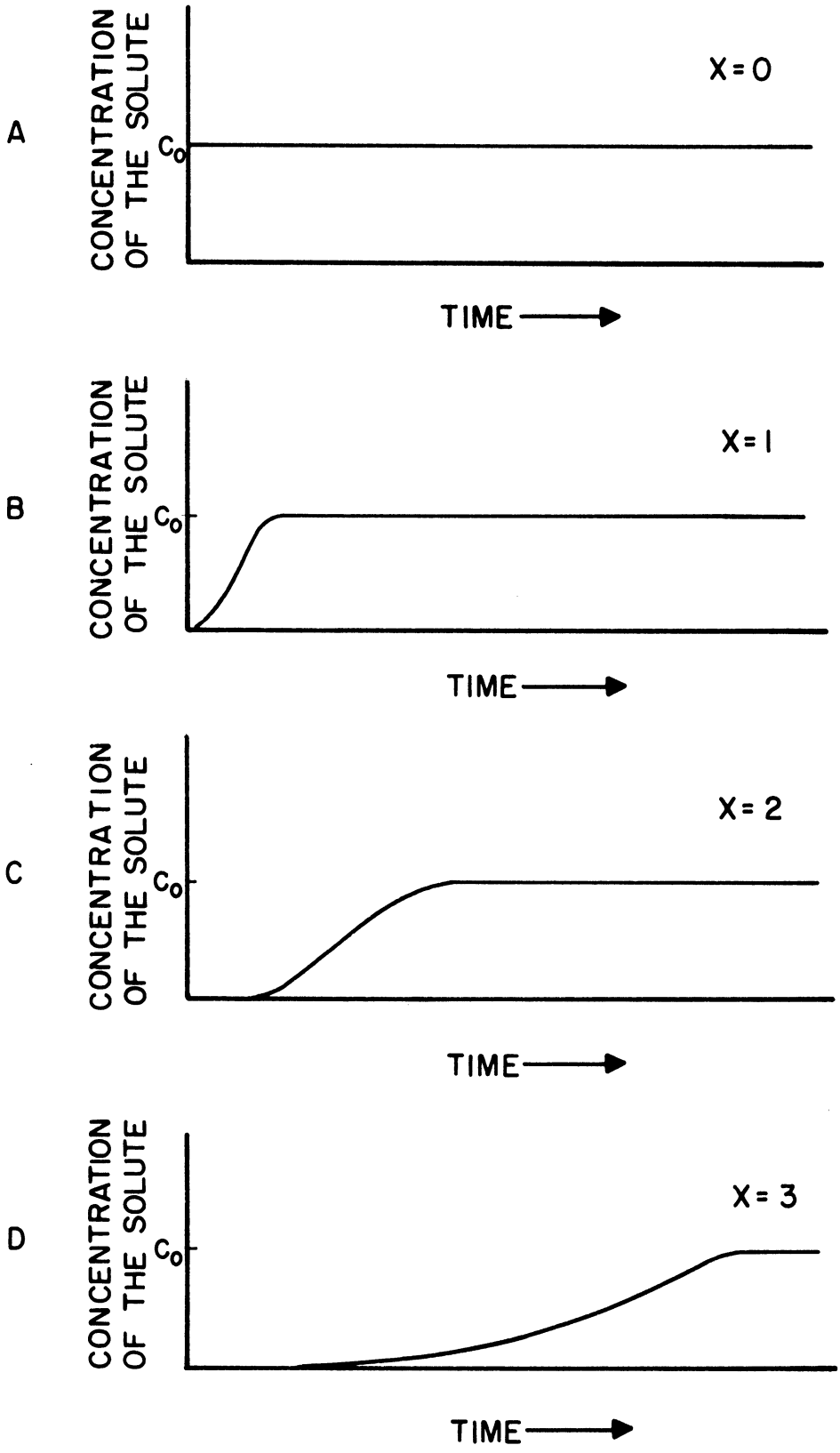

Figure 4. Break Through Curves for Different Bed Lengths.

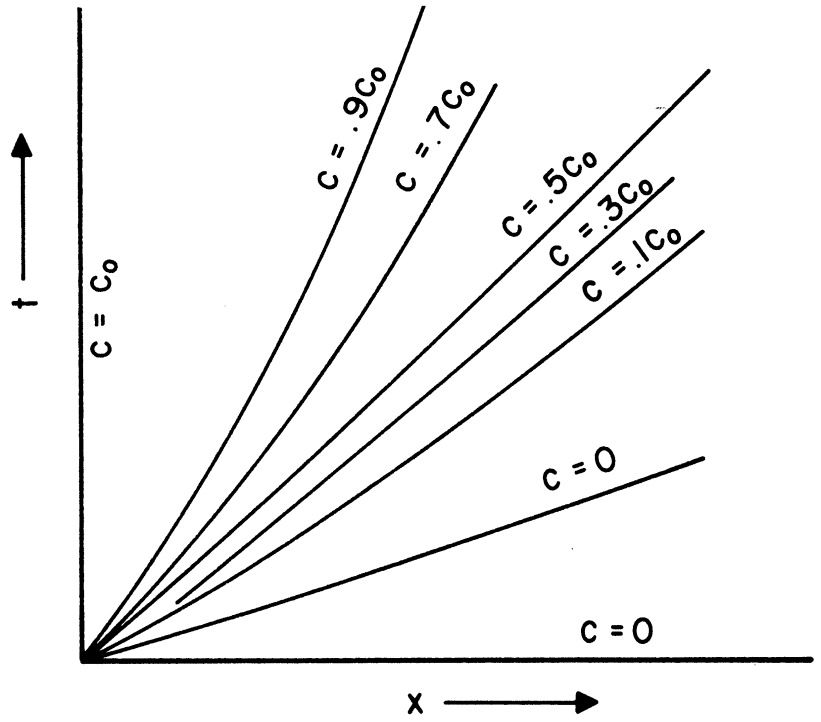

Figure 5. x-t Contour Diagram for a Chromatographic or an Ion-Exclusion Wave.

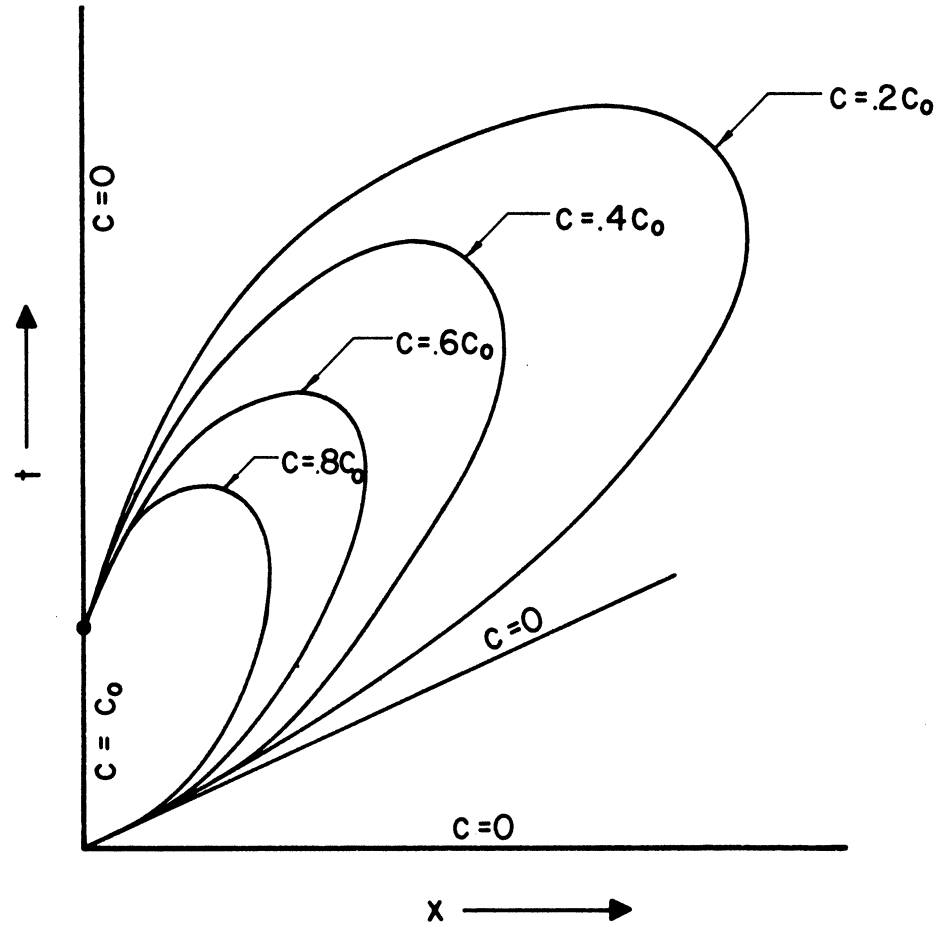

Figure 6. x-t Contour Diagram for a Chromatographic or an Ion-Exclusion Wave.

A cross section of the contour diagram taken at a constant value of t, along a horizontal line, represents the concentrations present along the length of the column at time equal to t. An instantaneous "appearance" of a chromatographic column is represented by this cross-section.

Figure 6 shows the contour diagram for the concentration of one component in a typical ion-exclusion process. As can be seen from the t-axis, a slug of the solution is first fed to the column and then pure solvent is passed through the column. The cross sections of the surface represented in the figure give the waves obtained in the effluent.

One concentration surface is obtained for each solute involved, and level curves may be drawn for each solute. Another set of concentration surfaces would be obtained for the concentration of the solutes in the solid phase. For equilibrium column operation, these are simply the values in equilibrium with the concentration of the liquid at all points in the x-t plane.

In the discussion on the various mathematical models, the x-t contour diagrams expected from the models are indicated. In a sense, the contour diagram is a graphical representation of the model. Certain characteristics of the concentration surfaces, such as slopes and crowding of the contour lines which can be visualized, are related to the inherent physical assumptions in the model. These relationships are brought out analytically wherever possible. In general, the author feels that if one were familiar with contour diagrams for the simpler models, some intuitive understanding of the column operation could be developed and it may be possible to make some predictions about the behavior of the more complex models.

Figure 7 shows the x-t contour diagrams that would be obtained if a solution were passed through a bed of inert solids. Assuming a slug flow of the liquid through the bed and assuming no longitudinal diffusion in the liquid, the material balance equation may be written as:

$$u \frac{\partial c}{\partial x} + \epsilon \frac{\partial c}{\partial t} = 0 \tag{6}$$

where u = the superficial velocity of the liquid.

ϵ = the porosity of the bed.

Since c is a function of x and t, the following relation between the partial derivatives is obtained.

$$\frac{\partial c}{\partial x} = - \left[\frac{dt}{dx}\right]_c \frac{\partial c}{\partial t} \tag{7}$$

$\left[\frac{dt}{dx}\right]_c$ in the above equation is considered at a constant value of c.

Substituting Equation (7) in Equation (6), Equation (8) is obtained.

$$\left\{u\left[\frac{dt}{dx}\right]_c - \epsilon\right\} \frac{\partial c}{\partial t} = 0 \tag{8}$$

Since $\frac{\partial c}{\partial t}$ cannot always be zero,

$$\left[\frac{dt}{dx}\right]_c = \frac{\epsilon}{u} \tag{9}$$

For each constant value of c, a level curve in the x-t plane must obey Equation (9). It must be a straight line with a slope equal to $\frac{\epsilon}{u}$. Thus, Equation (9) yields a family of parallel straight lines in the x-t plane as level curves for constant values of c. The value of c along any one of these lines is determined by the boundary conditions

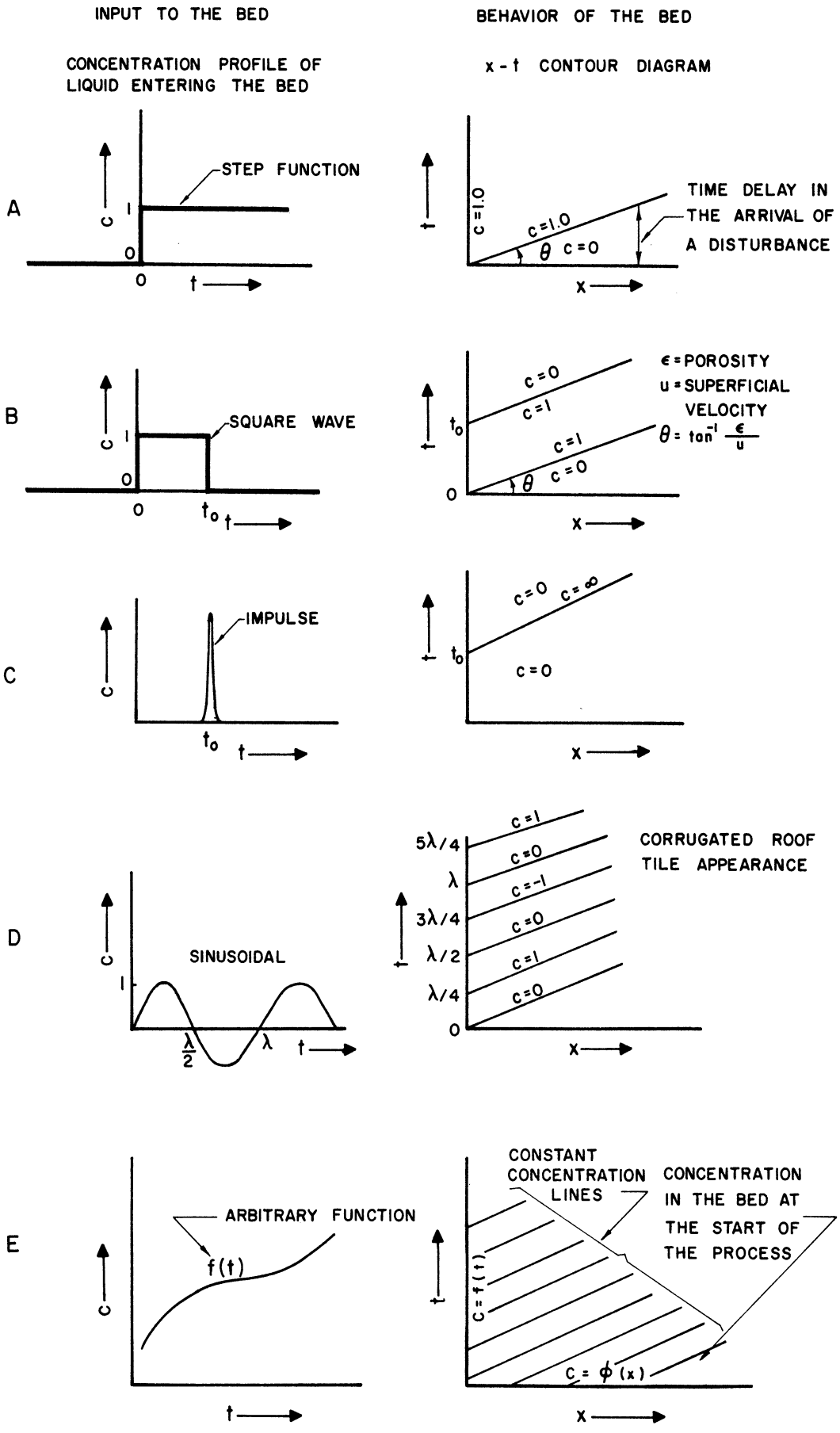

Figure 7. x-t Diagrams for a Bed of Inert Materials.

of the differential equation. As can be seen from Figure 7E, it is determined either by the concentration of the solution fed at the entrance of the bed or by the concentrations of the liquid present in the interstices of the bed at the start of the operation.

From Equation (9), $\frac{\epsilon}{u} x$ may be interpreted as the time required for the travel of a disturbance from the entrance of the bed to a point at the distance x. Graphically, it can seen from Figure 7A. If the porosity of the bed is increased, the time required for the travel is increased and the slope of the constant level lines, ϵ/u, is increased. If the velocity of the liquid is increased, the time for travel is decreased and the slope of the contour lines is reduced.

4. Various Models

As listed in the Table of Contents, the discussion of the various mathematical models considered will be given in the following order (of generally increasing complexity):

A. Equilibrium Column Operation

(i) Single Solute

(a) Linear Equilibrium (Simplest Model)

(b) Non-Linear Equilibrium

(c) Linear Equilibrium and Longitudinal Diffusion in the Liquid

(d) Arbitrary Equilibrium with Shrinkage and Swelling of the Solid

(ii) Two Solutes

(a) Independent Equilibria

(b) Interdependent Equilibria

B. Non-Equilibrium Column Operation

(i) Linear Equilibrium (One Solute)

(a) Diffusion in Solid as Controlling Mass Transfer Resistance

(b) Resistance in Liquid Film as the Controlling Mass Transfer Resistance

(c) Diffusion in Solid and Film Resistances in the Liquid

(d) Longitudinal Diffusion in the Liquid Added to Case (c)

(ii) Non-Linear Interdependent Equilibria (Two Solutes)

A. Equilibrium Column Operation

(i) Single Solute

(a) Linear Equilibrium

Mathematical Equations:

Material Balance:

$$u \frac{\partial c}{\partial x} + \epsilon \frac{\partial c}{\partial t} + (1-\epsilon) \frac{\partial Q}{\partial t} = 0 \qquad (10)$$

Equlibrium Relation:

$$Q = K c \qquad (11)$$

Feed History (Boundary Condition):

$$c = f(t) \quad \text{at} \quad x = 0 \qquad (12)$$

Initial Condition (of the column):

$$c = \varphi(x) \quad \text{at} \quad t = 0 \qquad (13)$$

Where

c = the concentration of the solute in the liquid. It is a function of x and t.

Q = the concentration of the solute in the solid.

x = the distance from the inlet end of the bed.

t = time.

ϵ = the porosity of the bed, i.e., the volume of the voids per unit volume of the bed.

K = the equilibrium constant, i.e., the ratio of the concentration of the solute in the solid to that in the liquid phase at equilibrium. K is independent of concentrations.

u = the superficial velocity of the liquid.

Equation (10) is the material balance for a differential section of the bed. Superficial velocity of the liquid and porosity of the bed are assumed to be constant. Equation (11) is the equilibrium relation between Q and c. The constancy of K indicates linear equilibrium. Equation (12) is the condition at the inlet of the bed. It is the concentration history of the liquid fed to the column, where f(t) is an arbitrary function. Equation (13) gives the initial condition obtaining throughout the column at the start of the operation, where $\varphi(x)$ is an arbitrary function.

Substitution of Equation (11) in (1) yields Equation (14).

$$u \frac{\partial c}{\partial x} + \{\epsilon + (1-\epsilon)K\} \frac{\partial c}{\partial t} = 0 \qquad (14)$$

Since c is a function of x and t,

$$\frac{\partial c}{\partial x} = - \left[\frac{dt}{dx}\right]_c \frac{\partial c}{\partial t} \qquad (15)$$

Substituting Equation (15) in Equation (14), Equation (16) is obtained

$$\left\{- u \left[\frac{dt}{dx}\right]_c + [\epsilon + (1-\epsilon)K]\right\} \frac{\partial c}{\partial t} = 0 \qquad (16)$$

Since $\frac{\partial c}{\partial t}$ cannot alwyas be zero, Equation (17) is obtained from Equation (16).

$$\left[\frac{dt}{dx}\right]_c = \frac{\epsilon + (1-\epsilon)K}{u} \qquad (17)$$

Equation (17) defines the condition that any level curve of constant c must fulfill. It can be seen from the equation that the level curves are parallel straight lines having a slope equal to the right side of the equation. The actual value of the concentration along any

one of these level curves depends on the boundary condition f(t) and the intial condition of $\varphi(x)$.

If ϵ is substituted, for the expression $\{\epsilon + (1-\epsilon)K\}$ in Equation (14), the resulting equation is identical to material balance equation for the case of flow through inert solids (compare with Equation (6) of the previous section). Consequently, the solution of the model under consideration is almost the same as that for a liquid passing through a bed of inert solids. Because of the equilibrium absorption by the solid, however, the capacity of the column for holding the solute has been increased and the effective porosity of the bed has been increased by $(1-\epsilon)K$. The volume fraction of the bed occupied by the solid, $(1-\epsilon)$, may be considered as partially pervious to the solute. The average residence time for a solute particle is increased, and the time delay for a disturbance in the value of c to propagate from the entrance of the bed to the point x is increased from the value $\frac{\epsilon}{u}x$ in the case of the bed on inert materials (discussed in the previous section) to the value $\frac{\epsilon + (1-\epsilon)K}{u}x$, as can be seen from Equation (17). In the above expression, the first term $\frac{\epsilon}{u}x$ is the time delay due to the porosity of the bed and the second term $\frac{(1-\epsilon)K}{u}x$ is the time delay due to equilibrium absorption of the solute by the solid. This is increased as K increases.

The x-t diagram in Figure 8 indicates that any arbitrary concentration profile initially present in the bed would travel across the bed without any distortion. If this model is applicable, a chromatographic band would travel without widening or narrowing. Any arbitrary concentration wave introduced in the feed to a column would be reproduced

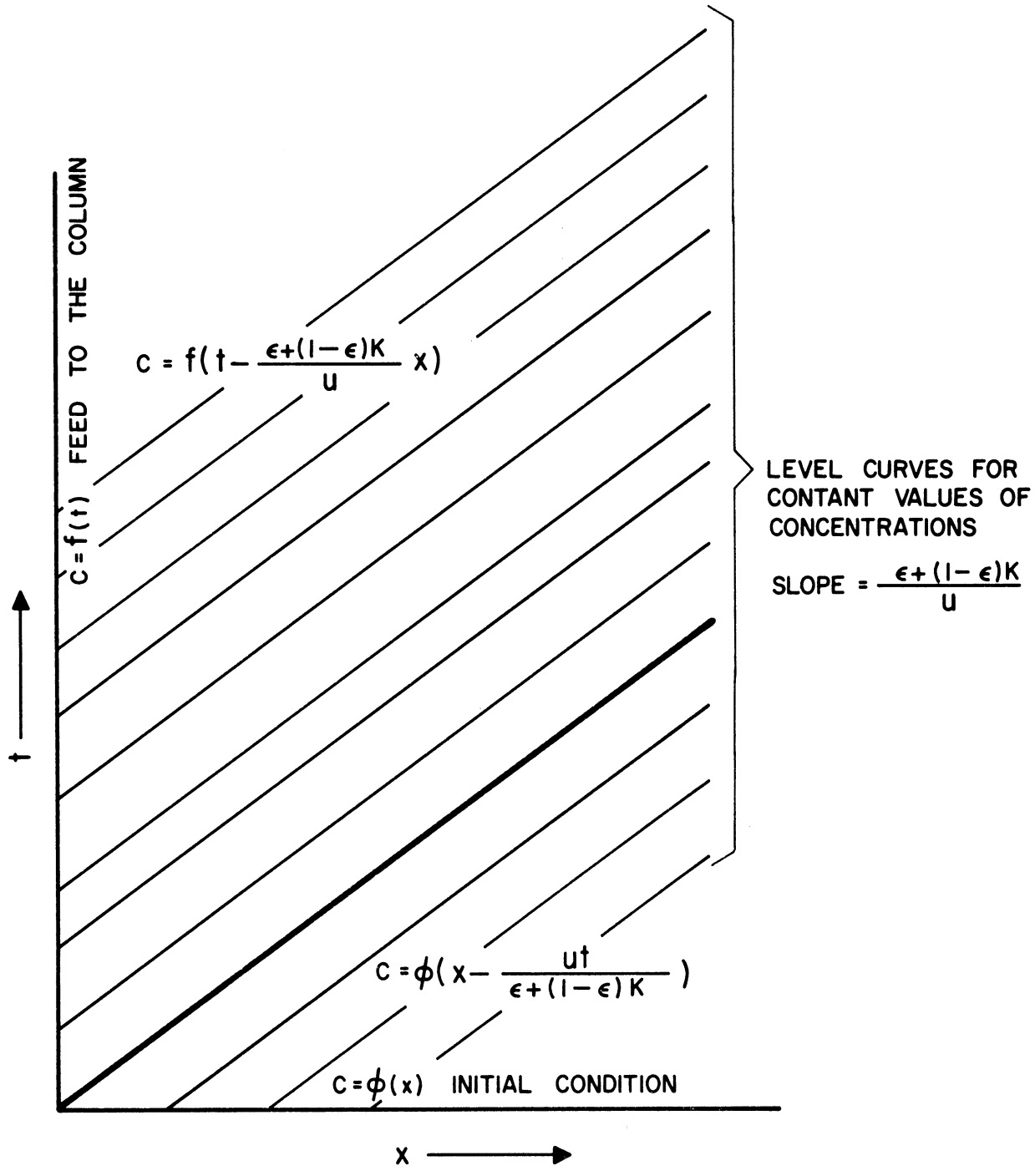

Figure 8. x-t Contour Diagram for Model A(i)(a) and for Arbitrary Boundary Conditions.

in the effluent without any distortion. It would, however, be displaced. The extent of the displacement would be greater for higher values of the equilibrium constant, K.

Figure 9 shows the x-t contour diagrams obtained for different concentration histories of the feed to the column.

(b) Non-Linear Equilibrium

Mathematical Equations:

Material Balance:

$$u \frac{\partial c}{\partial x} + \epsilon \frac{\partial c}{\partial t} + (1-\epsilon) \frac{\partial Q}{\partial t} = 0 \qquad (18)$$

Equilibrium Function:

$$Q = F(c) \qquad (19)$$

Feed History:

$$c = f(t) \quad \text{at} \quad x = 0 \qquad (20)$$

Initial Condition:

$$c = \varphi(x) \quad \text{at} \quad t = 0 \qquad (21)$$

Where

c = the concentration of the solute in the liquid. It is a function of x and t.

Q = the concentration of the solute in the solid.

x = the distance from inlet end of the bed.

t = the time.

ϵ = the porosity of the bed.

u = the superficial velocity of the liquid.

$F(c)$ = an arbitrary equilibrium function of c.

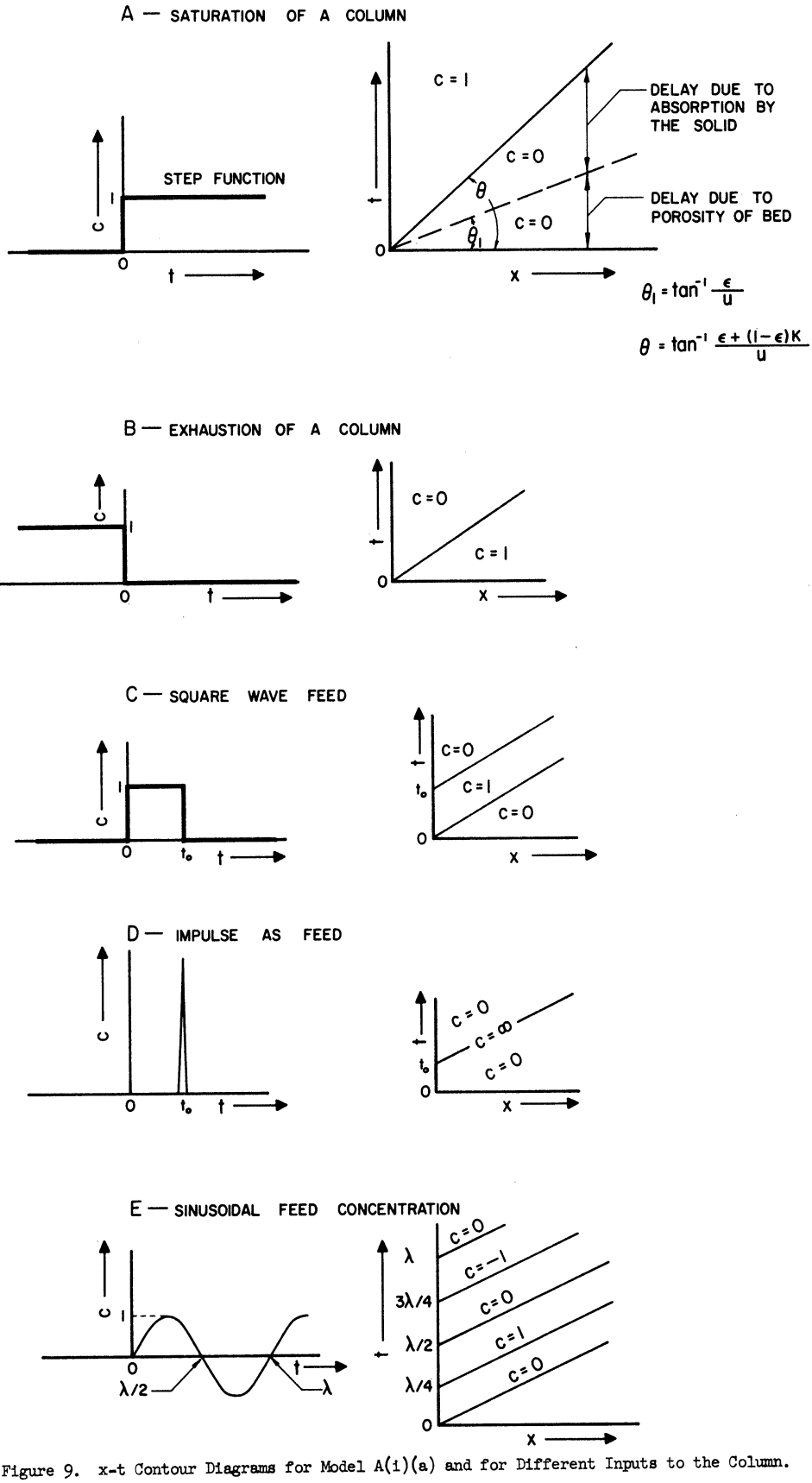

Figure 9. x-t Contour Diagrams for Model A(i)(a) and for Different Inputs to the Column.

Equation (19) defines an arbitrary non-linear equilibrium characteristic of the system. The rest of the equations and assumptions are the same as the ones discussed before for the case of linear equilibrium (Model A(i) (a)).

Since $Q = F(c)$,

$$\frac{\partial Q}{\partial t} = \left(\frac{dQ}{dc}\right) \frac{\partial c}{\partial t} = \frac{dF(c)}{dc} \cdot \frac{\partial c}{\partial t}$$

Substituting this in Equation (18)

$$u \frac{\partial c}{\partial x} + \left[\epsilon + (1-\epsilon) \frac{dF(c)}{dc}\right] \frac{\partial c}{\partial t} = 0 \qquad (22)$$

Substituting the relation (23) into Equation (22), Equation (24) is obtained

$$\frac{\partial c}{\partial x} = - \left[\frac{dt}{dx}\right]_c \frac{\partial c}{\partial t} \qquad (23)$$

$$\left\{- u \left[\frac{dt}{dx}\right]_c + \epsilon + (1-\epsilon) \frac{dF(c)}{dc}\right\} \frac{\partial c}{\partial t} = 0 \qquad (24)$$

At each constant value of c, $\frac{dF}{dc}$ is a definite number for a given system and the level curve for this value of c in the x-t plane satisfies the equation

$$- u \left[\frac{dt}{dx}\right]_c + \epsilon + (1-\epsilon) \frac{dF}{dc} = 0$$

or,

$$\left[\frac{dt}{dx}\right]_c = \frac{\epsilon + (1-\epsilon) \frac{dF}{dc}}{u} \qquad (25)$$

Equation (25) represents a family of straight lines with the slopes equal to the right hand side of the equation, which itself depends on the value of the concentration of the liquid for which the level curve is being considered.

Depending on the equilibrium function F(c), for a given concentration history of the feed to the column, f(t), the concentration in the effluent may show continuous variations or discontinuous jumps. These will be discussed in some detail below.

To illustrate the effect of different equilibrium functions, consider a column which is originally free of the solute. A feed containing a constant concentration is introduced into the column and the solid eventually gets saturated with the feed solution.

For two common types of non-linear equilibria shown in Figure 10, the behavior of the column will be different. The two types of equilibria considered are:

(i) the ratio of concentration in the solid to that in the liquid increases with the increased concentration of the liquid (i.e. $\frac{d^2F}{dc^2}$ is positive).

and

(ii) the ratio of concentration in the solid to that in the liquid decreases with increased concentration in the liquid (i.e. $\frac{d^2F}{dc^2}$ is negative).

Figures 11 and 12 show the behavior of the column for equalibria of type (i) above. The slope of the level curves for constant concentrations on the x-t diagram depends on the value of $\frac{dF}{dc}$ for the concentration for which the level curve (the straight line) is drawn. Since $\frac{dF}{dc}$ increases with increasing concentration, the slope of the level curves also increases. The concentration profiles in the bed show a broadening boundary between the saturated and unsaturated portions of

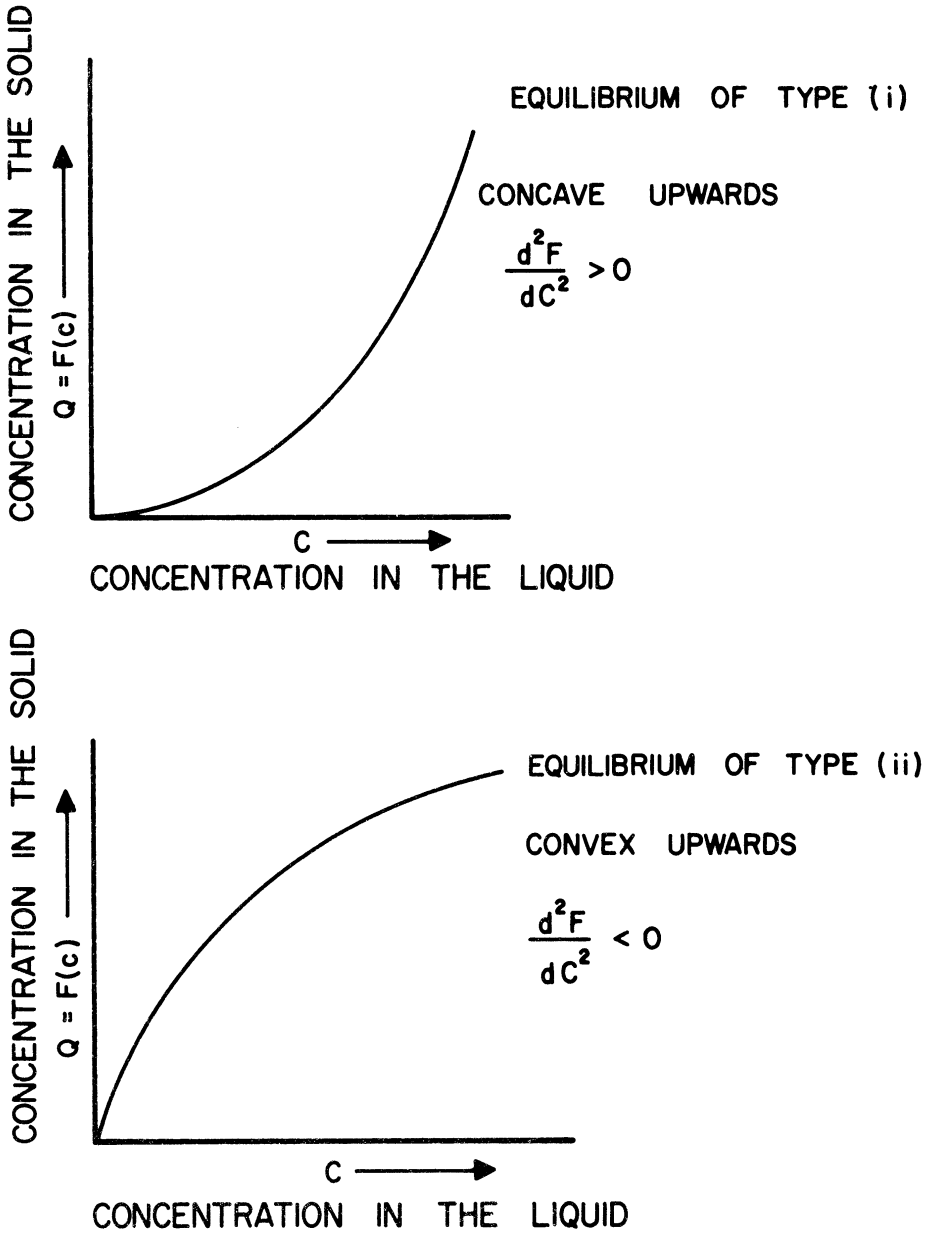

Figure 10. Two Common Types of Non-Linear Equilibria for a Single Solute.

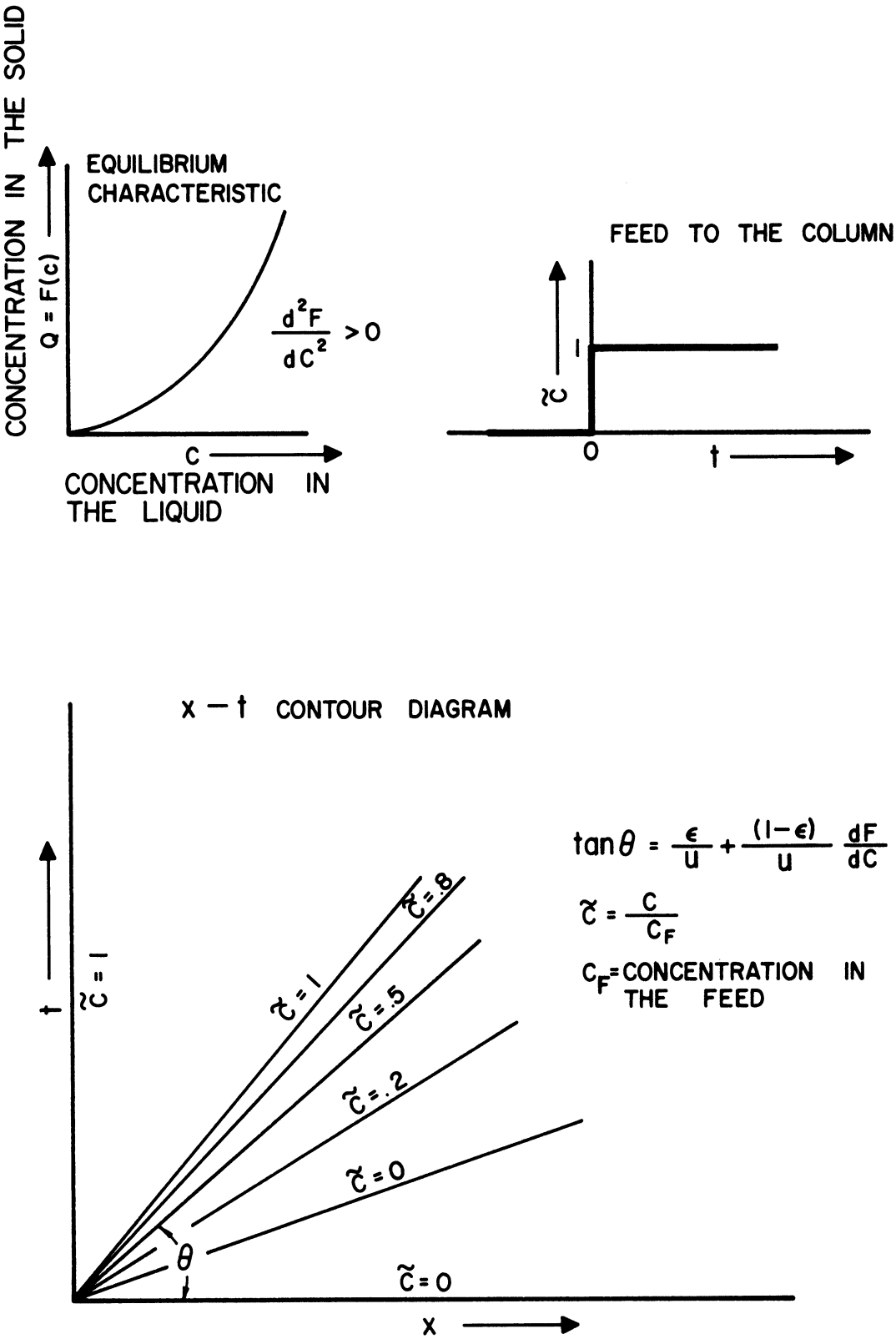

Figure 11. Saturation of an Equilibrium Column with Non-Linear Equilibrium of Type(i). Model A(i)(b).

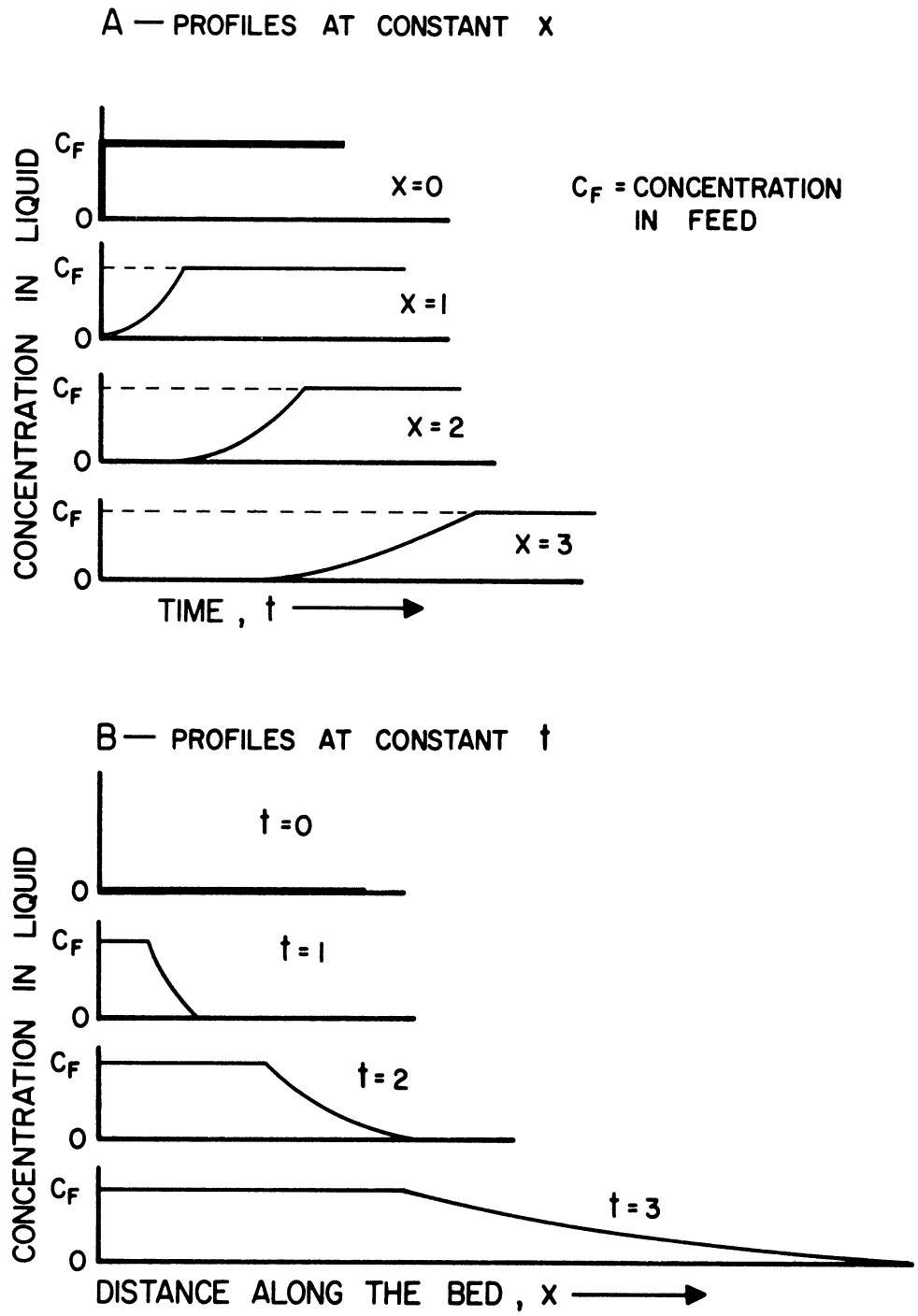

Figure 12. Cross Sections of the Surface Represented by x-t Diagram in Figure 11.

the bed as the solution is fed to the column or as time increases. See Figure 12B.

In Figure 13B, the curve ABEG is the concentration history of the effluent from a column of length x_o. At time equal to t_1 the column is saturated, and steady state is established. The shaded area ABEL represents the total amount of material retained by the column. This consists of the material retained in the pores of the column, equal to the area AMNL, and that retained by the solid saturated with the solute, equal to the area MBEN. The distance AM represents the delay in appearance of the break through curve due to the porosity of the column. The distances MB to MP represent the delay due to the absorption by the solid.

Let J be a point on the t-axis such that the area MJHN is equal to the area MBEN, which represents the total amount of solute retained by the saturated solid. The locus of the point t_o for different values of x_o is plotted as the dotted line on the x-t contour diagram on Figure 13A. This is a straight line of slope $\frac{\epsilon}{u} \quad \frac{(1-\epsilon)}{u} \quad \frac{F(c_F)}{c_F}$ where c_F is the concentration in the feed.

Consider the two contour diagrams given in Figure 14. Figure A is the actual diagram obtained for saturation of a column. It is the same as Figure 13A. Figure B, on the other hand, is a hypothetical contour diagram that would have been obtained if the equilibrium had been linear. The dotted line on this Figure 14B is the same as the dotted line on the Figure 13A. Figure 14B is identical to the previously discussed contour diagrams obtained for the simpler model with linear equilibrium (Model A(i) (a)). The effect of non-linear equilibrium has been

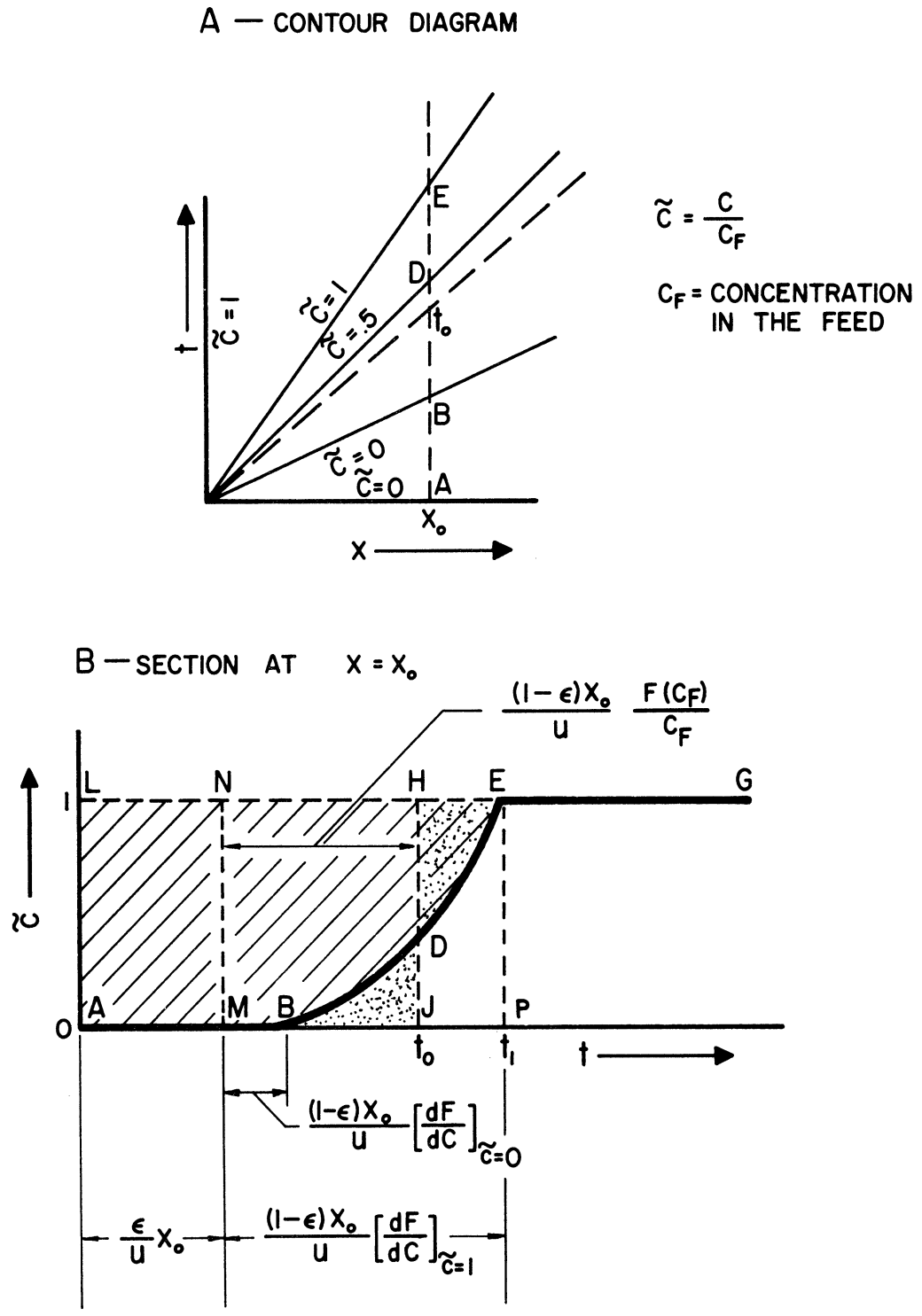

Figure 13. Overall Material Balance in Saturation of a Bed According to Model A(i)(b) for Equilibrium with $\frac{d^2F(c)}{dc} > 0$.

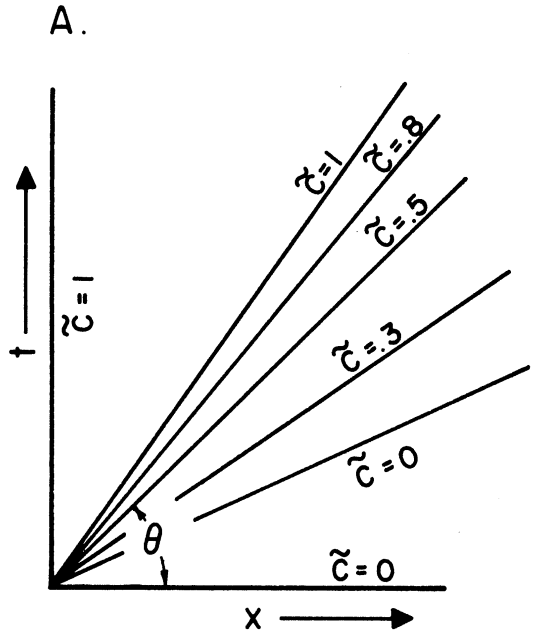

$$\theta = \tan^{-1}\left[\frac{\epsilon}{u} + \frac{(1-\epsilon)}{u}\frac{dF}{dC}\right]$$

$$Q = F(c)$$

$$\frac{d^2F}{dC^2} > 0$$

$$\tilde{C} = \frac{C}{C_F}$$

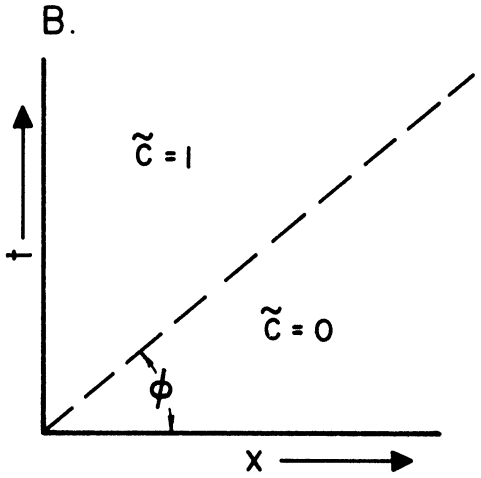

$$\phi = \tan^{-1}\left[\frac{\epsilon}{u} + \frac{(1-\epsilon)}{u}\frac{F(C_F)}{C_F}\right]$$

Figure 14. Smearing of a Discontinuous Section of a Concentration Surface by Non-Linear Equilibrium. Model A(i)(b).

to smear the sharp discontinuous edge of the concentration surface obtained in the case of linear equilibrium.

The above discussion and all the figures considered were for the saturation of a column and for the non-linear equilibrium of type (i) in which $\frac{d^2F}{dc^2} > 0$ (concave upwards). The following discussion on the saturation operation of a column considers the alternate case of non-linear equilibrium of type (ii) in which $\frac{d^2F}{dc^2} < 0$ (convex upwards). Subsequently, exhaustion operation of a column will be considered for both types of non-linear equilibria.

The case at hand illustrates an important characteristic of non-linear problems. "Self-sharpening" boundaries may be produced and "shock-fronts" and discontinuous concentration profiles may develope.

Concentration surfaces in the three dimensional (x, t, c) space that are given by Equation (25) above are sketched in Figure 15 for the two types of non-linear equilibria. Both the sketches are for saturation column operation. Sketch A shows the continuous surface for the equilibrium type (i); Figures 11 and 12 discussed above show the level curves and cross sections of this surface. Sketch B shows the continuous surface indicated by Equation (25) for the equilibrium type (ii). It is a physical impossibility to obtain the effluent curves predicted by the cross section of this surface, e.g., the curve ABDE in Figure 15B. Consequently, the continuous solution of the mathematical equations describing the model is not applicable and a discontinuous solution is suggested.

The x-t Contour Diagram in Figure 16 depicts the discontinuous solution for the case under consideration. The concentration surface has an edge of discontinuity and the various sections at constant t and at constant x would also show sharp boundaries.

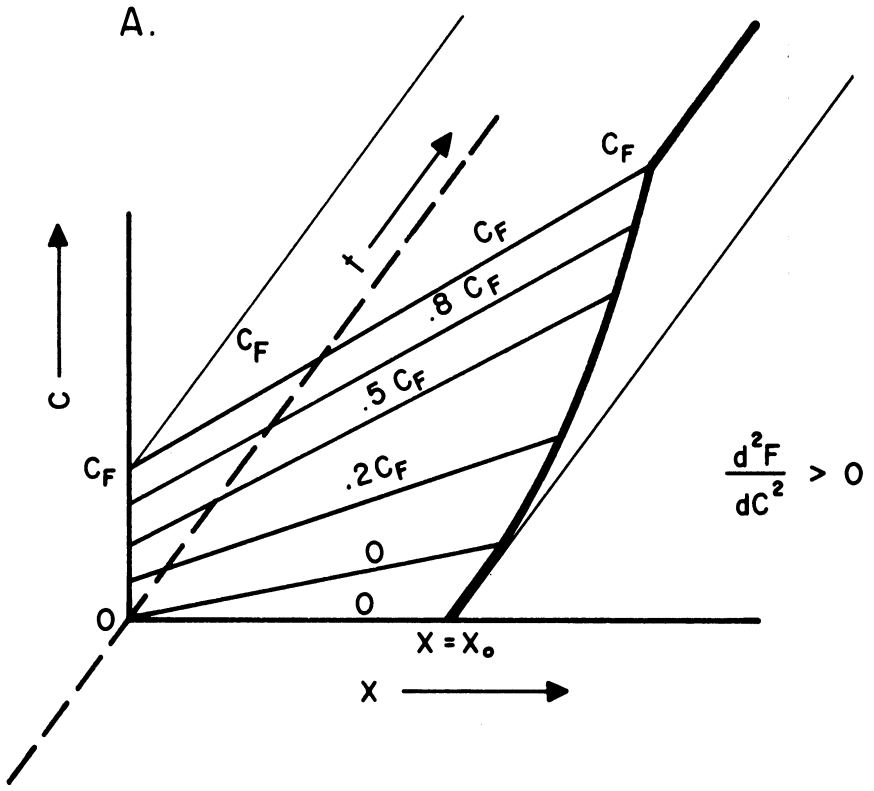

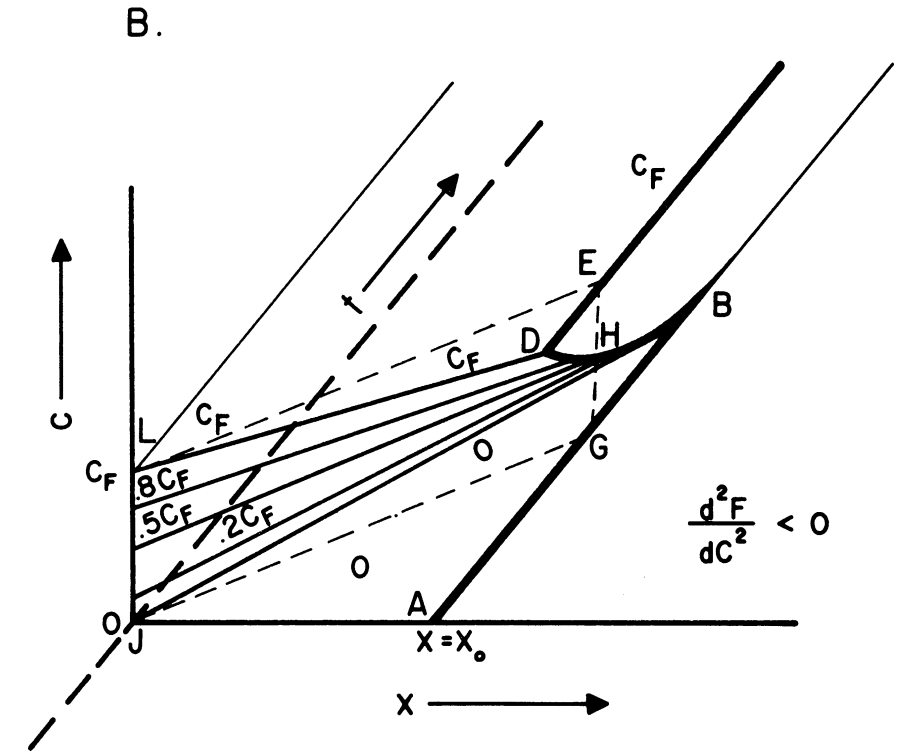

Figure 15. Concentration Surfaces for Saturation Column Operation with Non-Linear Equilibria.

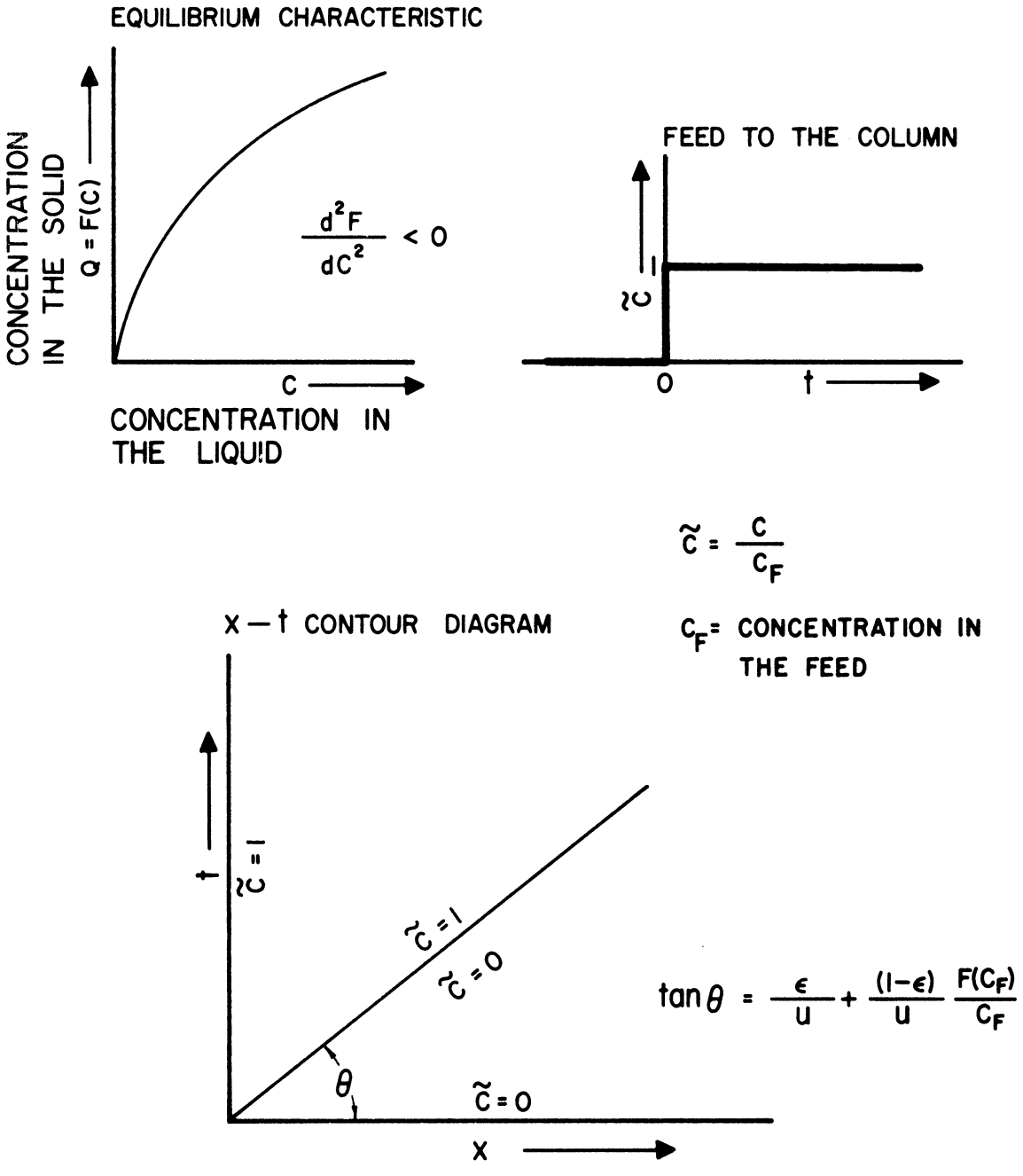

Figure 16. Saturation of an Equilibrium Column with Non-Linear Equilibrium of Type (ii).. Model A(i)(b).

The restriction imposed by the overall material balance dictates the shape and the location of the edge of discontinuity. As explained above with the aid of Figure 13B, the total amount of the solute retained by the bed can be determined from the effluent curve. The effluent curves for the case at hand are all step functions. If at the value of $x=x_1$, the "jump" in the effluent concentration occurs at $t=t_1$, then $t_1 c_F$ will represent the total amount of the solute retained by the bed, where c_F is the concentration of the solute in the feed. Considering the total amount of solute that can be retained in the voids in the bed and in the saturated solid,

$$t_1 c_F = \frac{\epsilon}{u} c_F x_1 + \frac{(1-\epsilon)}{u} F(c_F) x_1$$

The above equation gives the equation for the edge of discontinuity shown in the Contour Diagram on Figure 16. On Figure 15, the plane JLEG represents the discontinuity in the concentration surface. Consistant with overall material balance, areas of the three sided figures GBH and DEH are equal.

In terms of propagation of a disturbance, in the case of linear equilibria, a disturbance at the entrance of a bed is propagated with a uniform velocity and without any distortion; in the case of non-linear equilibria where $d^2F/dc^2 > 0$, a disturbance of increase in concentration is dissipated as it travels down the column; and in the case of non-linear equilibria where $d^2F/dc^2 < 0$, a disturbance of an increase in concentration produces a "shock front" that travels down the column.

The different slopes of the level curves given by Equation (25) may be considered as different velocities of propagation for different concentrations. If the equilibrium is concave upwards, the equilibrium

constant increases with the concentration and the regions of high concentration would have greater proportionate absorption by the solid and greater residence time in the bed then the regions of low concentration. Effectively, a region of low concentration would move faster through the bed then a region of high concentration. On the other hand, if the equilibrium is convex upwards, a region of high concentration would move faster through the bed than a region of low concentration. This difference in effective velocities of propagation through the bed between region of high and low concentrations produces broadening of some concentration profiles and sharpening of others.

The saturation operation of a column has been considered above. If a column were originally saturated with a solute and then it were to be exhausted by passing a solvent, almost reciprocal behaviors of the columns are obtained in the sense that the Contour Diagram for exhaustion of a column with equilibrium of type (i) is similar to the Contour Diagram for the saturation of a column with the equilibrium of type (ii). The following table may clarify this.

Figures 17 and 18 show the x-t Contour Diagrams for exhaustion of a column for the two types of non-linear equilibria.

	Equilibrium Type (i)	Equilibrium Type (ii)
	Concave Upwards	Convex Upwards
Saturation Column Operation	Continuous concentration surface and diffusing boundaries	Discontinuous concentration surface and sharp boundaries
Exhaustion Column Operation	Discontinuous concentration surface and sharp boundaries	Continuous concentration surface and diffusing boundaries

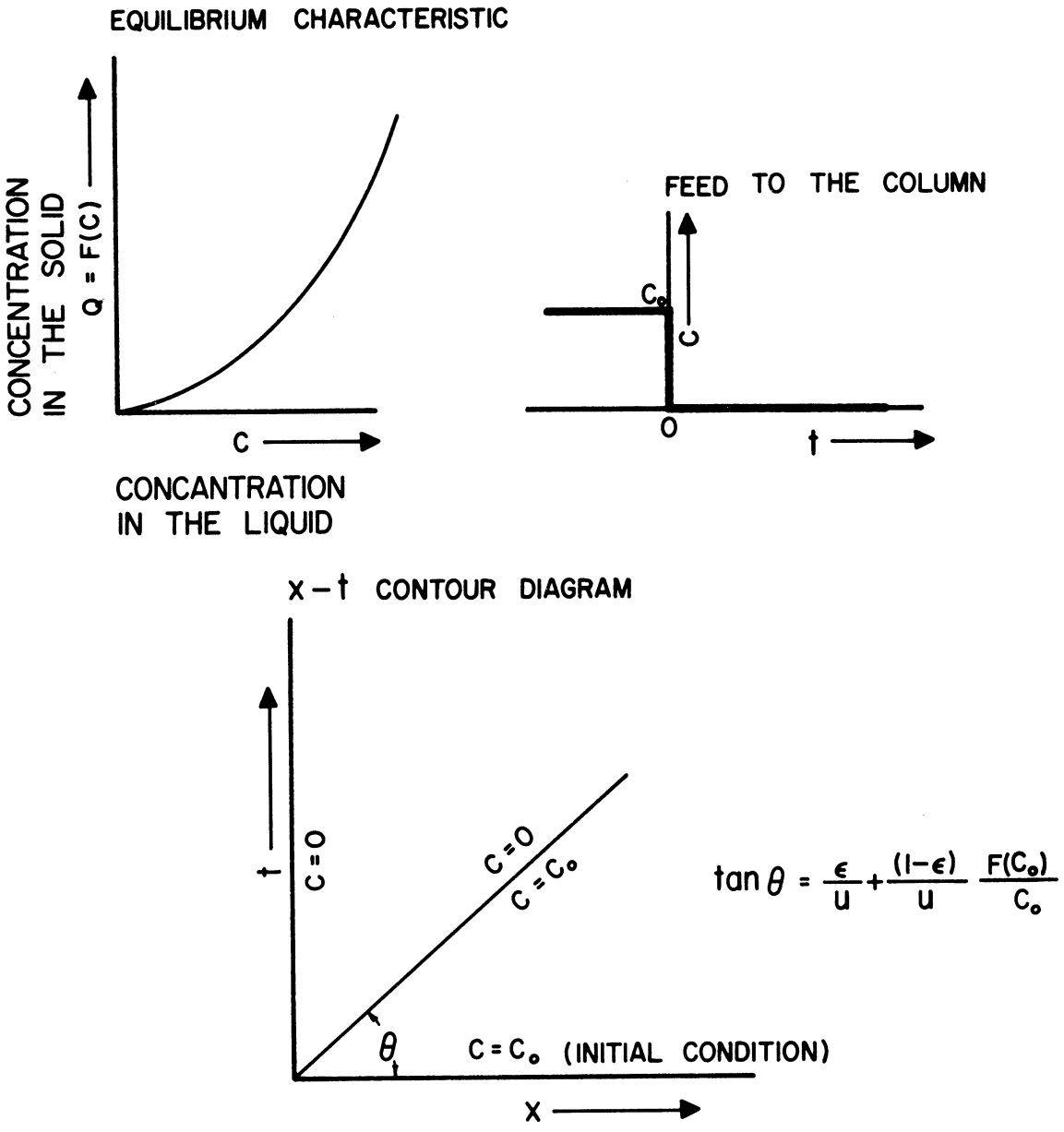

Figure 17. Exhaustion of an Equilibrium Column with Non-Linear Equilibrium of Type (i). Model A(i)(b).

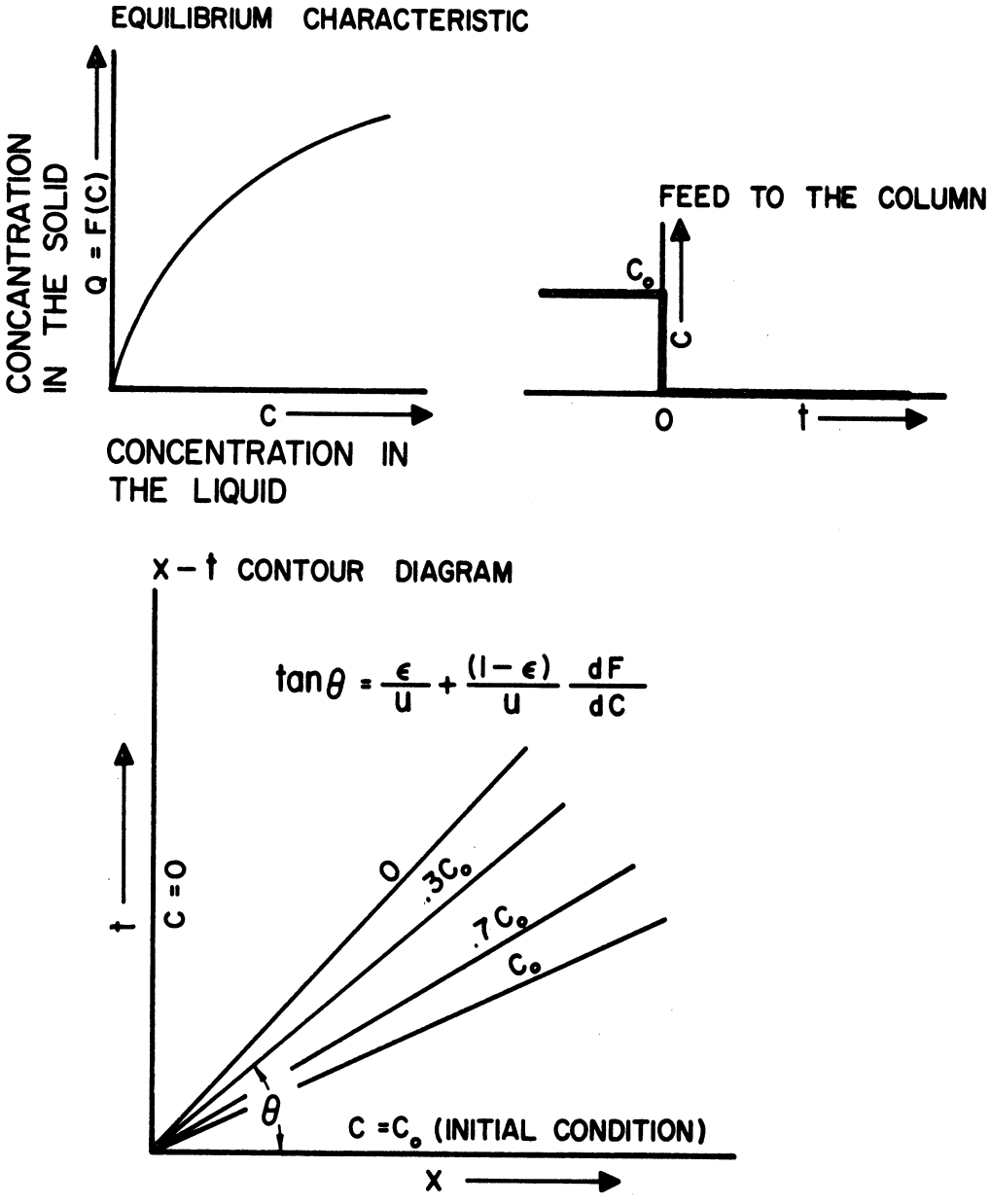

Figure 18. Exhaustion of an Equilibrium Column with Non-Linear Equilibrium of Type (ii). Model A(i)(b).

The understanding of the operation of saturation and the exhaustion column can be used to predict the performance of a column to which a slug of the solution containing the solute is fed.

Figure 19 shows the Contour Diagram for type (i) equilibrium. At point M the disturbance is that of increasing concentration (saturation of a column) and constant concentration profiles spread out in the x-t plane. The slope tan θ is given by

$$\left\{\frac{\epsilon}{u} + \frac{(1-\epsilon)}{u} \frac{dF(c)}{dc}\right\} .$$

At point A, the disturbance is one of decreasing concentration (exhaustion of a column) and overall material balance restrictions determine the slope of the line AB, which is given by

$$\tan \varphi = \left\{\frac{\epsilon}{u} + \frac{(1-\epsilon)}{u} \frac{F(c_F)}{c_F}\right\} . \qquad (25a)$$

Beyond point B, along the line BD, the maximum concentration is less than c_F. The broadening of the effluent waves shown in Figure B has increased so much that there is not enough material fed to the column. The concentration along the line BD hence decreases gradually from c_F to zero.

The slope of the curve BD also decreases gradually. At B, the slope is the same as that of AB. Along BD it decreases and asymptotically approaches a value equal to the slope of the line MN on the figure.

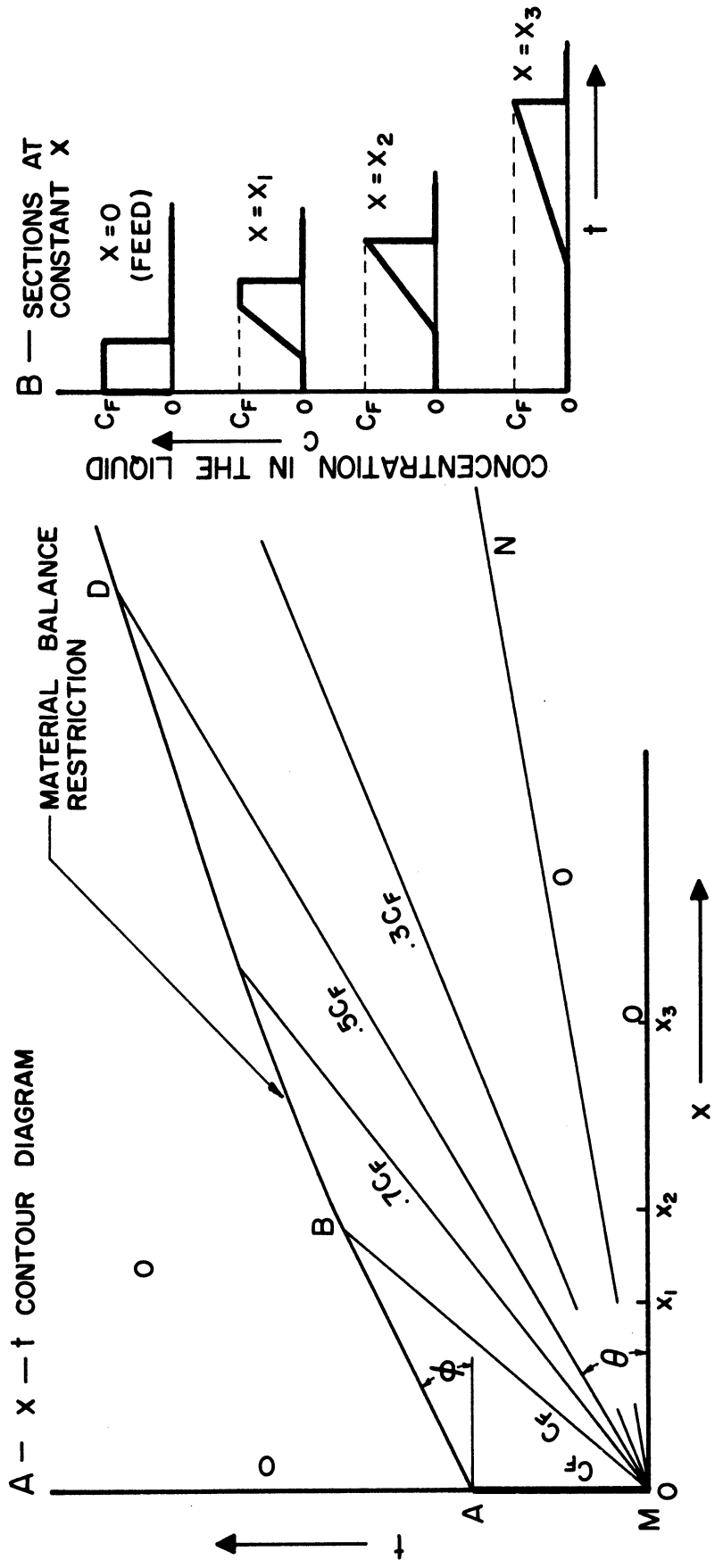

Figure 19. Model A(i)(b). Column Behavior for Non-Linear Equilibrium of Type (i) ($\frac{d^2F}{dc^2} > 0$).

If the equilibrium function, $Q = F(c)$ is known, the curve BD can be determined graphically, and the entire contour diagram shown in Figure 19 can be drawn. Detailed procedure for drawing this contour diagram is given in Appendix.

For equilibrium of type (ii), a somewhat similar contour diagram is obtained as shown on Figure 20. Comparison of Figures 19B and 20B shows that for non-linear equilibria, sharp edges are obtained in the concentration profiles. Depending on the type of non-linearity (i.e. the sign of $\frac{d^2F}{dc^2}$) either the leading or the trailing edge of the profile is sharp.

If a bed of solids had an arbitrary profile of the concentrations at the start of an operation, it would remain unaltered in shape and travel out of the bed at a constant velocity if the equilibrium were linear. In the case of non-linear equilibrium, the profile may get more or less steep as it progresses through the column. x-t contour diagrams can be drawn for any particular case as illustrated in Figure 21 and the profiles can be estimated quantitatively.

Figure 22 indicates the contour diagrams that would be obtained if the feed to a column were an impulse function.

(c) Linear Equilibrium and Longitudinal Diffusion in the Liquid

Mathematical Equations:

$$D_L \frac{\partial^2 c}{\partial x^2} - u \frac{\partial c}{\partial x} = \frac{\partial}{\partial t} (\epsilon c + (1-\epsilon) Q) \qquad (26)$$

$$Q = Kc \qquad (27)$$

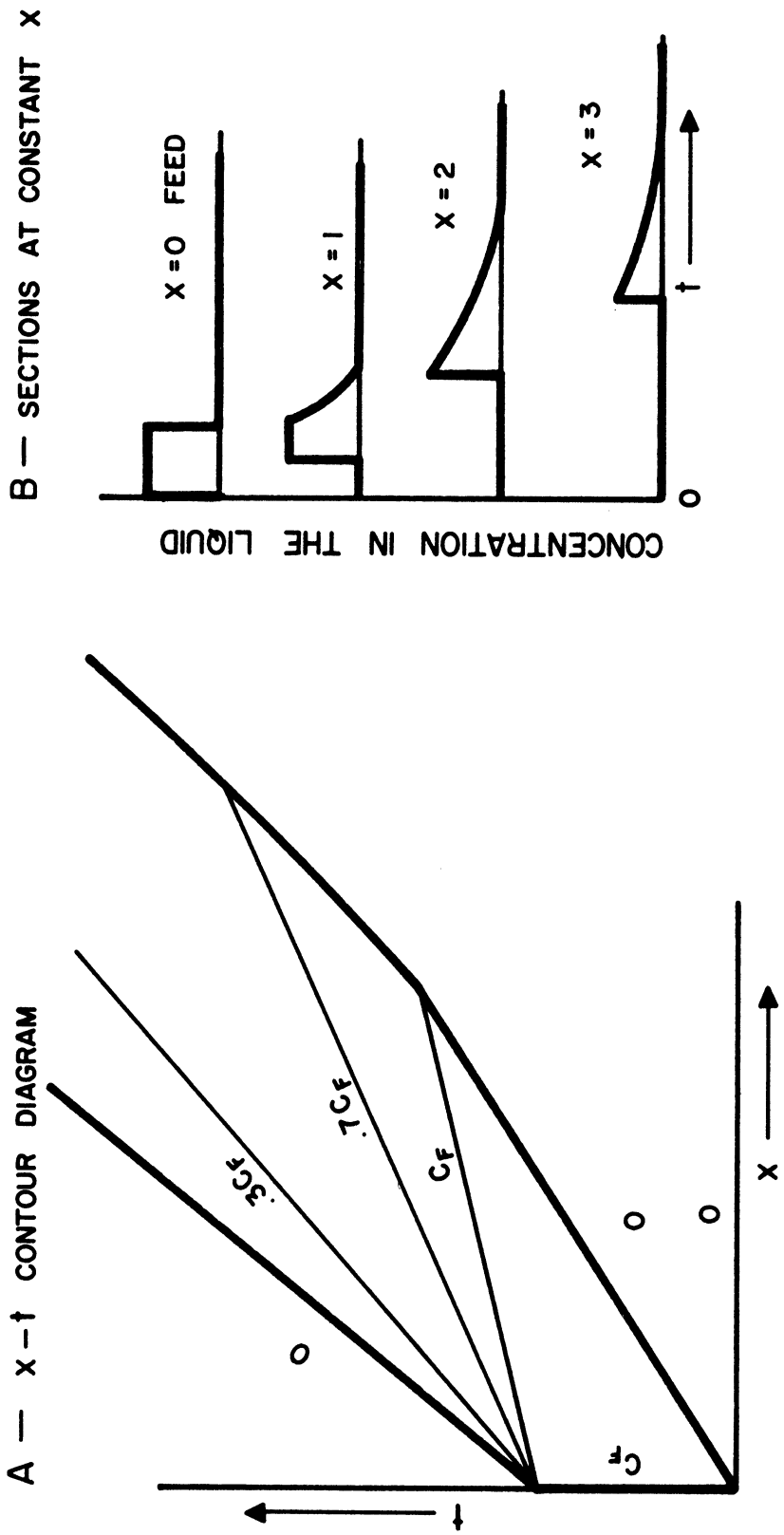

Figure 20. Column Behavior for Non-Linear Equilibrium of Type (ii) ($\frac{d^2F}{dc^2} < 0$). Model A(1)(b).

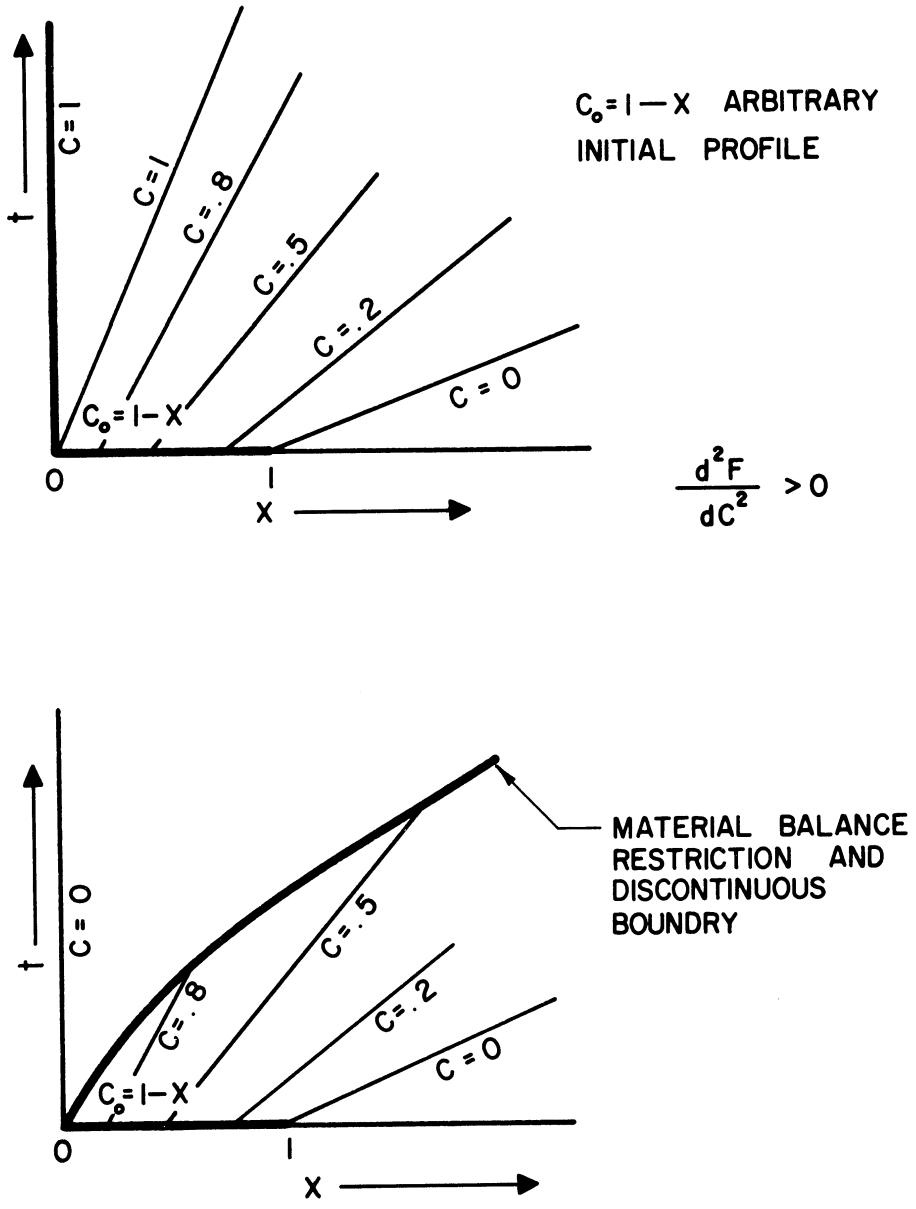

Figure 21. Contour Diagrams for Some Arbitrary Cases.

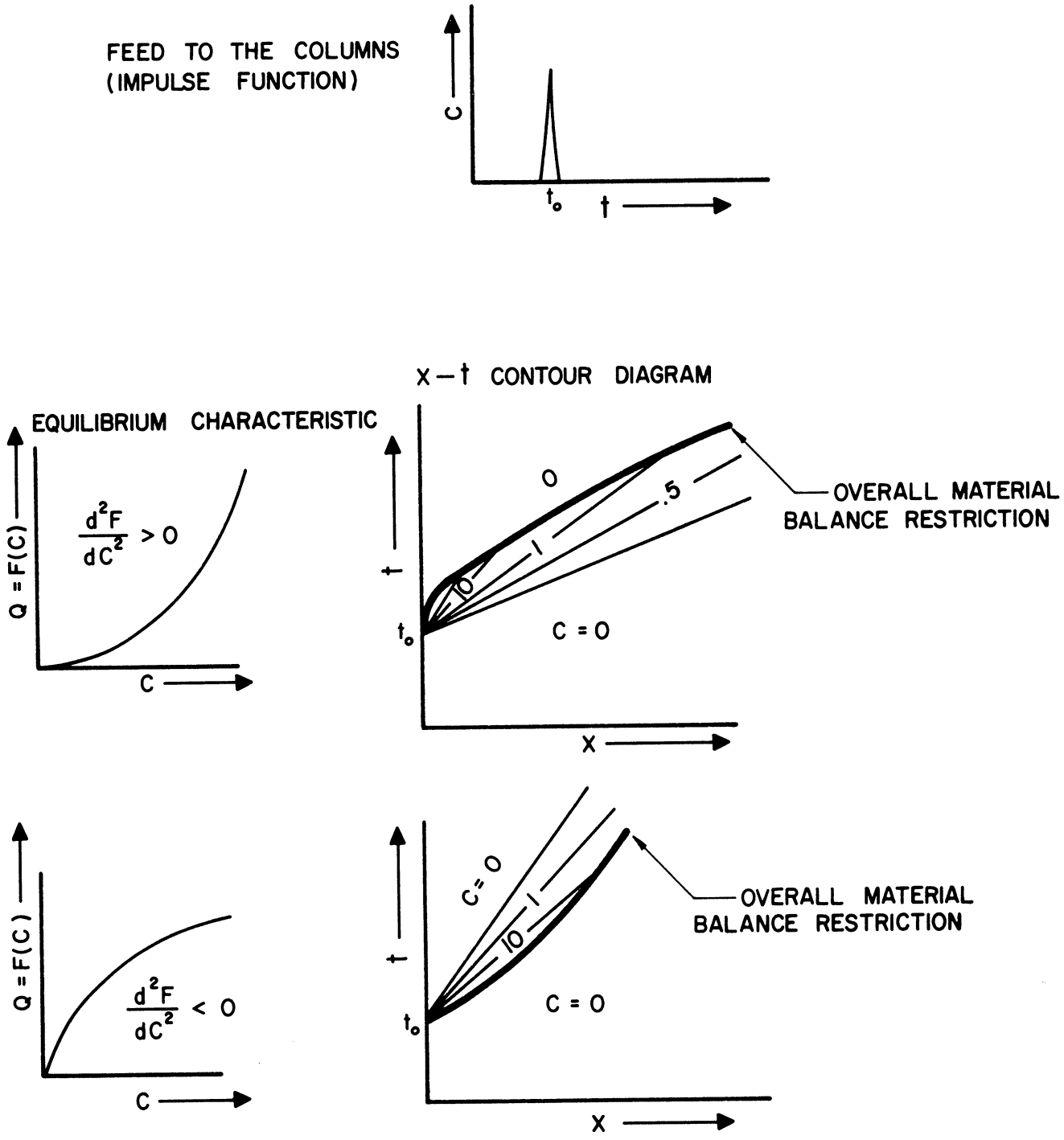

Figure 22. Response of an Equilibrium Column to an Impulse Function Model A(i)(b).

$$c = 0 \quad \text{at} \quad t = 0 \quad \text{for all} \quad x \tag{28}$$

$$c = c_F \text{ at} \quad x = 0 \quad \text{for all} \quad t \tag{29}$$

$$c \text{ is bounded as } x \text{ tends to } \infty \tag{30}$$

Where:

D_L is the longitudinal diffusivity in the liquid.

The other symbols in the equations are the same as defined in model A (i) (a). Equation (26) is the modified material balance in which the first term, $D_L \frac{\partial^2 c}{\partial x^2}$ is the net accumulation in a unit volume of the bed due to longitudinal diffusion in the bed. Equation (27) defines the linear equilibrium, K being a constant. Equation (28) is the initial condition of the bed and Equation (29) gives the condition at the inlet of the bed.

Equations (27) and (26), can be combined to give

$$D_L \frac{\partial^2 c}{\partial x^2} - u \frac{\partial c}{\partial x} - (\epsilon + (1-\epsilon)K) \frac{\partial c}{\partial t} = 0 \tag{31}$$

The following analytic solution of this partial differential equation is given by Carslaw and Jaeger (C1).

$$C = 1/2 \left\{ \operatorname{erfc} \frac{x - \frac{ut}{\epsilon + (1-\epsilon)K}}{2\sqrt{\frac{D_L t}{\epsilon + (1-\epsilon)K}}} + e^{\frac{ux}{D_L}} \operatorname{erfc} \frac{x + \frac{ut}{\epsilon + (1-\epsilon)K}}{2\sqrt{\frac{D_L t}{\epsilon + (1-\epsilon)K}}} \right.$$

where

$$\operatorname{erfc}(\beta) = \frac{2}{\sqrt{\pi}} \int_{\beta}^{\infty} e^{-x^2} \, dx$$

The above mathematical model is written for an infinite bed and the solution gives the concentration profiles in an infinitely long bed.

For a finite bed of length, L, Equation (30) would be replaced by the following boundary condition.

$$\left[\frac{\partial c}{\partial x}\right]_{x=L} = 0 \ .$$

The case of linear equilibrium without any longitudinal diffusion in the liquid was discussed above in model A (i) (a). The effect of longitudinal diffusion is to smear the sharp edges of the concentration surface in the (x, t, c) space. Under the usual operations of ion-exclusion and chromatographic columns, this "smearing" is small. [It will be discussed further in model B (i) (d)].

(d) Arbitrary Equilibrium with Shrinkage and Swelling of the Solid

During the operation of a column the concentrations of the materials present in the solid vary. Due to concentration changes some solids may swell or shrink in volume. For instance, in a 15% NaCl solution, the ion exchange resin, Dowex 50, shrinks to about 90% of its volume in water. This change in the volume of the solid phase is usually compensated by an opposite change in the volume of the liquid phase and the net change in the total volume is usually small. In effect, the solid absorbs additional solvent when it swells and discharges the solvent when it shrinks.

In the following equations, it is assumed that the porosity of the bed is a function of the concentration of the materials in the solid phase. This assumption is made in order to account for the swelling and the shrinking of the solid.

The following equations describe the model:

Material Balance:

$$\frac{\partial}{\partial x}[uc] + \frac{\partial}{\partial t}[\epsilon c + (1-\epsilon)\, Q] = 0 \tag{31}$$

Porosity Function:

$$\epsilon = \epsilon(Q) \tag{32}$$

Equilibrium Function:

$$Q = F(c) \tag{33}$$

Initial Condition of the Bed:

$$c = \phi(x) \text{ at } t = 0 \tag{34}$$

Feed History:

$$c = f(t) \text{ at } x = 0 \tag{35}$$

The porosity of the bed, ϵ, is a variable and cannot be factored out of the differentiation operation. The superficial velocity, u, is assumed to be a constant. "Slug flow of the liquid" and "no longitudinal diffusion in the liquid" are assumed.

It will be shown in the following that the solution of the above model is the same as the solution of the model* A(i) (b) with constant porosity which has been discussed above, provided that the equilibrium function, F(c), is replaced by a different function, $\overset{v}{F}(c)$. $\overset{v}{F}(c)$ may be considered as a hypothetical equilibrium function that incorporates the effect of the porosity changes. $\overset{v}{F}(c)$ is defined by the following equation.

$$F(c) = \frac{-\epsilon_o\, c + \epsilon c + (1-\epsilon)F}{1 - \epsilon_o} \tag{36}$$

---

* Equilibrium Column Operation, Single Solute, Constant Porosity, Non-Linear Equilibrium.

ϵ_o is the arbitrary value of porosity that should be used in the equations in the model A(i) (b).

Using $\overset{\vee}{F}(c)$ as the equilibrium function, the following equation gives the material balance for the model A(i) (b) with constant porosity.

$$u \frac{\partial c}{\partial x} + \frac{\partial}{\partial t} [\epsilon_o c + (1-\epsilon_o) \overset{\vee}{F}(c)] = 0$$

Substituting the value of $\overset{\vee}{F}(c)$,

$$u \frac{\partial c}{\partial x} + \frac{\partial}{\partial t} [\epsilon_o c - \epsilon_o c + \epsilon c + (1-\epsilon) F] = 0$$

The above equation is exactly the same as Equation (31). This means that the model A(i) (d) with variable porosity corresponds to model A(i) (b) with constant porosity, provided that the equilibrium function defined by Equation (36) is used in the latter model.

The solution of the model with variable porosity will show all the characteristics of the model A(i) (b) discussed above. The consideration as to whether $\frac{d^2 \overset{\vee}{F}}{dc^2}$ is positive or negative will be important in determining the exact solution.

For any particular situation under consideration, the function $\overset{\vee}{F}(c)$ can be obtained and then the entire x-t contour diagram or the concentration surface can be determined. The graphical procedure, described with the discussion of the model A(i) (b) can be used.

The following example will illustrate the effect of the shrinking and swelling of the solid on the shape of the effluent waves.

Consider a system with linear equilibrium characteristics. The equilibrium function will be given by the following equation.

$$Q = F(c) = Kc \qquad (37)$$

where K is a constant.

Let the porosity, also, be a linear function of the concentration of the liquid. Let it be given by the equation:

$$\epsilon = \alpha + \beta c \qquad (38)$$

α is the porosity of the bed when the concentration of the solutes is zero. If the solid swells with an increase in the concentration, the porosity will be reduced and β will be negative; on the other hand, if the solid shrinks with an increase in the concentration, the porosity will increase and β will be positive. Substituting Equations (37) and (38) in Equation (36),

$$\overset{\vee}{F}(c) = \left\{ - \epsilon_o c + (\alpha + \beta c)c - (1 - \alpha - \beta c)\, Kc \right\} \frac{1}{1-\epsilon_o}$$

Differentiating,

$$\frac{d\overset{\vee}{F}}{dc} = \frac{- \epsilon_o + \alpha + 2\beta c - K + \alpha K + 2\beta K c}{1 - \epsilon_o}$$

and

$$\frac{d^2\overset{\vee}{F}}{dc^2} = \frac{2\beta(1 + K)}{1 - \epsilon_o} \quad . \qquad (39)$$

If the solid swells with increase in concentration, β will be negative, d^2F/dc^2 will be negative and $\overset{\vee}{F}(c)$ will give non-linear equilibrium of type (ii) (Figure 10). If the solid shrinks with increase in concentration, $\overset{\vee}{F}(c)$ will show type (i) equilibrium. Figure 23 shows typical x-t contour diagrams and effluent histories.

The concentration surface represented in the x-t diagram A has sharp edges. If the edge AB is "rolled down", the surface of Figure B is produced. The edge DE adjusts to maintain the overall material balance. Surfaces like the one in Figure B are produced by non-linear equilibria

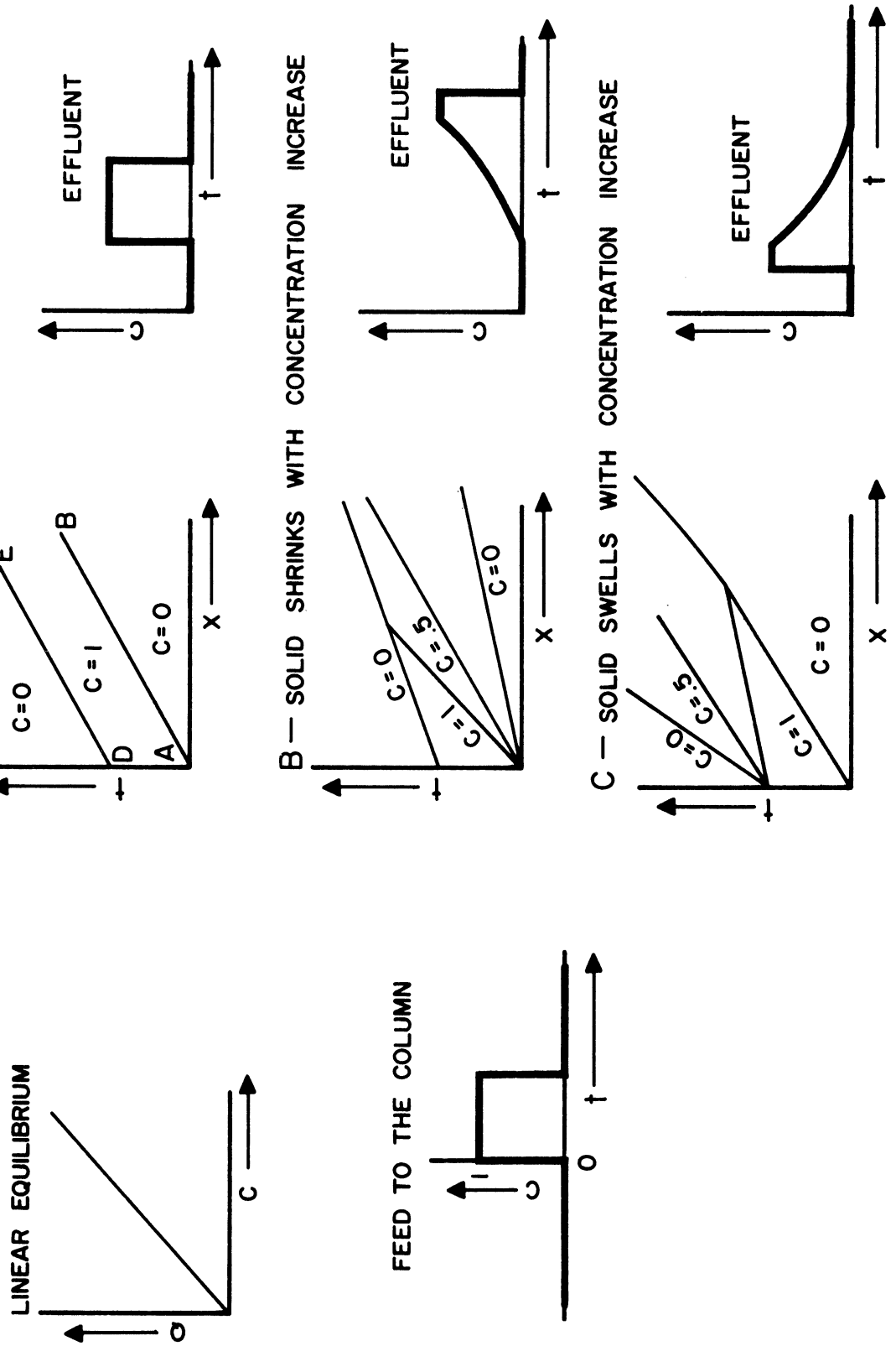

Figure 23. Effect of Swelling and Shrinking of the Solid on the Column Operation. Model A(1)(d).

that are concave upwards. From the diagram A, if the edge DE is rolled out the surface of Figure C is produced. Non-linear equilibria that are convex upwards produce this effect.

Consider a system in which the solid shrinks in volume as the concentration of the solute is increased. Let a slug of a solution be passed over a bed of the solid. As the forward edge of the slug of solution contacts the solid, the solid shrinks and discharges the solvent into the liquid phase. This dilutes the forward edge of the liquid. While the slug of the solution is passing over the solid, the solid remains "shrunk". As the tail end of the slug passes over, the solid swells and absorbs the solvent from the liquid phase. In effect, the solid discharges some solvent ahead of the slug of the solution and picks it up from some solvent behind the slug. This produces an overall displacement in the effluent wave if the concentration is plotted against the volume of effluent. The solvent discharged ahead of the slug of the solution produces dilution and trailing of the front edge. Absorption of the solvent from tail end of the slug increases the steepness of the tail end.

(ii) Two Solutes

(a) Independent Equilibria

For two solutes, in (x, t, c) space there will be two concentration surfaces - one for each solute. If the equilibria are independent, the level curves for the concentration surface for each solute can be drawn according to the methods considered above with the models for the single solute.

Figure 24 shows the contour diagram for the two solutes. For simplicity, it is assumed that both the solutes exhibit linear equilibrium characteristics. The feed to the column, shown on the t-axis in the diagram, is a mixture of the two solutes, whose concentrations in the feed are normalized to unity. In other words c_1 and c_2 in the figure may be interpreted as $c_1/(c_1)_F$ and $c_2/(c_2)_F$.

Depending on their equilibrium constants, the two concentration profiles of components 1 and 2 travel through the column at different velocities. The solute with the lower equilibrium constant travels faster and appears first in the effluent. Sections of the concentration surfaces at constant x give the effluent histories for different lengths of the column. If the length of the column is less than x_1, Figure 24, there would be a definite area of contamination of the waves for the solutes in the effluent. If the length of the column is greater than x_1, the waves exhibit a separation, whose magnitude can be obtained from the diagram.

If one or both the solutes show non linear equilibria, corresponding contour diagrams can be drawn and effluent histories can be determined.

(b) Interdependent Equilibria

Mathematical Equations:

Material Balances:

$$u \frac{\partial c_1}{\partial x} + \frac{\partial}{\partial t} (\epsilon c_1 + (1-\epsilon) Q_1) = 0 \qquad (40)$$

$$u \frac{\partial c_2}{\partial x} + \frac{\partial}{\partial t} (\epsilon c_2 + (1-\epsilon) Q_2) = 0 \qquad (41)$$

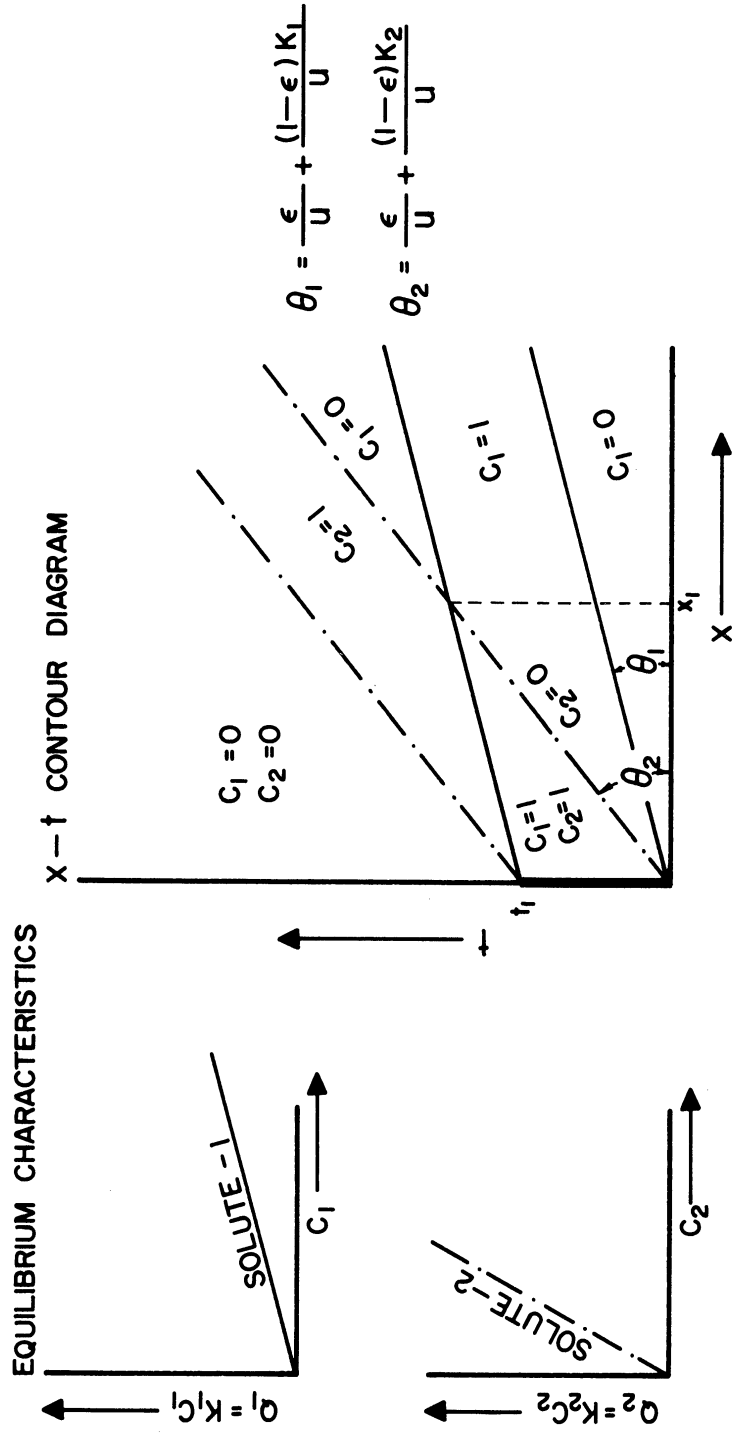

Figure 24. Equilibrium Column with Two Solutes. Independent Equilibria. Model A(ii)(a).

Variable Porosity:

$$\epsilon = \epsilon(Q_1, Q_2) \tag{42}$$

Interdependent Non-Linear Equilibrium Functions:

$$Q_1 = F_1(c_1, c_2) \tag{43}$$

$$Q_2 = F_2(c_1, c_2) \tag{44}$$

Initial Concentration Profiles:

$$c_1 = \varphi_1(x) \quad \text{at} \quad t = 0 \tag{45}$$

$$c_2 = \varphi_2(x) \quad \text{at} \quad t = 0 \tag{46}$$

Feed History:

$$c_1 = f_1(t) \quad \text{at} \quad x = 0 \tag{47}$$

$$c_2 = f_2(t) \quad \text{at} \quad x = 0 \tag{48}$$

Definition of the Symbols:

c_1, c_2 = the concentrations of the components 1 and 2 in the liquid.

Q_1, Q_2 = the concentrations of the components in the solid in the bed.

x = the distance in the bed from the entrance.

u = the superficial velocity.

t = time

ϵ = the porosity of the bed.

Equations (43) and (44) show the interdependent non-linear equilibrium characteristics.

The above set of equations has not been solved analytically for general arbitrary equilibrium functions. For any particular case the partial differential Equations (40) and (41) may be integrated stepwise either graphically or numerically.

An important effect of interdependent equilibria is that, for some systems, under certain conditions of column operation, the concentration of a component in the effluent from a column may be greater than its value in the feed.

To illustrate this effect, consider a bed of solids over which a slug of solution containing two solutes is passed. Initially the bed is free of both the solutes. The porosity of the bed remains constant. Solute 1 shows a linear equilibrium characteristic, and the value of the equilibrium constant, denoted by K_1, is independent of the concentration of the other solute. The equilibrium constant for the second solute is K_2^o if the solute 1 is not present and it is K_2^1 if the solute 1 is present. Following equations give the equilibrium relations under consideration:

$$Q_1 = K_1 c_1$$

$$Q_2 = K_2^o c_2 \quad \text{if} \quad c_1 = 0$$

and

$$Q_2 = K_2^1 c_2 \quad \text{if} \quad c_1 > 0$$

Figures 25 and 26 show the x-t contour diagrams and illustrate the concentration or the dilution effect depending on the relative values of K_1, K_2^o and K_2^1.

In Figure 25, the slope of the line AB is dictated by the K_2^1, the equilibrium constant that applies in the region of x-t plane in which the concentration of c_1 is greater than zero. The slopes of DE and BG are dictated by the constant K_2^o, since they represent the propagation of disturbance in the region in which $c_1 = 0$.

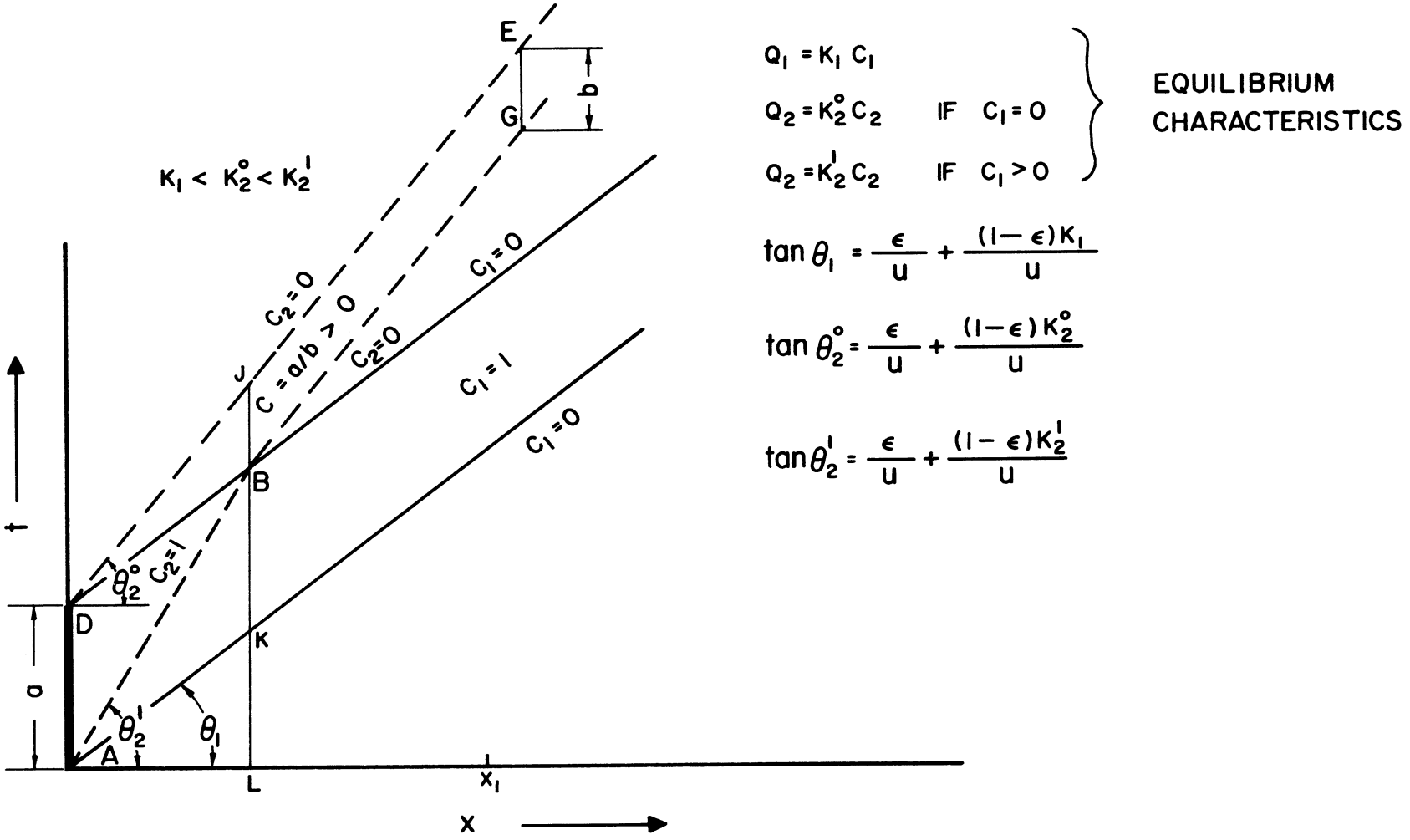

$Q_1 = K_1 C_1$

$Q_2 = K_2^\circ C_2$ IF $C_1 = 0$

$Q_2 = K_2' C_2$ IF $C_1 > 0$

EQUILIBRIUM CHARACTERISTICS

$$\tan\theta_1 = \frac{\epsilon}{u} + \frac{(1-\epsilon)K_1}{u}$$

$$\tan\theta_2^\circ = \frac{\epsilon}{u} + \frac{(1-\epsilon)K_2^\circ}{u}$$

$$\tan\theta_2' = \frac{\epsilon}{u} + \frac{(1-\epsilon)K_2'}{u}$$

Figure 25. Concentration Effect of Interdependent Equilibria. Model A(ii)(b).

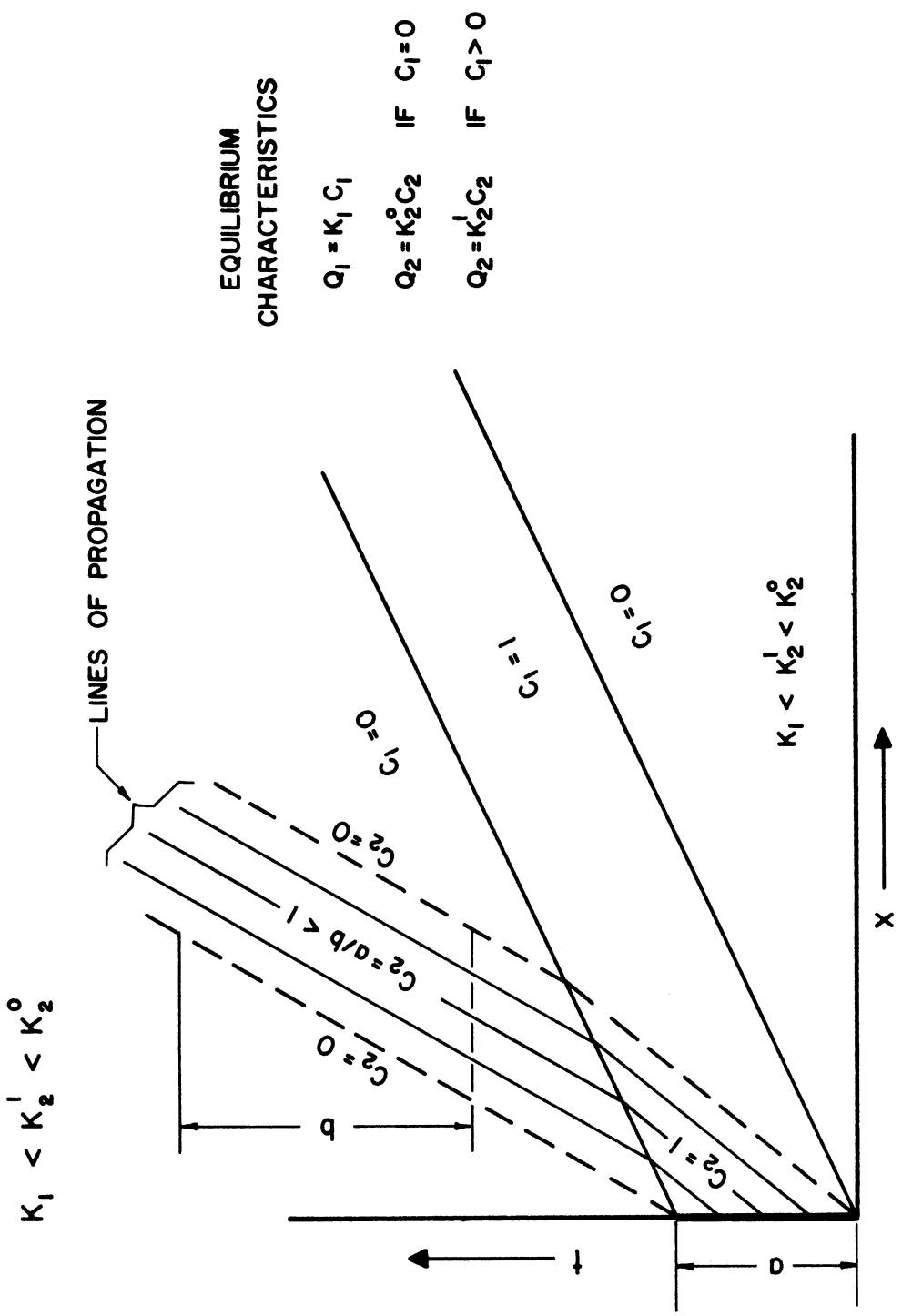

Figure 26. Dilution Effect of Interdependent Equilibria Model A(ii)(b).

Any section of the c_1 and c_2 surfaces at a constant value of x represents the effluent history for a bed of length of x. The integral under the effluent wave represents the total amount of the material fed to the column. Comparing the sections at the entrance of the bed and at $x = x_1$, the concentration of the component 2 in the region BGED can be determined to be $(\frac{a}{b})$ times the concentration in the feed.

An analytic expression giving the ratio $\frac{a}{b}$ in Figures 25 and 26 can be obtained as explained in the following. Let JBKL be a line parallel to t-axis, through the point B in Figure 25.

Then,

$$\begin{aligned} a &= \overline{BK} \\ &= \overline{BL} - \overline{KL} \\ &= \overline{AL}\,(\tan\theta_2^1 - \tan\theta_1) \\ &= \frac{\overline{AL}(1-\epsilon)}{u}\,(K_2^1 - K_1) \end{aligned}$$

and

$$\begin{aligned} b &= \overline{JB} \\ &= \overline{JL} - \overline{BL} \\ &= (a + \overline{AL}\tan\theta_2^0) - (a + \overline{AL}\tan\theta_1) \\ &= \frac{AL(1-\epsilon)}{u}\,(K_2^0 - K_1) \end{aligned}$$

Therefore,

$$\frac{a}{b} = \frac{K_2^1 - K_1}{K_2^0 - K_1} \qquad (48a)$$

Depending on the relative values of the equilibrium constants the ratio $\frac{a}{b}$ may be greater or less than unity, expressing thereby either the concentration or the dilution effect of interdependent equilibria.

Figure 27 illustrates that concentration of one solute and dilution of another may be produced simultaneously. The interdependent equilibrium characteristics chosen are typical of systems that may be encountered experimentally. The equilibrium absorption of each solute is increased by the presence of the other solute and increases further with the increase in the concentration of the other solute. For simplicity, K_1 is assumed to be independent of c_1 and K_2 independent of c_2. In general, K_1 would depend on c_1 and the sharp boundaries of the concentration surface c_1 in Figure 27 would be smeared out at either the leading or the trailing end depending on the type of non-linearity. The concentration surface, c_2, would be effected similarly if K_2 were a function of c_2. The effluent waves (compare Figure 28) in such cases would show leading or trailing edges instead of the steep profiles obtained here.

Figure 28 shows the sections of the x-t contour diagram of Figure 27 for different values of constant x. Solute 1 has a smaller equilibrium absorption by the solid and it appears first in the effluent. In the column the slug of the solute 1 moves faster. While the solution containing both the solutes is passing over a section of the column, the absorption of solute 2 is high. As the tail end of the slug of the faster

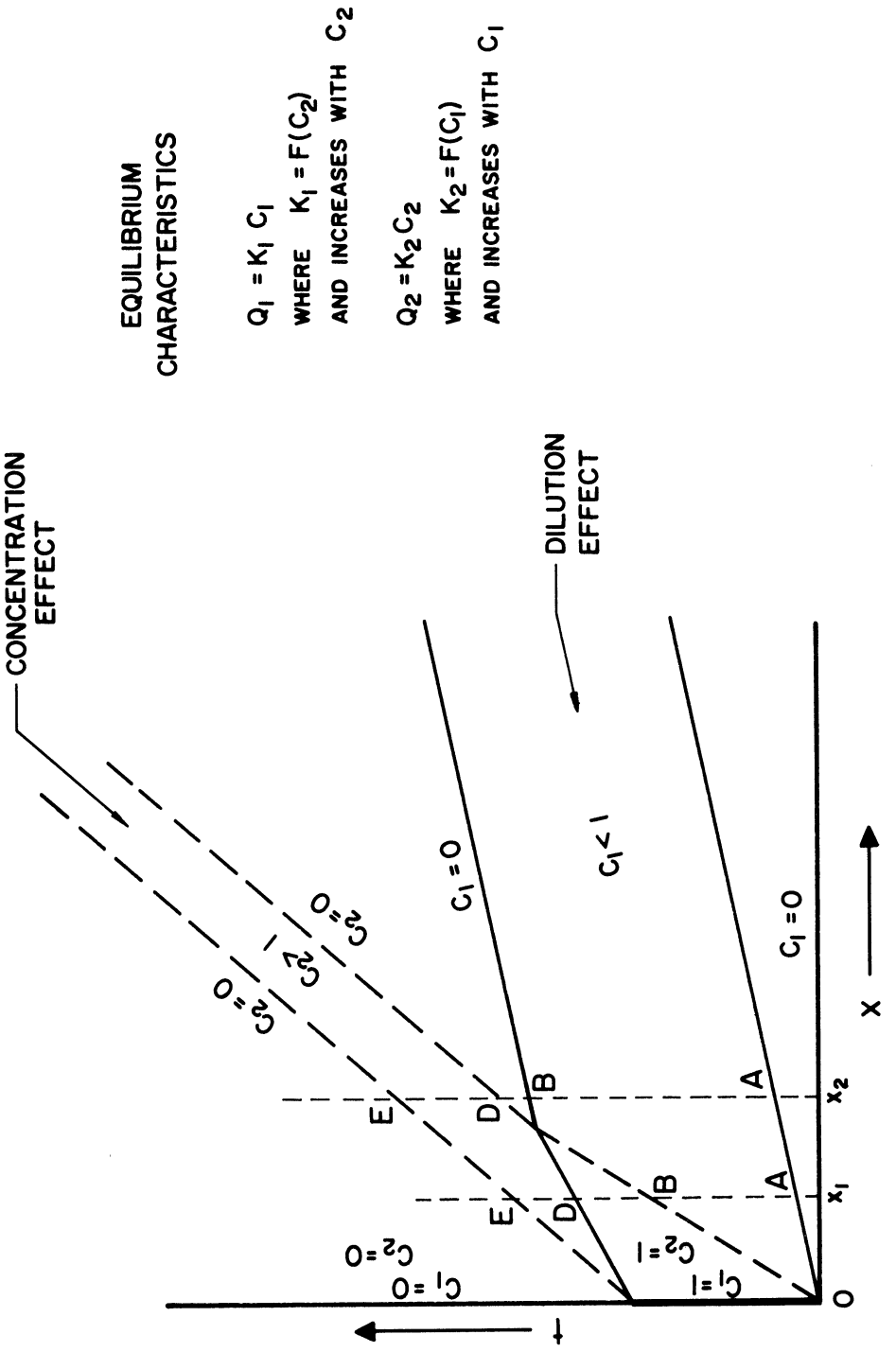

Figure 27. Simultaneous Concentration and Dilution Effects for Interdependent Equilibria. Model A(ii)(b).

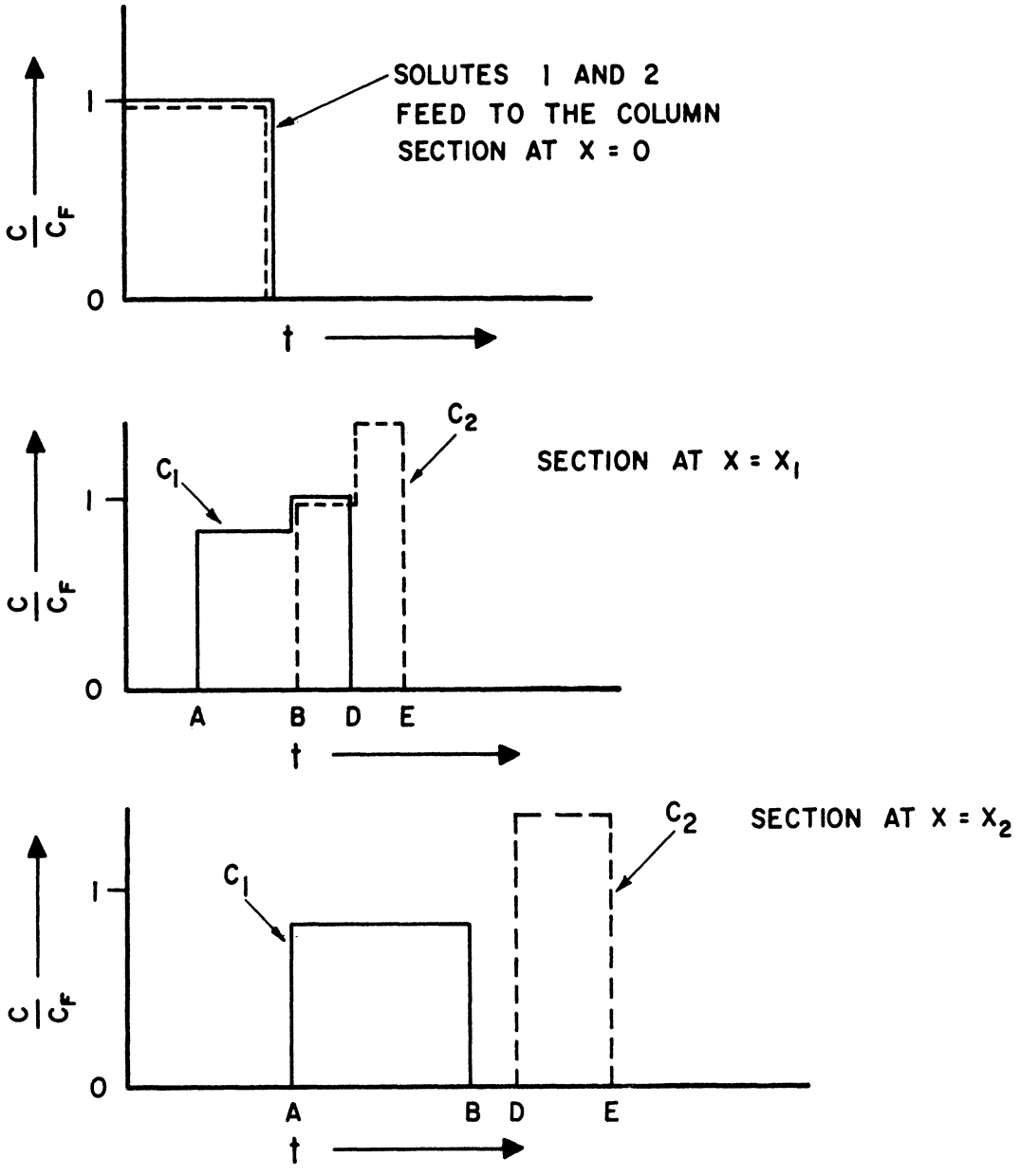

Figure 28. Effluent Waves from the Contour Diagram in Figure 27.

moving solute 1 passes over the section, the equilibrium constant for solute 2 is lowered and the solid discharges into the liquid the excess amount of solute 2. This causes the concentration of solute 2. As can be seen from Figures 27 and 28, eventually the waves separate and further interaction ceases.

B. Non-Equilibrium Column Operation

All the mathematical models discussed in the preceding sections assumed operation of a column such that the solid phase was always in equilibrium with the liquid surrounding it. It was assumed that there was no resistance to transfer of the solute between the solid and the liquid phases. Mathematically, this assumption was expressed by using equilibrium functions as the equations describing the relation between Q_i, the concentration of the solute, i, in the solid phase and $c_j (j=1,2,...)$, the concentrations of the various solutes in the liquid.

In practice, the resistances to mass transfer are seldom negligible. The following models consider these resistances and the rates of mass transfer.

The equilibrium characteristic of the system is still an important physical characteristic in these models, and the shape of the concentration surface obtained as the solution of the mathematical equations is strongly influenced by the nature of the equilibrium functions.

The effect of the mass transfer resistances is to distort the concentration surfaces that would have been obtained from an equilibrium column operation. Frequently, in actual ion exclusion and chromatographic column operations, these distortions are small and they merely round off

some of the sharp edges and the discontinuous jumps present in the surfaces representing equilibrium column operation. Even when the distortions are large, the positions of the "ridges" in the concentration surfaces, representing areas of high concentration in the x-t plane, are the same as they would be on the surface representing an equilibrium column operation. The slopes of these "ridges" may be considerably flattened and the exact shapes would be determined by the mass transfer resistances. In terms of the effluent concentrations, this means that, in place of discontinuous jumps in the concentrations that are obtained in equilibrium column operations, smooth variations in concentrations would be obtained; however, the approximate values of time at which rapid concentration changes take place would not change.

In most of the models discussed below, it is assumed that the equilibrium characteristics of the solute are linear, i.e., the ratio of the concentration of the solute in the solid to that in the liquid in equilibrium with the liquid, is a constant. This assumption makes the entire set of mathematical equations for many models linear and techniques of operational mathematics may be applied for solving them analytically. The solutions available in the literature will be discussed with the various models.

The assumption of linear equilibrium produces another useful simplification. For each model, the equations define a problem in partial differential equations. The solution of the equations, in general, will depend on the concentration history of the liquid entering the column. Let $f_1(t)$, $f_2(t)$ and $f_3(t)$ denote the concentration histories in the liquid for three cases. Let $c_1(x, t)$, $c_2(x, t)$ and $c_3(x, t)$ be

the corresponding solutions of a problem in partial differential equations. If the mathematical equations are linear, it can be shown that the following property holds:

If

$$f_3(t) = A\, f_1(t) + B\, f_2(t)$$

where A and B are constants,

Then

$$c_3(x, t) = A\, c_1(x, t) + B\, c_2(x, t)$$

Using this property, the response of a column to a square wave input can be estimated from the knowledge of its response to a step function input; and the behavior of an absorption column can be used to determine the behavior of a column through which a slug of a solution is passed. Consequently, in the linear models below, only the saturation behavior of the columns need be considered in detail.

During the operation of a column, the transfer of material takes place between the solid phase and the liquid phase. Depending on the physical characteristics of the system, the resistances to mass transfer in the two phases may be of the same order of magnitude or one or the other may be the predominant resistance. The three possible cases that arise are considered in the three models discussed below.

(i) Linear Equilibrium (One Solute)

(a) Resistance in Solid is the Controlling Resistance to Mass Transfer

In the following equations it is assumed that the transfer of materials in the solid follows the Fick's Law of Diffusion, where the rate of transfer is proportional to the concentration gradient and the diffusivity is a constant.

It is also assumed that the solid particles are spheres of uniform size, complete radial symmetry exists within each solid particle, the surface of the solid particles is always in equilibrium with the liquid surrounding it, there is no longitudinal diffusion in the liquid, there are no radial concentration or velocity profiles in the bed and the superficial velocity of the liquid and the porosity of the bed are constant.

Mathematical Equations:

Material Balance:

$$u \frac{\partial c}{\partial x} + \frac{\partial}{\partial t} (\epsilon c + (1-\epsilon)Q) = 0 \tag{49}$$

Diffusion in the solid (Laplacian in spherical coordinates):

$$D\left(\frac{\partial^2 q}{\partial r^2} + \frac{2}{r} \frac{\partial q}{\partial r}\right) = \frac{\partial q}{\partial t} \tag{50}$$

Equilibrium condition at the surface of the solid:

$$q = Kc \quad \text{at} \quad r = R \tag{51}$$

Symmetry in the solid spherical particles:

$$\left[\frac{\partial q}{\partial r}\right] = 0 \quad \text{at} \quad r = 0 \tag{52}$$

Average concentration in the solid:

$$Q = \left(\int_{r=0}^{r=R} 4\pi r^2 q \, dr\right) / \frac{4}{3} \pi R^3 \tag{53}$$

Initial condition of the column:

$$c = 0 \quad \text{for} \quad t = 0 \tag{54}$$

$$q = 0 \quad \text{for} \quad t = 0 \tag{55}$$

Feed History:

$$c = 1 \quad \text{at} \quad x = 0 \tag{56}$$

Definition of Symbols:

x = the distance from the inlet end of the column.

t = the time.

r = the distance of a point in a solid particle from the center of the particle.

c = the concentration in the liquid. It is a function of x and t.

q = the concentration within the solid particle. It is a function of x, r and t.

Q = the average concentration of the solute in the solid particle. It is a function of x and t.

ϵ = the porosity of the bed.

u = the superficial velocity of the liquid.

D = the diffusivity of the solute in the solid phase.

R = the radius of the solid particles.

K = the equilibrium constant.

C_F = the concentration in the feed.

Since the above problem is linear, Equation (56) which considers the feed concentration equal to 1 is no loss of generality. If the feed concentration were c_F, the entire solution would be multiplied by c_F.

Following transformation of the coordinates makes the problem dimensionless and simplifies the equations.

$$Z = D(1-\epsilon)\ x/uR^2 \tag{57}$$

$$\theta = (t - x\epsilon/u)(D/R^2) \tag{58}$$

$$\rho = r/R \tag{59}$$

The partial derivatives give the following relations:

$$\frac{\partial c}{\partial x} = \frac{\partial c}{\partial Z} \cdot \frac{\partial Z}{\partial x} + \frac{\partial c}{\partial \theta} \cdot \frac{\partial \theta}{\partial x}$$

$$= \frac{D(1-\epsilon)}{uR^2} \frac{\partial c}{\partial x} - \frac{D\epsilon}{uR^2} \frac{\partial c}{\partial \theta} \tag{60}$$

$$\frac{\partial c}{\partial t} = \frac{\partial c}{\partial Z} \cdot \frac{\partial Z}{\partial t} + \frac{\partial c}{\partial \theta} \cdot \frac{\partial \theta}{\partial t}$$

$$= \frac{D}{R^2} \frac{\partial c}{\partial \theta} \tag{61}$$

$$\frac{\partial Q}{\partial t} = \frac{D}{R^2} \frac{\partial c}{\partial \theta} \tag{62}$$

$$\frac{\partial q}{\partial r} = \frac{1}{R} \frac{\partial q}{\partial \rho} \tag{63}$$

$$\frac{\partial^2 q}{\partial r^2} = \frac{1}{R^2} \frac{\partial^2 q}{\partial \rho^2} \tag{64}$$

Using Equations (60) through (64), following relations are obtained.

From Equation (49),

$$\frac{\partial c}{\partial Z} + \frac{\partial Q}{\partial \theta} = 0 \tag{65}$$

From Equation (50),

$$\frac{\partial^2 q}{\partial \rho^2} + \frac{2}{\rho}\frac{\partial q}{\partial \rho} = \frac{\partial q}{\partial \theta} \tag{66}$$

From Equation (51) through (56),

$$q = Kc \quad \text{at} \quad \rho = 1 \tag{67}$$

$$\left[\frac{\partial q}{\partial \rho}\right] = 0 \quad \text{at} \quad \rho = 0 \tag{68}$$

$$Q = 3 \int_{\rho=0}^{\rho=1} \rho^2 q \, d\rho \tag{69}$$

$$c = 0 \quad \text{for} \quad \theta = 0 \tag{70}$$

$$q = 0 \quad \text{for} \quad \theta = 0 \tag{71}$$

$$c = 1 \quad \text{for} \quad Z = 0 \tag{72}$$

Equations (65) through (72) define the problem in partial differential equations. ρ, Z and θ are independent variables.

ρ = the distance of a point inside the solid particle as a fraction of the radius.

Z = a dimensionless measure of the distance from the inlet end of the bed.

θ = a dimensionless measure of the time at the point Z, whose value at the point Z indicates the interval of time elapsed since the arrival at the point Z, of the first slug of liquid that entered the bed.*

c, Q and q are the dependent variables.

$c = c(Z,\theta)$

$Q = Q(Z,\theta)$

and $q = q(\rho,Z,\theta)$.

---

* This concept of moving time coordinate has been explained in Section II, 1. Material Balances.

In the case of a system that shows non-linear equilibrium relationships, if the diffusion in the solid phase is the controlling resistance to mass transfer, all the above equations and manipulations are applicable, the only change being the equilibrium relationships given in Equations (51) and (67). In these equations, instead of having,

$$q = Kc \quad \text{at} \quad r = R \quad \text{or at} \quad \rho = 1,$$

the following equation will apply.

$$q = F(c) \quad \text{at} \quad r = R \quad \text{or at} \quad \rho = 1 \tag{73}$$

where F(c) is a function describing the equilibrium relationship between the solid and the liquid.

Introduction of a non-linear function, F(c), in Equation (73), would make the entire mathematical problem non-linear. General solution of this non-linear problem has not been obtained and for any particular case, the system of partial differential equations may be integrated numerically in a stepwise manner.

On the other hand, for the linear problem as described by Equations (49) through (56) and transformed into the dimensionless form of the Equations (65) through (72), a general analytic solution is available. The following discussion will be limited to the linear problem.

Solution of the Equations (65) through (72) would give a surface c as a function of Z and θ in (Z,θ, c) space. However, there would be one surface for each value of the equilibrium constant, K, in Equation (67). It is convenient to redefine some of the variables so as to "incorporate" the effect of the different values of the equilibrium constant in the dimensionless variables and get a general problem and a general solution for all values of the equilibrium constant. This is accomplished in the following.

Let

$$\bar{q} = q/K \tag{74}$$

$$\bar{Q} = Q/K \tag{75}$$

and

$$\bar{Z} = KZ = DK(1-\epsilon)x/uR^2 \ . \tag{76}$$

Then, in the following equations, the independent variables are $\bar{Z}$, θ and ρ. The dependent variables are:

$$c = c(\bar{Z},\theta)$$

$$\bar{Q} = \bar{Q}(\bar{Z},\theta)$$

$$\bar{q} = \bar{q}(\rho,\bar{Z},\theta)$$

Using Equations (74) through (76), following equations are obtained from the Equations (65) through (72).

$$\frac{\partial c}{\partial Z} + \frac{\partial \bar{Q}}{\partial \theta} = 0 \tag{77}$$

$$\frac{\partial^2 \bar{q}}{\partial \rho^2} + \frac{2}{\rho}\frac{\partial \bar{q}}{\partial \rho} = \frac{\partial \bar{q}}{\partial \theta} \tag{78}$$

$$q = c \quad \text{at} \quad \rho = 1 \tag{79}$$

$$\left[\frac{\partial \bar{q}}{\partial \rho}\right] = 0 \quad \text{at} \quad \rho = 0 \tag{80}$$

$$\bar{Q} = 3\int_{\rho=0}^{\rho=1} \rho^2 \, \bar{q} \, d\rho \tag{81}$$

$$c = 0 \quad \text{for} \quad \theta = 0 \tag{82}$$

$$\bar{q} = 0 \quad \text{for} \quad \theta = 0 \tag{83}$$

$$c = 1 \quad \text{for} \quad \bar{Z} = 0 \tag{84}$$

The solution of the problem in partial differential equations, described by the above Equations (77) through (84), is shown in Figures 29 and 30. The value of the concentration in the liquid phase, c, as a function of $\overline{Z}$ and θ is the solution of interest. Figure 29 shows the level curves for constant values of c on the $\overline{Z}$ - θ plane. Figure 30 is the enlarged plot of the corner of Figure 29 near its origin.

The solution given on Figures 29 and 30 is based on the analytic solution and the numerical values reported by Rosen (R1, R2). The analytic solution was obtained by use of operational mathematics (R1) and the numerical values for the special functions describing the solution were computed on a digital computer (R2). Rosen's solution will be discussed in more detail along with model B(i) (c).

Break through curves for the saturation operation of a column can be obtained (quantitatively) from Figures 29 and 30. From the length of the column and the physical and operating variables, the value of $\overline{Z}$ can be obtained.

$$\overline{Z} = \frac{DK(1-\epsilon)x}{uR^2} \tag{76}$$

At this value of $\overline{Z}$ a cross-section of the concentration surface may be taken either from Figure 29 or from Figure 30. Such a cross section would give a plot of concentration in the liquid versus the dimensionless time, θ. Figure 31 shows such cross sections. From the plot of concentration versus θ, a plot of concentration versus time, t, can be made by using the relation

$$\theta = \frac{D}{R^2}\left(t - \frac{\epsilon}{u}x\right) \tag{58}$$

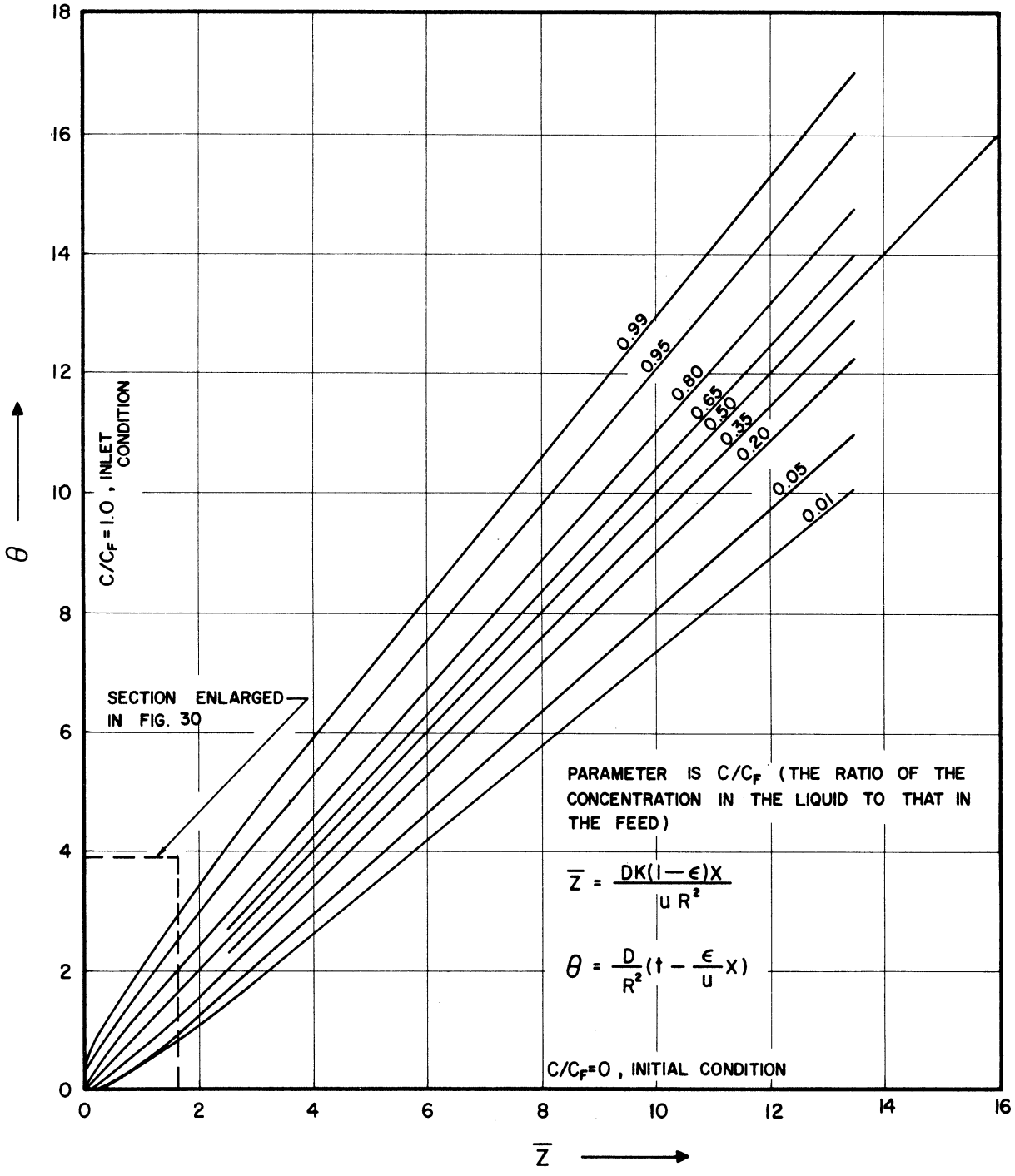

Figure 29. Contour Diagram for Saturation of a Column with Diffusion in the Particles as Controlling Resistance (Model B(i)(a)).

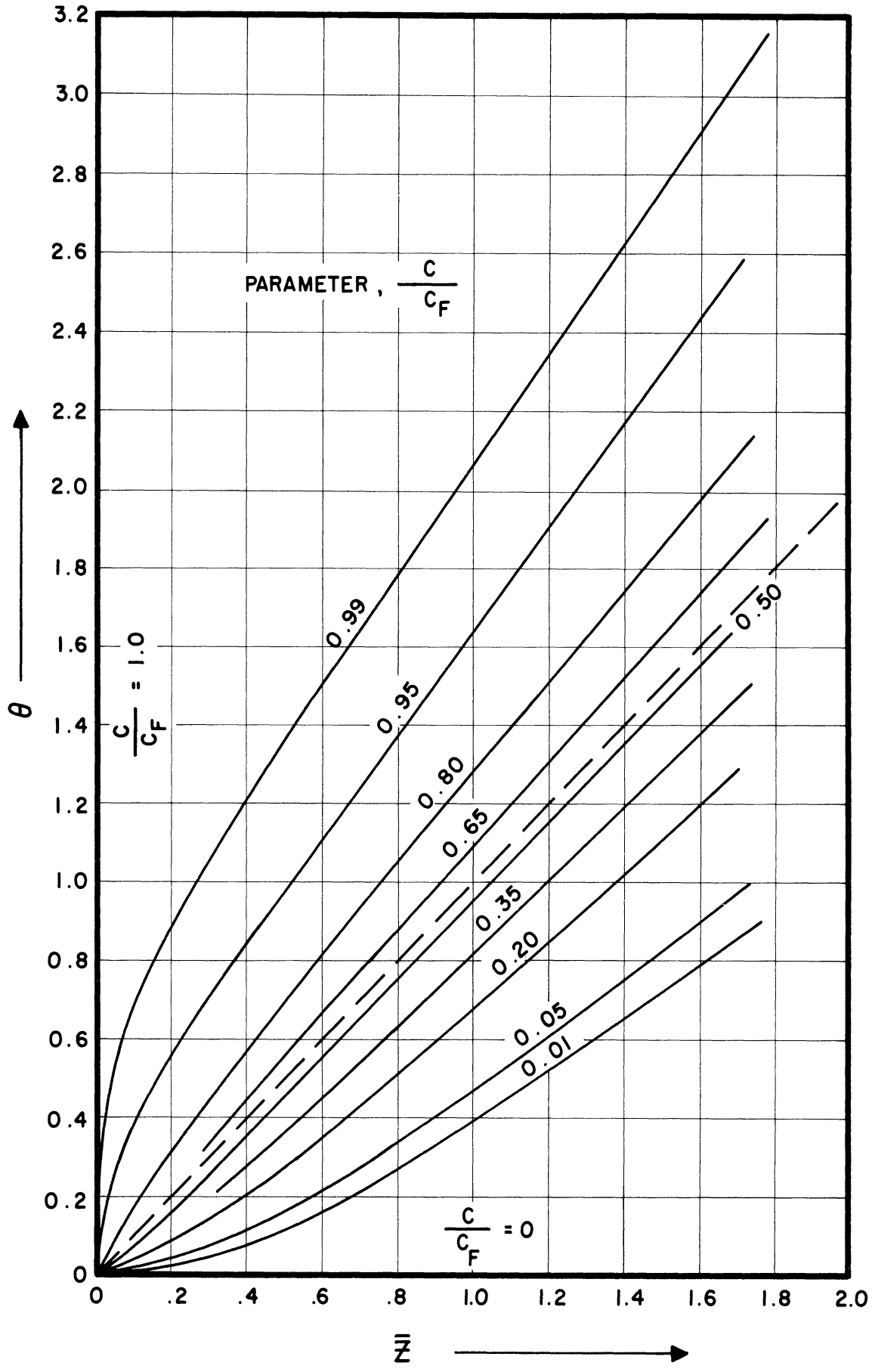

Figure 30. An Enlarged Section of Contour Diagram of Figure 29, as Indicated in Figure 29.

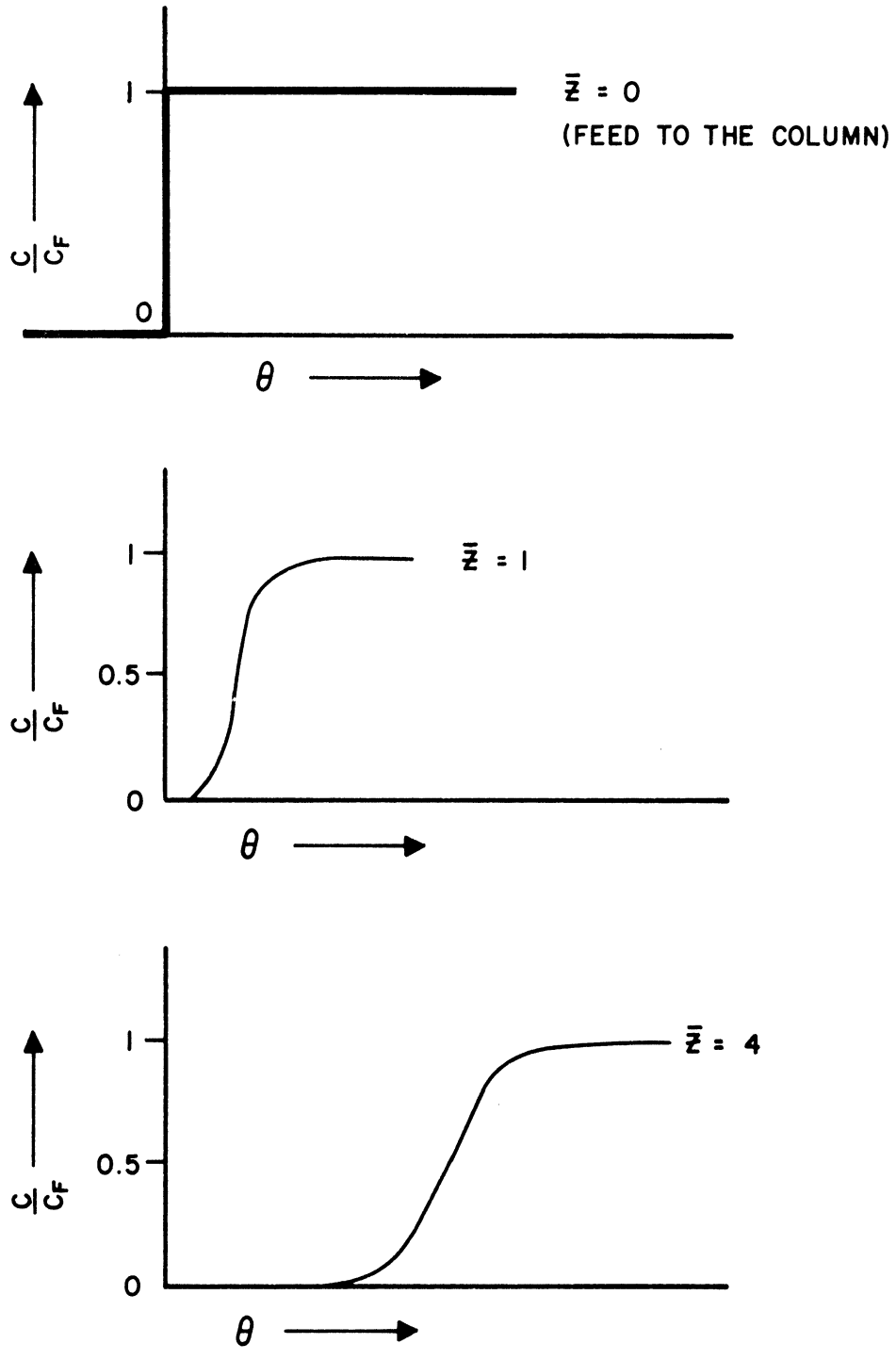

$$\theta = \frac{D}{R^2}\left(t - \frac{\epsilon}{u}x\right)$$

$$\bar{z} = \frac{DK(1-\epsilon)x}{uR^2}$$

Figure 31. Typical Cross Sections of the Concentration Surface in Figure 29.

The plot of concentration versus t would be very similar to the plot of concentration versus θ. The term $\frac{\epsilon}{u} x$ in the Equation (58) is the time required for the first slug of the solution entering the bed to traverse the distance x. For a given value of x, this represents a constant displacement between t and θ coordinates.

If a slug of a solution is fed to a column, the concentration history in the effluent can be determined from the break through curves for the saturation operation of a column, as shown in Figure 32.* The feed, as shown above in Figure 32C is a square wave. It may be considered to be made up of a sum of two step functions, shown in Figures 32A and B. Figure 32D is the saturation behavior of the column obtained from the general solution given in Figures 29 and 30. It would be the effluent history for feed shown in Figure 32A. Figure 32E is obtained by translating the curve in Figure 32D by t_o, and multiplying it by -1. It is the response to the feed shown in Figure 32B. The response to a slug input in the feed is obtained by adding the curves in Figures 32D and E. Figure 32F shows the effluent wave produced as the result.

Figure 33A is a sketch of the concentration surface in the three dimensional (x, t, c) space. The surface represents the solution of the equations describing the model. Figures 29 and 30 show the level curves of this surface plotted on the dimensionless $\bar{Z}$-θ plane instead of the x-t plane. The transformation of the x-t plane into $\bar{Z}$-θ plane can be

---

* The procedure described here is possible because the system of integro-differential equations describing the model under consideration are all linear.

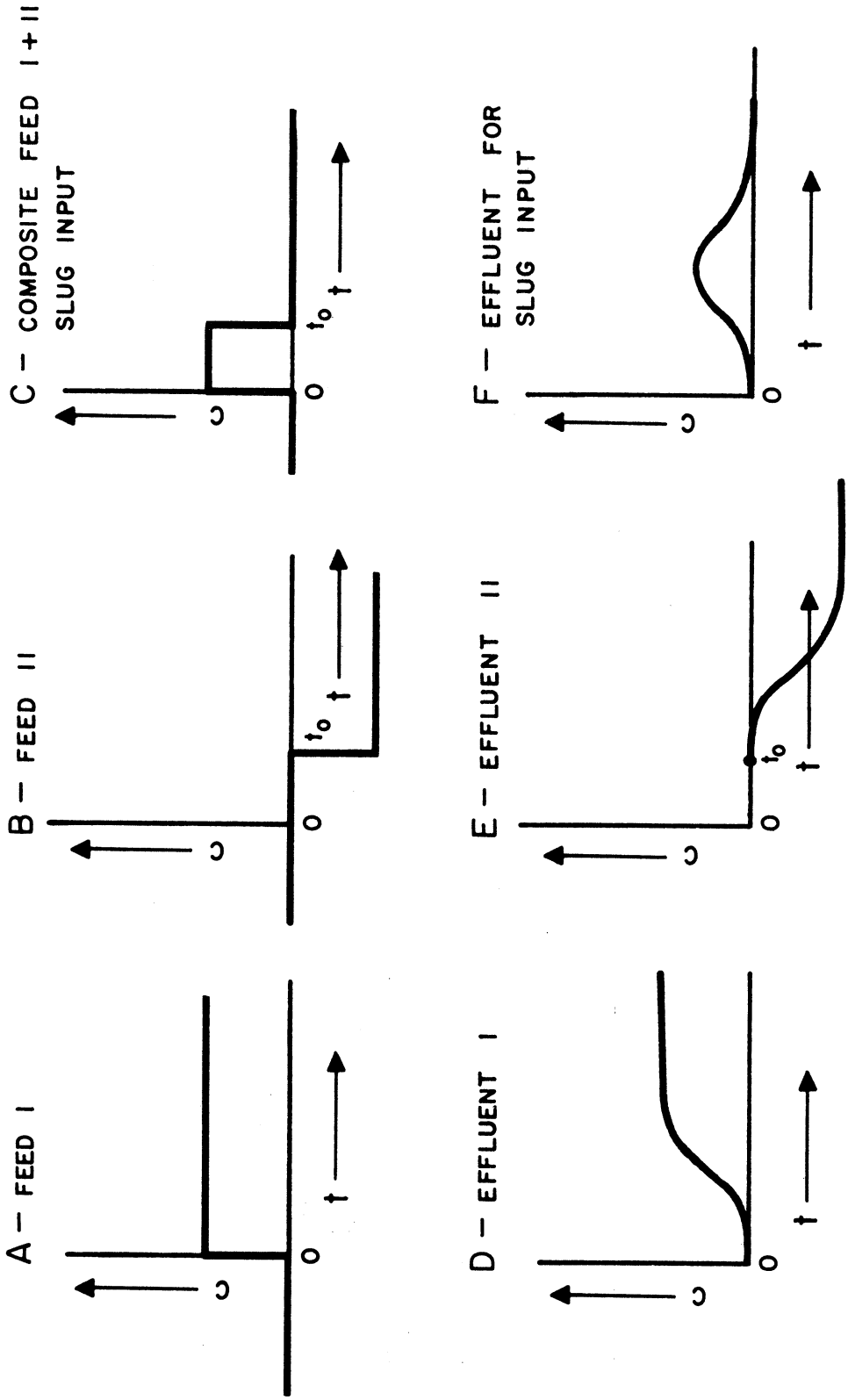

Figure 32. Estimation of the Behavior of a Column to a Slug Input (Figure F) from its Saturation Behavior (Figure D).

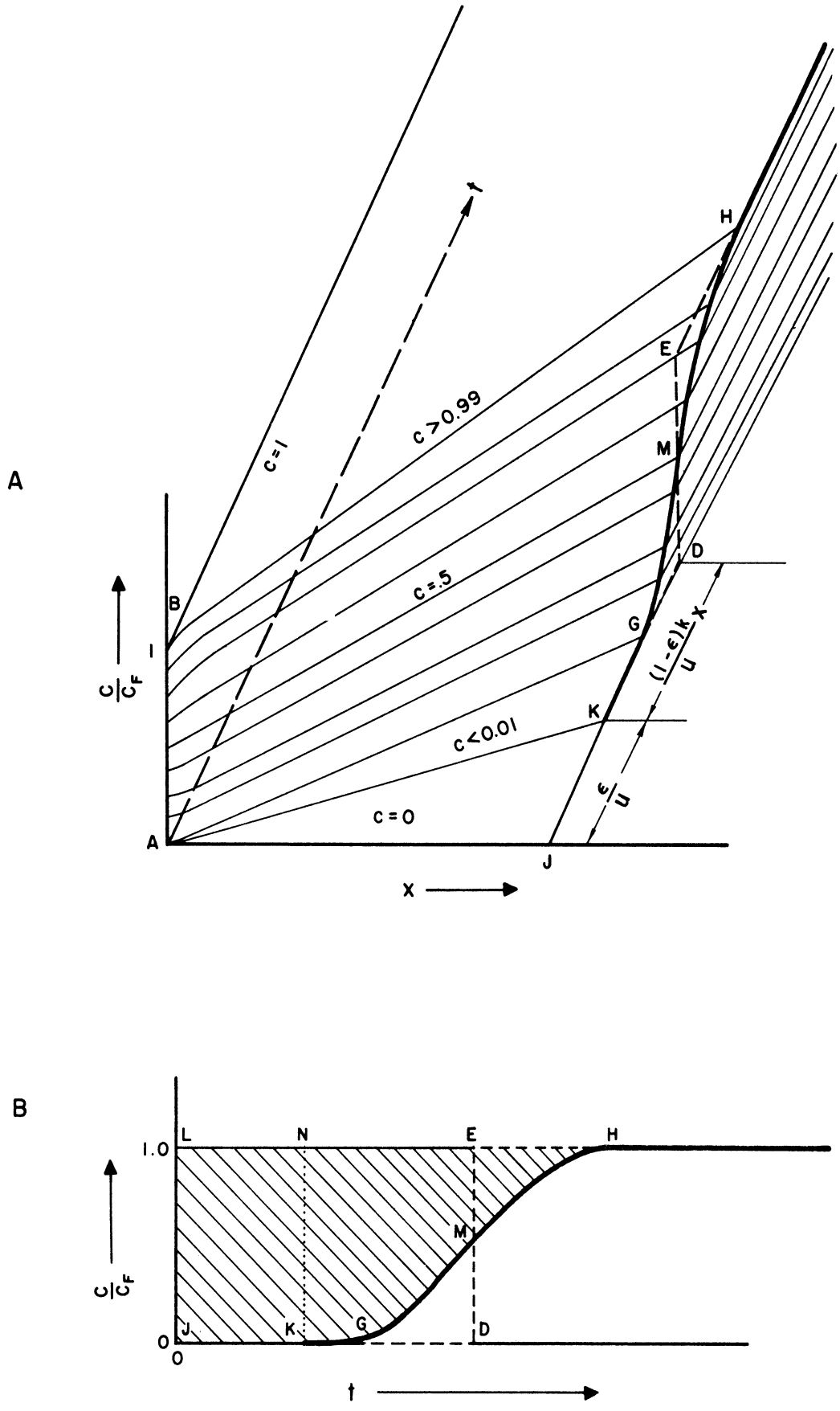

Figure 33. Concentration Surface for the Case of Diffusion in Solid as the Controlling Resistance to Mass Transfer, and Linear Equilibrium Characteristic for the Solute. (Model B(i)(a)).

understood by considering Figure 33A. The $\overline{Z}$-axis, where $\theta=0$ lies along the line AK. $\overline{Z}$ coordinate is proportional to the x coordinate. The θ-axis coincides with the t-axis. θ coordinate of any point is proportional to its distance parallel to the t-axis from the line AK.

The curve JKGMH in Figure 33A is a section of the surface for a constant value x. Figure 33B shows this section. The area JGMHL represents the total amount of the solute retained in the column. Of this, the area JKNL represents the amount retained in the voids in the column and the area KGMHN represents the amount retained in the solid phase.

If a vertical line ED were drawn in the figures such that area JDEL is equal to area JGMHL, then the curve JDEH would have been the break through curve for an equilibrium column operation if there had been no resistance to mass transfer.

For different values of x, the locus of the point D in the x-t plane would be a straight line with a slope of $[\frac{\epsilon}{u} + \frac{(1-\epsilon)K}{u}]$. (This would actually be the contour diagram for the equilibrium column operation for linear equilibrium. See Figure 9A.) On the $\overline{Z}$-θ plane of Figure 29 and 30 this would be a straight line with a slope equal to 1.

Corresponding to continuous curved surface in Figure 33A for the non-equilibrium column operation, the equilibrium column operation would give a discontinuous concentration surface. The discontinuity would be along the plane ADEB. The effect of mass transfer resistance has been to "roll out" this discontinuous surface. The boundary DE is "smeared" along GH. For consistancy of material balance, areas of the three sided figures GDM and MEH are equal.

It may be recalled that smearing of the discontinuous concentration surface is also obtained in an equilibrium column operation if the solute exhibits non-linear equilibrium. [See the section on Model A(i) (b) and Figures 14, 19, 20.] However, if a slug of a solution is fed to a column, the effect of non-linear equilibrium is to "smear" one edge and "sharpen" the other, where as the effect of mass transfer resistance is to "smear" both edges. Consequently, the effluent wave tends to be heavily skewed in the case of non-linear equilibria and it tends to be symmetrical in the case of linear equilibria with mass transfer resistances.

In the case of a system with non-linear equilibrium characteristics and appreciable mass transfer resistances, the effect of the latter would be to smear both the edges of an effluent wave, whereas that of the former would be to "smear" further one of the two edges and "cramp in" or "sharpen" the other edge. As to whether the leading or the trailing edge would be the more "smeared" one would depend on the sign of the curvature of the equilibrium isotherm.

Returning to Figures 29 and 30 which represent graphically the solutions of the model under the present consideration, it can be seen that for large values of x, the level curves are straight lines. This makes it possible to extrapolate the solution shown in Figure 29. On the Figure 29, the level curve for $c/c_F = 0.5$ is a straight line with slope equal to 1, and as explained above, it coincides with the line representing overall material balance (locus of the point D in Figure 33A). The level curves for values of c/c_F other than 0.5 are spread somewhat symmetrically about this line. This means that the break through curve

such as one shown in Figure 33B would be antisymmetric about the midpoint M, and the combination of two break through curves giving the response of the column to a slug of solution in the feed would be a symmetrical wave in the effluent.

For small values of $\overline{Z}$, however, as can be seen in Figure 30, the deviation from symmetry is appreciable and the effluent wave would be skewed. This skewness, in general, would be much smaller than that produced by the effect of non-linear equilibria. In industrial and laboratory practice $\overline{Z}$ is frequently in the range of 1 to 20.

In Figure 33A, the distance JD and the line AD depend on the equilibrium constant, the velocity of the liquid and the porosity of the bed. They are independent of the mass transfer resistance. The curve GMH depends on the mass transfer resistance. Figure 33 is the concentration surface for the saturation operation of a column. If the feed to the column is a slug of the solution, the concentration surface obtained is shown in Figure 34. For a constant value of x, the cross section of the surface gives the effluent wave. The shape of the wave is influenced by the mass transfer resistances. But the position of the wave on the time axis is independent of the mass transfer resistances. If the wave is symmetrical, the peak of the wave would be at the same value of time as the midpoint of the square wave that might be obtained for the equilibrium column operation. (See Figure 35.)

The spread of the effluent wave and the "smearing" of the sharp edges of concentration profiles in equilibrium column operation, depend on the ratio D/R^2 where D is the diffusivity and R is the radius of the spherical particles. As the particle size, R, is decreased, the mass

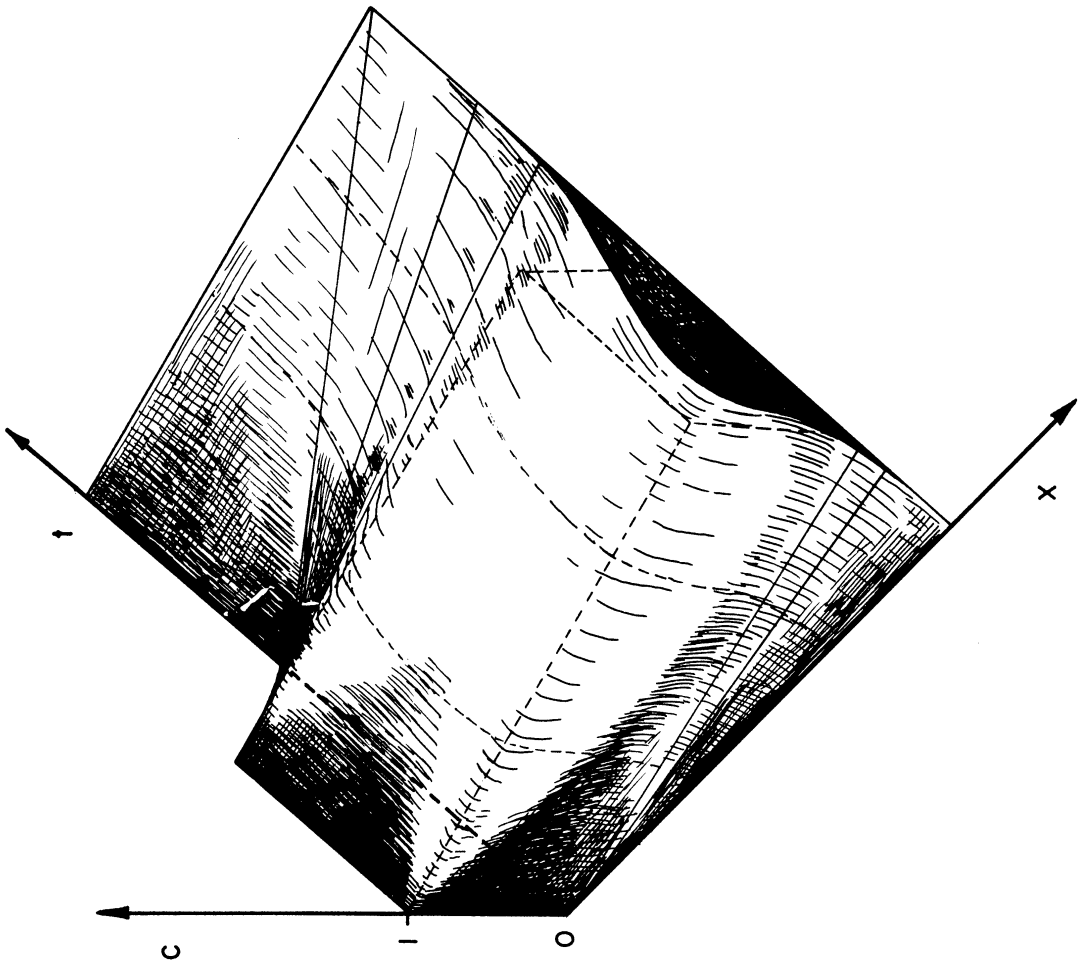

Figure 34. Concentration Surface for Model B(1)(a), where a Slug of Solution is the Feed to the Column.

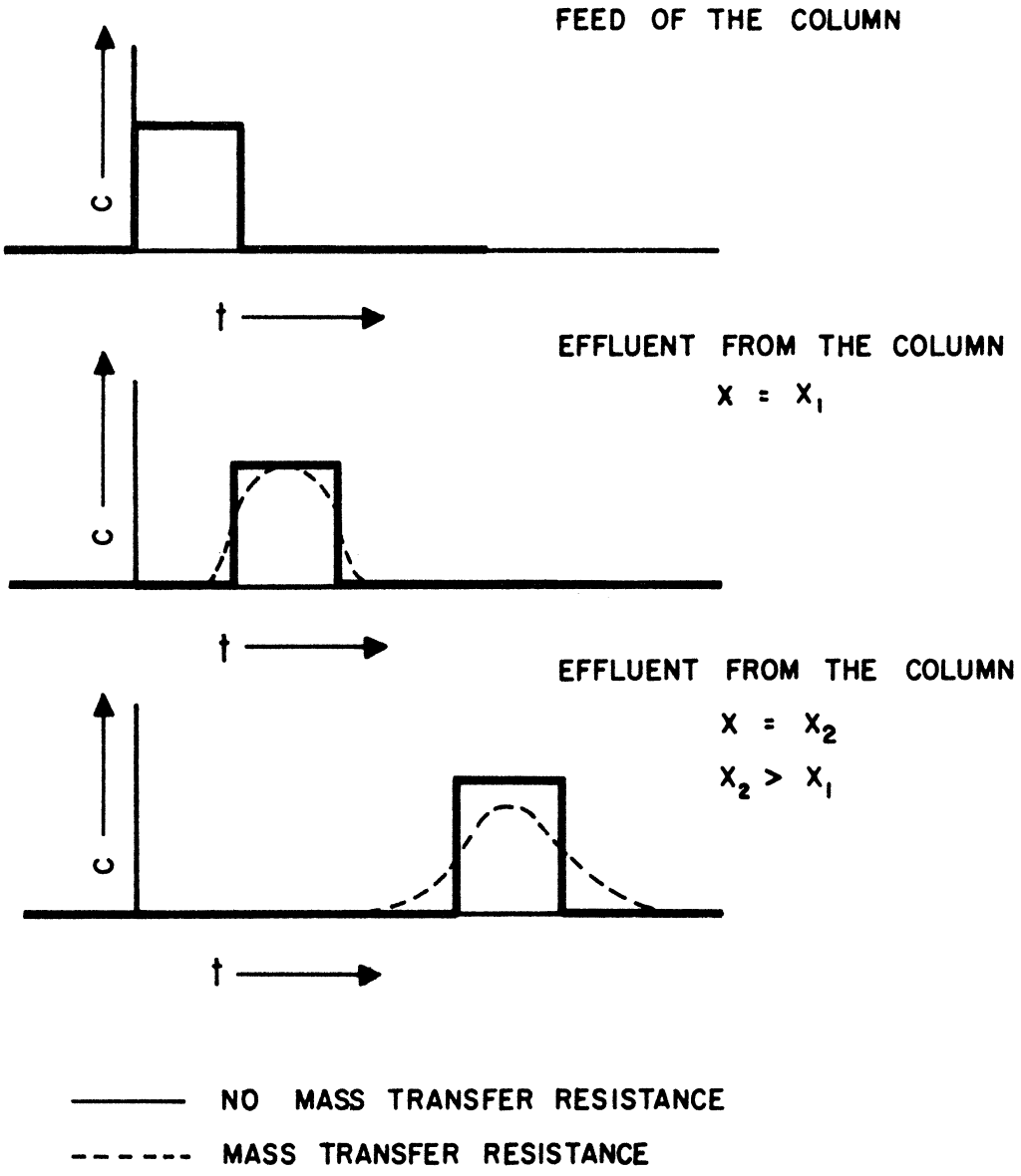

Figure 35. Effluent Waves for Equilibrium and Non-Equilibrium Column Operation for the Case of Linear Equilibrium Characteristics. (Models A(i)(a) and B(i)(a)).

transfer resistance is reduced and the "smearing" is reduced. Also as the diffusivity, D, in increased, "smearing" is reduced.

If a slug of solution is fed to a column, the effluent wave that would be predicted according to the model under present consideration, can be determined if the equilibrium constant and the diffusivity of the solute in the solid phase are known. The method for predicting the effluent wave by using Figures 29 and 30, has been described above. On the other hand, frequently, the effluent wave is determined in a laboratory and the equilibrium constant and the diffusivity are not known. The following describes a method for fitting the effluent data to obtain these constants, assuming linear equilibrium and the diffusion in solid as the controlling mass transfer resistance.

First of all, the behavior of the column, if it were to be saturated with the feed, is estimated from the effluent wave. As shown in Figure 32, the effluent wave, Figure 32F, may be supposed to be made up of two responses, viz. Figures 32D and 32E. The former, Figure 32D, is the saturation behavior of the column. Figure 36 shows the method of estimating the saturation behavior from the effluent wave. If t_o is the width of the feed slug, then for time equal to t_o after the start of the effluent wave, i.e., along the curve AB in the figure, the curve of saturation behavior and the effluent wave coincide. For values of time beyond the point B, any point F on the curve of saturation behavior is obtained by adding to any point D on the effluent wave, the value of the curve at the point E. The t-coordinate of E is less than that of D by the value t_o. The point E is always taken on the portion of the curve for the saturation behavior that has already been estimated.

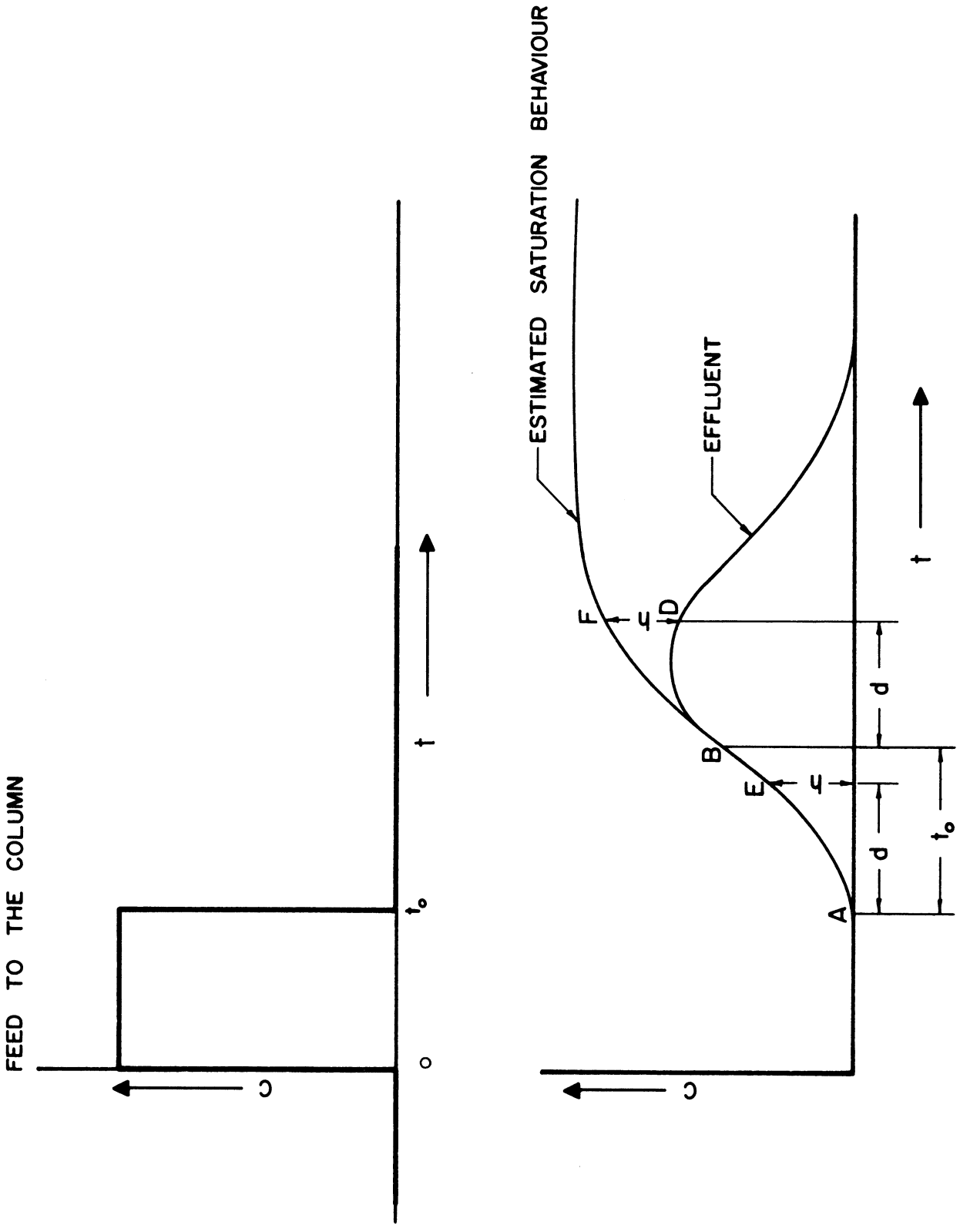

Figure 36. Estimation of the Saturation Behavior of a Column From the Effluent Wave.

The equilibrium constant and the diffusivity are estimated from the curve for the saturation behavior of the column. Figure 37 shows the method of determining the value of the equilibrium constant from the curve. The line GH parallel to the concentration axis, is drawn such that the areas of the three sided figures AGM and MHF are equal. As explained above, Figure 33B, the line GH in Figure 37 represents the break through curve that would have been obtained if there had been no mass transfer resistances. The value of K can be determined from the distance JG which is equal to $\frac{\epsilon}{u} x + \frac{(1-\epsilon)K}{u} x$.

Frequently the curve AMF, Figure 37, is antisymmetrical about the point M and the ordinate of M is 0.5 c/c_F. In such cases the effluent wave itself would be symmetrical about its peak and the position of the peak would be at the value of time equal to

$$\frac{\epsilon}{u} x + \frac{(1-\epsilon)K}{u} x + \frac{t_o}{2}$$

where t_o is the time for which the slug of the solution was fed to the column. Consequently in the case of symmetrical effluent waves, the value of the equilibrium constant can be determined directly from the position of the peak of the wave.

The value of diffusivity is determined from the shape of the curve for saturation behavior. It is necessary to prepare the following master plot for this purpose.

Figure 29 which was explained above, gives the solution of the partial differential equations describing the model under consideration. From the figure, one may obtain concentration in the liquid, c, as a

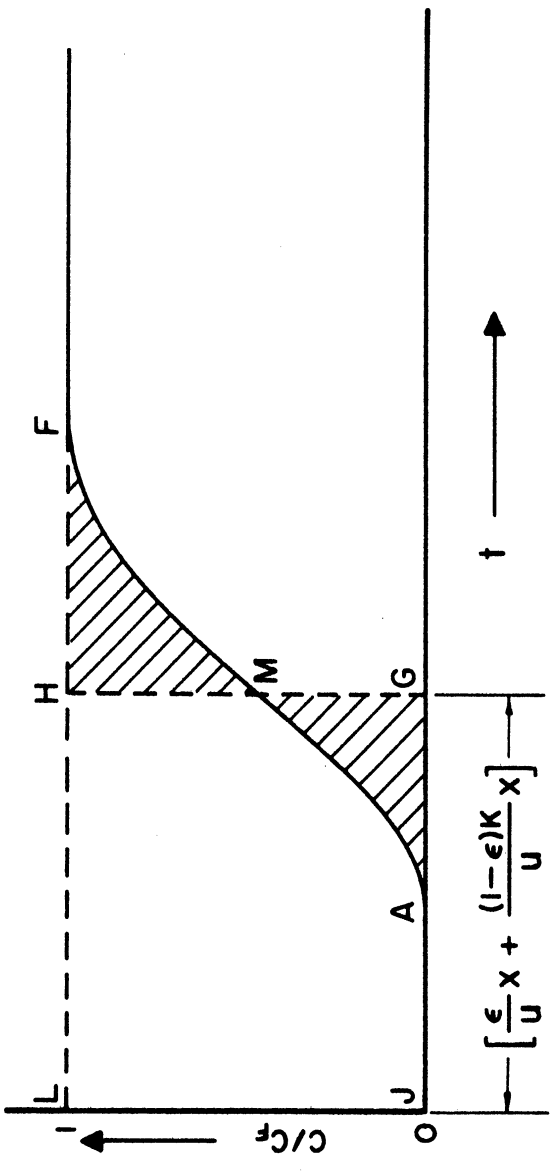

Figure 37. Determination of Equilibrium Constant from the Saturation Behavior of a Column. (Model B(i)(a)).

function of the dimensionless independent variables $\overline{Z}$ and θ.

$$\overline{Z} = \frac{DK(1-\epsilon)x}{uR^2} \tag{76}$$

$$\theta = \frac{D}{R^2}(t - \frac{x\epsilon}{u}) \tag{58}$$

Let $\overset{\vee}{\theta}$ be defined by Equation (85).

$$\overset{\vee}{\theta} = \theta/\overline{Z} \tag{85}$$

Then the concentration can be expressed as a function of $\overline{Z}$ and $\overset{\vee}{\theta}$,

where

$$\overline{Z} = \frac{DK(1-\epsilon)x}{uR^2} \tag{76}$$

and

$$\overset{\vee}{\theta} = \frac{\epsilon}{(1-\epsilon)K}\left(\frac{ut}{x\epsilon} - 1\right) \tag{86}$$

With the use of Figures 29 and 30 and the Equation (85), the concentration in the liquid can be evaluated numerically as a function of $\overline{Z}$ and $\overset{\vee}{\theta}$. Figure 38 shows this function. It may be noted that $\overline{Z}$ depends on the factor (DK/R^2) and that $\overset{\vee}{\theta}$ is independent of the diffusivity. Figure 38 is the master plot that is used in determining diffusivity from the curve of saturation behavior of the column. The abscissa $\overset{\vee}{\theta}$ is drawn on the logarithmic scale, so that for a given value of $\overline{Z}$, multiplying the abscissa of all the points by a factor would not alter the shape of the curve but merely translate it along the abscissa.

In order to determine the diffusivity of the solute in the solid particles, the curve of the saturation behavior of the column (estimated from the effluent data) such as the curve AEBF shown in Figure 36 is plotted on a semi-logarithmic scale. The ordinate is the ratio of the

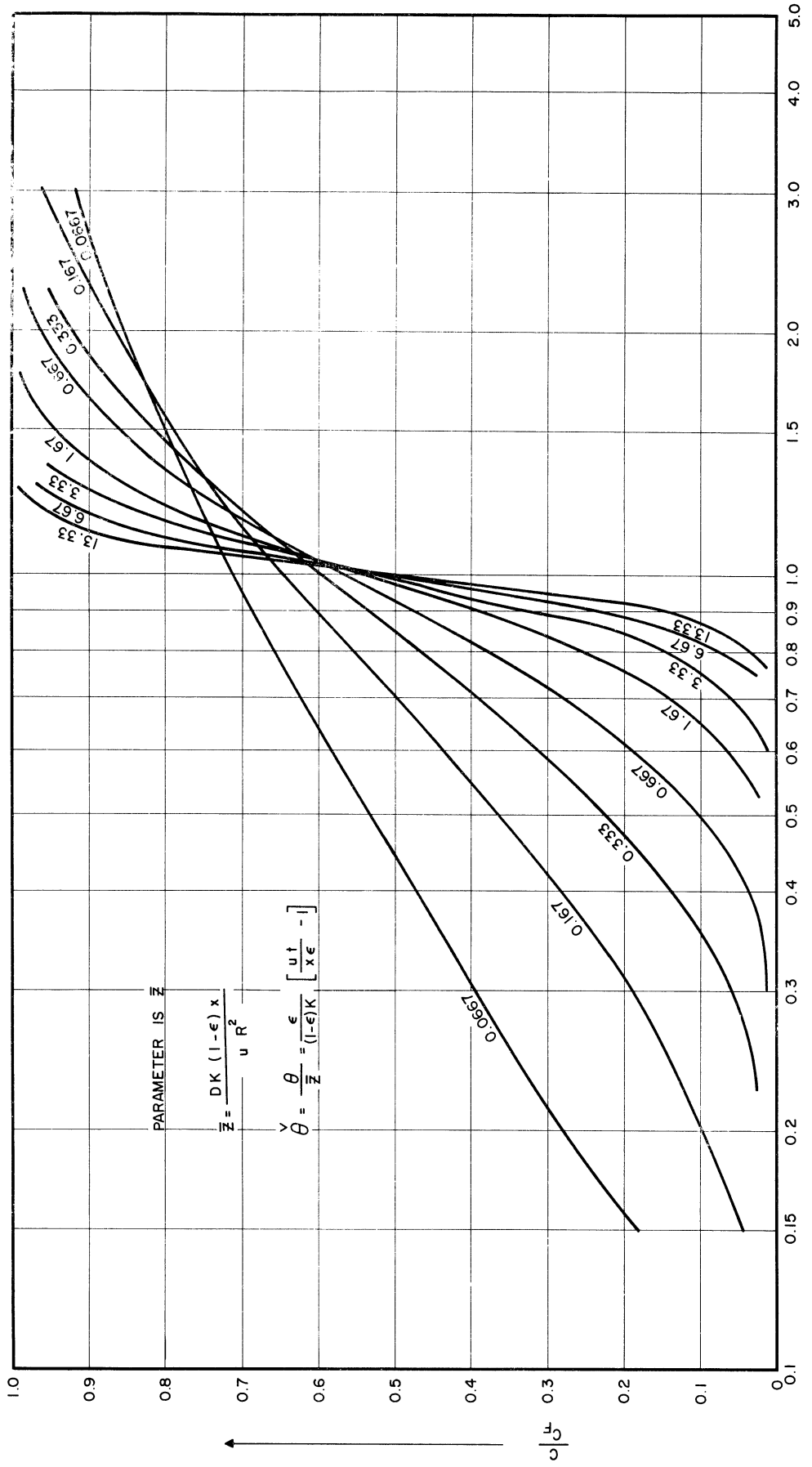

Figure 38. Concentration in the Liquid as a Function of $\overset{v}{\theta}$ and $\bar{Z}$, for Saturation of a Column with Diffusion in the Particles as the Controlling Resistance. (Model B(i)(a)). Master Plot for Fitting the Data.

concentration in the liquid to that in the feed (the concentration in feed is the same as the final concentration on the curve AEBF for large values of t) on the linear scale, and the abscissa is the quantity $(\frac{ut}{x} - 1)$ plotted on the logarithmic scale. This plot is now matched with the master plot.

The master plot may be made on a translucent paper and it may be superimposed on the above plot based on the data. The master plot may be moved along the abscissa until the curve based on data matches one of the curves on the master plot. The value of $\overline{Z}$ on the master plot for this match is the fit of the data. The error in the value of $\overline{Z}$ for this fit can be roughly estimated visually. This curve fitting described here is independent of the value of the equilibrium constant. Since $\overline{Z}$ is equal to $DK(1-\epsilon)x/uR^2$, the value of DK/R^2 can be determined. As described above, the value of the equilibrium constant K is determined independently from the position of the curve of saturation behavior or from the peak of the effluent wave. Using this and the value of DK/R^2, diffusivity, D, can be determined.

Summarizing, for a model assuming linear equilibrium characteristics of the solute, and the diffusion in the solid as the controlling resistance to mass transfer, Figures 29, 30 and 38 give generalized solutions for the saturation behavior of a column. Since the entire mathematical problem is linear, the solutions are linearly additive and the response of the column if a slug of the solution is introduced into it, can be obtained from Figures 29 and 30, if the equilibrium constant and the diffusivity are known. Conversely, from the effluent curves, the diffusivity and the equilibrium constant can be determined with the help of Figure 38.

In the above discussions, the mass transfer in the solid was assumed to obey Fick's Law of Diffusion. It is possible to assume other mechanisms of mass transfer in the solid phase and different set of mathematical equations would describe the model. Hiester and Vermeulen (H2) have reported a solution that is applicable if it is assumed that the rate of mass transfer in the solid is given by Equation (86).

$$\text{rate} = k_s \left(c_s^* - \bar{c}\right) \tag{86}$$

where rate is the rate of mass transfer per unit surface area

c_s^* = the concentration in the solid that would be in equilibrium with the concentration in the liquid.

$\bar{c}$ = the concentration of the solute in the solid. (It is assumed to be a constant throughout a solid particle.)

and

k_s = a proportionality constant that is independent of the concentrations.

(b) Resistance in the Liquid Phase is the Controlling Resistance to Mass Transfer

In the following equations it is assumed that there are no concentration gradients within a solid particle. The mass transfer to the solid takes place through a liquid film and the driving force for the mass transfer is the difference between the concentration in the bulk of the liquid and the concentration that would be in equilibrium with the solid.

Mathematical Equations:

Material Balance:

$$u \frac{\partial c}{\partial x} + \frac{\partial}{\partial t} (\epsilon c + (1-\epsilon)Q) = 0 \tag{87}$$

Mass Transfer through the liquid film:

$$(1-\epsilon) \frac{\partial Q}{\partial t} = k\bar{S}(c-c^*) \tag{88}$$

Equilibrium condition at the surface of the solid:

$$Q = Kc^* \tag{89}$$

Initial condition of the column:

$$c = 0 \quad \text{for} \quad t = 0 \tag{90}$$

$$Q = 0 \quad \text{for} \quad t = 0 \tag{91}$$

Feed History:

$$c = 1 \quad \text{at} \quad x = 0 \tag{92}$$

Definition of the Symbols:

x = the distance from the inlet end of the column.

t = time.

c = the concentration of the solute in the liquid. It is a function of x and t.

Q = the concentration of the solute in the solid. It is a function of x and t.

c^* = the concentration in liquid that would be in equilibrium with the solid. It is a function of x and t. [Equation (89) may be considered to be the definition of c^*.]

ϵ = the porosity of the bed.

u = the superficial velocity of the liquid.

K = the equilibrium constant.

$\overline{S}$ = the surface area of the solid particles per unit volume of the bed. If the particles are uniform spheres of radius, R, the value $\overline{S}$ is given by the expression $3(1-\epsilon)/R$.

k = the mass transfer coefficient across the liquid film. It is the amount of a material transferred per unit area of interface in unit time for a unit concentration difference across the liquid film.

The "regenerator" problem in heat transfer, that considers the unsteady state temperatures when a fluid at a high temperature is passed through a bed of inert solids gives identical equations as the ones above if the concentrations are substituted for the temperatures, the mass transfer coefficient is substituted for the heat transfer coefficient and the equilibrium constant is substituted for the ratio of heat capacities of the solid and the fluid.

The problem in heat transfer has been solved and the solution and generalized curves have been reported by Schumann (S2) and Furnas (F1). With the substitution of the constants indicated above, their solutions and curves can be used for the model under present consideration.

Much of the general discussion of the preceding model that considered diffusion in the solid as the controlling resistance to mass transfer is applicable to the present model. The mathematical problem is linear and the solutions may be added linearly. The effect of the mass

transfer resistance on the concentration surface is to smear the edges that would be obtained for equilibrium column operations. Except for very small columns, the location of the effluent waves would be independent of the value of the mass transfer coefficients and only the shapes would be influenced by the value of the mass transfer coefficients.

(c) Diffusion in Solid and Film Resistance in the Liquid

Mathematical Equations:

Material Balance:

$$u \frac{\partial c}{\partial x} + \frac{\partial}{\partial t} (\epsilon c + (1-\epsilon)Q) = 0 \tag{93}$$

Diffusion in the Solid:

$$D(\frac{\partial^2 q}{\partial r^2} + \frac{2}{r} \frac{\partial q}{\partial r}) = \frac{\partial q}{\partial t} \tag{94}$$

Mass Transfer through Liquid Film:

$$k\bar{S}(c-c^*) = + D\bar{S}[\frac{\partial q}{\partial r}]_{r=R} \tag{95}$$

Equilibrium Function:

$$q = Kc^* \quad \text{at} \quad r = R \tag{96}$$

Symmetry in the solid particles:

$$\frac{\partial q}{\partial r} = 0 \quad \text{at} \quad r = 0 \tag{97}$$

Average concentration in the solid:

$$Q = (\int_{r=0}^{r=R} 4\pi r^2 q \, dr) / \frac{4}{3} \pi R^3 \tag{98}$$

Initial condition of the column:

$$c = 0 \quad \text{for} \quad t = 0 \tag{99}$$

$$q = 0 \quad \text{for} \quad t = 0 \tag{100}$$

Feed History:

$$c = 1 \quad \text{at} \quad x = 0 \tag{101}$$

Definition of the symbols:

x = the distance from the inlet end of the column.

t = time.

r = the distance of a point in a solid particle from the center of the particle.

c = the concentration of the solute in the liquid. It is a function of x and t.

q = the concentration within the solid particle. It is a function of x, r and t.

Q = the concentration of the solute in the solid. It is a function of x and t.

c^* = the concentration in a liquid that would be in equilibrium with the solid. It is a function of x and t. [Equation (96) may be considered to be the definition of c^*.]

ϵ = the porosity of the bed.

u = the superficial velocity of the liquid.

R = the radius of the solid particles.

$\bar{S}$ = the surface area of the solid particles per unit volume of the bed. If the particles are uniform spheres of radius, R, the value S is given by the expression $3(1-\epsilon)/R$.

K = the equilibrium constant.

D = the diffusivity of the solute in the solid phase.

k = the coefficient for mass transfer across the liquid film. It is the amount of a material transferred per unit area of interface in unit time for a unit concentration difference across the liquid film.

Equation (95) states that the rate of mass transfer across the liquid film is the same as the rate of mass transfer into the solid phase from its surface.

The assumptions on which the above equations are based have been mentioned with the equations describing the preceding two models, both of which may be considered as special cases of the present model.

Equations (93) through (101) define a problem in integro-differential equations. It has been solved by Rosen (R1) by use of operational calculus. The analytic solution has been obtained in the form of special integrals that have been evaluated numerically on a computer (R2) for several values of dimensionless variables and parameters. A table of the numerical values and dimensionless plots of the breakthrough curves for different parameters are available in Reference (R2).

(d) Longitudinal Diffusion in the Liquid Added to Model (c)

The addition of the longitudinal diffusion in the liquid changes the material balance Equation (93) to Equation (102)

$$D_L \frac{\partial^2 c}{\partial x^2} - u \frac{\partial c}{\partial x} = \frac{\partial}{\partial t} (\epsilon c + (1-\epsilon)Q) \qquad (102)$$

where

D_L = the longitudinal diffusivity in the liquid.

All the other Equations (94) through (101) from the preceding model are applicable. An additional boundary condition is required on c, which is given by the Equation (103).

$$\frac{\partial c}{\partial x} = 0 \quad \text{at} \quad x = L \tag{103}$$

where

L = the length of the column.

Equations (94) through (103) define the mathematical problem. Analytic solution of the problem has been reported by Kasten, Lapidus & Amundson (K1). Numerical evaluation of the solution is difficult since it involves integration and summation of infinite series of terms involving exponential and Bessel functions.

On the concentration surface in (x, t, c) space, the effect of longitudinal diffusion is similar to that of mass transfer resistances, viz. "smearing" of sharp edges. Figure 39 shows the difference in the range of smearing. The restriction of the overall material balance discussed along with Figure 33B in the section on model B (i) (a) applies in every case of "smearing".

(ii) Non-Linear Interdependent Equilibria. (Two Solutes)

For the case of mass transfer resistance in the liquid and diffusion in the solid, mathematical equations similar to the Equations (92) through (101) may be written for each solute. The equilibrium function (93) will be non-linear and in general would be a function of the concentration of both solutes. If the mass transfer is controlled either by the resistance in the solid or by that in the liquid, simpler equations corresponding to those given with models B(i) (a) and (b) may be written.

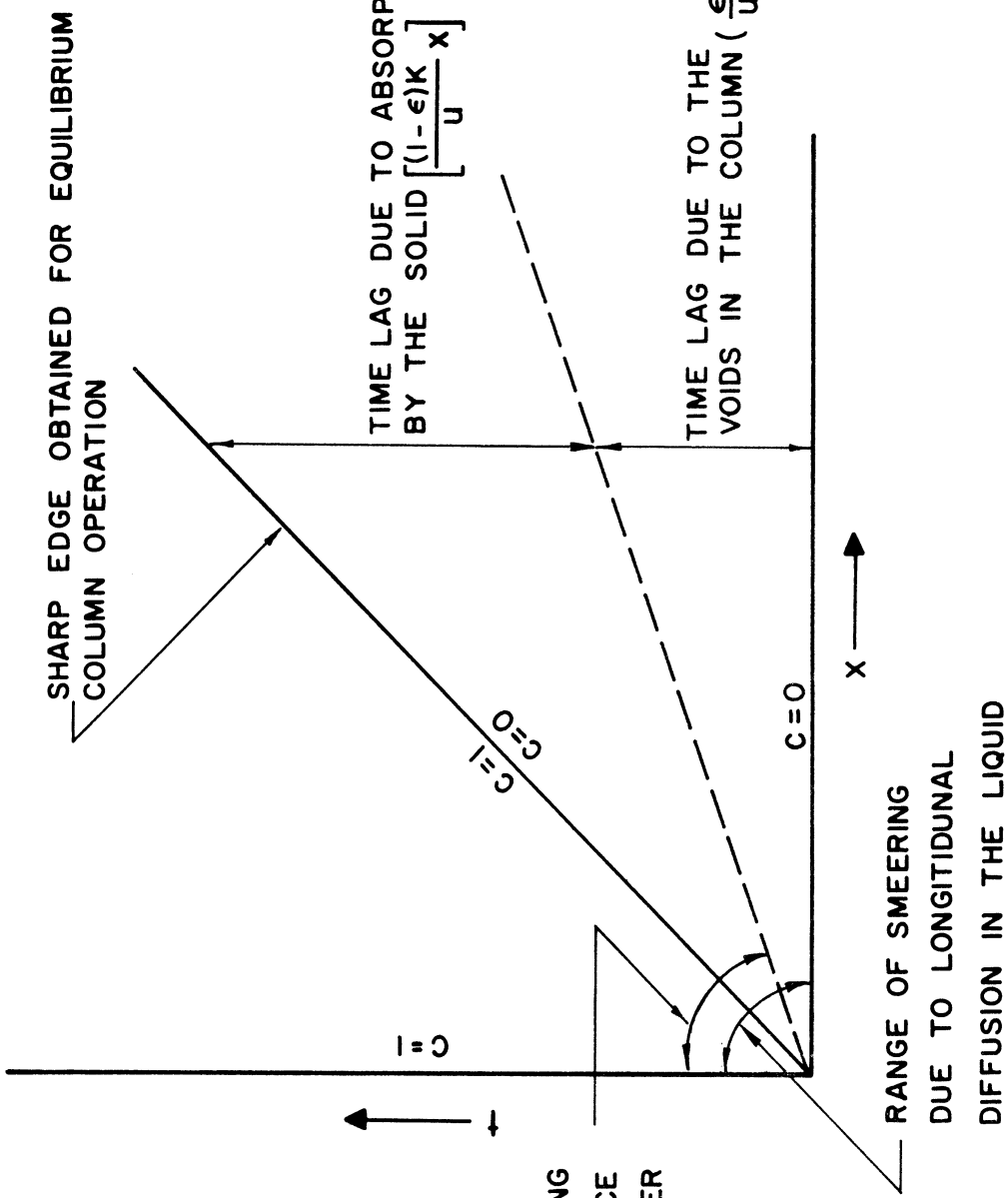

Figure 39. x-t Contour Diagram for Equilibrium Column Operation (Saturation) and the Areas of "Smearing" Due to Resistance to Mass Transfer and Longitudenal Diffusion in the Liquid.

The general mathematical problem has not been solved analytically. For any particular case, the equations may be solved numerically. Availability of a digital computer has made the numerical solution feasible.

A rough estimate of the solution for this general case can be made by degenerating the problem into simpler models discussed in the preceding sections, and drawing x-t Contour Diagrams for the simplified cases. For instance the extent of "smearing" due to mass transfer resistances may be roughly estimated by assuming approximately linear equilibria.

Because of interdependent equilibria, concentration and dilution of the solutes would take place, see Model A (ii) (b). Some estimate of this effect can be obtained by considering equilibrium operation of a column for the system under consideration and drawing approximate x-t Contour Diagrams. An estimate of the effect of shrinkage and swelling of the resin may also be obtained by considering equilibrium column operation.

5. Some Comments on Analytic, Graphical and Numerical Solutions of Various Models

Analytic solutions in general are possible only for the simpler of the mathematical models. They are useful because of their general applicability. Numerical values for these solutions can be evaluated to any desired accuracy.

At times, however, the analytic solutions are obtained by defining special transforms and the solutions are expressed in terms of very complex integrals and infinite series. Numerical evaluation of these solutions for any practical problem may be very difficult because the series may not converge rapidly and there may be terms involving multiplication of very large numbers by very small numbers.

The x-t Contour Diagrams and the concentration surfaces may be considered as graphical solutions. For some models it may be easier to obtain the contour diagram than the analytic solutions, e.g., in the case of equilibrium column operation for non-linear equilibrium, Model A(i) (b), the contour diagram can be plotted readily from the equilibrium isotherm.

A generalized plot of breakthrough curves based on an analytic solution of the model may also be considered a graphical solution.

Graphical solutions are a strong visual aid to understanding the models. If the behavior of an experimental column is known, the graphical solutions help select the models that might fit the data.

Numerical solutions are obtained only for a particular set of parameters and for a particular system. The procedures for obtaining the numerical solutions have their own breed of problems such as the stability and convergence of the numerical iterative and repititive procedures used, as well as convergence of the numerical solution to the "true" analytical solution.

The numerical solutions have been feasible with the advent of the high speed digital computers. Nevertheless, for a particular problem the space grids and the time intervals may have to be so small that the computation time required may make the numerical solution impractical. With large numbers of calculations an additional problem of the cummulative round off errors of the computation may make it difficult to get a good numerical solution.

Automatic computers have made it possible to get a "general numerical solution" of a problem. The entire computer program by itself may be considered as the general solution. The act of feeding the values

of the parameters in the program and running the program on a computing machine may be considered analogous to the act of computing numerical values by substituting values of parameters in a general analytic solution.

6. Related Literature and Literature Credits

For general background and discussion of many of the specific models considered in this section of the thesis, the author is indebted to many workers in various fields such as chromatography, ion exchange and ion exclusion.

For overall survey, following books have been very useful.

Keulemans: Gas Chromatography (Ref. K2)

Nachod (Ed): Ion Exchange Technology (Ref. N1)

Vermeulen: Chapter on Adsorption Processes in Advances in Chemical Engineering, Vol. II (Ref. V1)

Equilibrium column operation for single solute with non-linear equilibrium has been discussed by De Vault (D1). His mathematical development has been used in this thesis for the model. Sillen (S8) has considered the same model from a slightly different point of view.

Sillen (S7,S8) has also explained the transformation of coordinates that simplify the material balance equation for the unsteady state operation of fixed beds, and has used graphical aids for equilibrium column operations with single solutes. He has attempted calculations for ion-exchange beds graphically.

In the cases of non-equilibrium column operations, problems with linear equilibrium relationships have received considerable attention.

Rosen (R1) has solved analytically the problem considering diffusion in the solid phase and mass transfer resistance in the liquid film surrounding it. He has also obtained the numerical values of his solution with the help of a digital computer and reported (R2) them in form of generalized plots. His solutions and his plots have been used in discussion of some of the models in this thesis. Wicke (W1) obtained an analytic solution of the same problem and left it in the form of La Place transform. Lowan (L2) has given a method of obtaining the numerical solution of the same problem. Selke et al. (S3) have given a method of incremental calculations using constructions similar to Schmidt method (used in calculations for unsteady state heat transfer problems).

Thomas (T2) and Kasten, Lapidus and Amundson (K1) have solved the problem considering diffusion in the solid phase as the only mass transfer resistance. Glueckauff (G1) has treated the same problem and has considered various approximations.

Furnas (F1) and Schumann (S2) have solved and reported generalized curves for the "regenerator" problem in heat transfer and their solution as discussed with Model B(i) (b) above is applicable if the resistance in the fluid film is the only mass transfer resistance.

An added complication of longitudinal diffusion in the liquid is considered by Lapidus and Amundson (L1). Their analytic solution is difficult to evaluate numerically.

A general problem of fixed beds with axial and radial diffusions in the beds has been solved by Amundson (A1,A2) by use of operational methods. The mathematical steps are explained and analytical

solutions are given. Numerical evaluation of the solutions is difficult. Sigmund, Munro and Amundson (S6) have considered the problem of moving beds mathematically.

Thomas (T1) has obtained an analytic solution for fixed bed ion exchange operation assuming no mass transfer resistances and second order reaction kinetics. Hiester and Vermeulen (H2) have shown that Thomas' solution can be used for the following cases after suitable substitutions:

(i) if mass transfer in the liquid film is the controlling resistance

(ii) if mass transfer in the solid is the controlling resistance and it can be described by a constant coefficient of mass transfer in the solid, defined in the manner similar to that in which the mass transfer coefficient in the liquid film is generally defined.

Opler and Hiester (O1) have obtained numerical values for Thomas' solution (T1) mentioned above, with the help of a digital computer and they have reported tables of values for different parameters (O1). Hiester and Vermeulen (H2) have given generalized plots of the same solution. Hiester, Radding, Nelsen and Vermeulen (H1) have worked out a method of extending Thomas' solution to combine the solid and the liquid phase resistances (i) and (ii) above and to estimate ion exchange column performance under non-linear equilibria.

III. COMPARISON OF MODELS TO ION EXCLUSION* DATA

1. Ethylene Glycol-Water-Dowex 50 System

A. Available Data

Simpson and Wheaten (S9) have reported data on effluent waves obtained when a slug containing a solution of ethylene glycol in water is fed to a column of Dowex 50.* Figure 40 is a reproduction of the figures given in the reference mentioned above.

They used resin beds of approximately 100 ccs. (column 0.6 in. x 22 in.). The feed solutions contained 10% of ethylene glycol by weight. The data were obtained at room temperature. Unless mentioned otherwise on Figure 40, for each run, the feed was 5 ccs., the flow rate was 0.134 gal./(sq.ft.)(min.), the cross linkage of the resin was 8% divinyl benzene and the mesh size of the resin particles was 50 - 100 mesh.

The zero point on the abscissa (effluent volume) in Figure 40, represents that point at which the feed solution entered the resin bed.

The variables that have been studied are the following:

Cross linkage of the resin in Figure 40A.

The amount of feed solution in Figure 40B.

Resin particle size in Figure 40C.

Liquid flow rates in Figure 40D.

B. Selection of the Model

Model B(i) (a) discussed in the preceding section was selected for fitting the data. This model assumes a non-equilibrium column

---

* For description of ion exclusion and details about ion exchange resin, refer to Sections 1 and 11 of the Detailed Discussions in Part I of this dissertation.

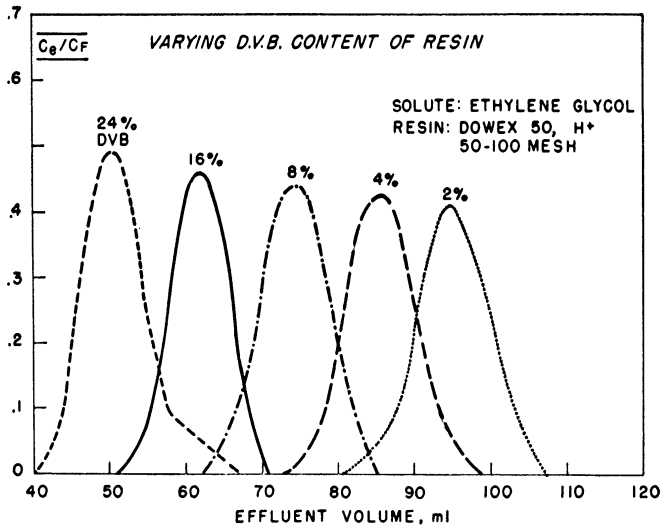

A

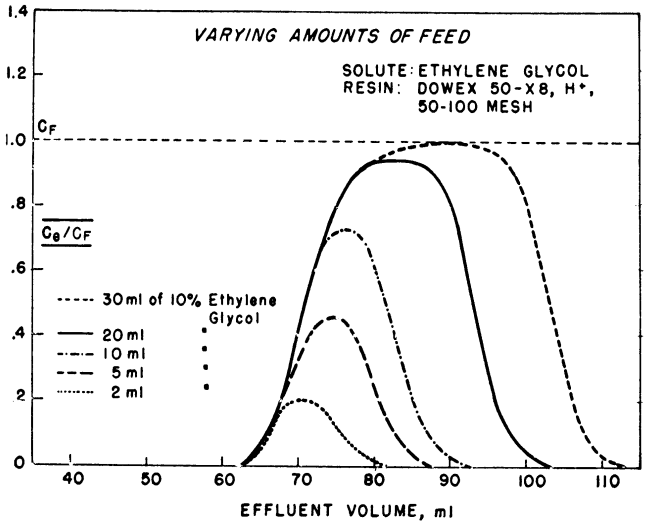

B

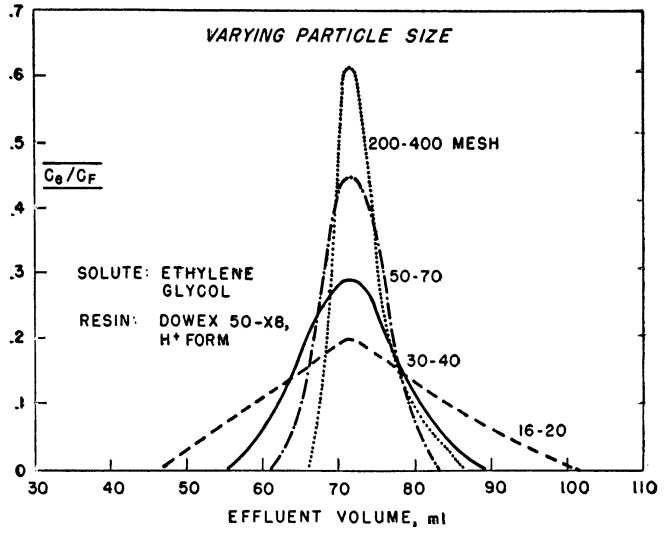

C

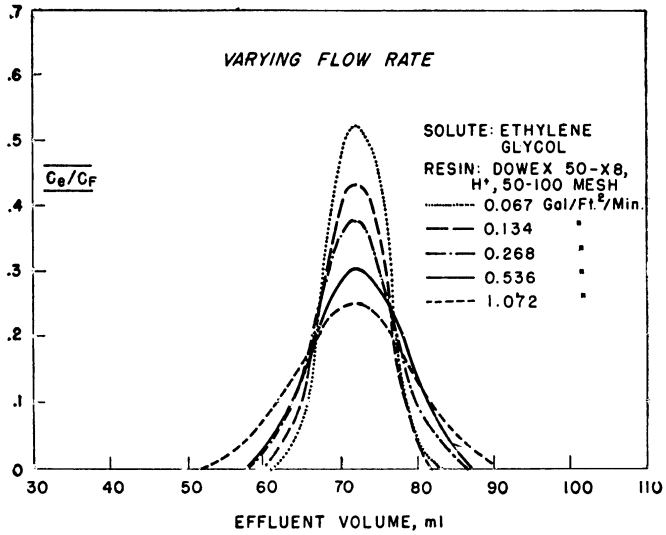

D

Figure 40. Ion Exclusion Data for the System Ethylene Glycol-Water-Dowex 50 [Reproduced from Simpson and Wheaton (S9)].

operation in which the diffusion of the solute in the solid phase is the controlling mass transfer resistance. Linear equilibrium between the solid phase and the liquid phase is assumed. Slug flow of the liquid and no longitudinal diffusion in the liquid are also assumed. The final selection of the model is somewhat arbitrary, although the following factors are taken into consideration.

The effluent waves obtained in Figure 40A are nearly symmetrical, suggesting that the equilibria are likely to be linear in the concentration range of interest. Solid-liquid equilibria for Dowex-50 are generally linear if the solute is a non-electrolyte and they are non-linear if the solute is an electrolyte. For equilibrium distribution of glycerol - a molecule structurally similar to ethylene glycol - between aqueous and resin phase, approximately linear equilibrium characteristics are obtained (S4, S5). This suggests that a model assuming linear equilibrium may fit the data.

The structural similarity between glycerol and ethylene glycol also suggests that the diffusivities of the two materials in Dowex 50 may be of the same order of magnitude. Diffusivities of glycerol have been obtained in Part I of this dissertation. They are a fraction of its diffusivity in water. The mass transfer coefficient for the transfer of materials through the liquid film can be estimated from generalized correlations for flow through packed beds (C2, S3).

Even for the lowest flow rates and the finest resin particles used, the comparison between the mass transfer coefficients and the diffusivities shows that the total resistance to the mass transfer is determined by the low diffusivities. This suggests that a model assuming that the diffusion in the solid phase controls the rate of mass transfer may be applicable.

C. Fit of the Model to the Data

The values of equilibrium constants for distribution of ethylene glycol between water and Dowex 50 are not known. The diffusivities of ethylene glycol in Dowex 50 are also not known.

The effluent waves given in Figure 40A are used to fit the model and the values of the equilibrium constants and the diffusivities for the resins with different cross-linkages are obtained from each effluent wave in the Figure 40A. The method of determining diffusivities and the equilibrium constant from the effluent wave is described in detail in the section discussing model B(i) (a).

Table I shows the values obtained by fitting the data of Figure 40A to the model B(i) (a).

TABLE I

DIFFUSIVITIES OF ETHYLENE GLYCOL IN DOWEX 50 AND EQUILIBRIUM DISTRIBUTION OF ETHYLENE GLYCOL BETWEEN DOWEX 50 AND WATER

Resin Crosslinkage % DVB (Dowex 50)	Equilibrium Constant for Ethylene Glycol Concentration in resin/Concentration in aqueous phase	Diffusivity of Ethylene Glycol in the Resin Phase $cm^2/sec \times 10^6$
24	$0.19 \pm .03$	$.35 \pm .1$
16	$0.37 \pm .03$	$1.3 \pm .2$
8	$0.54 \pm .03$	$1.3 \pm .3$
4	$0.72 \pm .03$	$1.9 \pm .5$
2	$0.86 \pm .03$	$2.1 \pm .6$

The data in Figures 40B, C and D are for a resin with 8% divinyl benzene. The physical constants for this cross linkage determined from Figure A as mentioned above, are used to predict the data reported in Figures B, C and D.

Figure 41B shows the effluent curves predicted by the model where the amount of feed is a variable. Data of Figure 40B are reproduced in Figure 41A for comparison with the predicted curves. Actually in this prediction, all that is required is the assumption of a linear mathematical model. The predicted curves of Figure 41A are independent of the mechanism describing the mass transfer process. The effect of different amounts of feed is to change the time interval to between the two responses to step functions that have to be added (refer to Figure 32).

For different particle size, the predicted effluent waves are shown in Figure 42B. Figure 42A shows the data of Figure 40C for comparison.

Figure 43 shows the predicted waves and data for different liquid flow rates.

As can be seen from Figures 41, 42 and 43, the model is adequate to explain the data.

2. Glycerol-Sodium Chloride-Water-Dowex 50 System

A. Available Data

(i) Physical Characteristics

(a) Equilibrium Data

For resin with 8% divinyl benzene, and at room temperature, very accurate equilibrium data have been reported by Shurts and White (S4, S5). Figures 44 and 45 are reproduced from the references cited. Their

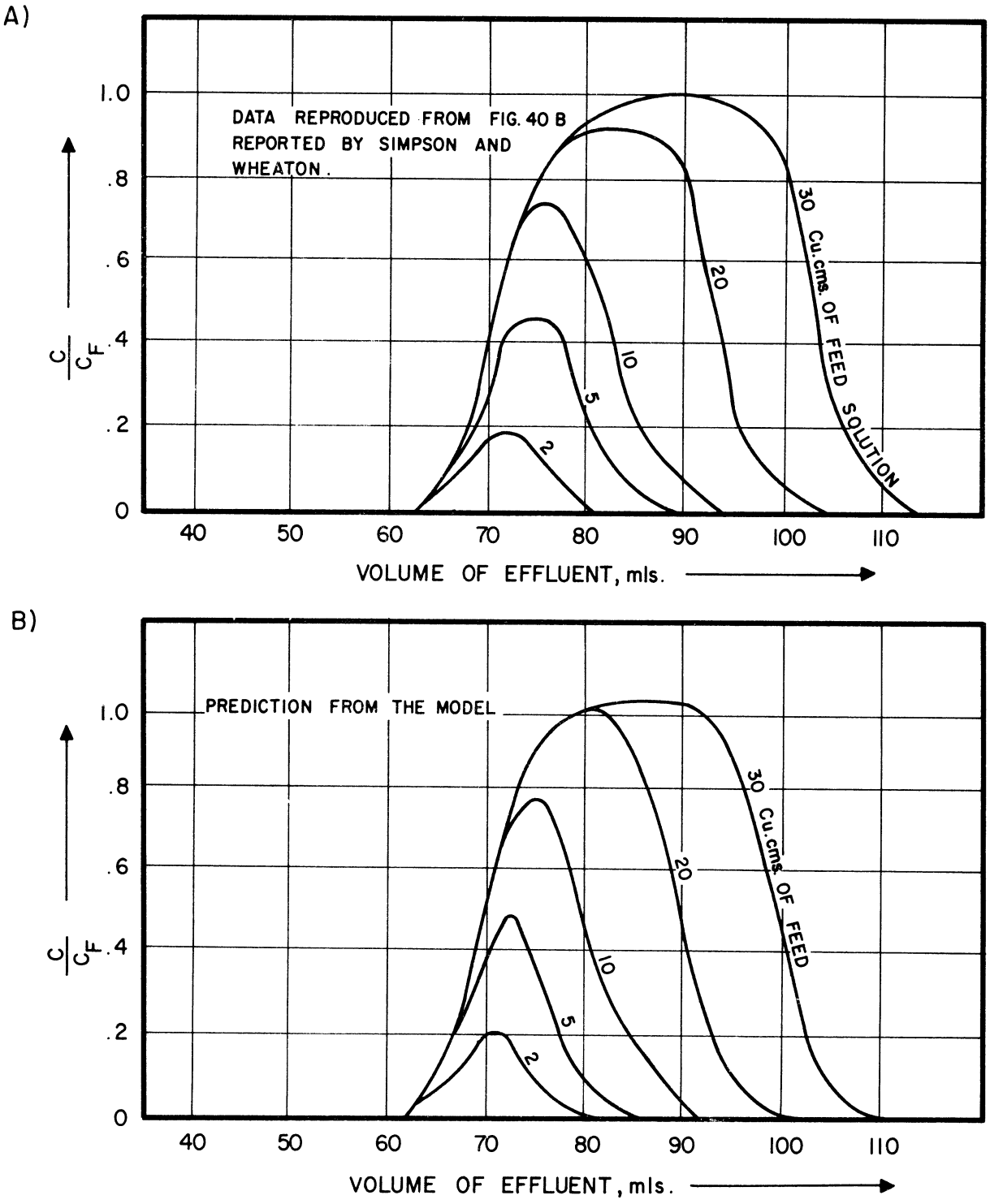

Figure 41. Comparison of Data with the Model. (Amount of Feed Solution as a Variable) (Feed: 10% Ethylene Glycol Solution; Resin Size: 50-100 Mesh; Flow Rate: 0.134 gls/(sq ft.) (min))

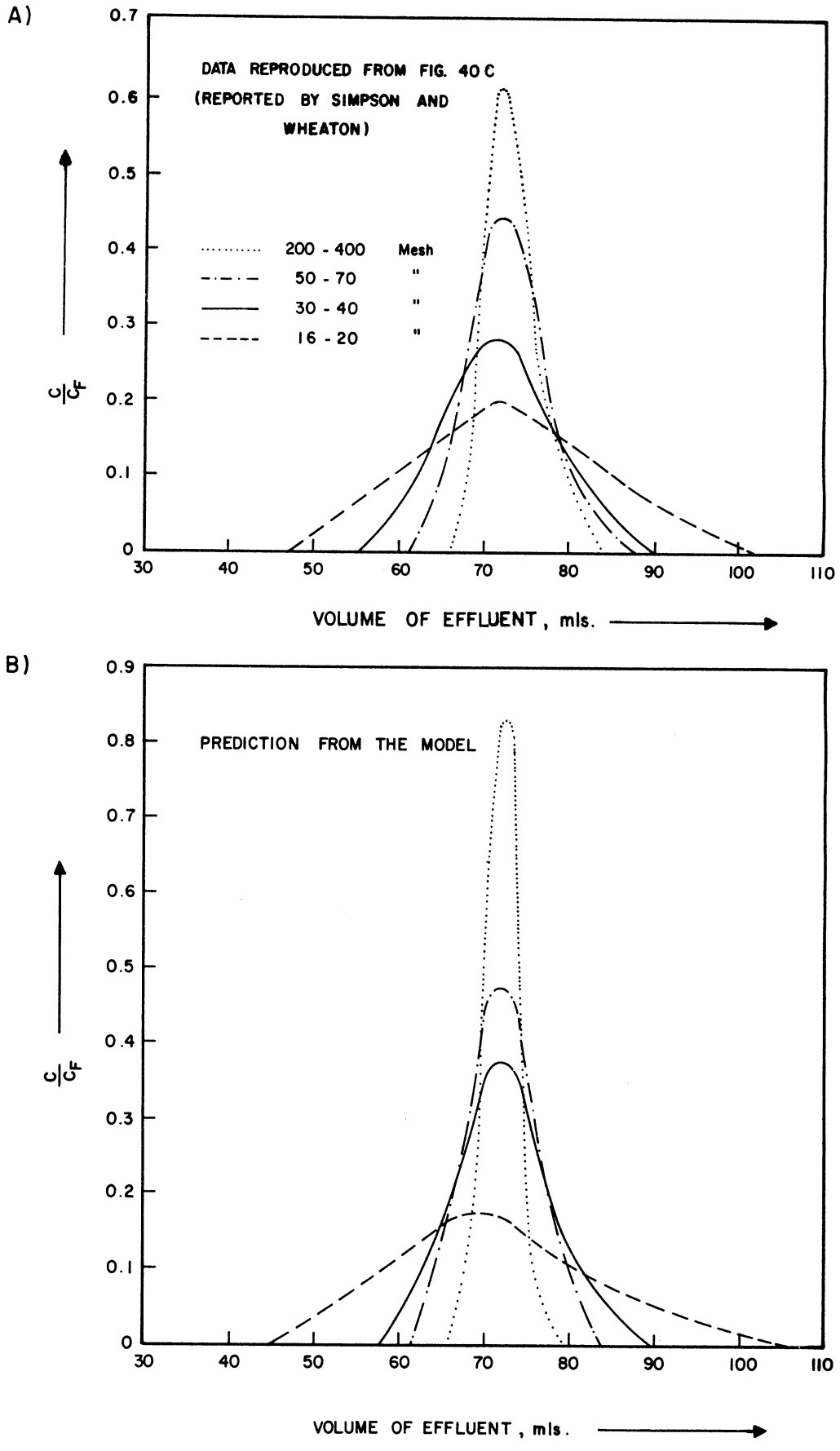

Figure 42. Comparison of Data with the Model. (Particle Size as the Variable). (Feed: 5 ml of 10% Ethylene Glycol Solution; Flow Rate: 0.134 gls. (sq ft.)(min.))

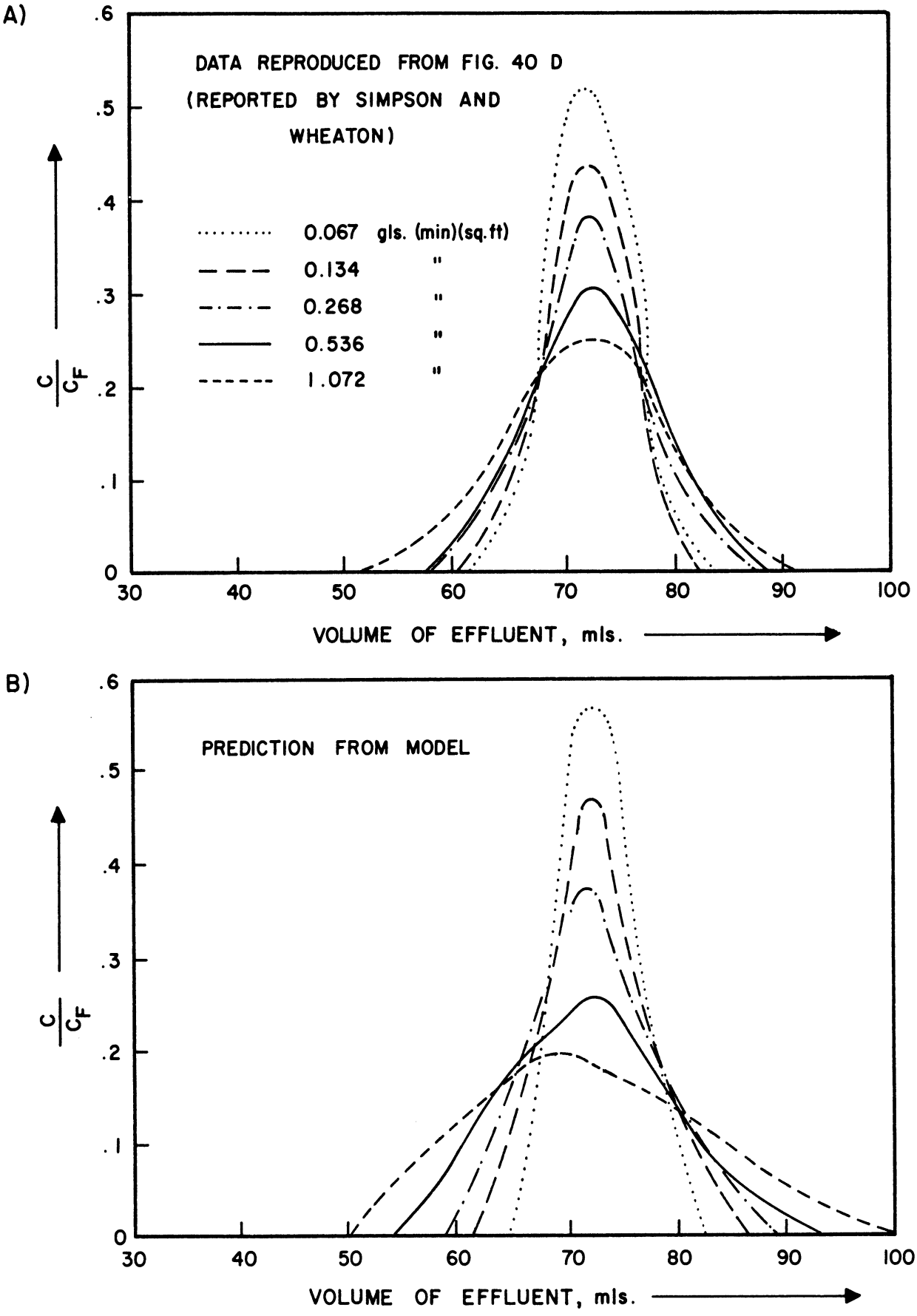

Figure 43. Comparison of Data with the Model. (Flow Rate as the Variable) (Feed: 10% Ethylene Glycol Solution - 5 mls. Resin Size: 50-100 mesh).

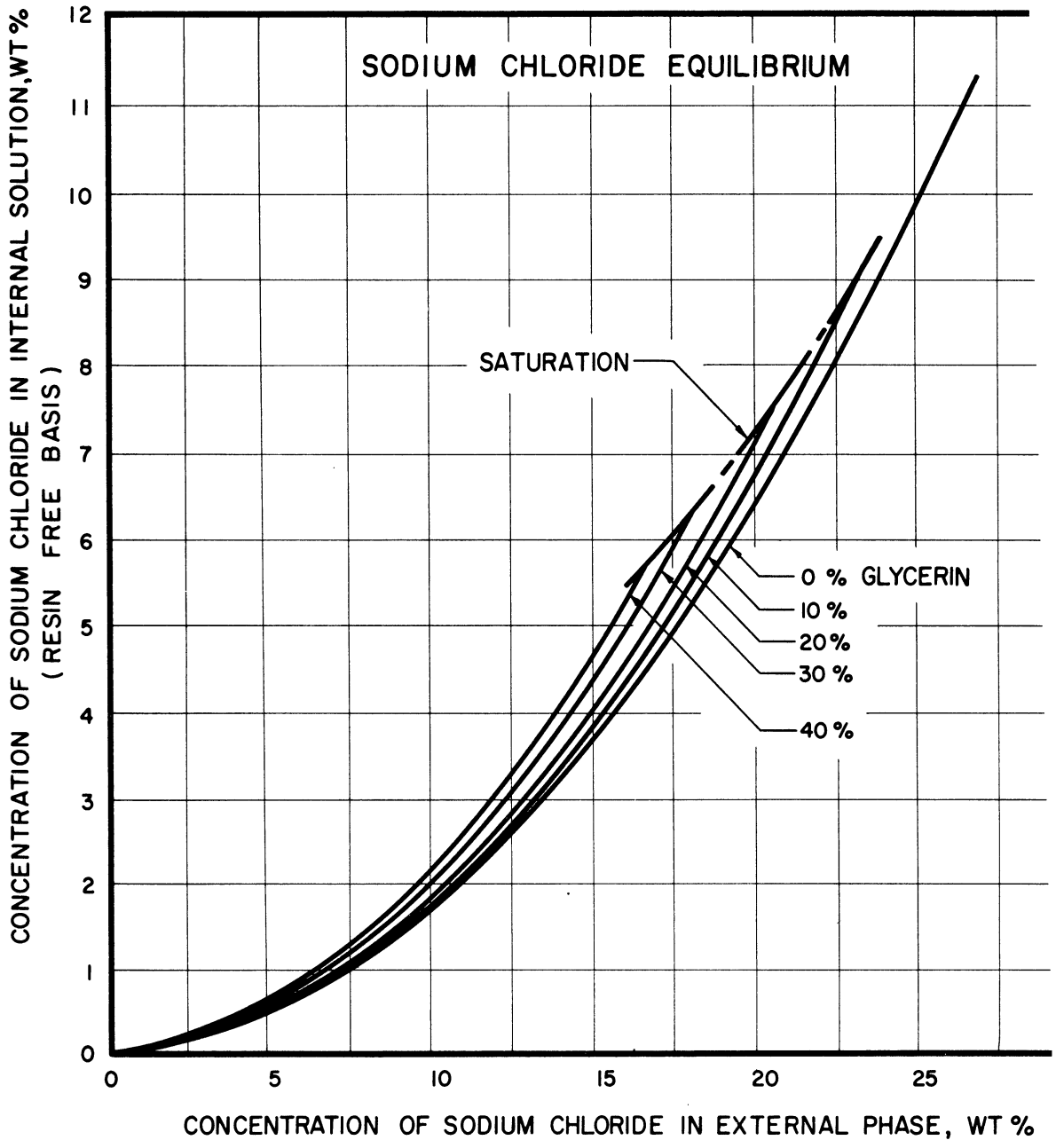

Figure 44. Equilibrium for NaCl in the System Glycerol-NaCl-Water-Dowex 50. (Reproduced from Shurts (References 84, 85)).

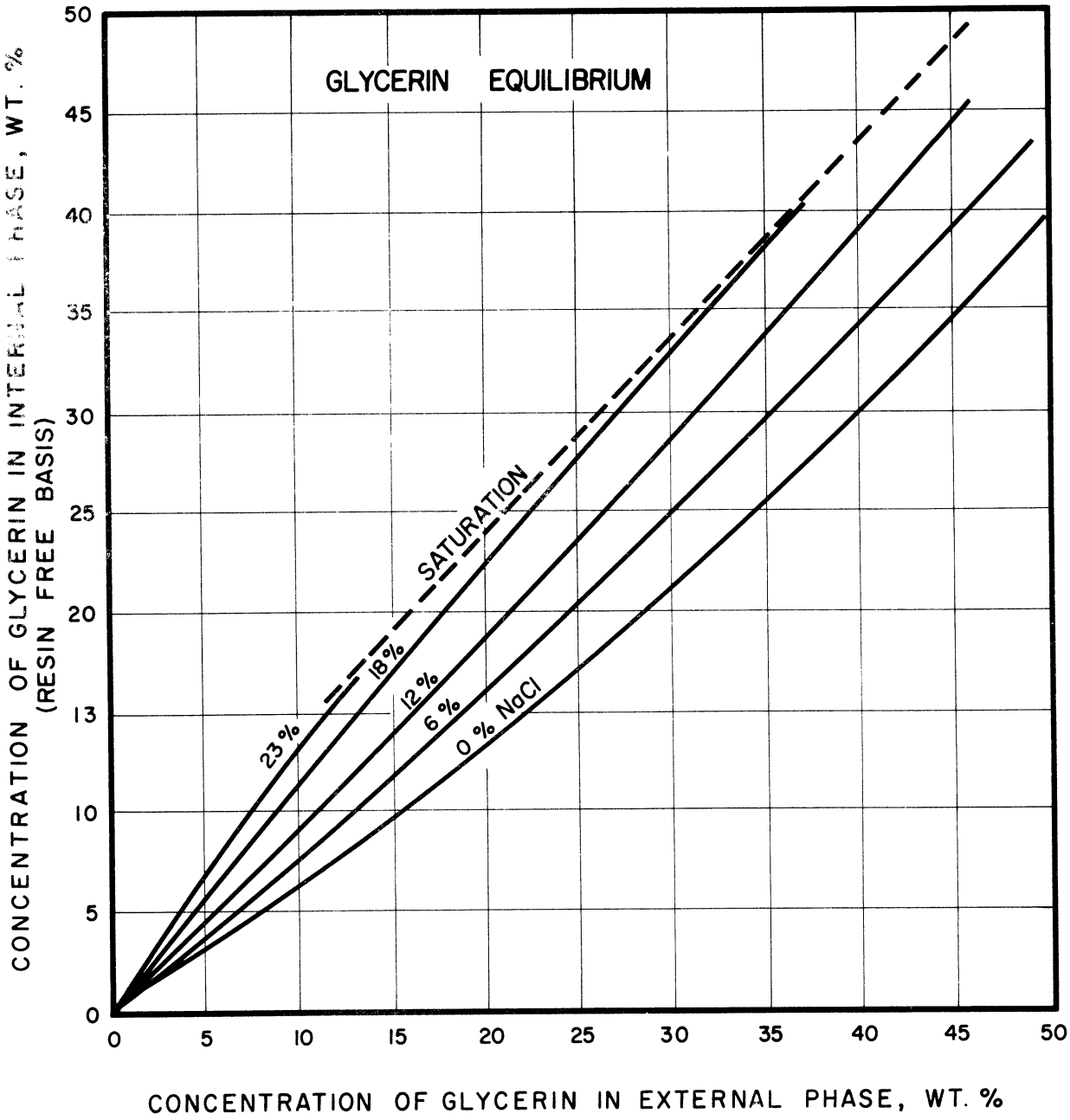

Figure 45. Equilibrium for Glycerol in the System Glycerol-NaCl-Water-Dowex 50. (Reproduced from Shurts (Reference S4, S5)).

correlation expresses the concentration of the solutes (on resin free basis) in the solid phase as a function of the concentrations in the liquid phase. From their correlation and their data on swelling of resin, equilibrium constants expressing the ratio of concentration in gms./liter in the resin phase to that in the liquid phase were computed. Figures 46 and 47 show the equilibrium constants as a function of concentration.

If q is the concentration in gms./liter of the resin phase and c is the concentration in gms./liter in the liquid phase, then the equilibrium constant, K, is given by

$$K = q/c \qquad (104)$$

In order to draw the contour diagram for non-linear equilibrium, it is necessary to know $\frac{dq}{dc}$. If K is constant, $\frac{dq}{dc} = K$. In the system under consideration K is not a constant and Figure 48 gives the value of $\frac{\partial q_s}{\partial c_s}$ as a function of the concentrations. Subscript "s" denotes Sodium Chloride.

Some equilibrium data for different resin cross-linkages and different temperatures are reported in Part I of this thesis.

(b) Data on Resin Shrinkage

Shurts and White (loc. cit.) have reported the ratios of the diameter of Dowex 50 x 8% DVB in solutions of various concentrations to that in water. They have also reported the change in total volumes for the system. The volume of the resin decreases when the solutes are present. The change in total volume is very small with change in concentration. Figure 49 gives the porosity of the bed as a function of the

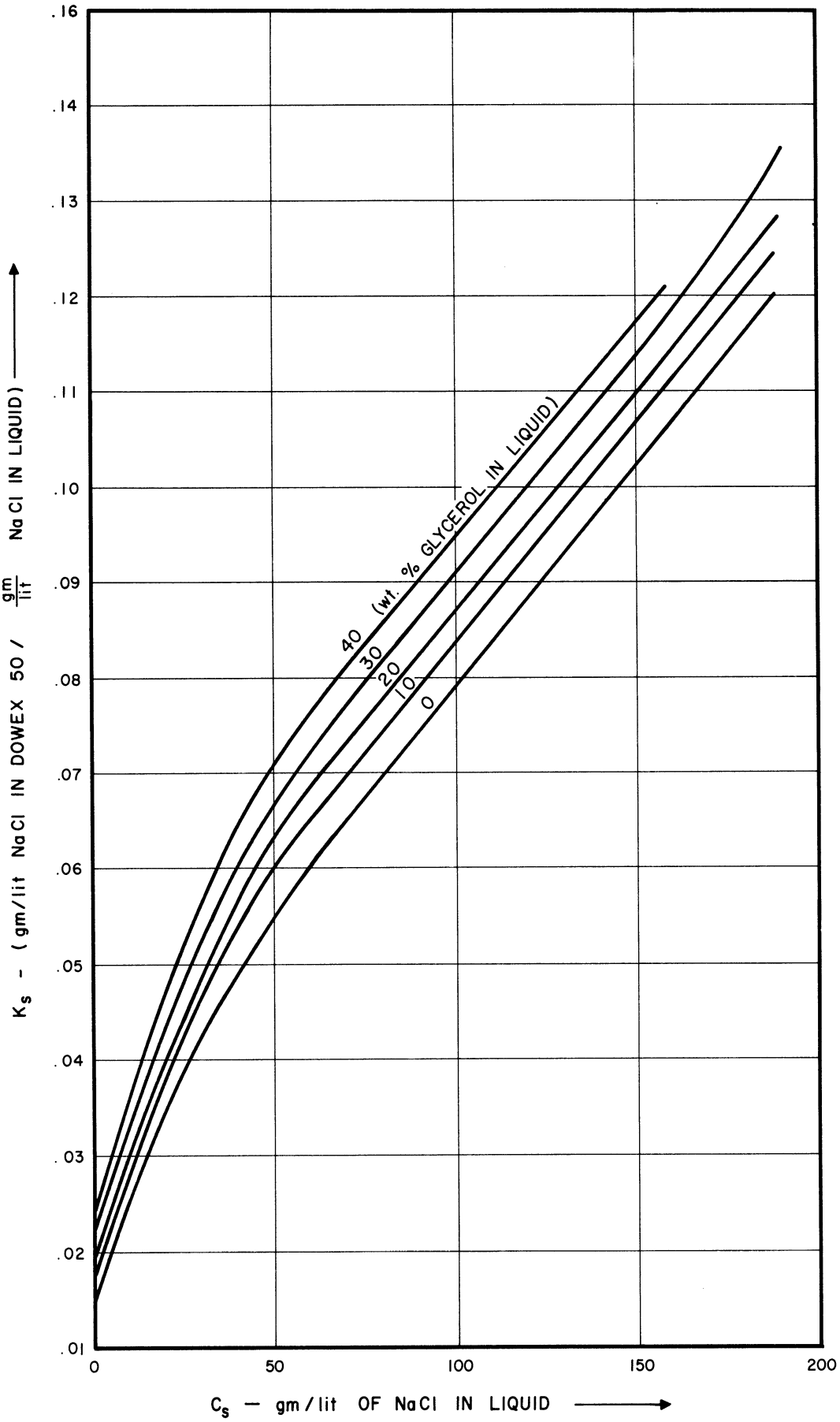

Figure 46. Equilibrium Constant for NaCl in the System Glycerol - NaCl - Water - Dowex 50. (Curves based on Shurts' Data Reference S4, S5).

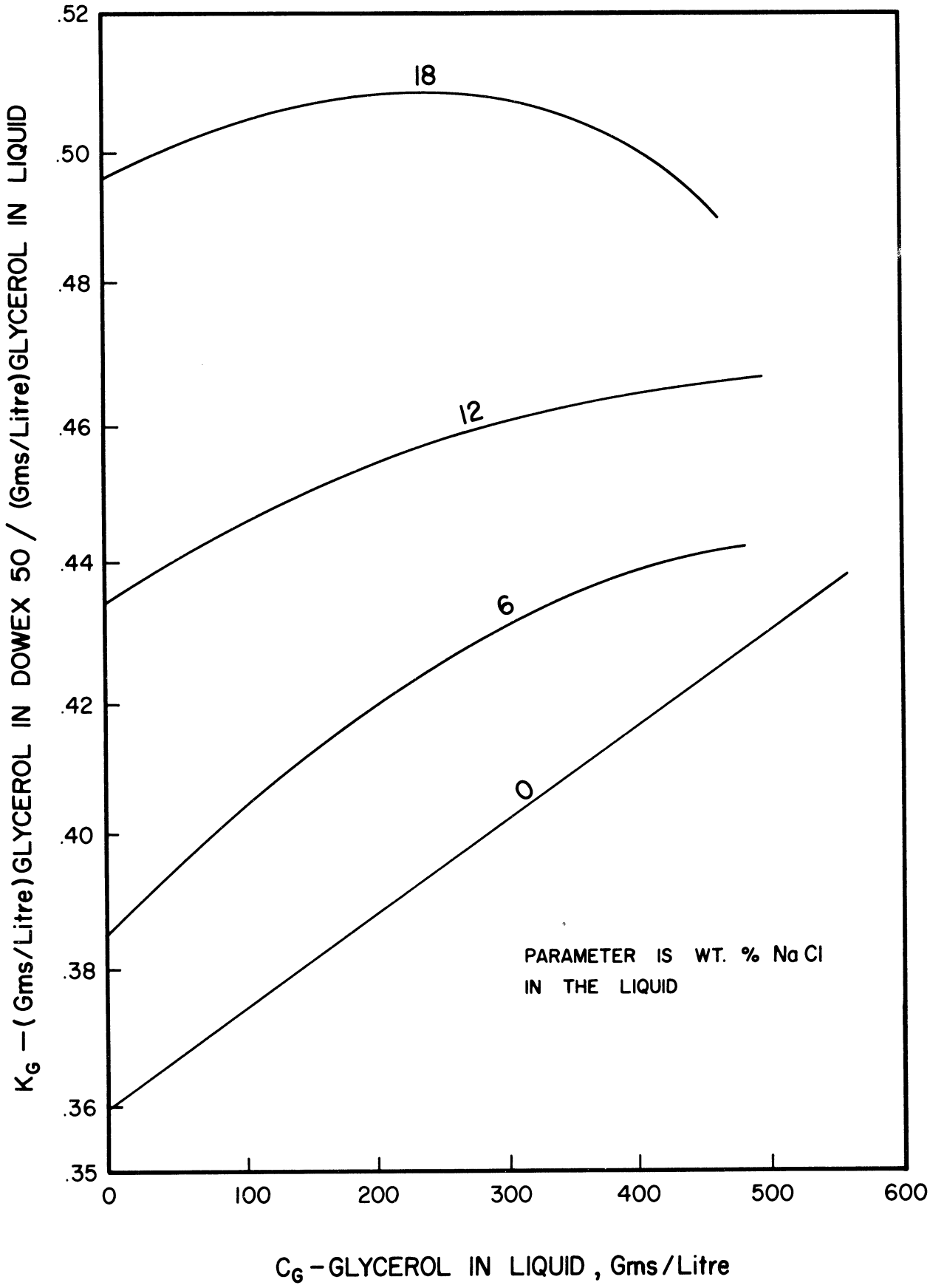

Figure 47. Equilibrium Constant for Glycerol in the System. Glycerol - NaCl - Water - Dowex 50. (Curves based on Shurts' Data. Reference S4, S5).

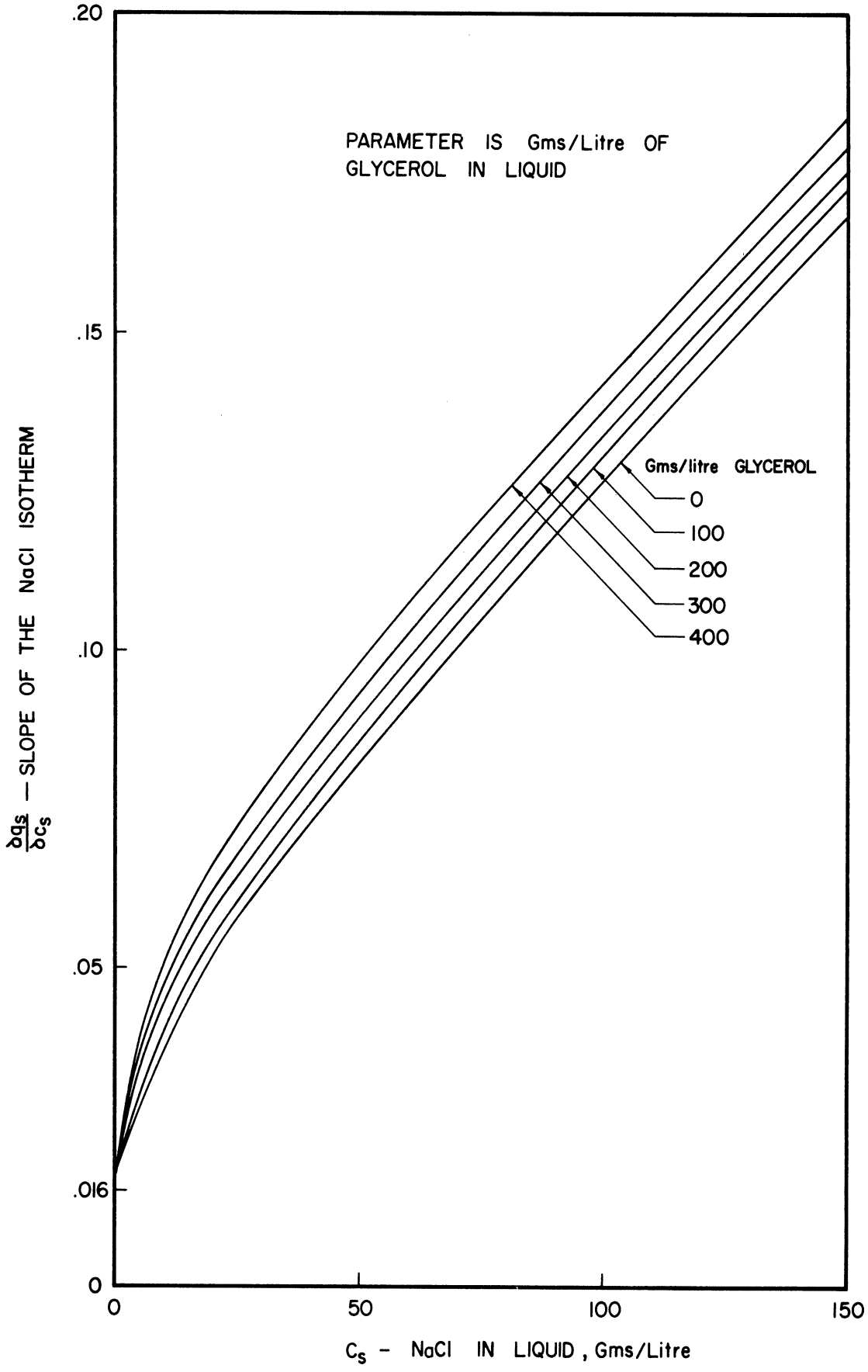

Figure 48. Slope of the Equilibrium Isotherm for NaCl in the System Glycerol-NaCl-Water-Dowex 50. (Curves based on Shurt's Data Reference S4, S5).

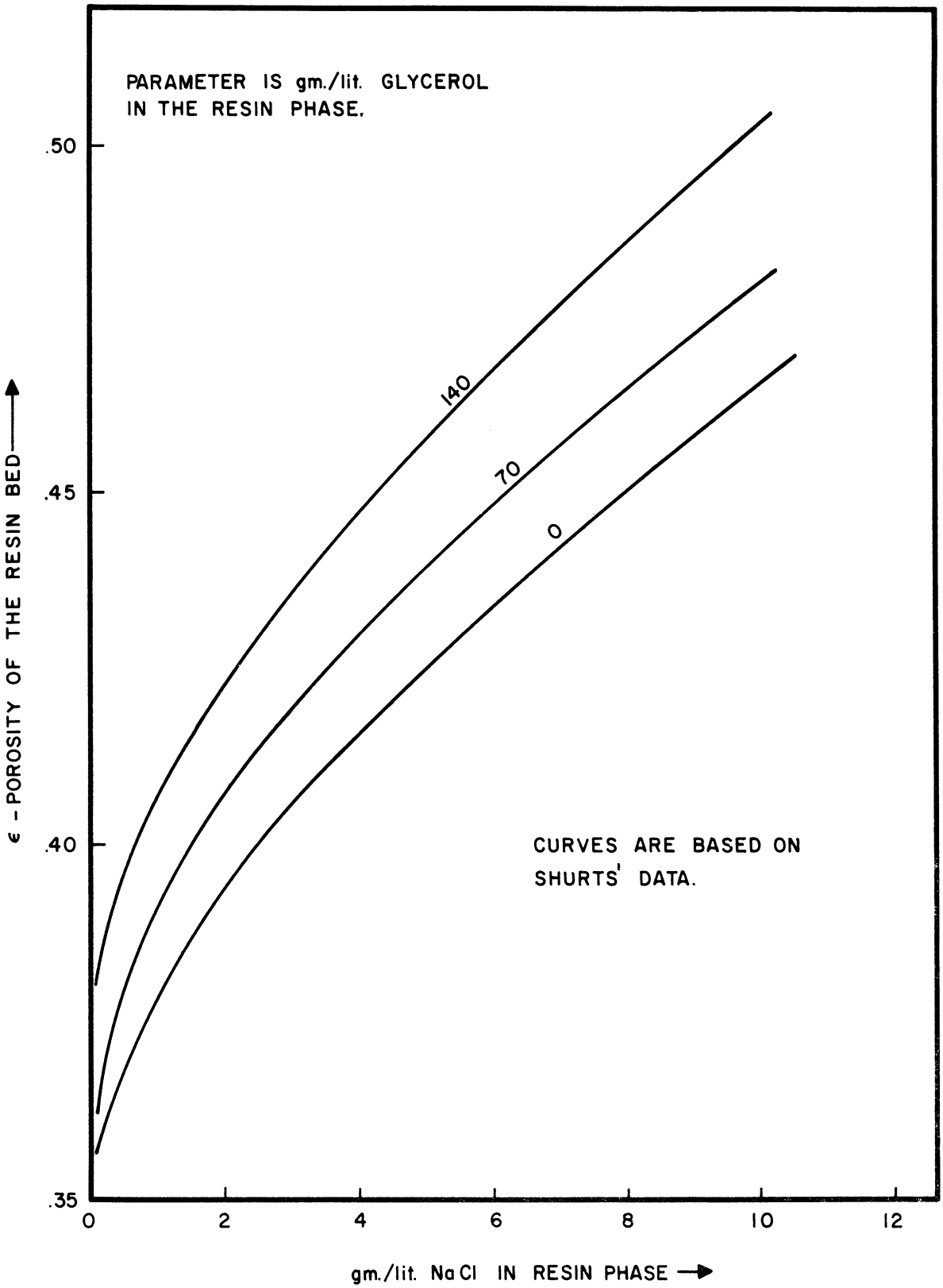

Figure 49. Porosity of the Bed as a Function of Concentrations in the Resin Phase.

concentration in the resin on the assumption that the effect of the presence of the solutes in the resin phase is to decrease the volume of the solid, increase the volume of the liquid by a corresponding amount and thus change the porosity of the bed. Porosity of the bed when no solutes are present is assumed as 35%.

Figure 50 gives the porosity of the bed as a function of the concentration of the solutes in the liquid, assuming an equilibrium between the liquid and the solid in addition to the assumptions mentioned above.

(c) Diffusivities of Sodium Chloride and Glycerol in Dowex 50

For different amounts of divinyl benzene cross linkage and different temperatures, the diffusivities are reported in Part I of this thesis.

For 8% DVB and room temperatures, the diffusivity of glycerol is 0.58×10^{-6} cm^2/sec and that of sodium chloride is 1.4×10^{-6} cm^2/sec.

(ii) Ion-Exclusion Data

Data available from the operation of a laboratory column are reported by Wheaton and Bauman (W2) and Asher and Simpson (A3).

Figure 51 reproduces Wheaton and Bauman's data (W2). They used a 100 ml. column (1.5 cm.x 55 cm.). The flow rate was 1 ml./min. The resin cross linkage was 8% DVB. The resin size was 50 - 100 mesh. The feed to the column was 15 ccs of a solution containing 4% Glycerol and 4% Sodium Chloride by weight.

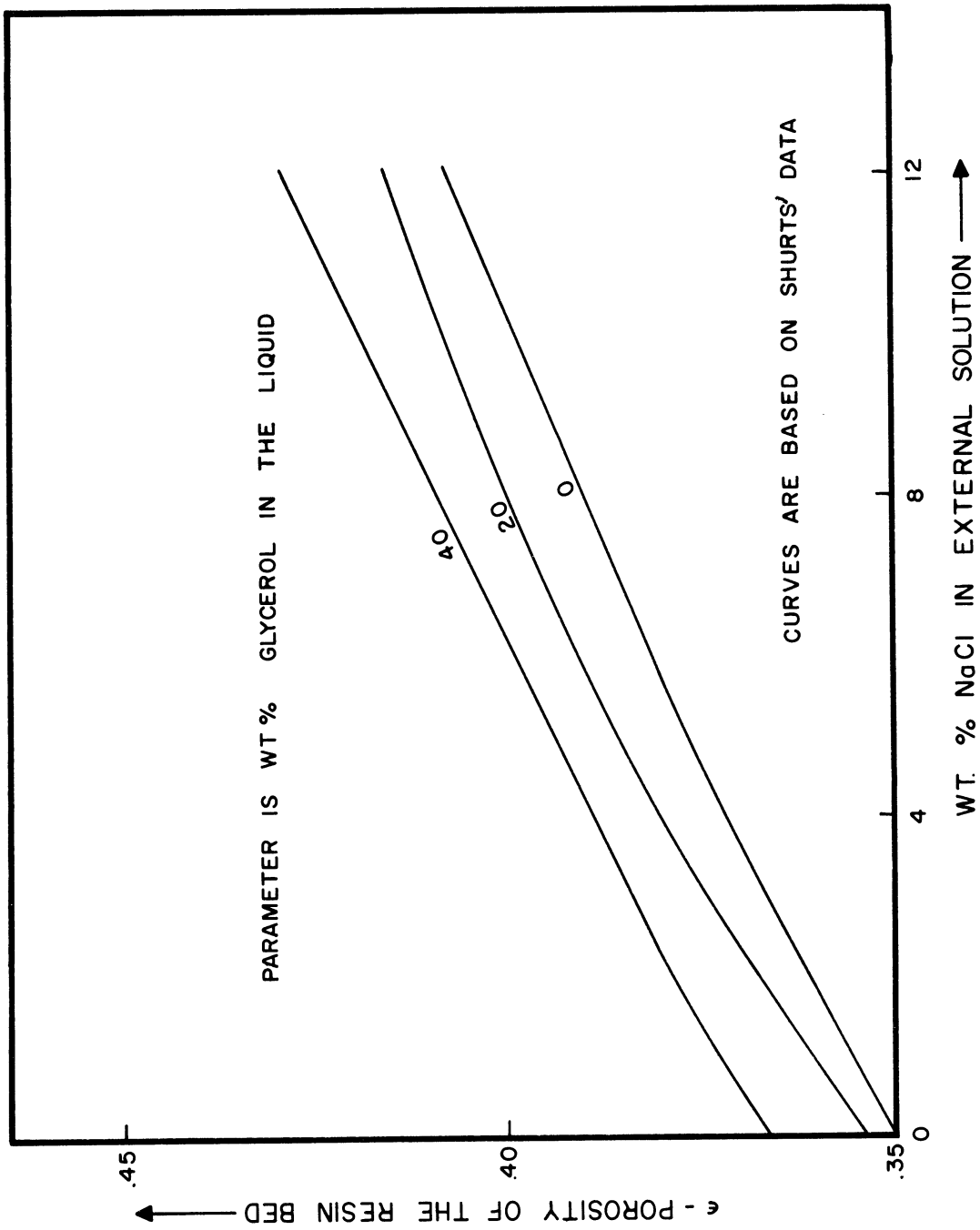

Figure 50. Porosity of the Bed as a Function of Concentration in the Liquid (assuming Equilibrium Between the Liquid and the Resin).

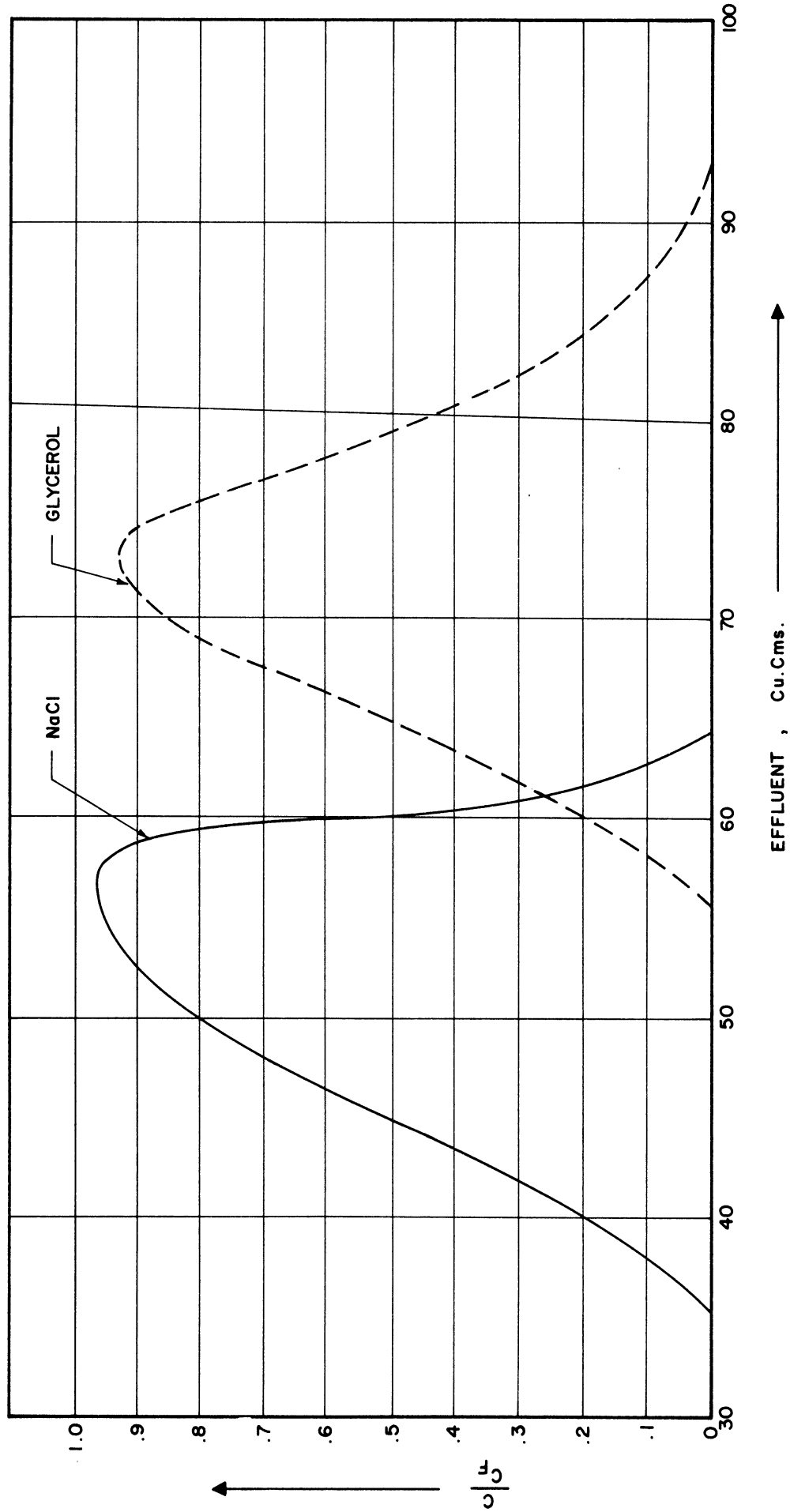

Figure 51. Wheaton and Bauman's (W2) Curves. Resin: Dowex 50 x8; Feed: 15 cu. cms. (15% of Bed Volume)
4% Glycerol 4% NaCl.

Figures 52 and 53 reproduce two of the typical data curves reported by Asher and Simpson (A3). They used a 0.6" x 60" column. The flow rate was 0.5 gls/(sq.ft.)(min.). The resin cross linkage was 8% DVB. The resin size was 50 - 100 mesh.

Prielipp and Keller have reported data from operation of a pilot plant column (P1). They had 4.5 cu. ft. of resin (12" x 70"). The other conditions were generally the same as those used by Asher and Simpson (loc. cit.). Their data show the same general characteristics as those of Asher and Simpson. No attempt has been made to fit this data in the present thesis.

B. Comparison of Data to Various Models

(i) Wheaton and Bauman's Data

In the following, various models are considered in increasing order of complexity. The solution of each model is compared with the data and the disagreement between the model and the data is used to indicate as to which of the more complex models should be used subsequently.

Abbreviations used in the following list of models:

E.C.O.	Equilibrium Column Operation
L.Eq.	Linear Equilibrium
Rsn. Shr.	Resin Shrinkage Considered
non-L. Eq.	Non-Linear Equilibrium
R. Dif.	Diffusion in resin phase is the controlling mass transfer resistance
(NaCl)	for NaCl
(Gly)	for Glycerol.

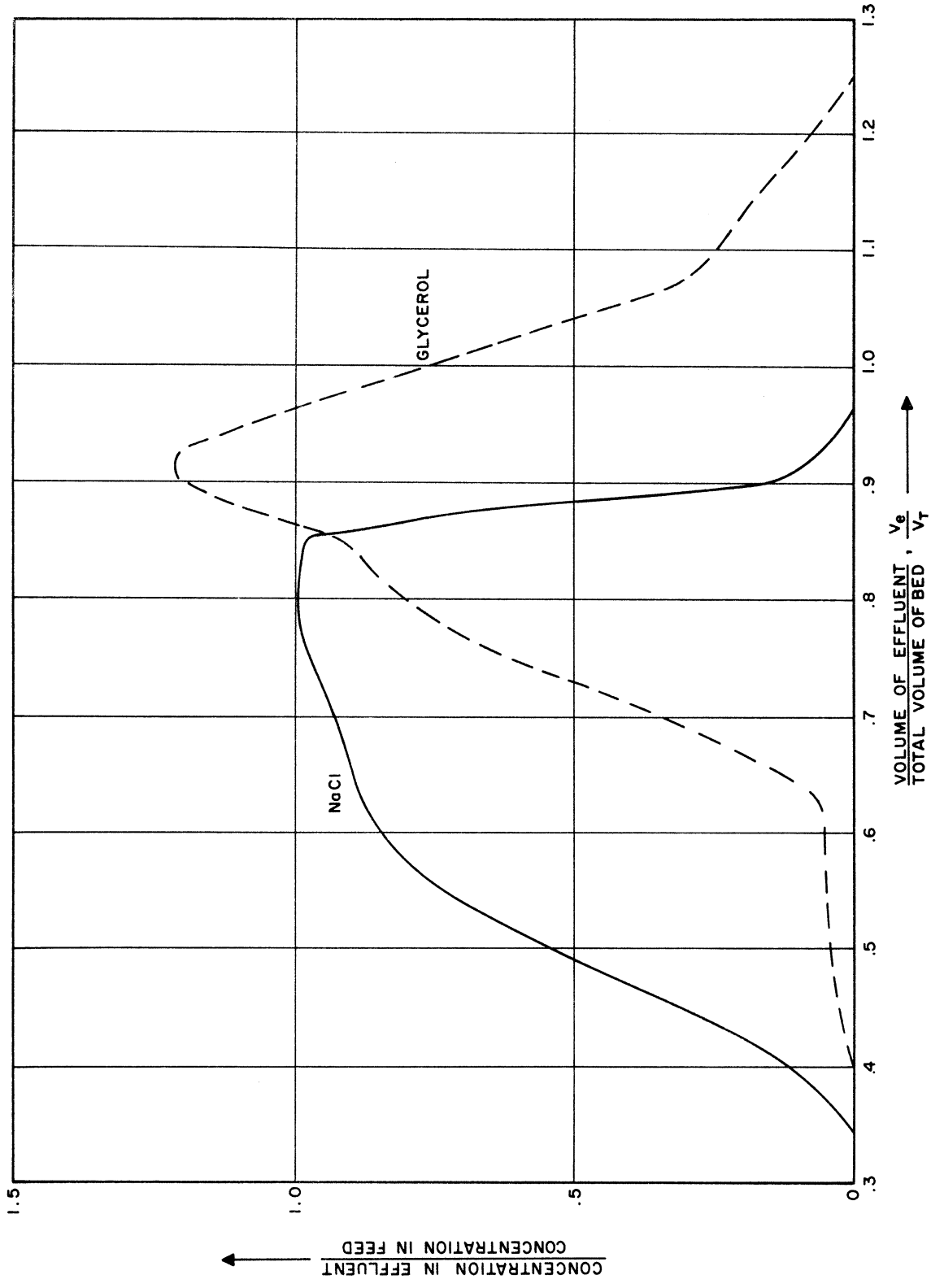

Figure 52. Asher and Simpson's (A3) Curves. Resin: Dowex 50 x 8; Feed: 35% of Bed Volume. 35.3% Glycerol; 10% NaCl; Room Temperature 80°C.

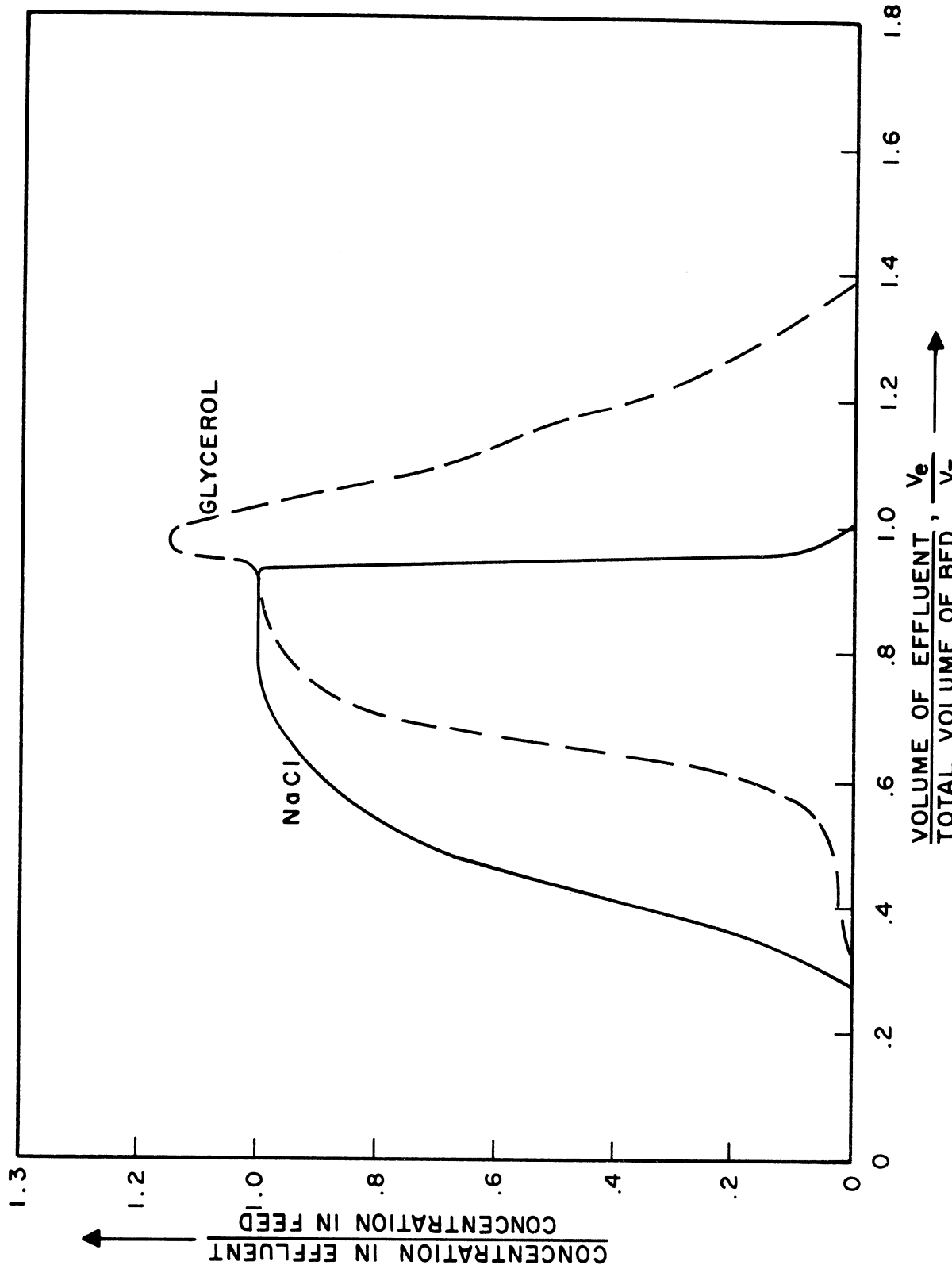

Figure 53. Asher and Simpson's (A3) Curves. Resin: Dowex 50 x 8; Feed: 0.50 V_T of 10.1% NaCl; 30.2% Glycerol; Room Temperature 80°C.

List of models considered below:

Model 1:	E.C.O.;	L. Eq.(NaCl);	L. Eq.(Gly)	
Model 2:	E.C.O.;	non-L. Eq.(NaCl);	L. Eq.(Gly)	
Model 3:	E.C.O.;	non-L. Eq.(NaCl);	L. Eq.(Gly);	Rsn. Shr.
Model 4:	R.Dif.;	L. Eq.(NaCl);	L. Eq.(Gly)	
Model 5:	R.Dif.;	non-L. Eq.(NaCl);	L. Eq.(Gly);	Rsn. Shr.
Model 6:	E.C.O.;	non-L. Eq.(NaCl);	non-L. Eq.(Gly);	Rsn. Shr.
Model 7:	R.Dif.;	non-L. Eq.(NaCl);	non-L. Eq.(Gly);	Rsn. Shr.

Model 1:

It is assumed that the column operates as an equilibrium column. The equilibrium characteristics for both solutes are approximated by an equilibrium constant for each solute which is independent of the concentrations. There is slug flow in the liquid and there is no longitudinal diffusion.

The equilibrium constants are approximated from Figures 46 and 47. Considering that the concentrations of the solutes are in the range of 0 to 4% by weight, equilibrium constant for glycerol is taken as 0.35 and that for sodium chloride is taken as 0.035.

The porosity of the bed is assumed to be 35% of the volume of the bed.

Figure 54 gives the contour diagram for the concentration surface that may be expected. Instead of an x-t plot, a plot of effluent volume (as a measure of time, t) versus the volume of the bed (as a measure of the distance in the bed, x) is made. The effluent waves according to this model are given in Figure 55. The separation between the solutes has

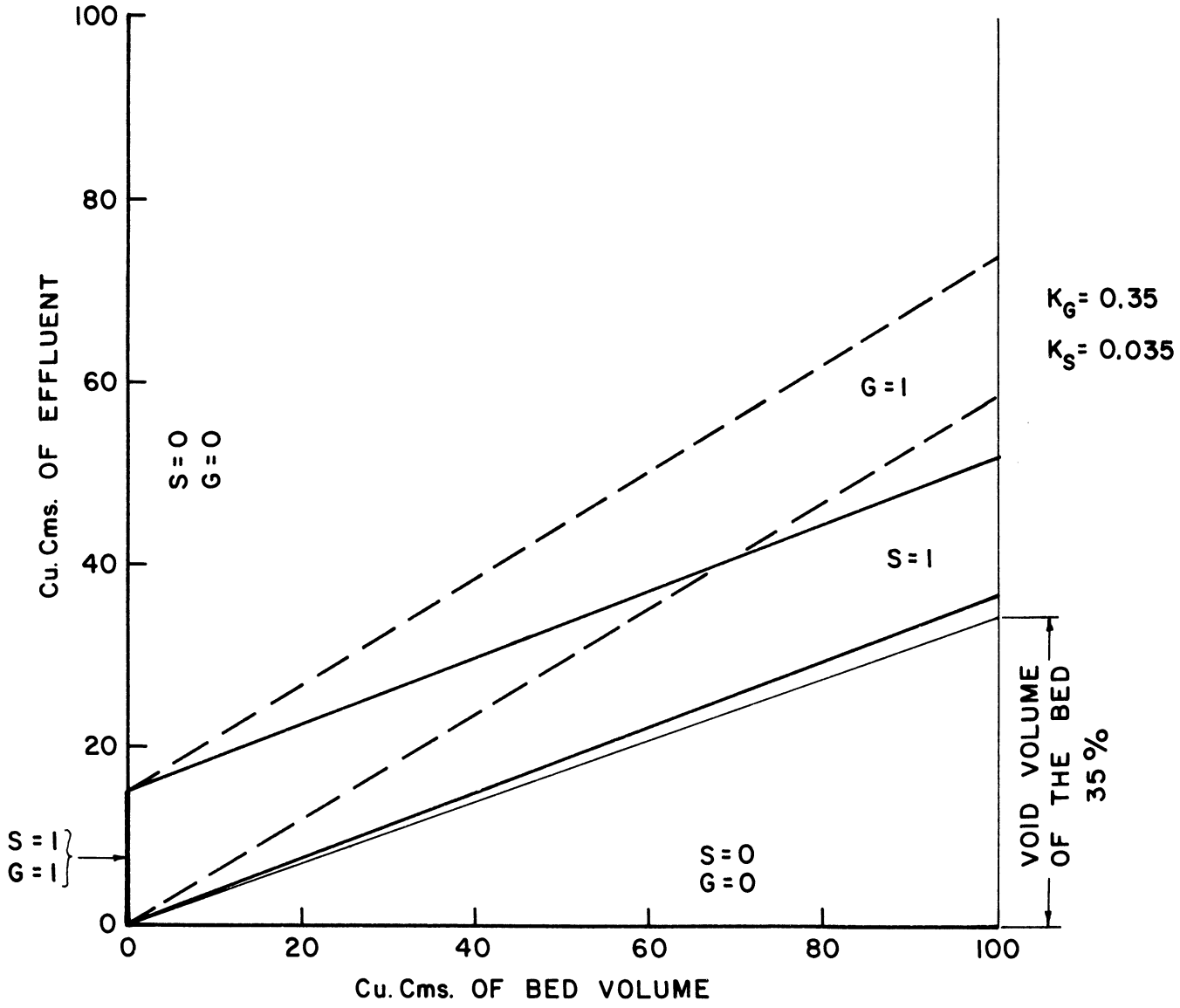

Figure 54. Contour Diagram for Model 1 for Wheaton and Bauman's Curves.

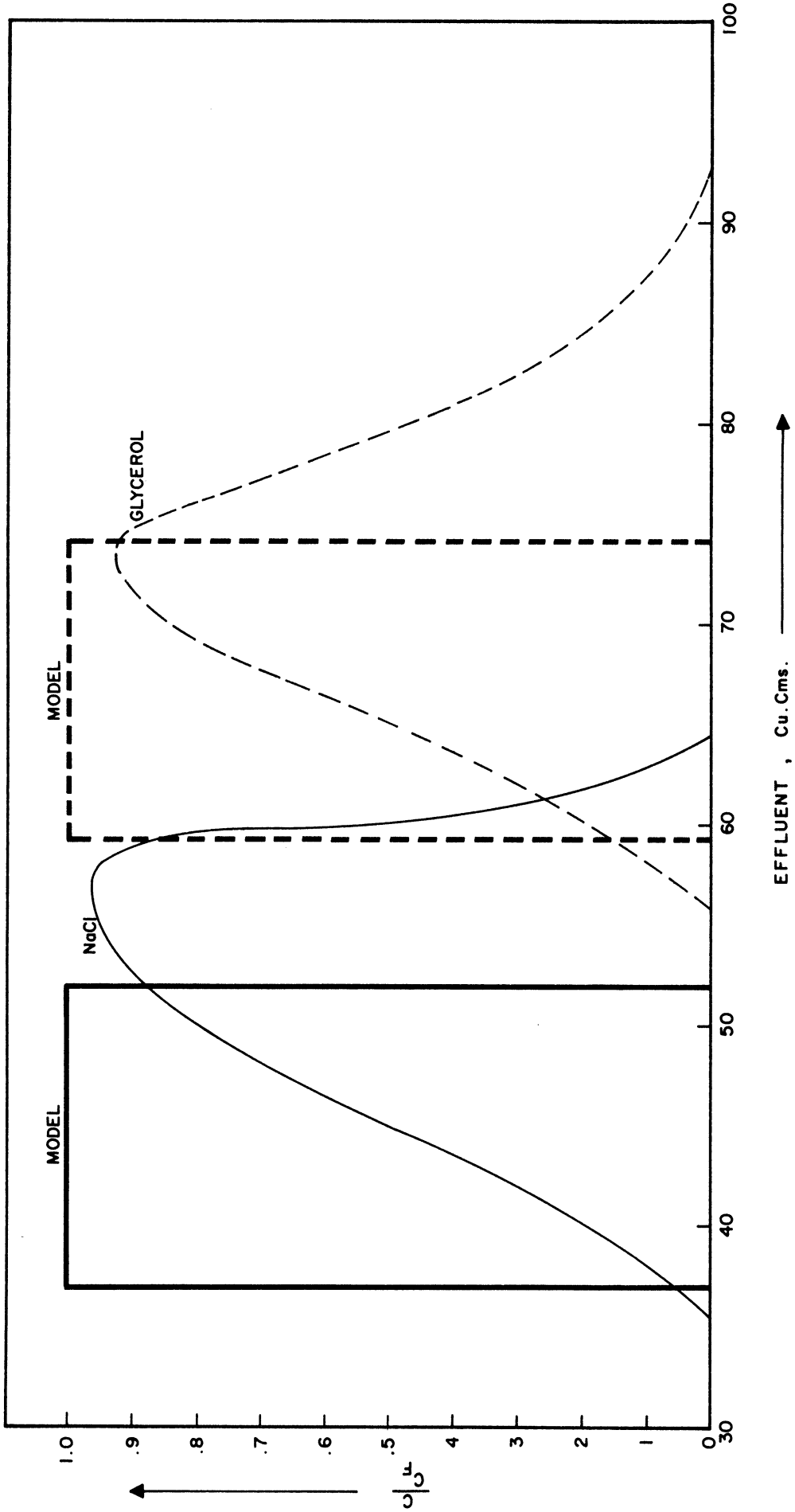

Figure 55. Effluent Curves Predicted by Model 1.

been accomplished in the column. The data are also shown on Figure 55 for comparison.

The data curve for NaCl is skewed. This may be because of non-linear equilibrium for NaCl as can be seen from Figure 44. The equilibrium isotherm is concave upwards and its effect would be to smear the leading edge of the effluent wave (for small values of effluent volume) and have the trailing edge sharp. The next model considers the non-linear equilibrium for NaCl.

Model 2:

The equilibrium characteristics of NaCl and glycerol are assumed to be independent of each other. The equilibrium for NaCl is non-linear and the characteristics are given by the curves on Figures 46 and 48 for the parameter of 0% glycerol.* The column operates as an equilibrium column. Other assumptions are the same as in the previous model.

Figure 56 gives the Contour Diagram. Because of the very low values of equilibrium absorption for NaCl, the effect of non-linearity in spreading the leading edge of NaCl wave is not significant at all.

Figure 57 shows the effluent waves obtained from the model. The slanting from the vertical of the leading edge for NaCl wave of data is very large.

Consideration of the volume change of the resin particles with concentrations may explain the difference. The resin shrinks with increasing concentration. In the process it discharges some water into the

---

* The effect of non-linearity in NaCl equilibrium is to "spread" the leading edge of NaCl wave. The concentration of glycerol in the leading edge of NaCl wave is zero, as can be seen from the Contour Diagram, Figure 56.

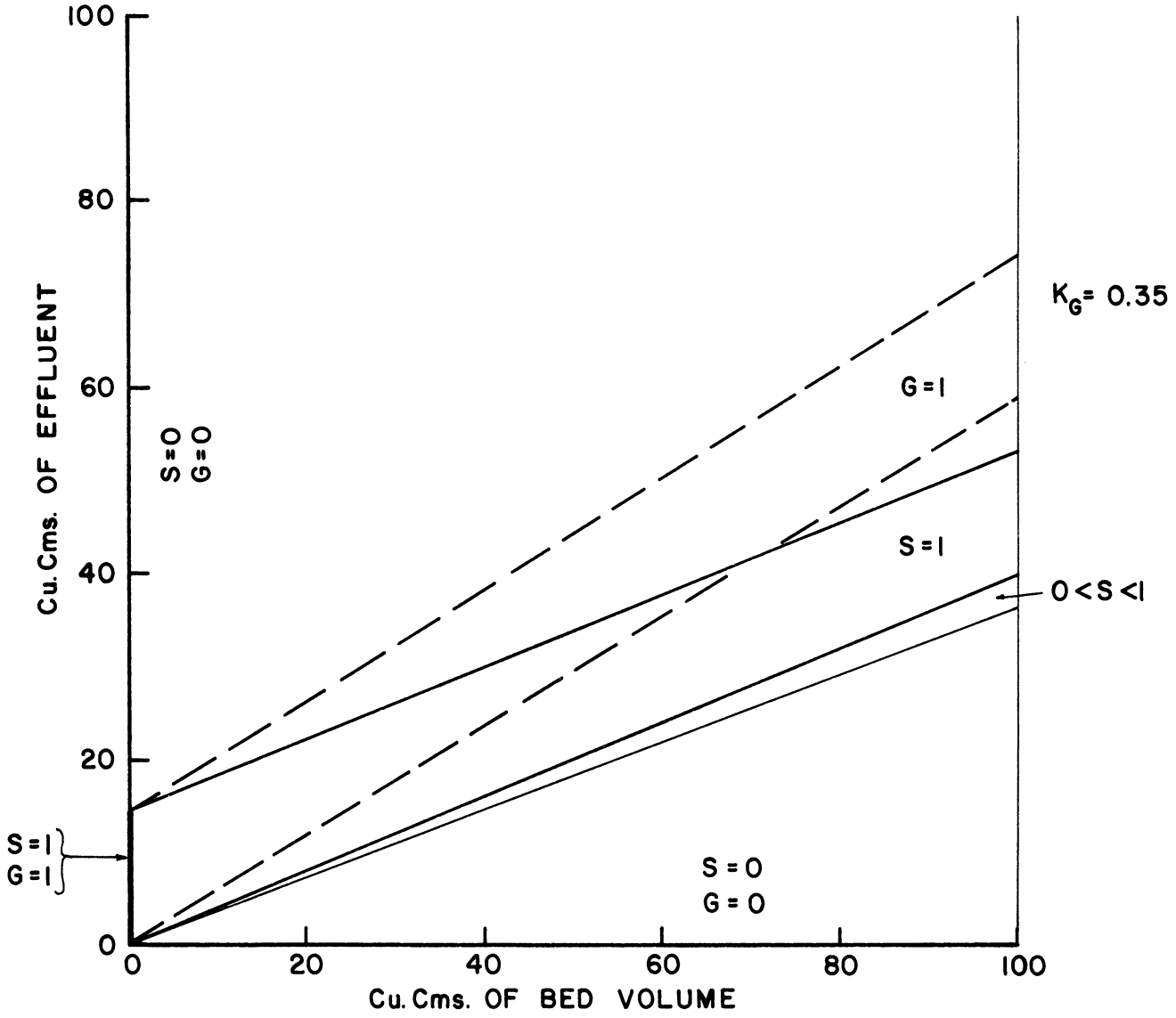

Figure 56. Contour Diagram for Model 2. G(or S) is the Ratio of the Concentrations of Glycerol (or NaCl) in the Liquid to that in the Feed Solution.

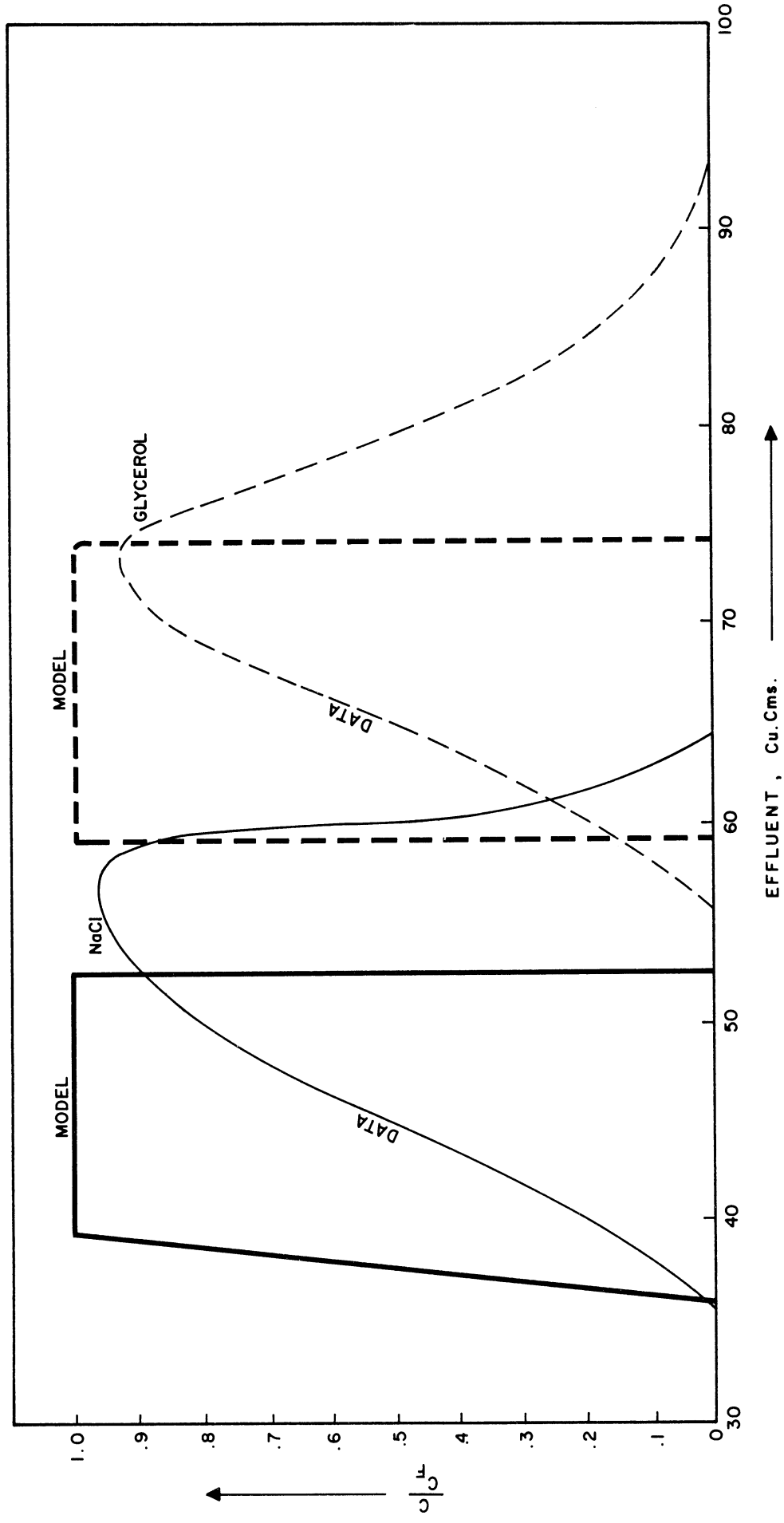

Figure 57. Effluent Curves Predicted by Model 2.

leading edge, thus diluting it.* As a consequence, the peak of the wave is delayed and this may also explain partly the discrepancy between the position of the glycerol wave predicted by the model and that reported in data. The next model considers the effect of shrinkage.

Model 3:

Equilibrium for glycerol is assumed linear. That for NaCl is non-linear and same as in Model 2. There is equilibrium column operation. The porosity of the bed is a function of the concentration of the liquid as shown in Figure 50. (This accounts for the change in volume of the solid with concentration.)

Figure 58 gives the Contour Diagram. Figure 59 gives the effluent curves from the model. The dilution of leading edge of NaCl wave is partly explained, but not completely. The shrinking of the resin particles during the flow conditions may produce effectively a greater amount of dilution than what is estimated from volume changes measured under static conditions.

Further smearing of the leading edge of NaCl would be produced by mass transfer resistances. Also the mass transfer resistances may account for the spreading of the glycerol wave. As discussed in the previous section, along with data on Ethylene Glycol, the resistance in the solid phase is likely to be the most important mass transfer resistance. The following model considers the diffusion in the solid as the controlling mass transfer resistance. For convenience of obtaining a solution of the model, the case assuming linear equilibria will be considered.

---

* Model A(i)(d) in the section on Mathematical Models discusses more details, and shows the method of obtaining the Contour Diagram.

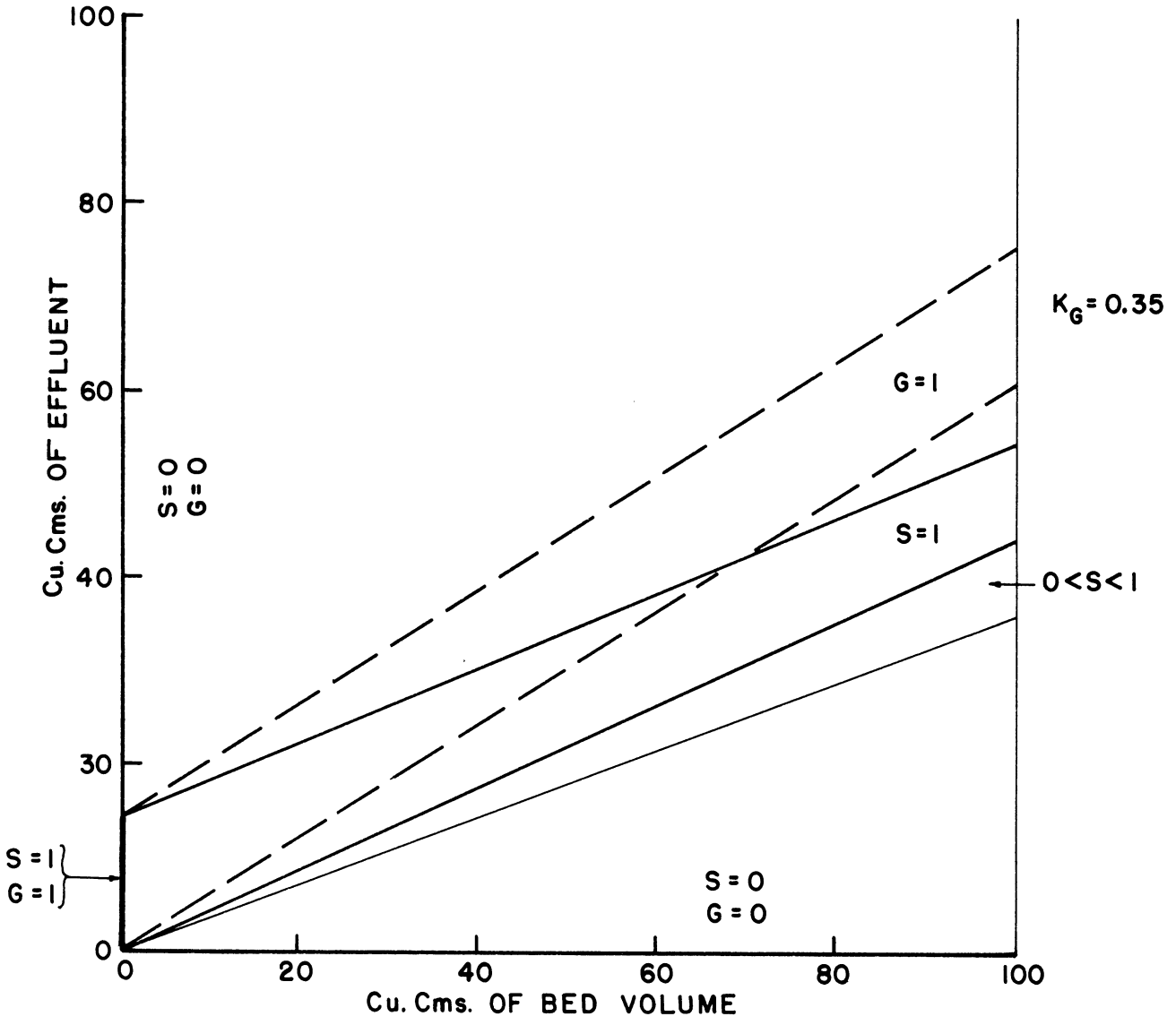

Figure 58. Contour Diagram for Model 3. G(or S) is the Ratio of the Concentrations of Glycerol (or NaCl) in the Liquid to that in the Feed Solution.

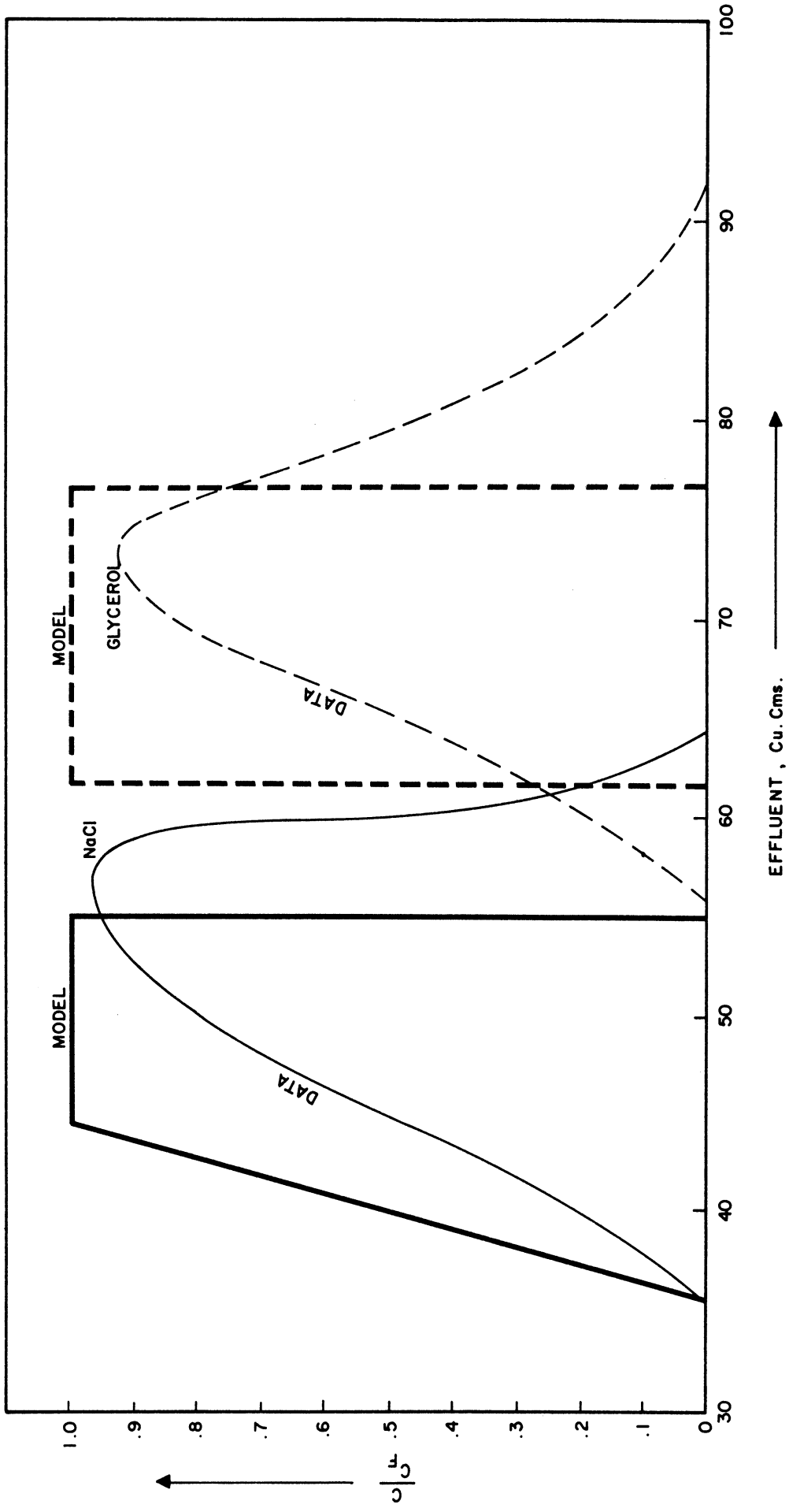

Figure 59. Effluent Curves Predicted by Model 3.

Model 4:

Linear equilibrium is assumed for both solutes. Diffusion in the solid phase is the controlling mass transfer resistance for both solutes.* Slug flow of the liquid and no longitudinal mixing in the liquid are assumed.

Equilbrium constants for Sodium Chloride and Glycerol are estimated as 0.035 and 0.35 as in Model 1 above. The diffusivity in the resin is taken as 0.58×10^{-6} and 1.4×10^{-6} cm^2/sec for Glycerol and Sodium Chloride respectively. The Contour Diagrams and the effluent wave for both solutes are determined according to the method described in the section on Mathematical Models, Model B(i)(a). The generalized solution given in Figures 29 and 30 is used.

For the experimental conditions under which the data curves were obtained, the value of $\overline{Z}$ for use in Figures 29 and 30, is 2.96 for glycerol and 0.675 for sodium chloride. Break through curves are obtained by taking cross sections of the surface represented by Figures 29 and 30 at the values of $\overline{Z}$ mentioned above and then converting the θ coordinate of the cross section into a convenient scale. From the break through curves, effluent waves may be obtained as shown in Figure 32.

The dimensionless time coordinate, θ, on Figures 29 and 30 is given by the following equation.

$$\theta = \frac{D}{R^2} \left(t - \frac{\epsilon}{u} x\right) \qquad (58)$$

---

* Model B(i)(a) in the section on Mathematical Models discusses more details and shows the method of using the generalized solution given in the section.

Where

D = the diffusivity of the solute in the solid phase.

R = the radius of the solid particles.

t = the time.

ϵ = the porosity of the bed.

u = the superficial velocity of the liquid.

x = the distance from the inlet end of the column.

Let V be the volume of the bed between the inlet end of the bed and the point at a distance x from the inlet end.

Let V_e be the volume of the effluent that has flown out of the bed. This volume is measured from the time at which the feed was first introduced into the bed.

Let A_x be the area of the cross-section of the column.

Then,

$$V_e = uA_xt$$

$$V = A_xx$$

and

$$t = \frac{x}{u} \cdot \frac{V_e}{V} \tag{105}$$

Substituting this value of t, in Equation (58),

$$\theta = \frac{D}{R^2} \frac{x}{u}\left(\frac{V_e}{V} - \epsilon\right) \tag{106}$$

In Equation (106), for a given value of x, there is a definite value of V and the equation defines a relation between the dimensionless time θ used in the generalized plots of Figures 29 and 30 and the volume of the effluent, V_e, from a column of length x. From the concentration surface represented in the generalized plots, the break through curve may

be determined as a plot of the concentration in the liquid versus θ. Using Equation (106), a plot of concentration in the liquid versus volume of the effluent can be determined from this break-through curve. The data curves under the consideration are plotted on the latter coordinates and can be compared with the curves given by the model.

Figure 60 shows the Contour Diagram for the case under consideration. First, the Contour Diagram for the saturation operation of column is obtained from the generalized diagram of Figures 29 and 30 directly by multiplying $\overline{Z}$ and θ coordinates by appropriate constants and by translating the θ coordinate. The Contour Diagram for the case where the feed is a slug of the solution (as in Figure 60) is obtained from the Contour Diagram for the saturation operation of a column in the same way as an effluent wave is obtained from a break through curve (refer to Figure 32).

The effect of mass transfer resistance as can be seen in Figure 60 is to spread the sharp edges obtained in Figure 54. In the case of sodium chloride the leading and the trailing edges do not interfere with each other. In the case of glycerol, on the other hand, the spreading of the sharp edges is greater (because of lower diffusivity) and the leading and the trailing edges interfere with each other and region for $G = 1$ on Figure 60 vanishes for long columns. The maximum concentration of glycerol in the effluent wave would be less than that in the feed for long columns.

Figure 61 shows the effluent curves obtained from the model. Data curves are plotted on the same figure for comparison.

The effluent wave for glycerol in Figure 61 agrees with the data curve in "shape" and "spread" of the wave. The data curve, however,

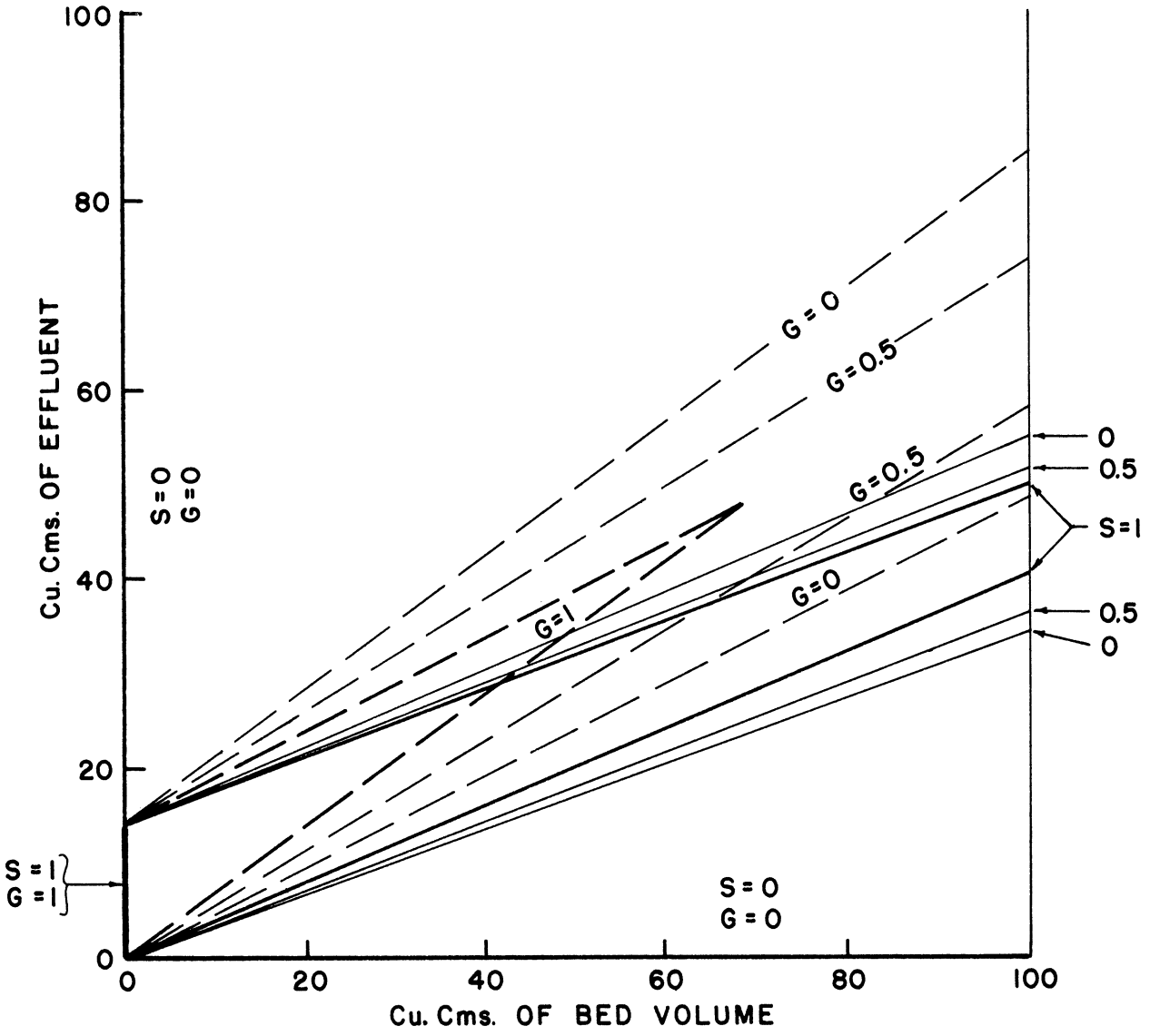

Figure 60. Contour Diagram for Model 4. (Diffusion in Solid Phase and Linear Equilibria) G(or S) is the Ratio of the Concentrations of Glycerol (or NaCl) in the Liquid to that in the Feed Solution.

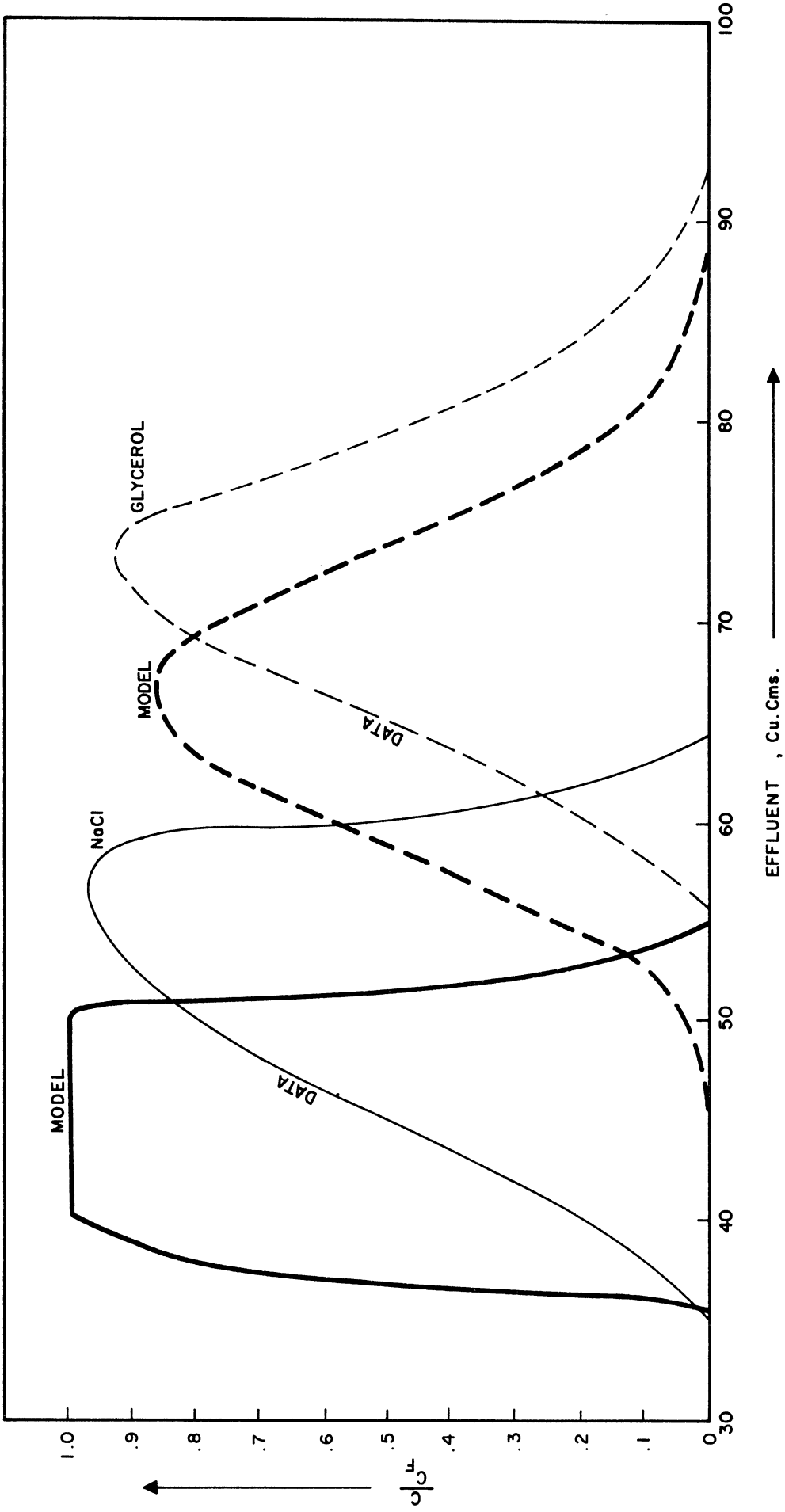

Figure 61. Effluent Curves Predicted by Model 4.

appears later than what is predicted by the model. If the curve given by the model were moved along the abscissa, the agreement with the data would be very good.

The position of the glycerol wave along the abscissa depends on the equilibrium characteristics of the system and the porosity characteristics of the bed; it is independent of the mass transfer resistances or the mass transfer mechanisms.* The agreement in the "shape" and "spread" of the curve between the data and the model suggests that diffusion in the solid phase adequately accounts for the effect of mass transfer on the effluent wave. The assumption of linear equilibrium for glycerol is probably valid since the effluent data curve is symmetrical.

If the shrinking of the resin with the increases in concentrations of the solutes were taken into account, the predicted glycerol wave would shift in the direction of the data curve. The shift is produced because the resin discharges water ahead of the effluent waves, diluting the leading edge of the salt wave and delaying the trailing edge.

The following model considers the effect of shrinking and swelling of the resin.

Model 5:

Diffusion in the solid is assumed to be the controlling resistance to mass transfer. The equilibrium for glycerol is assumed to be linear. The equilibrium for sodium chloride is assumed to be non-linear but independent of the concentration of glycerol. The resin shrinks when it comes in contact with sodium chloride and consequently the porosity of the bed increases with increase in concentration of sodium chloride. The equilibrium and the porosity functions used are the same as those used in Model 3 above.

---

* This has been discussed in the section on Mathematical Models, Models B(i).

The mathematical problem considering diffusion in the solid with non-linear equilibrium characteristics has not been solved. Some estimate of the solution, however, can be obtained by considering the contour diagram for Model 3 shown in Figure 58 (which is for the case of non-linear equilibrium, changing porosity, and no mass transfer resistances), and the Contour Diagram for Model 4 shown in Figure 60 (which is for the case of diffusion in solid with linear equilibrium). The effect of mass transfer resistances may be considered to be that of producing a certain spread of the boundaries given by the equilibrium operation of the column. From comparison of Contour Diagrams in Figures 54 and 60, this "spread" may be estimated for each sharp boundary. As an approximation the same amount of "spread" may be introduced graphically on the Contour Diagram (Figure 58) given for the operation with non-linear equilibrium. The resultant effluent waves may be obtained from the cross section of the estimated Contour Diagram.

Figure 62 shows the effluent waves estimated as described above for the model under consideration. As can be seen from the figure, the leading edge of NaCl data curve is "slanted" more to the right than what is predicted by the model; the dilution of the leading edge in the data is greater than what is predicted. Comparison of Figures 55, 57 and 61 shows that the non-linear equilibrium and the mass transfer resistances produce only a little dilution of the leading edge. Assumption of greater mass transfer resistances would "smear" the leading edge further but would not make it nearly "slant" to the right on Figure 62. Some mechanism that effectively introduces extra amount of water in the leading edge would explain further "slanting" of the leading edge in Figure 62 and further shift

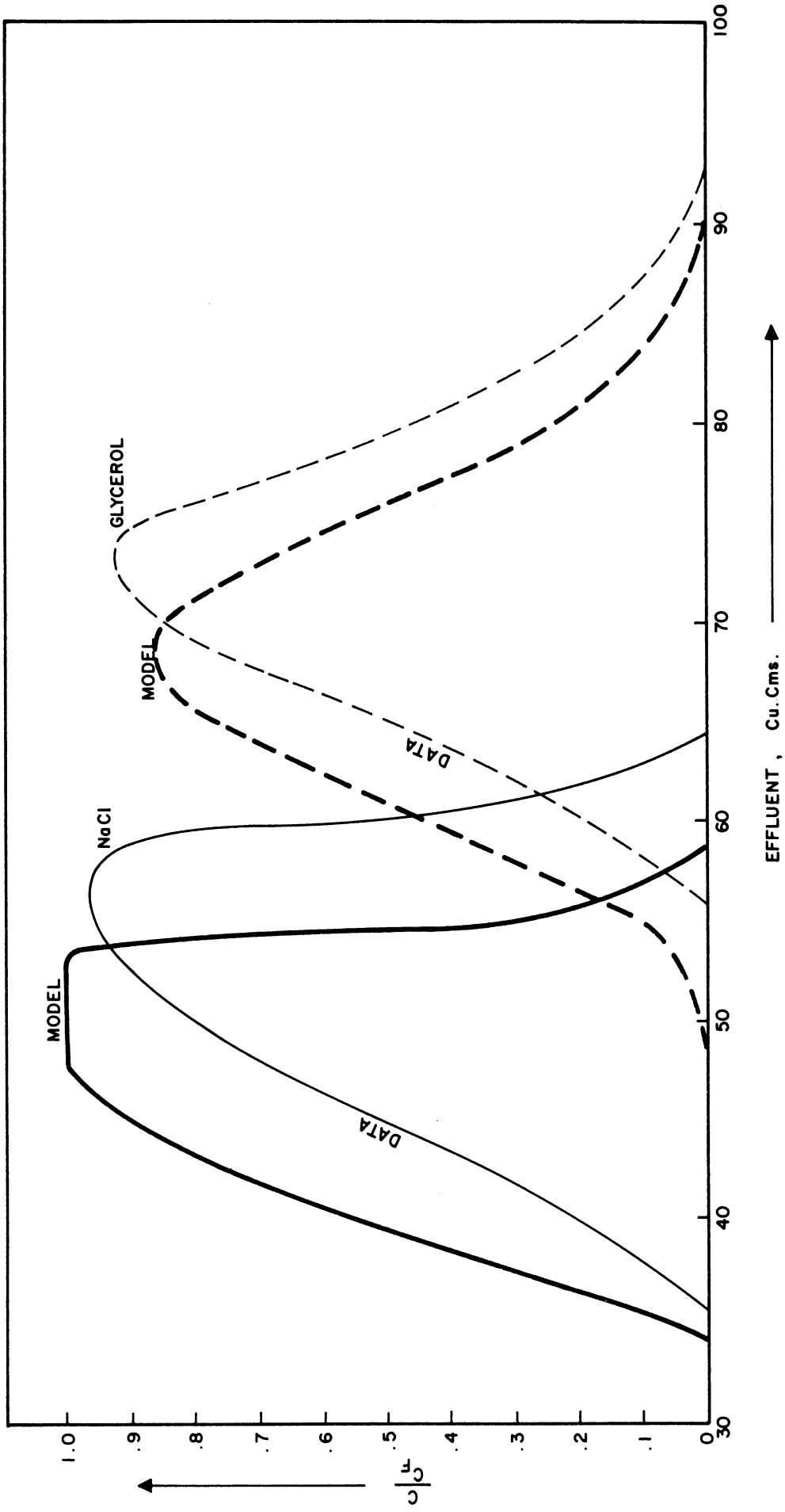

Figure 62. Effluent Curves Predicted by Model 5.

of the trailing edge of sodium chloride wave as well as the shift in the glycerol wave.

The effect of the concentration of NaCl on the equilibrium characteristics of glycerol have not been considered in above models. The following model considers the case of interdependent equilibria.*

Model 6:

Equilibrium Column operation and "no resistance to mass transfer" are assumed.

The equilibrium constant for glycerol is assumed to be dependent on the concentration of sodium chloride. (From Figure 47 it is taken as 0.34 for 0% NaCl and 0.36 for 4% NaCl.) It is assumed to be independent of the concentration of glycerol.

The equilibrium constants for sodium chloride and the effect of shrinkage of resin are assumed to be same as in Model 3.

Contour Diagram in Figure 63 shows the concentration effect of the interdependent equilibrium on the glycerol wave. The concentration of glycerol in the effluent is given as 1.07 times that in the feed.*

Since the concentration of glycerol is very small (0 to 4%), its effect on NaCl equilibrium is neglected.

Figure 64 shows the effluent curve predicted by the model. This may be compared with Figure 59 to see the effect of interdependent equilibria. The increase in the concentration of glycerol due to this effect may account for the difference in the peak heights for glycerol waves between the model and the data curves in Figures 61 and 62.

---

* For more details, see section on Mathematical Models, Model A(ii)(b).

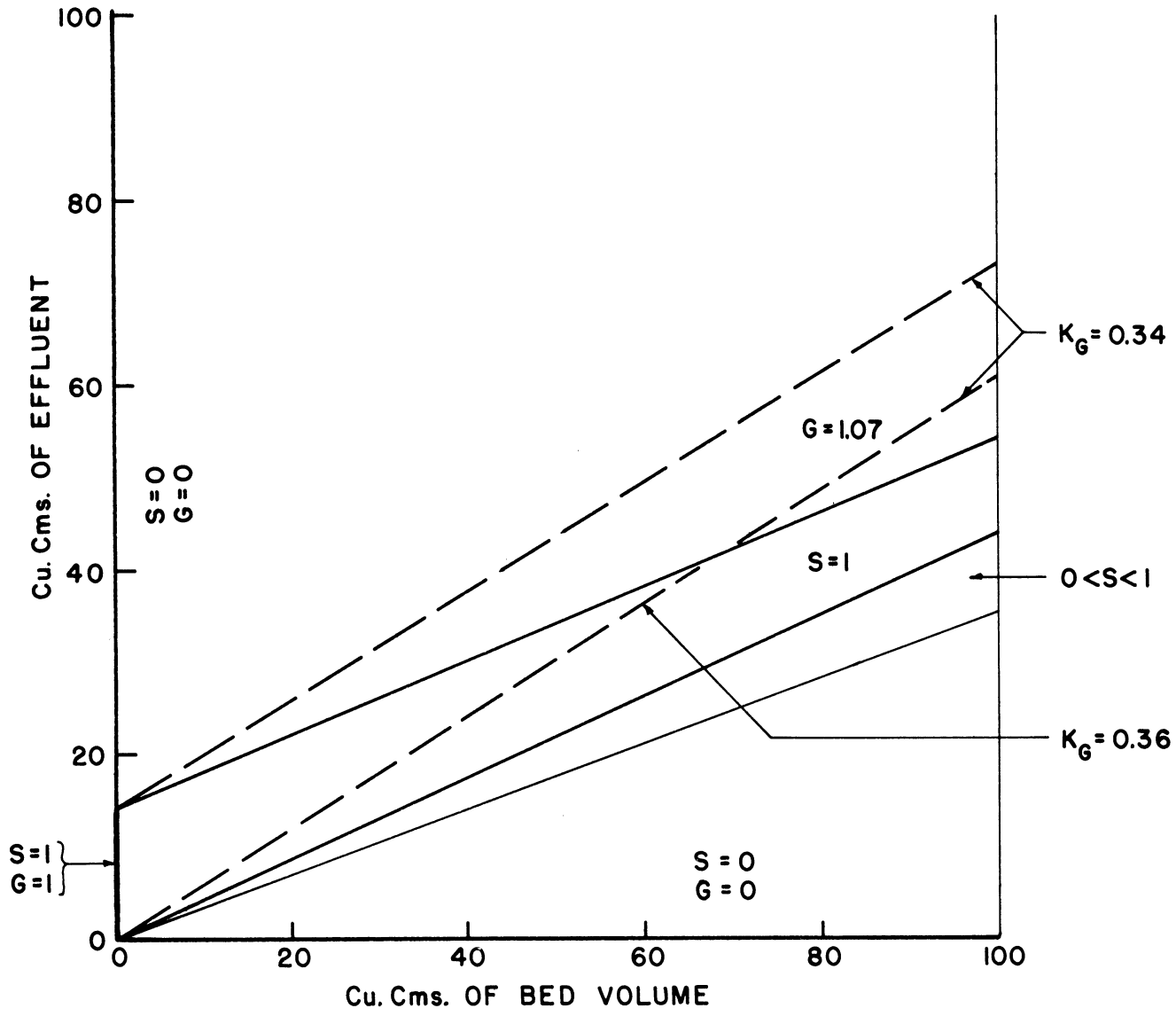

Figure 63. Contour Diagram for Model 6. G(or S) is the Ratio of the Concentrations of Glycerol (or NaCl) in the Liquid to that in the Feed Solution.

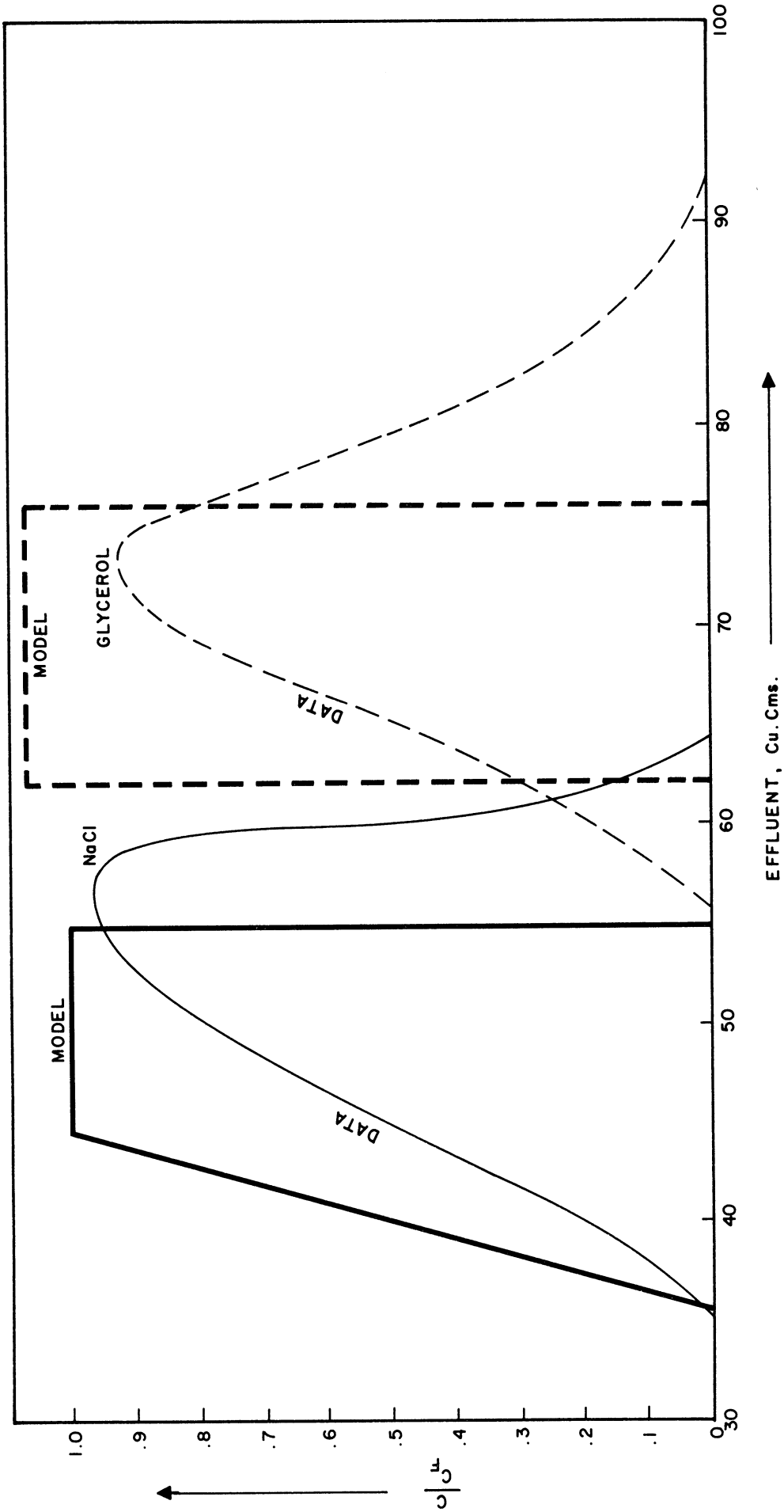

Figure 64. Effluent Curves Predicted by Model 6.

Model 7:

It is assumed that mass transfer rates are controlled by the rates of diffusion of the solutes in the solid phase. The equilibrium characteristics of the system are the same as those in Model 6.

Figure 65 shows the effluent curve predicted by the model. It is obtained from the solution of Model 6 by adding the effect of mass transfer resistances.* Comparison with Figure 62 shows that the effect of interdependent equilibrium is to concentrate the glycerol wave and increase the maximum concentration in the wave.

General Comments on Fitting Wheaton and Bauman's Data:

Figure 51 shows the data curves reported by Wheaton and Bauman (W2).

Consider the curve for glycerol. Assuming linear equilibrium and diffusion in the solid as the controlling mass transfer resistance, the "shape" and "spread" of the glycerol curve are explained adequately (see Figure 61). Consideration of the effect of the concentration of sodium chloride on the equilibrium constant of glycerol explains the peak height (see Figure 65).

The location of the glycerol wave along abscissa is not explained by the above models. Assumption of any other model for mass transfer rates would not explain this discrepancy, since the "location" of the wave does not depend on the mass transfer resistances.

Some mechanism that produces a "delay" in the wave is required. The shrinkage of resin may explain some delay since the resin discharges water ahead of the wave and picks up the water when the concentration wave has passed.

---

* In the same manner, the solution of Model 5 was obtained from that of Model 4.

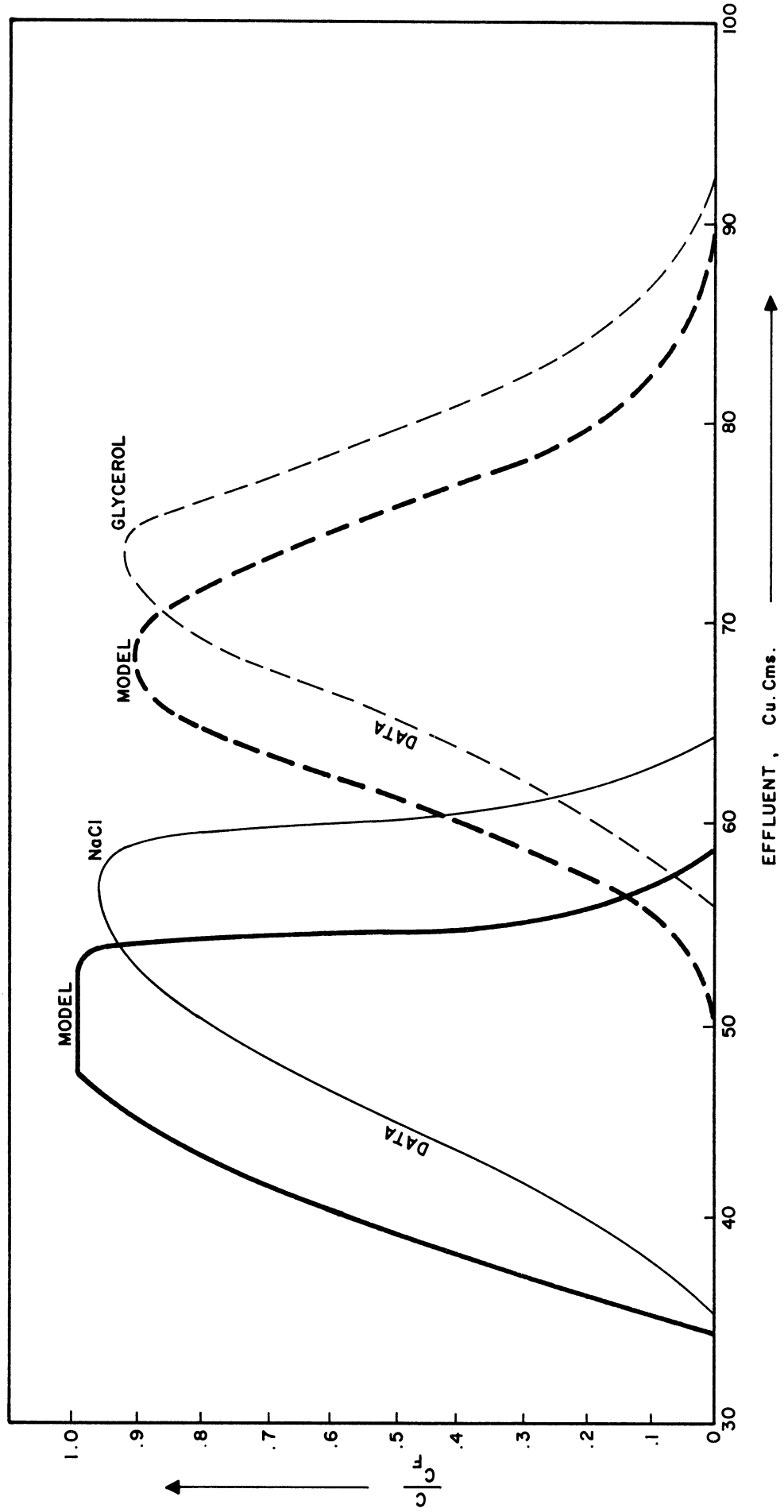

Figure 65. Effluent Curves Predicted by Model 7.

Now consider the sodium chloride curve reproduced in Figure 66. The leading edge DLE is "spread out" and "slanted to the right". The line BJ gives the leading edge predicted for linear equilibrium and for no mass transfer resistance. The effect of mass transfer resistances is to diffuse the edges BJ and HG about equally. The effect of non-linear equilibrium is to spread the edge BJ but not disturb the edge HG. In both cases - mass transfer resistances and non-linear equilibrium - the edge BJ is spread such that the area ABJK remains constant.* The "average" position of the predicted leading edge would remain the same as that of BJ and the "average" position of the predicted trailing edge would remain the same as that of GH.

In the data curve, however, the leading edge is slanted very much to the right, and the area ADLEK is much greater than that of ABJK. The trailing edge has also been moved to the right.

This would be the effect of large value of equilibrium constant. A value of effective equilibrium constant may be defined empirically to fit the data. Similar effective equilibrium constant may be defined empirically for glycerol to account for the shift between the data and the predicted curves.

Another possibility is to assume a mechanism that introduces diluting water in the leading edge of sodium chloride wave. This would displace the trailing edge GH by the amount equal to the amount of diluting water added. The leading edge would be diluted continuously, and it would slant to the right of a plot such as Figure 66. The area under

---

* This area represents the total amount of sodium chloride that would have been retained by the column in the case of a saturation column operation.

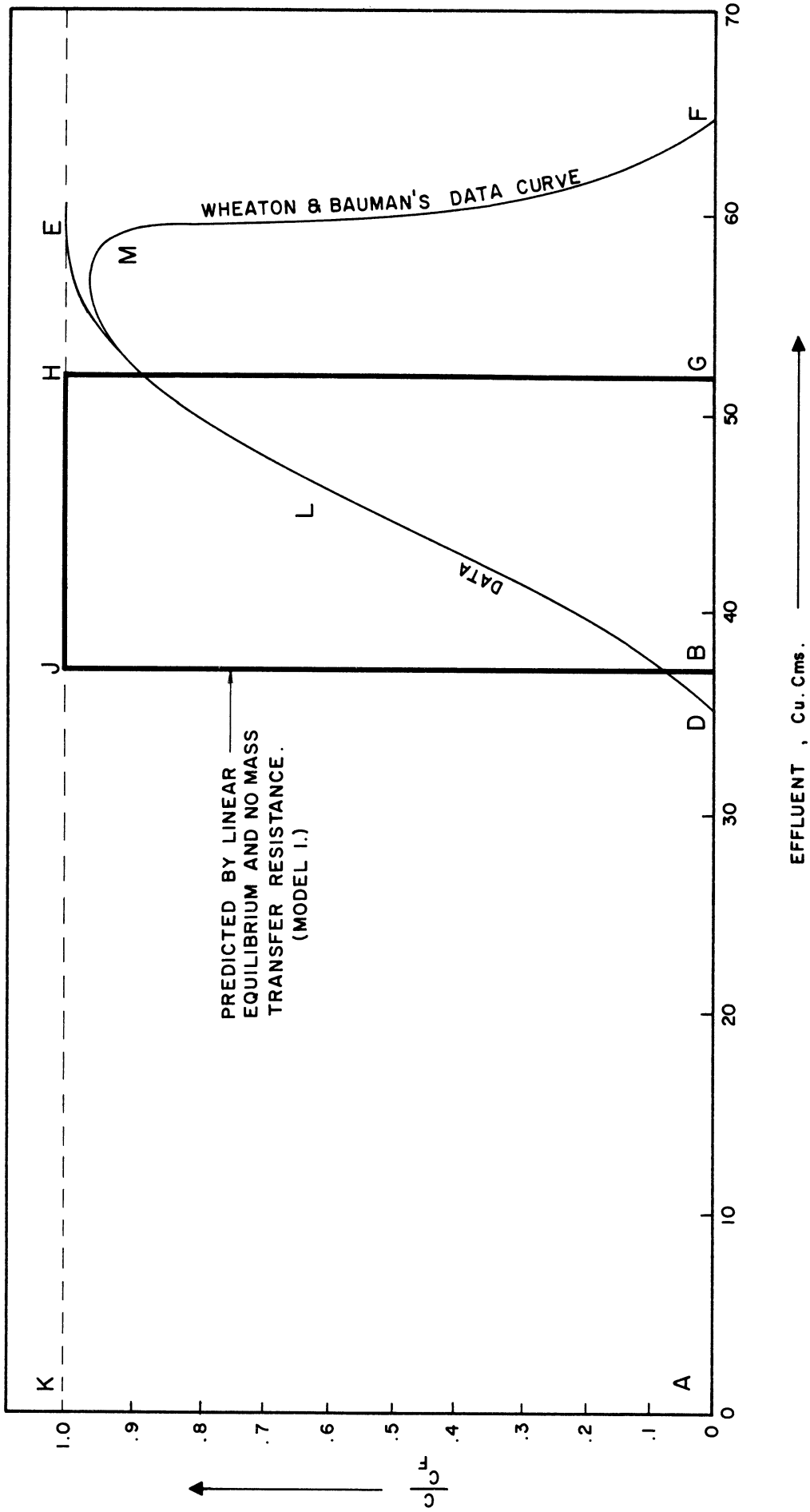

Figure 66. Aid to the Discussion of the Fit of Models to Data Curve for NaCl.

the wave, representing the total amount of the throughput of sodium chloride, would be maintained as constant.

This effect is produced when the resin particles shrink and discharge water in the process. However, from the data on resin shrinkage (S4, S5) the expected amount of dilution water accounts only for about half of the shift of the edge GH. The slant of the leading edge is also only partially explained.

A mechanism that discharges water into the leading edge of the sodium chloride wave and does not remove this water back from the liquid until the glycerol wave has passed that point in the bed, would explain the "slanting" of the leading edge of NaCl wave, the shift of the trailing edge of NaCl wave and the shift of the glycerol wave.

An additional complication arises in the consideration of the glycerol wave. The volume of the resin is much more sensitive to the concentration of sodium chloride than to the concentration of glycerol. The resin shrinks in the presence of sodium chloride and swells when the sodium chloride concentration is reduced. This means that any section of a bed would discharge water as the leading edge of NaCl comes in contact with it, and it would absorb water as the trailing edge of the NaCl wave passes by. Since the glycerol wave lags behind a little, this would produce additional concentration effects in the glycerol wave and would reduce the shift in the glycerol waves that was produced due to the diluting water discharged in the sodium chloride wave.

Wheaton and Bauman's data curves discussed above were obtained using low concentrations of the solutes in the feed to the column (4% glycerol and 4% NaCl). The following considers typical data curves

reported by Asher and Simpson (A3) where the concentration in feed is about 10% NaCl and 30% glycerol.

(ii) Asher and Simpson's Data

The following discussion is limited to the curves given in Figure 52. These may be considered as typical of the data reported by Asher and Simpson (A3).

In contrast to the data of Wheaton and Bauman (Figure 51) considered above, the feed under the present consideration contains a much higher percentage of glycerol and NaCl. Consequently, the effect of non-linear and interdependent equilibria would be important.

The equilibrium constant K for glycerol would vary from .34 for zero concentration of the solutes to 0.43 for the composition of the feed. The equilibrium constant for NaCl would vary from .016 to 0.1.

Consider the simple model assuming no mass transfer resistances and linear equilibria for both glycerol and NaCl. The equilibrium constants are estimated as 0.385 and 0.55 for K_G and K_S respectively, where subscripts "G" and "S" represent glycerol and NaCl. Figure 67 gives the contour diagram expected.

The non-linearity of the equilibria is such that the isotherms are concave upwards both for glycerol and NaCl (Figures 44 and 45). This means that on the Contour Diagram of Figure 67, the leading edges AD and AE would be "spread out" and the trailing edges BF and BG would remain sharp.

Because of interdependent equilibria, there would be concentration of glycerol in the region BFG and the degree of concentration can be

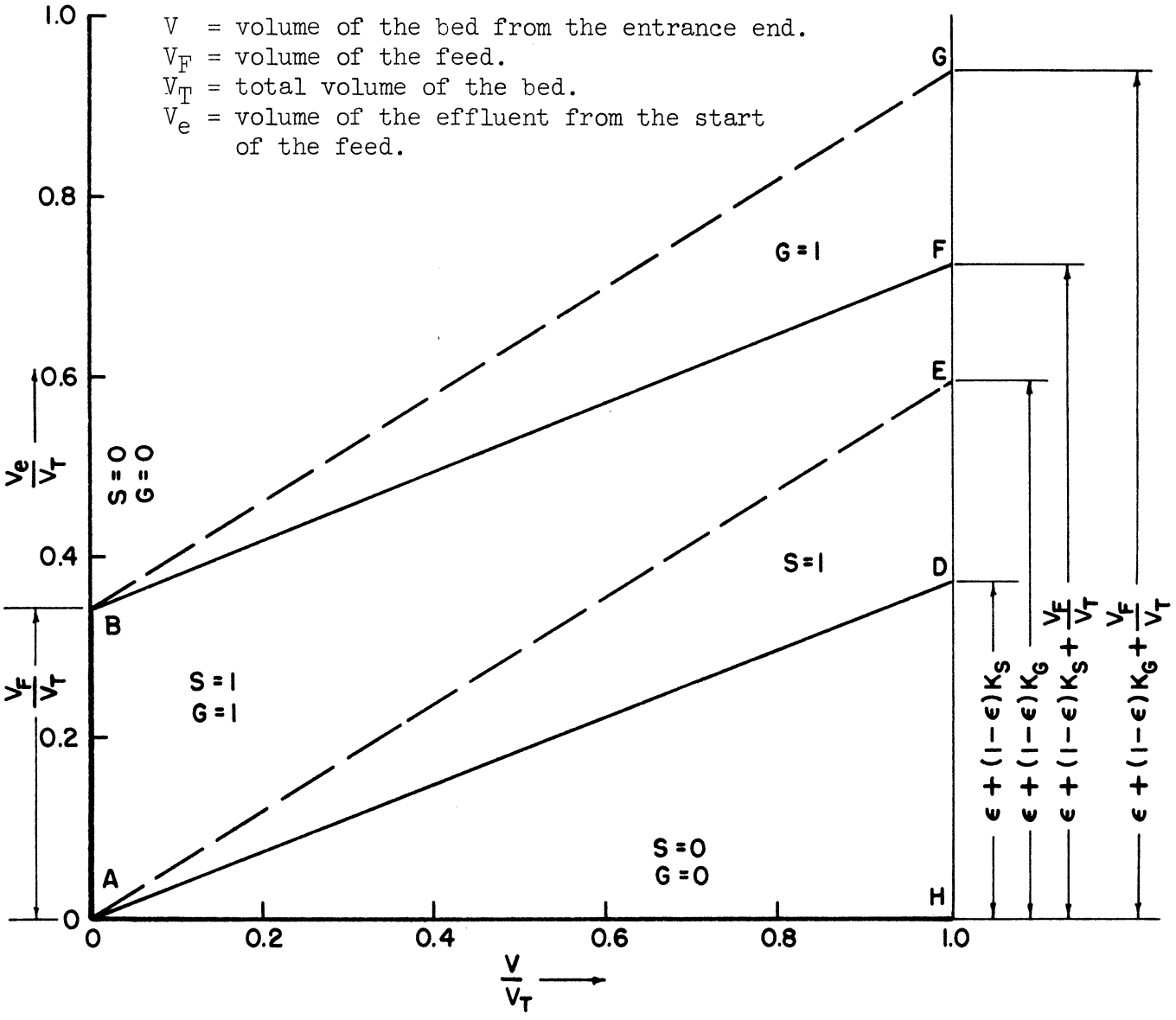

Figure 67. Contour Diagram for Equilibrium Column Operation Assuming Linear Equilibria. G(or S) is the Ratio of the Concentrations of Glycerol (or NaCl) in the Liquid to That in the Feed Solution.

calculated from the slope of the line BF and the equilibrium constants for glycerol in presence and in absence of salt solution.* Since the edge BF would remain sharp, the change in concentration of NaCl is sharp and the change in concentration of glycerol would also be sharp. In the region AED, there would be dilution of NaCl because of interdependent equilibria.* Since the edge AE would be "spread out", this dilution would be gradual.

Figure 68 shows the Contour Diagram obtained for an equilibrium column operation when the effects of non-linear equilibria mentioned above are taken into account. The edges AD and AE in Figure 67 have spread into the regions ADD' and AEE' respectively. Figures 46, 47 and 48 have been used for estimating values of equilibrium constants and slopes of equilibrium isotherms.

Figure 69 shows the Contour Diagram obtained if the effect of change in porosity due to resin shrinkage with the increase in concentration of the solutes is taken into consideration. Data on porosity given in Figure 50 have been used in drawing the Contour Diagram.

Figure 70 shows the effluent curves predicted from the Contour Diagram in Figure 69. Data curves from Figure 52 are reproduced on Figure 70 for comparison.

The trailing edge for NaCl data curve appears later than predicted by the model. The leading edge of NaCl data curve is slanted further to the right than predicted by the model. The discrepancy is

---

* For details see discussion on Model A(ii)(b) in the section on Mathematical Models.

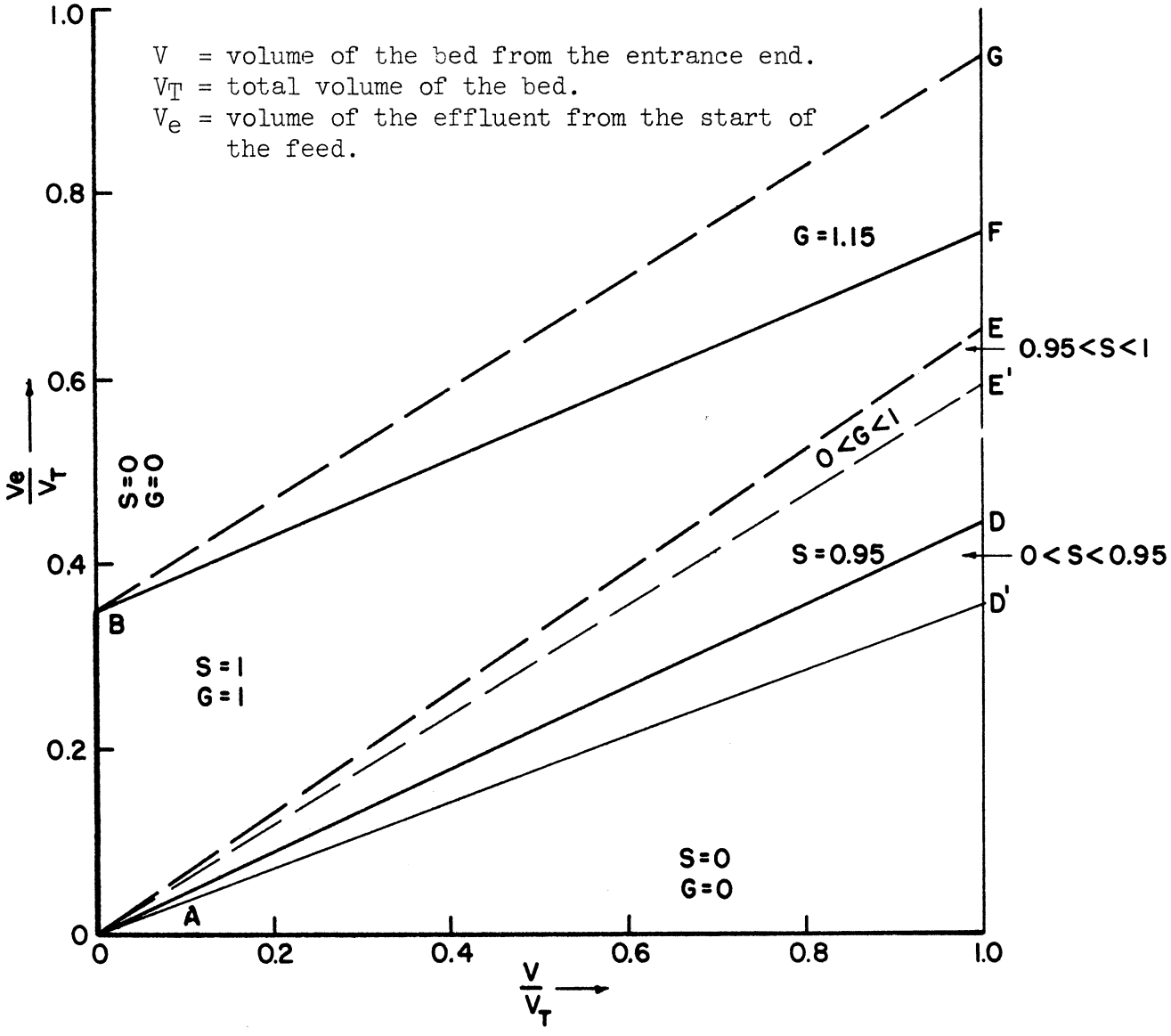

Figure 68. Contour Diagram for Equilibrium Column Operation and Non-Linear Interdependent Equilibria. G(or S) is the Ratio of the Concentrations of Glycerol (or NaCl) in the Liquid to That in the Feed Solution.

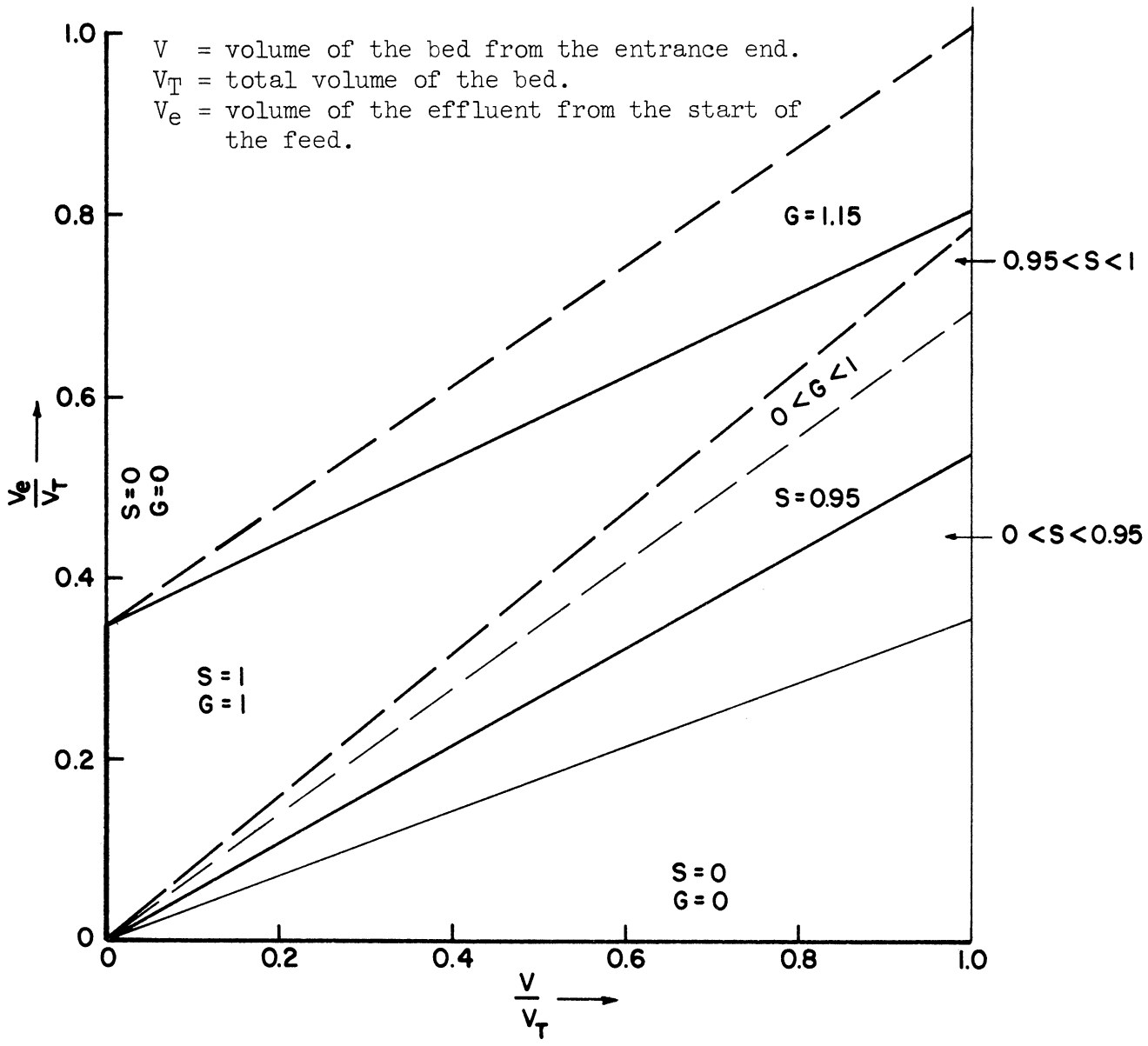

Figure 69. Contour Diagram Considering the Effect of Resin Shrinkage. (Equilibrium Column Operation). G(or S) is the Ratio of the Concentrations of Glycerol (or NaCl) in the Liquid to That in the Feed Solution.

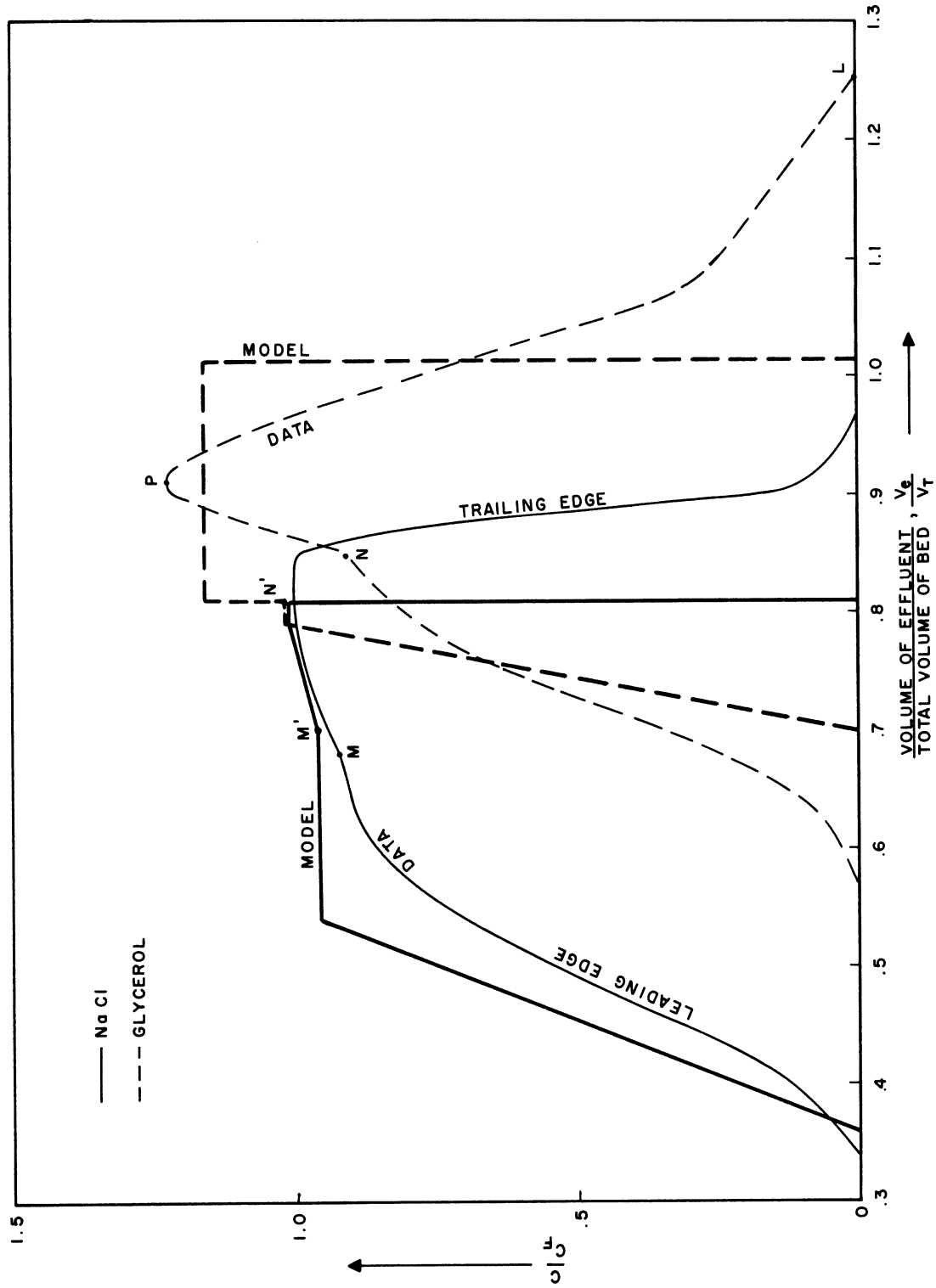

Figure 70. Effluent Curves Predicted by the Model Assuming Equilibrium Column Operation, Non-Linear Equilibrium characteristics and Changing Porosity of the Bed.

similar to that obtained in the case of Wheaton and Bauman's data (see Figure 59). As explained before, this discrepancy cannot be accounted for by consideration of mass transfer resistances, and a mechanism that would increase the amount of water added into the leading edge is required.

The consideration of an equilibrium column operation explains many of the essential characteristics of the data curves. The "slanting" of the leading edges of the NaCl and the glycerol curves are mainly due to the dilution produced by resin shrinkage, and secondarily due to non-linear equilibria. The inflection at the points M and M' (Figure 70) in the leading edge of the NaCl curve occurs at the same time at which the concentration of glycerol starts rising, and it is caused by the interdependent equilibrium characteristics. The inflection at the points N and N' (Figure 70) in the leading edge of the glycerol curve is also the result of interdependent equilibrium characteristics, and consequently, it occurs at the same time at which the concentration of NaCl decreases rapidly. The concentration of glycerol in the effluent peak is greater than that in the feed. This "concentration effect" is partly due to the lowering of the equilibrium absorption of glycerol as the concentration of NaCl is decreased and partly due to swelling and water absorption of the resin as the concentration of NaCl is decreased.

The models considered in this thesis do not explain the shape of the part NPL (Figure 70) of the glycerol data curve. If mass transfer resistance is introduced into the model represented in Figures 69 and 70, the effluent curves that are obtained are shown in Figure 71. The trailing edge of the data curve is spread out very much more than what is expected from the model.

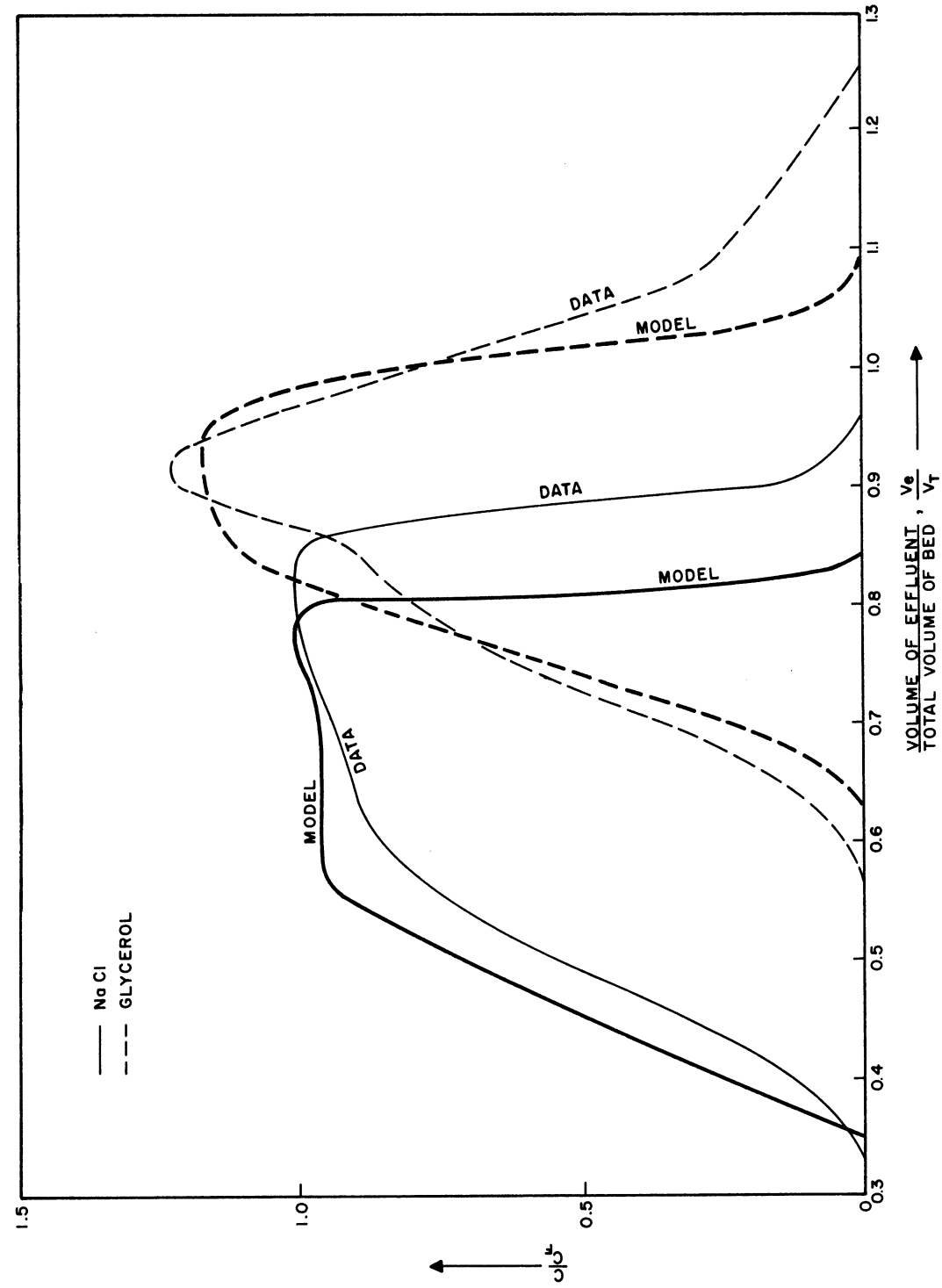

Figure 71. Effluent Curves Predicted by the Model Assuming Non-Linear Equilibrium Characteristics, Changing Porosity of the Bed and Diffusion in the Solid as the Controlling Resistance to Mass Transfer.

A possible qualitative explanation for this disagreement with the models is the difficulty of displacing concentrated glycerol solution from the voids of the resin bed with water. In the operation of an ion exclusion column, a limited quantity of the feed solution is followed by pure solvent. In the column, the solvent follows the band of the solution and "slug flow" of the solvent with complete displacement of the liquid in the voids has been assumed in the above models. Because of the high viscosity of concentrated glycerol solutions, such a displacement may be difficult and considerable dispersion and spreading of the trailing edge of the glycerol wave may be produced.

In the case of Wheaton and Bauman's data discussed above, only dilute solutions were involved and a model considering diffusion of the solutes in the solid phase was adequate to explain the shape of the glycerol wave. For dilute solutions, it would be easier to obtain "slug flow".

Asher and Simpson's data curves, under the present consideration, (Figure 52) were obtained at 80°C. The same authors (A3) have reported some data obtained at room temperature with concentrated feed solutions. Their data at room temperature, reproduced in Figure 72, show much more dispersion and spreading of the trailing edge of the glycerol curve. At the same time the trailing edge of the NaCl curve also shows approximately the same amount of spreading in Figure 72. Consequently, the mechanism that produces the dispersion of the trailing edges operates on the bulk of the band of the concentrated solution passing through the column. This is consistant with the explanation for the trailing edge of glycerol wave speculated above.

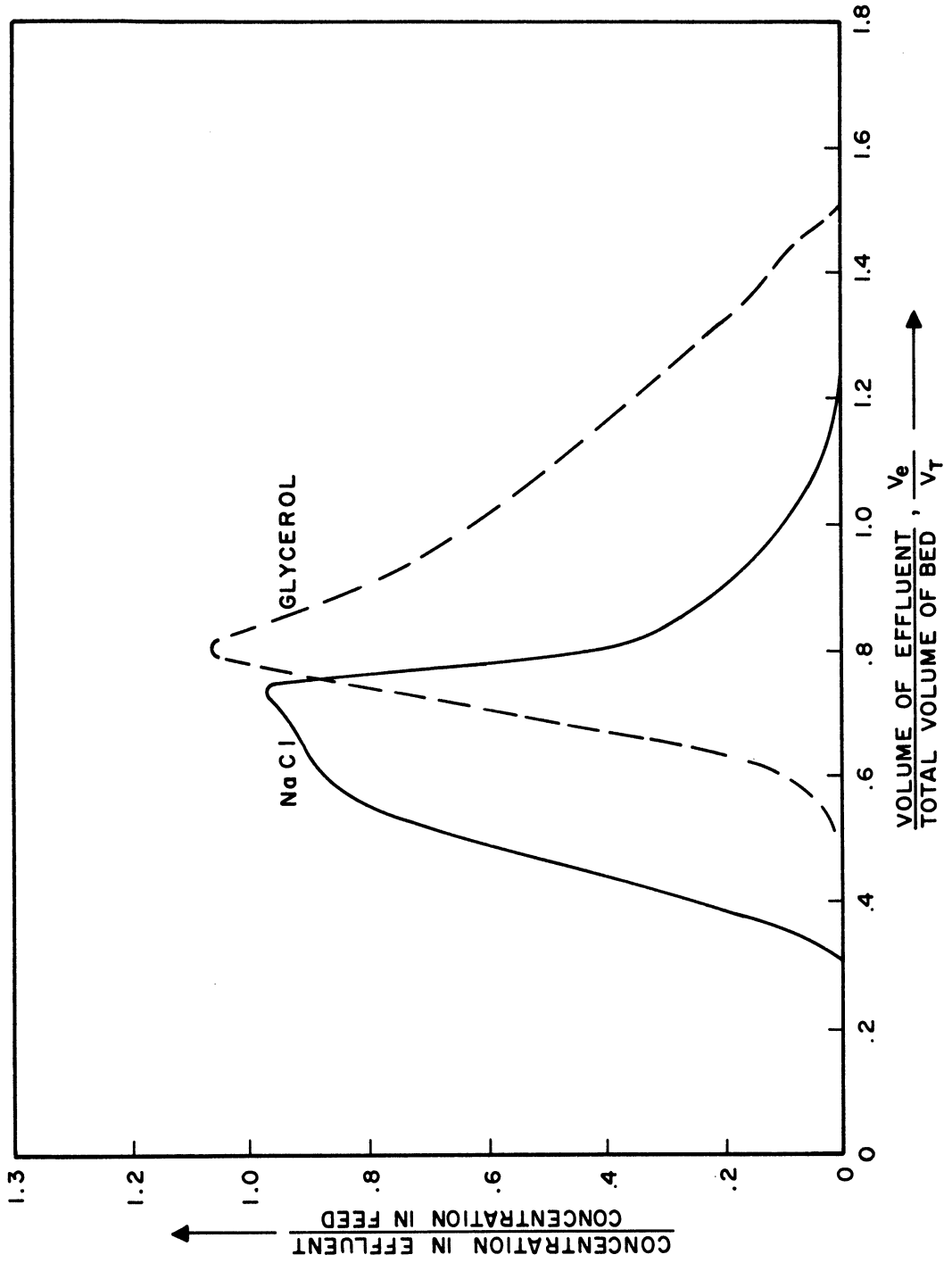

Figure 72. Asher and Simpson's (A3) Curves. Resin: Dowex 50 x 8; Feed: 0.35 V_T of 10% NaCl; 35.3% Glycerol; Room Temperature 80°C.

The equilibrium characteristics assumed for drawing Contour Diagrams and obtaining solutions of models are based on Shurts and White's data (S4,S5) which were obtained at room temperature. Asher and Simpson's data curves, Figure 52, considered above were obtained at higher temperature. The effect of temperature on equilibrium characteristics, however, is not large for resin with 8% divinyl benzene (used by Asher and Simpson) as can be seen from Figures 8 and 9 of Part I of this thesis. The small effect, in any event, does not alter the estimated Contour Diagrams significantly. Since the type of non-linearity and the nature of interdependence of the equilibria remains the same at high temperatures, the shape and general characteristics of the effluent waves predicted by the models are not effected by the temperature. In the case of models considering diffusion in the resin, the values of diffusivities at high temperatures were obtained from Figures 5 and 6 of Part I of this thesis.

In the preceding discussion two typical sets of data curves, Figures 51 and 52, have been treated in considerable detail in order to illustrate a simple and rapid method of predicting column behaviors if some estimate of the equilibrium and mass transfer characteristics is available. The models considered here explain the data to a limited extent. The inadequacy of the models and the "type" of mechanisms necessary for explaining the data was brought out by the method of analysis used. Additional data reported by Asher and Simpson (A3) and Prielipp and Keller (P1) have been considered by the author and similar limited agreement with the models was obtained. Same "kind" of inadequacies of the models was indicated by the analysis.

IV. CONCLUSIONS
(For Part II)

1. Data for ion exclusion column operation with the system Ethylene Glycol-Water-Dowex 50 can be reproduced within the estimated experimental accuracy by a mathematical model that makes the following assumptions. (This is Model B(i) (a) in the section on Mathematical Models):

(i) The equilibrium is linear for the distribution of glycol between the resin phase and the aqueous phase.

(ii) Mass transfer rates are controlled by "diffusion" the solid phase, and its mechanism is described by Fick's Law of diffusion.

(iii) There is a "slug flow" of the liquid and there is no longitudinal diffusion in the liquid.

2. Only some of the characteristics and parts of the effluent curves from the data for ion exclusion column operation with the system Glycerol-NaCl-Water-Dowex 50 can be reporduced by the various mathematical models considered in this study. The dilution of the leading edge of the NaCl effluent curve is only partially reproduced by the effects of resin shrinkage and non-linear equilibrium characteristic. Models that consider the flow patterns and velocity profiles in the liquid are required to account for the long trailing edge in the glycerol effluent curve.

3. Consideration of the equilibrium column operation predicts the location of the effluent curves and also general description of the "shapes" of effluent curves, such as "symmetrical" and "skewed" curves.

The order of magnitudes of the effects of the change in volume of the solid and those of interdependent equilibria can be estimated by considering equilibrium column operations.

4. The effect of mass transfer resistances is to distort the effluent curves predicted for equilibrium column operation in such a fashion that the sharp edges are "smeared"; but the "average" position of the curve and the total area under the curve are unaltered.

5. Except for very short columns, generally symmetric effluent waves are produced by "linear effects" such as mass transfer resistances and skewed waves are produced by "non-linear effects" such as non-linear equilibria and swelling and shrinkage of the solid.

6. If the porosity of a bed is a function of the compositions, for an equilibrium column operation, its effect is equivalent to the effect of non-linear equilibrium characteristics on the system with constant porosity. [Model A(i) (d) in the section on Mathematical Models discusses this quantitatively.]

7. x-t Contour Diagrams provide a visual aid for understanding the effect of different variables on the effluent curves. They also facilitate graphical estimation of effluent curves. The extent of concentration and dilution effects due to interdependent equilibria can be estimated graphically. Solutions of complex models for which analytic solutions are not available may also be estimated graphically by constructing approximate Contour Diagrams.

APPENDIX

ADDITIONAL DISCUSSION OF THE MODEL A(i) (b) (Equilibrium Column Operation for a Single Solute with Non-Linear Equilibrium)

The following discussion will be limited to the case of non-linear equilibrium of type (i), Figure 10, in which the equilibrium isotherm is concave upwards and d^2F/dc^2 is positive.* The concepts and methods described here can be extended to systems showing other types of equilibrium isotherms.

Let a column, initially free of solute, be saturated by passing a solution containing a constant concentration of the solute. Figure 11 shows the x-t Contour Diagram obtained for such an operation and Figure 15A shows the sketch of the concentration surface in the three dimensional (x, t, c) space. This surface is a ruled surface and it may be visualized as having been generated by the movement of a straight line that starts in the x-t plane, always remains parallel to the x-t plane, always intersects the c-axis, and swings towards the t-axis as it "rises up" along the c-axis. The relation between the slope of the projection of the above generating line on the x-t plane and its "height" along the c-axis is given by Equation (25).**

$$\left[\frac{dt}{dx}\right]_c = \frac{\epsilon}{u} + \frac{(1 - \epsilon)}{u} \frac{dF}{dc} \qquad (25)$$

---

* The Nomenclature in this section is the same as that used in the discussion of Model A(i) (b) in the section on Mathematical Models.

** Derivation of Equation (25) is given in the section on Mathematical Models, Model A(i) (b).

Figure 11 shows the level curves of this surface. Since for $0 < c < 1$, all the level curves pass through the origin of the x-t plane, along each level curve Equation (107) which is obtained by integrating Equation (25) will apply.

$$t = \left[\frac{\epsilon}{u} + \frac{(1 - \epsilon)}{u} \frac{dF}{dc}\right] x \qquad (107)$$

The value of $\frac{dF}{dc}$ in Equation (107) is taken at the same value of concentration for which the Equation (107) describes the level curve.

Now, consider a section of the concentration surface at a constant value of x, shown in Figure 73. This will be the concentration history for a certain bed length. The curve SR is also described by Equation (107). The concentration c as a function of time t is implicitly defined by Equation (107) for a constant value of x. At time t_1 let the concentration in the liquid be c_1 as shown in Figure 73.

Then,

$$\text{Area ASGH} = \int_{c=o}^{c=c_1} t \; dc$$

$$= \int_{c=o}^{c=c_1} \left(\frac{\epsilon}{u} x + \frac{(1-\epsilon)x}{u} \frac{dF}{dc}\right) dc$$

$$= \frac{\epsilon x}{u} c_1 + \frac{(1-\epsilon)x}{u} F(c_1)$$

$$= c_1\left(\frac{\epsilon x}{u} + \frac{(1-\epsilon)x}{u} \frac{F(c_1)}{c_1}\right)$$

and,

$$\text{Area SGJ} = c_1 t_1 - c_1\left(\frac{\epsilon x}{u} + \frac{(1-\epsilon)x}{u} \frac{F(c_1)}{c_1}\right) \qquad (108)$$

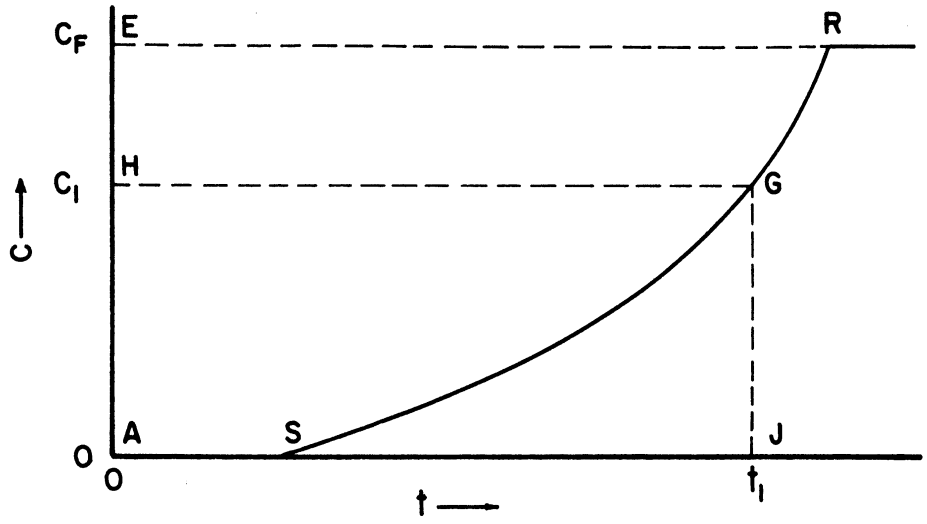

Figure 73. Cross-Section of the Concentration Surface for Saturation Column Operation. (Model A(i)(b)).

Equation (108) is very useful for drawing x-t Contour Diagram if a slug of solution is the feed to the column. Figure 19A shows the Contour Diagram expected in such a case and Equation (108) is useful in determining the line BD in Figure 19A which represents the restriction due to overall material balance.

The construction of an x-t Contour Diagram such as Figure 19A is carried out in detail in the following.

Let c_F be the concentration of the solute in the feed and let Figure 75A describe the feed to the column. A slug of the solution is fed to the column for time t_o.

On the x-t Contour Diagram, Figure 74, the feed to the column is represented on the t-axis, i.e., the line for x=0. Along MA, $c=c_F$ and along BD, c=0.

Through the point M, several straight lines are drawn according to the Equation (107) for different values of c in the range $0 \leq c \leq c_F$. These give the level curves for the saturation column operation.

Through the point A, one straight line AB is drawn with a slope* equal to

$$\frac{\epsilon}{u} + \frac{(1 - \epsilon)}{u} \frac{F(c_F)}{c_F}$$

This line represents the sharp boundary of the exhaustion column operation. The slope of this line is determined by the ratio $F(c_F)/c_F$ which is the equilibrium constant at $c=c_F$ in the above expression.

---

* See Figure 17, Equation (25a) and general discussion in the section on Mathematical Models, Model A(i) (b).

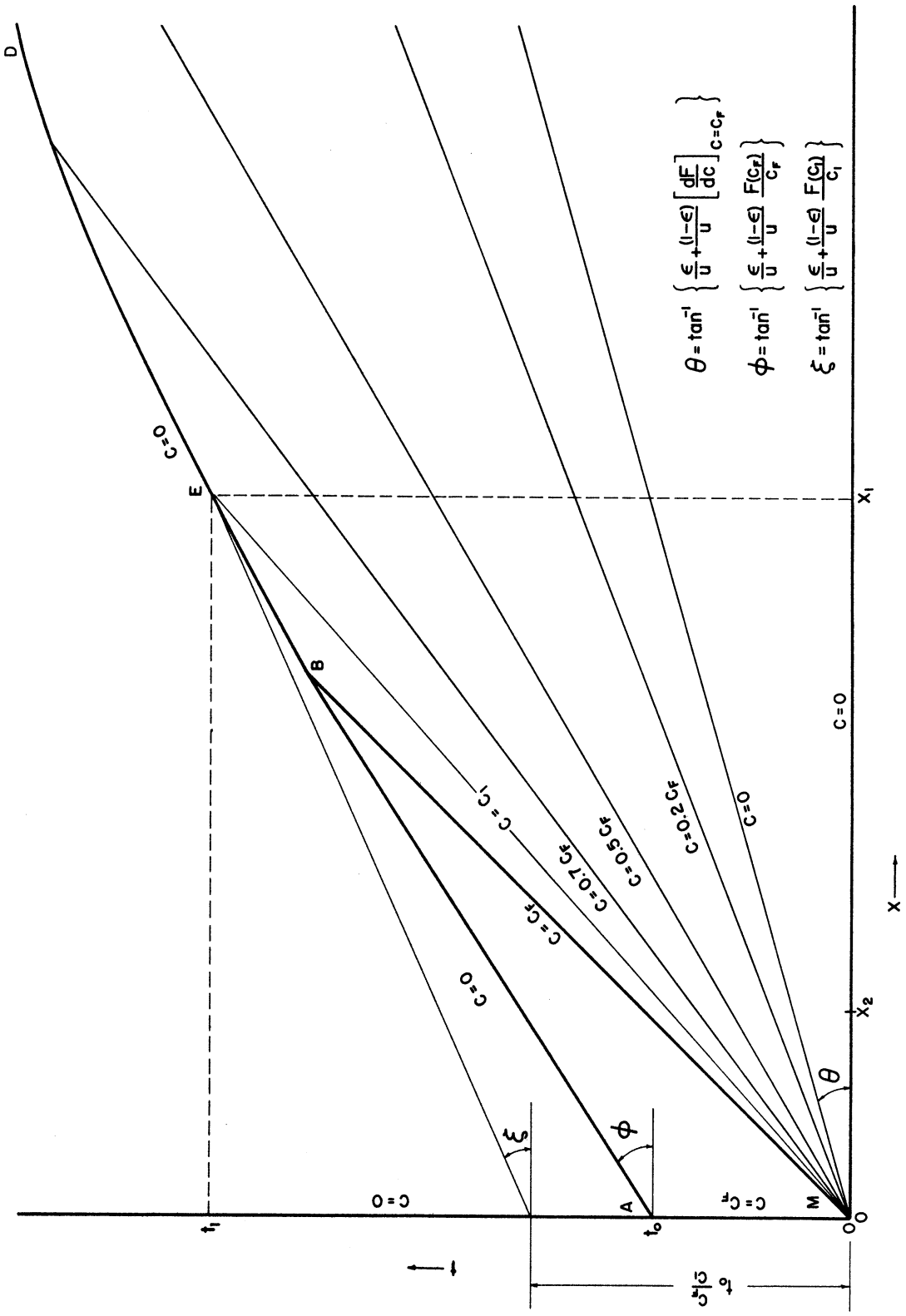

Figure 74. Construction of x-t Contour Diagram for Equilibrium Column Operation for Non-Linear Equilibrium of Type (i). (Model A(i)(b)).

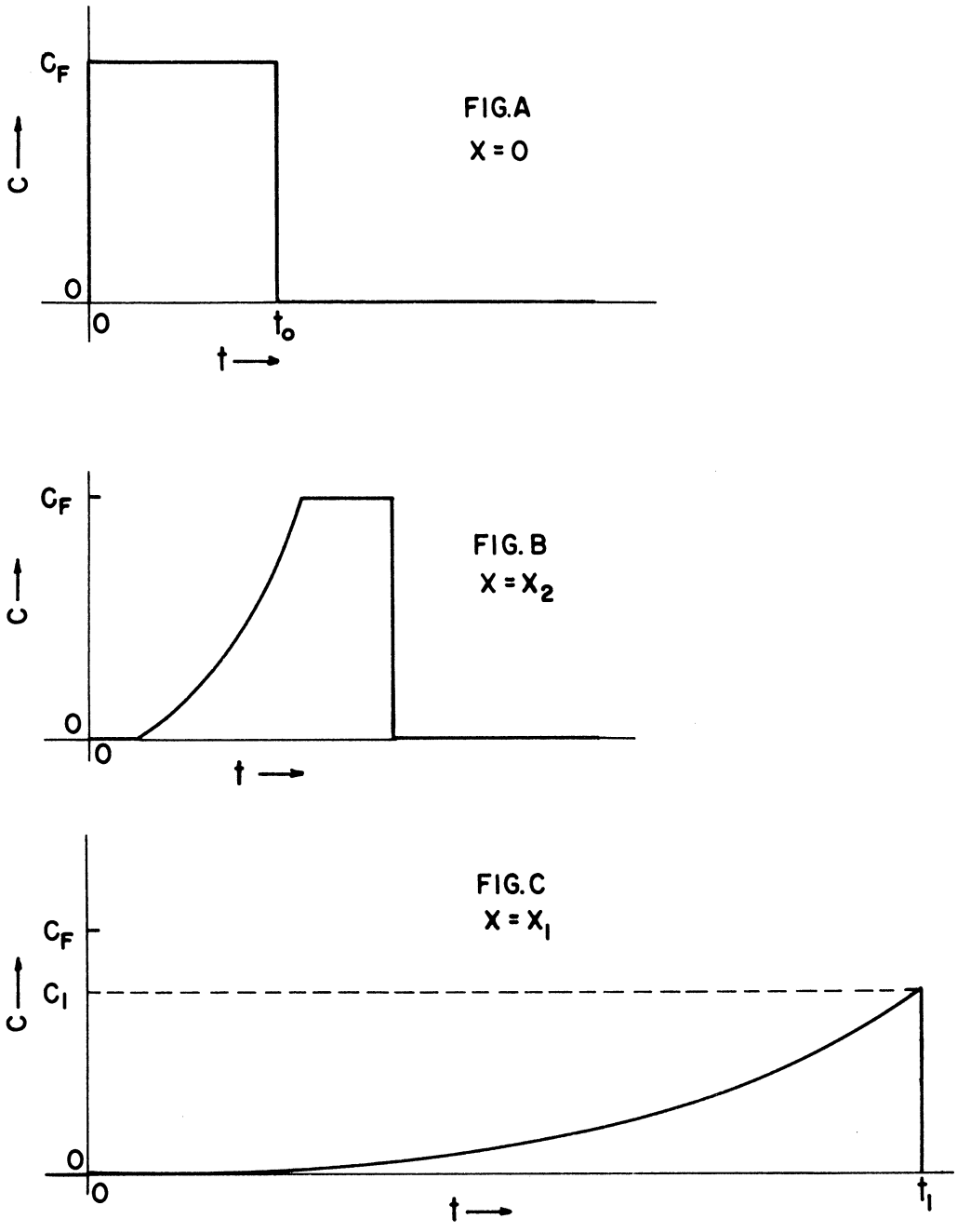

Figure 75. Effluent Concentration Curves Obtained as Cross-Sections of the Concentration Surface Represented in Figure 74.

B is the point of intersection of the lines AB and MB. The line MB is the level curve for $c=c_F$ constructed above. The triangle ABM represents the region where $c=c_F$. For short columns, the value of x will be low and a line parallel to t-axis at the low values of x will pass through the region ABM. In such a case the concentration of effluent versus time for short columns would give a curve such as the one shown on Figure 75B. The concentration will rise from zero to c_F, stay at c_F for awhile and then drop sharply to zero.

If the value of x is large, such that the line parallel to t-axis at that value of x does not intersect the triangle ABM, then the maximum concentration in the effluent from such a large column would be less than the concentration in the feed. The effluent curve would still show gradually increasing concentration in the leading edge and a sharp drop in the trailing edge as shown in Figure 75C. The area under the curve of effluent concentration versus time in any case represents the total amount of the solute that is passed through the column and consequently the areas under the curves given in Figures 75A, B and C will be equal.

Consider a level curve for $c=c_1$. Let E be the point of intersection between the level curve and the material balance restriction line BD. Let x_1 and t_1 be the coordinates of the point E. Let Figure 75C represent the concentration profile along a line parallel to t-axis at $x = x_1$.

Figure 75C is equivalent to the three sided figures SEJ on Figure 73, and hence the right hand side of the Equation (108) would give the area under the curve in Figure 75C. Equating this area to the area

under the curve in Figure 75A, Equation (109) is obtained.

$$c_1 t_1 - c_1 \left\{\frac{\epsilon x_1}{u} + \frac{(1-\epsilon)x_1}{u} \frac{F(c_1)}{c_1}\right\} = c_F t_o \qquad (109)$$

Since the point E lies on the level curve for $c=c_1$, from Equation (107), Equation (110) is obtained.

$$t_1 = \left\{\frac{\epsilon}{u} + \frac{(1 - \epsilon)}{u} \left[\frac{dF}{dc}\right]_{c=c_1}\right\} x_1 \qquad (110)$$

Equations (109) and (110) can be solved simultaneously to give the values of x_1 and t_1, the coordinates of the point E. The entire curve BD can thus be determined by taking various values of c_1 and solving Equations (109) and (110) simultaneously for each value of c_1 to obtain the coordinates of the points along the curve BD.

There is a convenient way of solving Equations (109) and (110) graphically. For any value of c_1, the level curve on the x-t diagram represents Equation (110). Equation (109) is also an equation of a straight line on the x-t diagram with the intercept on the t-axis equal to $c_F t_o/c_1$, and the slope equal to

$$\frac{\epsilon}{u} + \frac{(1 - \epsilon)}{u} \frac{F(c_1)}{c_1}$$

Intersection of the two straight lines gives the point E on the curve BD, and by taking different values of c_1, the entire curve BD can be constructed.

It may be noted that for the value of $c_1 = c_F$, Equation (109) represents the straight line AB on the x-t Contour Diagram on Figure 74.

BIBLIOGRAPHY FOR PART II

A1 Amundson, N. R. Ind. Engr. Chem., 48, (1956), 26.

A2 Amundson, N. R. Ind. Engr. Chem., 48, (1956), 35.

A3 Asher, D. R. and Simpson, D. W. J. Phy. Chem., 60, (1956), 518.

C1 Carslaw, H. S. and Jaeger, J. C. Conduction of Heat in Solids. (Oxford Univ. Press. See Ed. 1959), 388.

C2 Chilton, T. H. and Colburn, A. P. Ind. Eng. Chem., 26, (1935), 1183.

D1 DeVault, D. Jour. Amer. Chem. Soc., 65, (1943), 532.

F1 Furnas, C. C. Amer. Inst. Chem. Engr. Trans. 24, (1930), 142.

G1 Glueckauf, E. Trans. Faraday Soc. 51, (1955), 1540.

H1 Hiester, N. K., Radding, S. B., Nelson, R. L. Jr., and Vermeulen, T. A. I. Ch. E. Jour. 2, (No.3), (1956), 404.

H2 Hiester, N. K. and Vermeulen, T. Chem. Engr. Prog. 48, (1952), 505.

K1 Kasten, P. R., Lapidus, L., and Amundson, N. R. J. Phys. Chem. 56, (1952), 683.

K2 Keulemans, A. I. M. Gas Chromatography. New York: Reinhold Pub. Corp., edited by C. G. Verver, 1957.

L1 Lapidus, L., and Amundson, N. R. J. Phys. Chem. 56, (1952), 984.

L2 Lowan, A. N. Phil Mag. 7, (1934), 914.

N1 Nachod: Ion Exchange Technology. Ed. Nachod, F.C., and Schubert, J. Academic Press, 1956.

O1 Opler, A. and Hiester, N. K. Tables for Predicting the Performance of Fixed Bed Ion Exchange and Similar Mass Transfer Processes. Stanford Research Inst., Stanford, Calif., 1954.

P1 Prielipp, G. E. and Keller, H. W. J. Amer. Oil Chem. Soc. 33, (March, 1956), 103-108.

R1 Rosen, J. B. J. Chem. Phy. 20, (No. 3), (1952), 387.

R2 Rosen, J. B. Ind. Eng. Chem. 46, (1954), 1590.

S1 Sargent, R. and Rieman, W. (III). Journ. Phy. Chem. 61, (1957), 354.

S2 Schumann, T. E. W. Jour. Franklin Inst. 208, (1929), 405.

S3 Selke, W. E., Bard, Y., Pasternak, A. D., and Aditya, S. K. A. I. Ch. E. Journ. 2, (No. 4), (1956), 468.

S4 Shurts, E. U. of M. Thesis 1954.

S5 Shurts, E. and White, R. R. A. I. Ch. E. Journ. 3, (No. 2), (1957), 183.

S6 Sigmund, C. W., Munro, W. D., and Amundson, N. R. Ind. Engr. Chem. 48, (1956), 43.

S7 Sillen, L. G. Arkiv för Kemi. 2, (No. 34), (1950), 477.

S8 Sillen, L. G. Arkiv för Kemi. 2, (No. 35), (1950), 499.

S9 Simpson, D. W. and Wheaton, R. M. Chem. Eng. Progress. 50,(No. 1), (January, 1954), 45-49.

T1 Thomas, H. C. Ann. N.Y. Acad. Sci. 49, (1948), 161.

T2 Thomas, H. C. J. Chem. Phys. 19, (1951), 1213.

V1 Vermeulen, T. Advances in Chem. Engr. II, Acadamic Press, (1958), 147-208

W1 Wicke, E. Kolloid-z. 86, (1939), 295.

W2 Wheaton, R. M. and Bauman, W. C. Annals of the N.Y. Acad. of Sciences. 57, Art. 3, (November 11, 1953), 159-176.